Development of a Methodology for Estimating

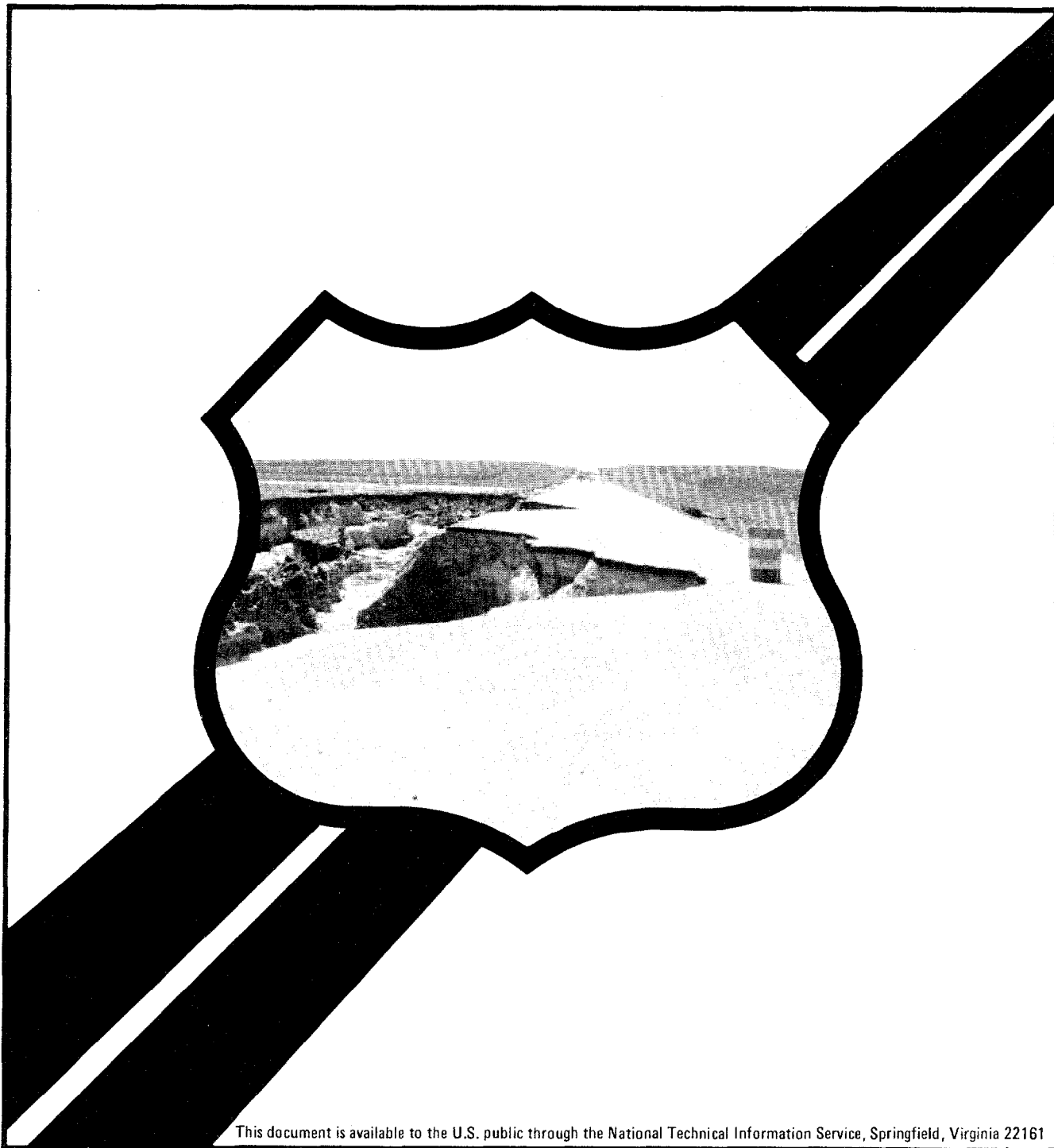# Embankment Damage Due to Flood Overtopping

U.S. Department
of Transportation

**Federal Highway
Administration**

Co-sponsored by:

**U.S. Department of Agriculture
Forest Service
Washington , D.C. 20590**

FOREWORD

This report describes a series of large-scale hydraulic model experiments to simulate floods overtopping highway embankments. Test conditions included embankments with and without pavement, with and without grass cover, with a range of headwater and tailwater elevations, and with a limited number of protective measures. The report will be of interest to hydraulic engineers for State highway agencies, consultants and other Government agencies who deal with flood damage evaluations of highway embankments or who deal with evaluations of dam safety in general.

Sufficient copies of the report are being distributed to provide a minimum of two copies to each FHWA regional office, one copy to each FHWA division office and one copy to each State highway office. Direct distribution is being made to the division offices.

Richard E. Hay, Director
Office of Engineering and
   Highway Operations
   Research and Development
Federal Highway Administration

NOTICE

1. Report No. FHWA/RD-86/126	2. Government Accession No.	3. Recipient's Catalog No.

4. Title and Subtitle	5. Report Date
DEVELOPMENT OF A METHODOLOGY FOR ESTIMATING EMBANKMENT DAMAGE DUE TO FLOOD OVERTOPPING	March 1987
	6. Performing Organization Code

7. Author(s) Y. H. Chen and Bradley A. Anderson	8. Performing Organization Report No.

9. Performing Organization Name and Address	10. Work Unit No. (TRAIS)
Simons, Li & Associates, Inc. 3555 Stanford Road P.O. Box 1816 Fort Collins, Colorado 80522	FCP 35H4-042
	11. Contract or Grant No. DTFH61-82-C-00104
	13. Type of Report and Period Covered

12. Sponsoring Agency Name and Address	13. Type of Report and Period Covered
Office of Engineering & Highway Operations R&D Federal Highway Administration 6300 Georgetown Pike McLean, Virginia 22101-2296	Final Report Sept. 1982 - March 1986
	14. Sponsoring Agency Code

15. Supplementary Notes

FHWA Contract Manager (COTR): J. Sterling Jones (HNR-10)

Co-sponsored by:
U.S. Dept. of Agriculture
Forest Service, Washington, D.C. 20013

16. Abstract

The objectives of this study are to conduct laboratory tests and develop a methodology to quantitatively determine embankment damage and assess protective measures. During the study, available literature and field data were collected. The embankments used in this study are 6 ft (1.8 m) high, 10 to 22 ft (3.0 to 6.7 m) in crest width, and 3 ft (0.9 m) in length, with slope varying from 2:1 to 3:1. The embankment surfaces include both with and without protective measures (pavement, grass, mattresses, Geoweb, soil cement, Enkamat, and others). The flood overtopping depths ranging from 0.5 to 4 ft (0.15 to 1.22 m), discharges ranging from 1 to 25 cfs/ft (0.1 to 2.32 cms/m) and tailwater conditions ranging from 10 percent water-surface drop to free fall. A computer model was developed to determine hydraulics of overtopping flow and associated erosion damage. This model was verified using field data and laboratory test results, and was utilized to generate charts for estimating embankment damage.

17. Key Words	18. Distribution Statement
Embankment, Erosion, Protection, Soil, Velocity, Shear Stress, Flood Overtopping, Headwater, Tailwater, Free Fall, Mathematical Model	No restrictions. This document is available to the public through the National Technical Information Service, Springfield, Virginia 22161.

19. Security Classif. (of this report)	20. Security Classif. (of this page)	21. No. of Pages 215	22. Price

Form DOT F 1700.7 (8-72)   Reproduction of completed page authorized

METRIC CONVERSION FACTORS

For readers who prefer metric units rather than inch-pound units, the conversion factors for the terms used in this report are listed below:

Multiply	By	To Obtain
ft (feet)	0.3048	m (meters)
ft/s (feet per second)	0.3048	m/s (meters per second)
ft/ft (feet per foot)	1.0	m/m (meters per meter)
ft^2 (square feet)	0.0929	m^2 (square meters)
ft^3/s (cubic feet per second)	0.0283	m^3/s (cubic meters per second)
in (inches)	25.4	mm (millimeters)
lb, avdp (avoirdupois pound)	0.4536	kg (kilograms)
lb/ft^2 (pounds per square foot)	4.882	kg/m^2 (kilograms per square meter)
lb/ft^3 (pounds per cubic foot)	16.02	kg/m^3 (kilograms per cubic meter)
mi (miles)	1.609	km (kilometers)

TABLE OF CONTENTS

iii

LIST OF TABLES

LIST OF TABLES (continued)

LIST OF FIGURES

LIST OF FIGURES (continued)

LIST OF FIGURES (continued)

INTRODUCTION

Embankment damage due to flood overtopping is a relatively new issue for highway engineers because traditionally they have ignored the consequences of floods larger than the "design flood." There have been several attempts to develop an approximate method of estimating embankment damage, but all attempts lacked the benefit of a set of controlled experimental data and differ by several orders of magnitude.

Numerous protection materials have been utilized for protecting embankments from flood erosion. These measures reduce embankment erosion mainly in two ways: (1) protect or strengthen soil to increase its resistance to erosion, and (2) increase surface roughness to reduce flood erosive force. Materials commonly utilized include vegetation, riprap, soil cement, and mats. Information about the performance of various materials available to protect embankments from damage due to flood overtopping is quite limited.

The objectives of this project were to perform a review of literature, collect field data, and conduct laboratory tests to develop a methodology to quantitatively determine embankment damage and to assess protection measures. During this project the following sources of literature were searched:

- ASCE (complete index of all publications of journals, conferences, proceedings, papers).

- U.S. Army Corps of Engineers (experimental model studies).

- National Technical Information Services (current published searches and bibliography of abstracts).

- Federal Highway Administration (index of research and development reports).

- Hydromechanics and Hydraulic Engineering Abstracts (Delft Hydraulics Laboratory, Indices, The Netherlands).

1

- Literature identified by Federal Highway Administration (FHWA) and United States Forest Service (USFS).

Seventy-nine reports and papers were identified as potentially useful to the study. These reports were reviewed to:

- Identify important parameters that control embankment damage.

- Investigate the failure mode of embankments.

- Assess effects of pavement, vegetation, and other protection measures on embankment stability.

- Assess erosion rate of embankment due to flood overtopping and other factors.

Field data of roadway erosion caused by flood overtopping were collected at five sites in Arkansas, three sites in Missouri, seven sites in Wyoming, one site in Colorado, and five sites in Arizona. These field data were analyzed and utilized to evaluate the methodology developed for determining embankment damages due to flood overtopping.

Embankment overtopping tests were conducted. The embankments tested in this study were 6 ft (1.8 m) high, 10 to 22 ft (3.0 to 6.7 m) in crest width, and 3 ft (0.9 m) in length, with slope varying from 2:1 to 3:1. The embankment surfaces which were tested included various combinations of two surface materials (bare soil and pavement) and five protective measures (grass, mattresses, geoweb, soil cement, and enkamat). Two base soils forming the embankments were tested and included soils classified as clay and as sandy clay. The flood overtopping conditions include overtopping depths ranging from 0.5 to 4 ft (0.2 to 1.2 m), discharges ranging from 1 to 25 ft^3/s-ft (0.031 to 0.77 m^3/s-m), and tailwater conditions ranging from 10 percent water surface drop to free fall.

The literature review, field data, and laboratory data were analyzed to develop embankment erosion equations considering the configuration and

material characteristics of the embankment and hydraulics of overtopping flow. A mathematical model was developed and verified using the collected field data and laboratory data. This model was then utilized to generate design charts for estimating embankment damages caused by floods of various overtopping depths and tailwater conditions.

This report presents the study results. The following sections deal with description of predominant modes of embankment failure, collection of field embankment damage data, the laboratory embankment test program, the hydraulics of overtopping flow, the parameters and equations governing embankment erosion, the development of a procedure for determining embankment erosion due to flood overtopping, and the evaluation of embankment protection measures.

DESCRIPTION OF PREDOMINANT MODES OF EMBANKMENT FAILURE

1. General

Roadway embankments are subjected to several types of failure during floods, including erosion due to flood overtopping, piping and liquefaction, and possibly mass wasting due to slip circle failure. The most common type of failure during flooding is caused by excessively high flood waters overtopping and eroding the embankment. Failures due to piping and liquefaction require a substantial amount of time for saturation of a soil matrix. This may be possible where embankments serve as a detention type structure or for longer-duration floods. Mass wasting also require some significant degree of soil saturation due to a longer flood event and occurs as flood waters recede, leaving saturated banks in an unstable condition. These types of embankment failure are briefly discussed first. Then, failure due to flood overtopping is focused upon, as the purpose of this study is to understand and develop methods of predicting damage caused by flood overtopping.

2. Piping and Liquefaction

Piping and liquefaction can occur when a soil has an effective stress which approaches zero. This commonly occurs in two situations: (1) an upward flow of water of such magnitude that the total upward force of water equals the total soil weight in an unloaded situation, and (2) the occurrence of a shock or vibration which produces a volume decrease in a loose soil skeleton, transferring the effective stress from the soil particle to the pore water. When either of these situations occur, the soil becomes essentially a fluid which flows and is easily moved and eroded by water either overtopping or flowing through the embankment. This type of failure for roadway embankments is not expected to be common unless the soil is quite permeable, and there is considerable ponding time and potential for embankment saturation. However, this failure factor required consideration when roadway embankments serve a dual purpose of providing detention for excess storm water.

4

3. Mass Wasting by Slip Circle Failure

An alternate form of embankment failure is caused by local mass wasting. If the embankment becomes saturated and possibly undercut by flowing water, blocks of the embankment may slump or slide downslope. Various forces are involved in mass wasting. These forces are associated with the downslope gravity component of the slope mass. Resisting these downslope forces are the shear strength of the earth's materials and any additional contributions from vegetation via root strength or man's slope reinforcement activities. When a slope is acted upon by water flowing over or through it, an additional set of forces is added. These forces are associated with removal of material from the toe of the slope, fluctuations in groundwater levels, and vibration of the slope. A slope may fail if stable material is removed from the toe. When the toe of a slope is removed, the slope loses more resistance by buttressing than it does by downslope gravitational forces. The slope materials may then tend to move downward into the void in order to establish a new balance of forces or equilibrium. Oftentimes, this equilibrium is a slope configuration with less than original surface gradient. The toe of the failed mass can provide a new buttress against further movements. However, if this buttress is removed by erosion, the force equilibrium may again be upset. For slope toes acted upon by erosive water, the continual removal of toe material can upset the force balance.

4. Flood Overtopping

Once floodwater overtops an embankment, erosion of the embankment will occur when locally high velocities over the embankment create a high erosion force which exceeds the strength of embankment resisting erosion. Failure of the embankment is also caused by large standing waves occurring on the embankment.

The primary mode of embankment failure due to flood overtopping begins by erosion of the downstream shoulder and slope. Figure 1 shows the progression of this type of failure where dashed lines show erosion at times t_1, t_2,

5
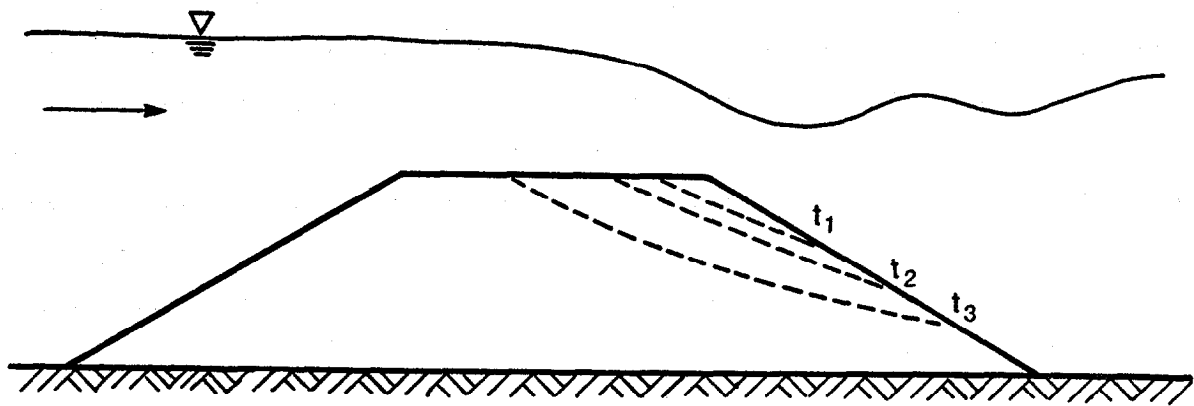
Figure 1. Erosion of the downstream shoulder.

and t_3. As water flows over the roadway it accelerates near the break point between the roadway shoulder and the downstream slope. Within a range of tailwater condition an undulating hydraulic jump with standing wave is created just downstream of the breakpoint. The energy dissipation in the hydraulic jump and the high velocities due to acceleration will greatly increase the erosion force of the water. Embankment is scoured from the area near the break point, forming a nick point which progresses upstream. The area downstream is also eroded from turbulence in the hydraulic jump.

Another mode of failure occurs when the toe of the embankment slope erodes. Figure 2 shows this type of embankment erosion failure. With low tailwater, often as the water accelerates over the top of an embankment it passes through critical depth and then forms an undulating hydraulic jump near the toe. The toe erosion may also be initiated by water flowing through the embankment and then down the slope. As the toe is eroded, the material above it becomes unstable and more erodible as erosion works its way up the embankment in the form of a headcut or slide.

On an earth embankment the erosion process will form a breach. Breaching will not be uniform over the entire embankment length, because weaker areas of embankment will fail first and cause the flow to concentrate at the failed sections. Continued washout of the embankment will occur from lateral erosion along with overtopping erosion of the embankment.
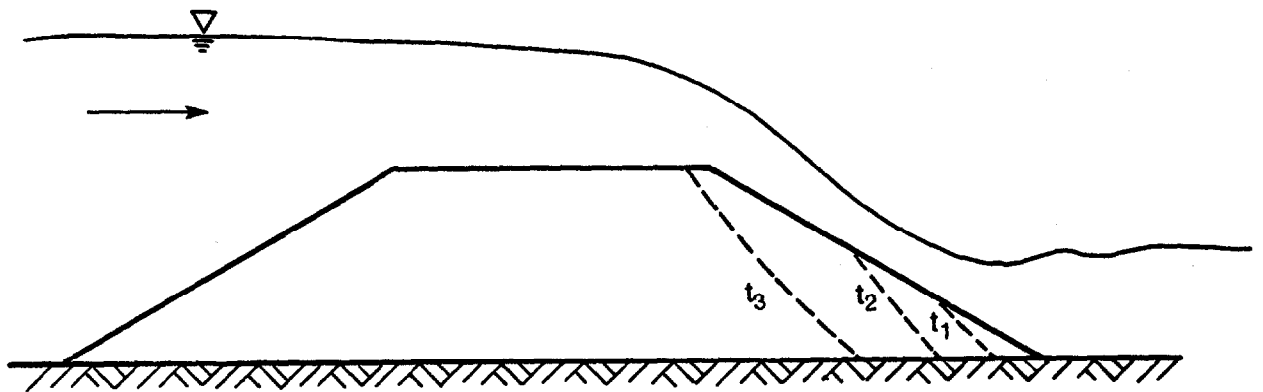
Figure 2. Erosion of the toe.

8

COLLECTION OF FIELD EMBANKMENT DAMAGE DATA

1. Field Data Collection Procedure

Roadway embankment damage data due to flood overtopping were collected at 21 sites by a joint force of personnel from the FHWA; State Highway Agencies; U.S. Geological Survey; and Simons, Li & Associates, Inc. (SLA). These field sites included data collected from five sites in Arkansas and three sites in Missouri due to the December 1982 flood, four sites in Wyoming and one site in Colorado due to the May 1983 flood, five sites in Arizona due to the September 1983 flood, and three sites in Wyoming due to the August 1985 flood. The following procedures were generally utilized in collecting these data:

(1) FHWA and State Highway Agency identified potential sites.

(2) FHWA invited the SLA team members to visit the study sites if time and budget allowed. SLA team members have visited all the sites except those in Arizona to acquaint themselves with the damage conditions; visit local residents to comprehend the flooding history; and collect soil and stage data, such as soil samples, high water marks, and photographs.

(3) FHWA contracted the U.S. Geological Survey to determine flood conditions based on indirect methods and facts collected following the flood. The USGS estimated peak streamflow, maximum depth and peak flow over the roadway, headwater and tailwater elevations, velocity over the roadway, and duration of the flood for all sites damaged by the 1983 flood, except those in Wyoming and Colorado. SLA project team made estimates for these sites.

(4) State Highway Agency personnel provided descriptions of the damage to the highway embankment, some cross-sectional data, and itemized the cost for repair.

2. Presentation of Field Data

Table 1 summarizes the estimated flood conditions and table 2 summarizes the embankment characteristics and damage conditions for the 21 flood sites. These data were utilized to verify the methodology for determining embankment damage due to flood overtopping as described in "Development of a Procedure for Determining Embankment Erosion Due to Flood Overtopping." Details of field data were presented elsewhere.[1,2]

9

Table 1. Flood data at field study sites.

Site	Peak Overtopping Conditions								
	Peak Discharge (ft^3/s)	Average Depth (ft)	Maximum Depth (ft)	Length (ft)	Duration (hours)	Average Velocity (ft/s)	Maximum Velocity (ft/s)	Headwater Elevation (ft)	Tailwater Elevation (ft)
1. Castor River at Zalma, State Highway 51, Bollinger County, MO	19,500	2.7	3.0	1,795	26	4.7	5.4	380.7-381.8	379.6-380.3
2. Black River at Hilliard, County Highway W, Dutler County, MO	35,300	4.5	6.7	1,370	41	5.7	6.2	66.2	65.9
3. Little Black River near Grandin County Highway K, Ripley County, MO	9,370	2.8	3.6	700	9	5.8	5.9	417.0	414.2
4. Spring River at Imboden, AR	98,500	6.5	10.5	1,863	22	10.5	12.6	310.5	307.6
5. Eleven Point River near Ravenden Springs, AR, at Arkansas State Highway 93 at Dalton, AR	17,500	2.5	3.7	1,255	15	6.5	7.8	348.3	344.63
6. South Fork Little Red River at Clinton, AR	6,290	2.6	3.3	508	10	5.2	6.3	515.7	514.8
7. Illinois Bayou near Scottsville, AR, at Arkansas State Highway 164	10,100	2.7	4.0	672	12	6.6	8.0	479.0	474.8
8. West Fork Point Remove Creek near Hattieville, AR, at Arkansas State Highway 247	10,300	1.2	2.0	3,118	12	4.2	5.1	317.3	315.3
9. Gravel Road 1-1/2 Miles North of Hillsdale, WY	60	---	1.0	80	80	3.0	---	---	Low
10. Morrie Street at Crow Creek in Cheyenne, WY	---	---	1.0	---	12	4	6	---	Low
11. Earth Road in Granite Reservoir, WY	300	---	1.0	120	10	---	5	---	---
12. Wyoming State Highway 487 at Sand Creek near Shirley Basin	6,680	---	2.3	1,134	42	---	---	7,005.8	Free Fall

Table 1. (continued)

Site	Peak Overtopping Conditions								
	Peak Discharge (ft^3/s)	Average Depth (ft)	Maximum Depth (ft)	Length (ft)	Duration (hours)	Average Velocity (ft/s)	Maximum Velocity (ft/s)	Headwater Elevation (ft)	Tailwater Elevation (ft)
13. Taft Hill Road at Cache la Poudre River in Fort Collins, CO	500	----	0.5	300	30	---	7	---	Low
14. Gila River at U.S. Highway 70 (Bylas Bridge)	27,000	2.5	3.4	2,100	38	5.1	5.5	2,583.4	2,577.3
15. San Francisco River at U.S. Highway 666 at Clifton, AZ	7,200	2.6	4.0	2,700	4	8.7	10.5	3,457.5	3,456.0
16. Gila River at State Higway 87 near Sacaton, AZ (milepost 148.0)	26,000	2.1	3.1	2,240	60	5.6	5.8	1,283.1	1,280.9
17. Peak Canyon at Interstate Highway 19 near Nogales, AZ (milepost 14)	6,200	1.5	1.8	1,100	---	3.6	4.0	3,357.2	3,354.8
18. Santa Cruz River at Cortaro Road near Tucson, AZ	23,000	3.9	5.3	1,600	44	3.6	7.1	2,151.9	2,149.8
19. Prairie Ave., Cheyenne, WY	4,200	---	2.5	---	3	---	8.5	Δh (H.E. - T.E.= 3 ft)	
20. Windmill Road, Cheyenne, WY	5,500	---	3.0	---	3	---	13	Δh (H.E. - T.E.= 3 ft)	
21. Ridge Road, Cheyenne, WY	5,700	---	1.5	---	3	---	12	Δh (H.E. - T.E = 5 ft)	

11

Table 2. Summary of embankment characteristics and damage.

	Embankment Characteristics					Damage				
Site	Width/ Height (ft)	Soil Type	Width of Pavement (ft)	Side Slope	Vege- tation on Slope	Length (ft)	Width (ft)	Volume (yd^3)	Cost of Repairs	Time of Closure (hours)
1. Castor River at Zalma, State Highway 51, Bollinger County, MO	24/4	Sandy, Low- Cohesive	20 (bituminous)	1.5:1	Fescue- bermuda	600 (shoulder)	---	200	5,150	26
2. Black River at Hilliard, County Highway W, Dutler County, MO	28/4	Sandy, Low- Cohesive	22 (bituminous)	---	Fescue	75 (shoulder and pavement)	---	---	1,450	41
3. Little Black River near Grandin County Highway K, Ripley County, MO	24/10	Sandy -Clay	20 (oil aggregate)	1.5:1	Fescue	400 (shoulder and embankment)	---	700	3,000	9
4. Spring River at Imboden, AR										
5. Eleven Point River near Ravenden Springs, AR, at Arkansas State Highway 93 at Dalton, AR										
6. South Fork Little Red River at Clinton, AR										
7. Illinois Bayou near Scottsville, AR, at Arkansas State Highway 164	26/10	Sandy-Silt, Noncohesive	20	2.5:1	Grass	155 (washed)	20-55	2,000	---	---
8. West Fork Point Remove Creek near Hattieville, AR, at Arkansas State Highway 247	26/6	---	20	2:1	Grass	2,500 (shoulder and 1000' pavement)	---	920	---	---
9. Gravel Road 1-1/2 Miles North of Hillsdale, WY	20/3	d_{50}=0.5 mm (surface) d_{50}=0.13 mm (subsurface) Noncohesive	0	3:1	Sparse	80	17	190	---	---
10. Morrie Street at Crow Creek in Cheyenne, WY	34/4	d_{50}=0.12 mm silt & clay content = 24-42 Percent, Low-Cohesive	24	2.5:1	Sparse	25	54 (breached)	330	---	---

12

Table 2. (continued)

Site	Embankment Characteristics					Damage				
	Width/ Height (ft)	Soil Type	Width of Pavement (ft)	Side Slope	Vegetation on Slope	Length (ft)	Width (ft)	Volume (yd^3)	Cost of Repairs	Time of Closure (hours)
11. Earth Road in Granite Reservoir, WY	20/4	d_{50}=2.7 mm Noncohesive	0	2.5:1	Sparse	120 (damaged) 20 (breached)	10-35 (damaged) 70 (breached)	210	---	---
12. Wyoming State Highway 487 at Sand Creek near Shirley Basin	45/10	d_{50}=0.4 mm PI=10	35	2:1	Sparse	1,100	70	9,600	300,000	>1,000
13. Taft Hill Road at Cache la Poudre River in Fort Collins, CO	30/8	Sandy Low-Cohesive	24	3:1	Sparse	230 (shoulder) 70 (pavement)	30 (shoulder) 5 (pavement)	350	---	300
14. Gila River at U.S. Highway 70 (Bylas Bridge)	45/6	Sandy silt d_{50} = 0.4 mm	34	4:1	Sparse	1,500	---	45,500	830,000	310
15. San Francisco River at U.S. Highway 666 at Clifton, AZ	45/5	Sand/gravel d_{50} = 4 mm	35	3:1	Sparse	---	---	---	85,000	70
16. Gila River at State Highway 87 near Sacaton, AZ (milepost 148.0)	50/5	Sandy d_{50} = 0.50 mm Low-Cohesive	40	6:1	Sparse	1,000	---	1,060	51,000	80
17. Peak Canyon at Interstate Highway 19 near Nogales, AZ (milepost 14)	58/5	Sandy d_{50} = 0.30 mm Low-Cohesive	38	3:1	Sparse	500	---	1,000	48,000	2
18. Santa Cruz River at Cortaro Road near Tucson, AZ	44/-	---	24	2:1	Sparse	---	---	---	---	---
19. Prairie Ave., Cheyenne, WY	35/5	Sandy clay d_{50} = 0.9 mm, PI = 4.3	24	4:1	Sparse	50	15	450	8,400	---
20. Windmill Road, Cheyenne, WY	40/5	Sand silt d_{50} = 1.0 mm	30	3:1	Sparse	100	15	980	26,000	---
21. Ridge Road, Cheyenne, WY	40/5	Sandy silt d_{50} = 0.6 mm	30	3:1	Sparse	60	10	390	7,300	---

13

The field data are limited in that they consist of overtopping condition at peak flow, total embankment damage after the flood, and limited soil data. However, these field data are useful for verification of the modeling assumptions and of the methodology that is developed using data from controlled laboratory conditions.

LABORATORY EMBANKMENT TEST PROGRAM

The details of the hydraulic model utilized to collect the laboratory data and the characteristics of the embankment soils tested by the model are presented in this section. The calibration of the hydraulic model is documented and provided along with a description of the embankment construction procedures. This section also presents the details of the embankment test program, the schedule of tests, flow conditions tested by the model, and data collection procedures. Finally, a review of the procedures utilized to edit, review, and analyze the data is presented.

1. Test Facilities and Instrumentation

The embankment overtopping tests were conducted in an outdoor testing facility at the Engineering Research Center (ERC) of Colorado State University. The outdoor testing facility was designed to conduct tests upon full-scale roadway embankments. The utilization of a testing facility which allows full-scale tests minimized the inaccuracies inherent with modeling the physical processes associated with the hydraulic and sediment transport mechanics of embankment erosion.

Testing the erosion of the full-scale embankments necessitated the fabrication of a large moveable flume and construction of a prototype section of roadway embankment. The design features of the flume included a headbox and tailwater control section, an embankment test section, and a data collection carriage mounted on the flume walls. An inlet diffuser was installed as an integral part of the headbox. A series of four outlet gates provided the tailwater control for the flume. The flume also includes a 60-foot (18.3-meter) section of 8-inch (203-mm) pipe to pass water from the headbox to the downstream embankment slope. This allowed for setting the initial tailwater conditions during the high tailwater tests. The flume utilized for this study is depicted in figures 3 and 4.

15

POINT GAGE &
VELOCITY PROBE

INLET DIFFUSER

CARRIAGE

90' x 11' x 3' FLUME

36"

|← HEADBOX →|← ——————— EMBANKMENT TEST SECTION ——————— →|← OUTLET GATES →|
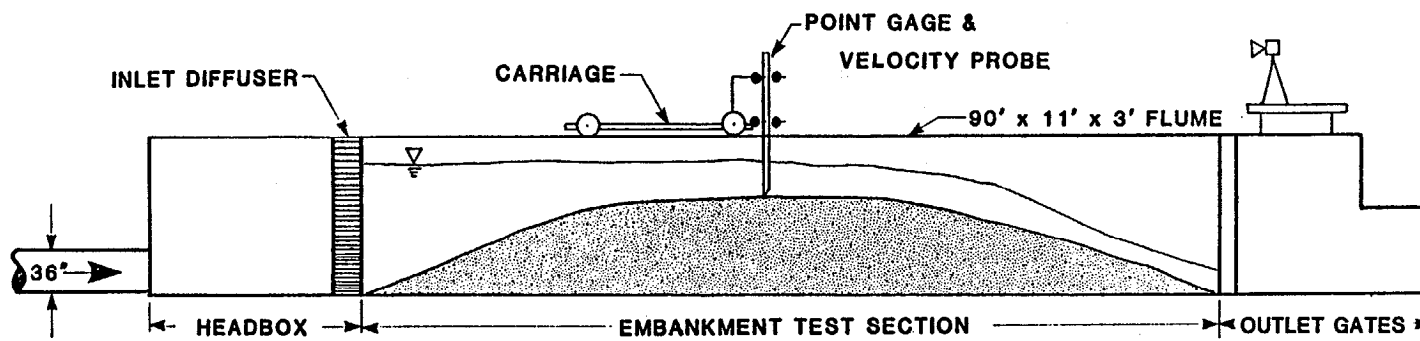
Figure 3. Profile of testing facility.
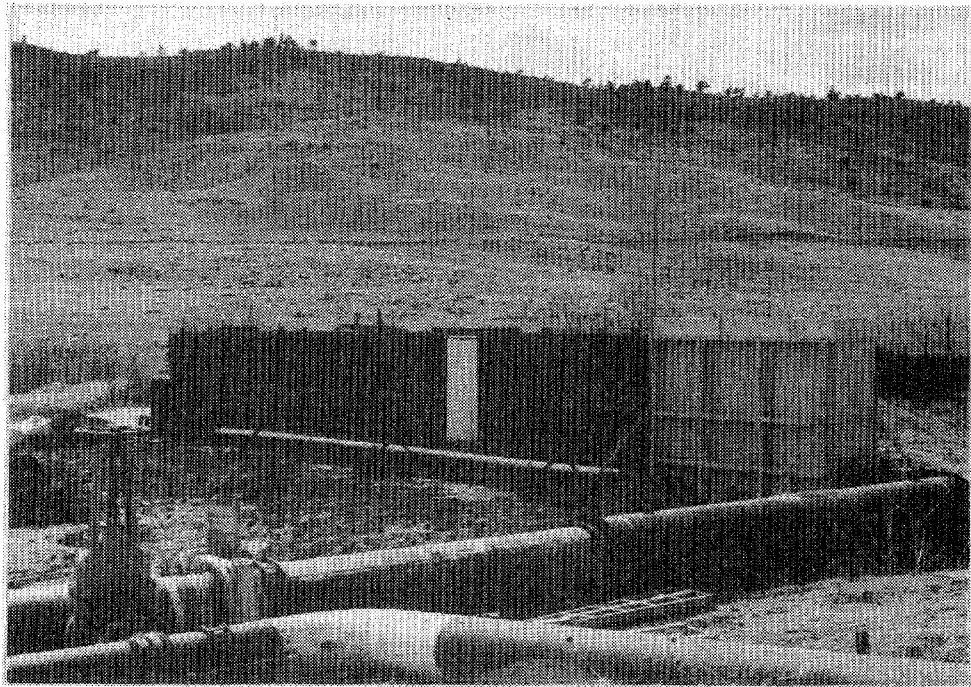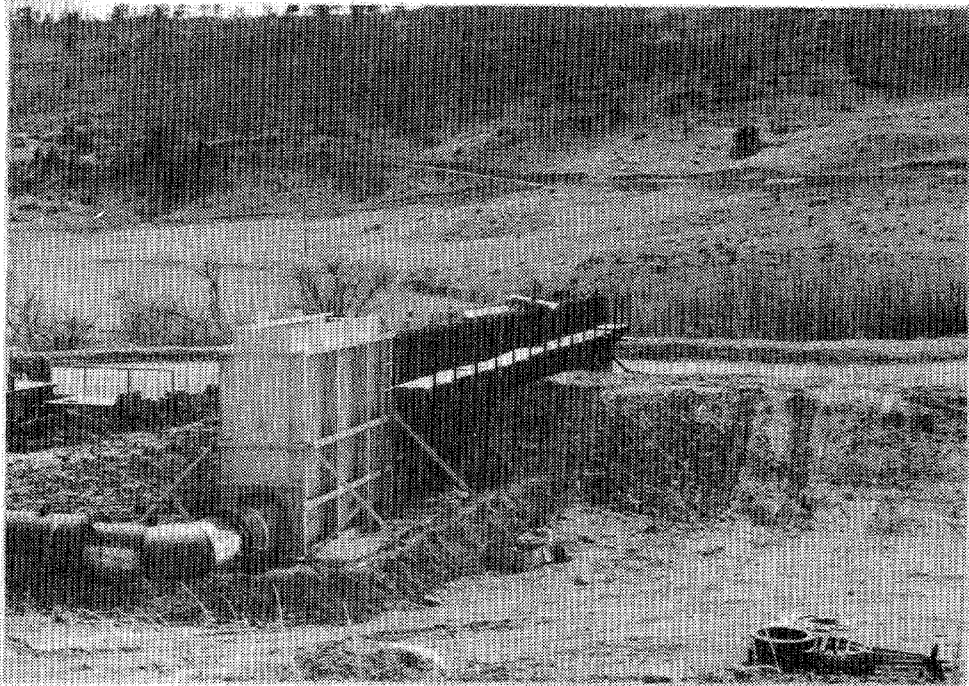
Figure 4. Testing facility

17

Extensive modifications to the property leased from Colorado State University were made to allow for a recirculating water supply and full-scale embankment construction. An embankment approximately 300 ft (91.4 m) in length was constructed in accordance with AASHTO guidelines. Unpaved and paved sections of roadway embankment were included in combination with sideslopes ranging from 4:1 (horizontal to vertical) to 2:1. The embankment sideslopes were vegetated with a seed mixture approved by representatives of the Federal Highway Administration.

The discharge required for the testing was provided by a pumping plant owned and operated by SLA. The pumping plant, consisting of an Aurora Diesel 8V-92T engine (435 BHP at 2100 rpm), provided in excess of 75 ft^3/s (2.1 m^3/s) to the flume. If needed, an additional 30 ft^3/s (0.8 m^3/s) could have been provided by a 300-hp, 24-inch (0.6-m) electric pump owned by Colorado State University. The source of water for the testing was a detention pond constructed at the testing site. The experimental facilities were designed to recirculate the design discharge from the flume to the detention pond and back to the pump pit. A plan view of the test site illustrating the recirculating water supply system and roadway embankment is presented in figures 5 and 6.

As indicated by figure 6, the test site was sufficiently large and was arranged to allow for stockpiling and mixing a variety of soil materials. The stockpiled soil materials were utilized during the construction and testing of the roadway embankment for the fixed-flume tests and duplicated the soils which composed the 300-ft (91.4-m) roadway embankment. The test site was also designed to allow for moving the flume to test successive sections of the 300-ft (91.4-m) roadway embankment. A 40-foot (12.2-m) telescoping section of 36-inch (0.9-m) pipe was utilized in conjunction with successive lengths of 36-inch (0.9-m) pipe to move the flume to the required locations.

SECTION A-A

y = 3' AVERAGE

EXISTING GROUND

8'

RETURN FLOW CHANNEL

SEDIMENT DETENTION POND

CROSS FLOW NOTCH

BERMS

PUMP FOREBAY

TAILBOX

A

A

36" GATE VALVE

12" BYPASS & VALVES (3) & ORIFICE

FLUME

Ⓐ FUEL OIL TANK & BERM
Ⓑ PUMP STAND
Ⓒ ENGINE
Ⓓ PUMP & GEAR
Ⓔ PUMP PIT
Ⓕ PUMP

36" Ø PIPE 40 SEGMENTS

90° ELBOW R = 6'

ORIFICE

HEADBOX

0   12'   24'

APPROXIMATE SCALE

120'x40' COVERED FLUME

TEE

40"x36"x34" TELESCOPING SECTION

36" GATE VALVE

24" Ø PIPE

24" GATE VALVE

24" 90° 3 SEG. ELBOW

ORIFICE OR VENT

Ⓕ

Figure 5. Site layout.

Figure 6. Overview of the testing facilities.

The data collected during the testing program included discharge, velocity, depth, water-surface profile, and embankment profile. The discharge rate in the flume was determined by utilizing a calibrated elbow meter installed in the water supply line. The device was connected to a manometer tube and the difference in water heads across the elbow meter determined. The difference in water heads coupled with the calibration curve for the meter provided the discharge. The calibration curve for the discharge measuring device is provided in figure 7. During the testing, data collection was facilitated by the use of a carriage which traversed the length of the flume. The carriage provided support for the point gauge and the instrumentation for velocity measurements. The point gauge measured the elevations of the bed and water surface. Velocity measurements were taken by a Marsh-McBirney 201 electromagnetic current meter capable of measuring velocities from 0 to 20 ft/s (0 to 6.1 m/s).

2. Verification of Flow Hydraulics

An understanding of the hydraulics of water flowing over an embankment is essential to understanding the erosion process. Consequently, a series of rigid-bed embankment tests were conducted to evaluate the hydraulic variables. Table 3 summarizes the various flow conditions generated during this series of tests.

The data collected during each test included discharges, water-surface elevations, and velocity measurements. The data were analyzed to determine the velocity distribution and coefficient of discharge for free flow and submerged flow conditions. The results of the analysis are presented in "Hydraulics of Flow Over an Embankment."

3. Characteristics of Embankment Soils

During this study a soil testing program was performed to evaluate all fill material used for construction of the embankment test sections. Soil materials were selected based on specifications provided by the Federal

21
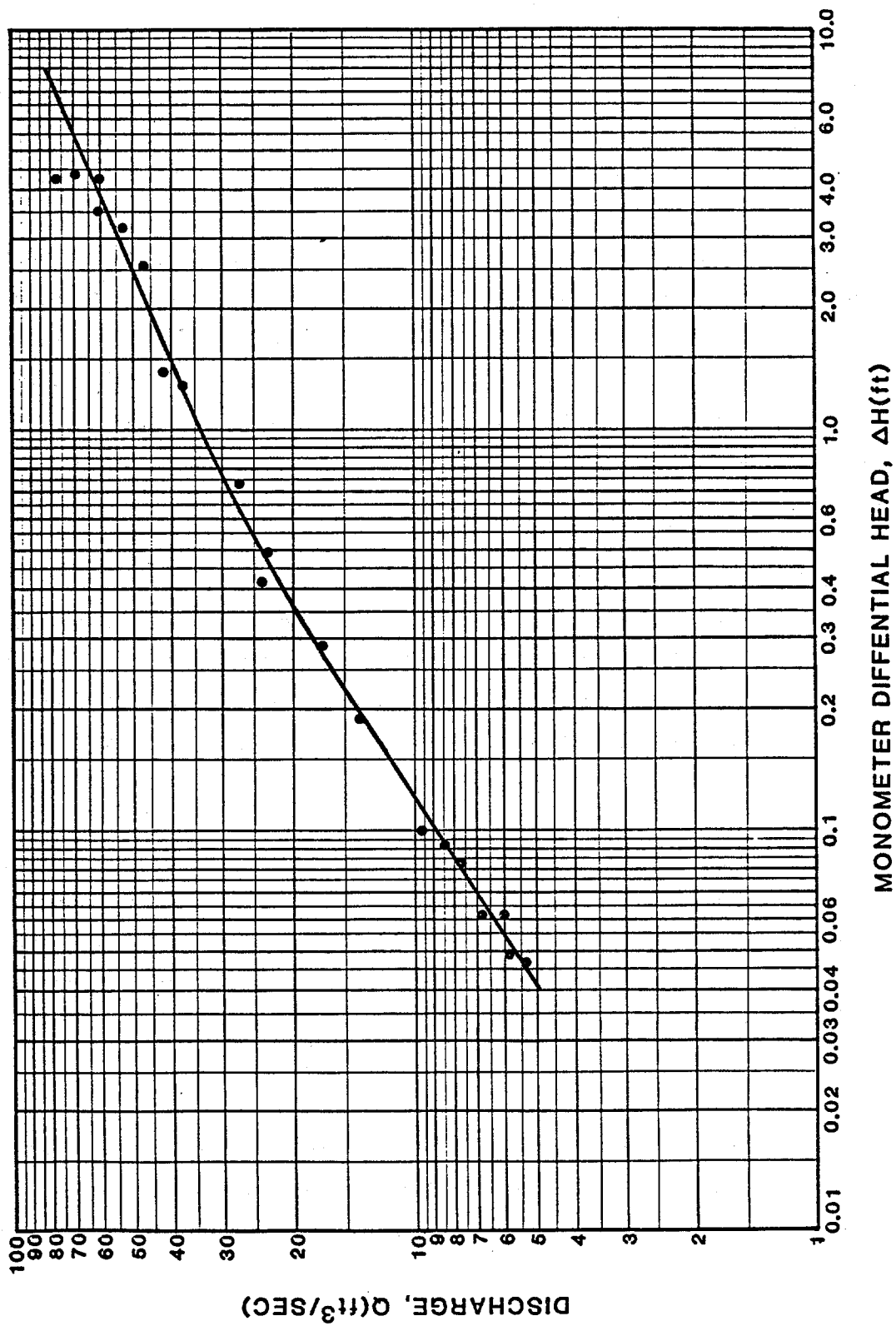
Figure 7. Calibration curve for discharge measurements.

Table 3. Flow overtopping conditions of rigid
          embankment runs.

Run	Overtopping Depth, h (ft)	Water Surface Drop (Percent)	Discharge (ft^3/s)
1	0.5	20	2.0
2	0.5	40	2.5
3	1.0	10	4.9
4	1.0	20	6.2
5	1.0	40	6.4
6	2.0	10	22.5
7	2.0	20	22.9
8	2.0	40	23.4
9	2.0	75	24.0
10	4.0	10	72.0
11	4.0	20	78.5
12	4.0	40	75.0

Highway Administration and included a clayey sand mixture, as well as a sandy, more erosive soil.

Two sources of embankment material were tested for comparative purposes before selecting the initial testing material, hereafter referred to as soil type I. Following a series of flood overtopping tests, a soil composed of a higher percentage of sand, hereafter referred to as soil type II, was utilized to construct additional test sections.

Laboratory and field tests were performed to classify and determine the engineering properties of the fill material. The soil tests, conducted in accordance with ASTM procedures, provided information concerning soil classification, grain-size distribution, Atterberg limits, hydraulic conductivity, critical shear stress, shear strength, compaction characteristics, and dispersivity.

Soil type I was classified as a clay of low plasticity (CL) by the Unified Soil Classification. According to the AASHTO classification system, the material was classified to be an A-6 soil. The grain-size distribution curve for soil type I is provided on figure 8. In general, soil type I contained approximately 40 percent sand and 60 percent silt plus clay. Results of the laboratory analyses are presented in table 4. A comparison of the selected laboratory analyses of soil type I before and after embankment construction is also provided in table 4.

Soil type II was classified as a SM-SC by the Unified Soil Classification and a A-4(0) by the AASHTO classification system. The grain-size distribution curve is provided on figure 9. Soil type II was created by mechanically mixing a sandy material with soil type I, which produced a soil with approximately 20 percent more sand than soil type I. The results of the laboratory analyses conducted for soil type II are presented in table 5.

Figure 8. Size distribution for soil type I.
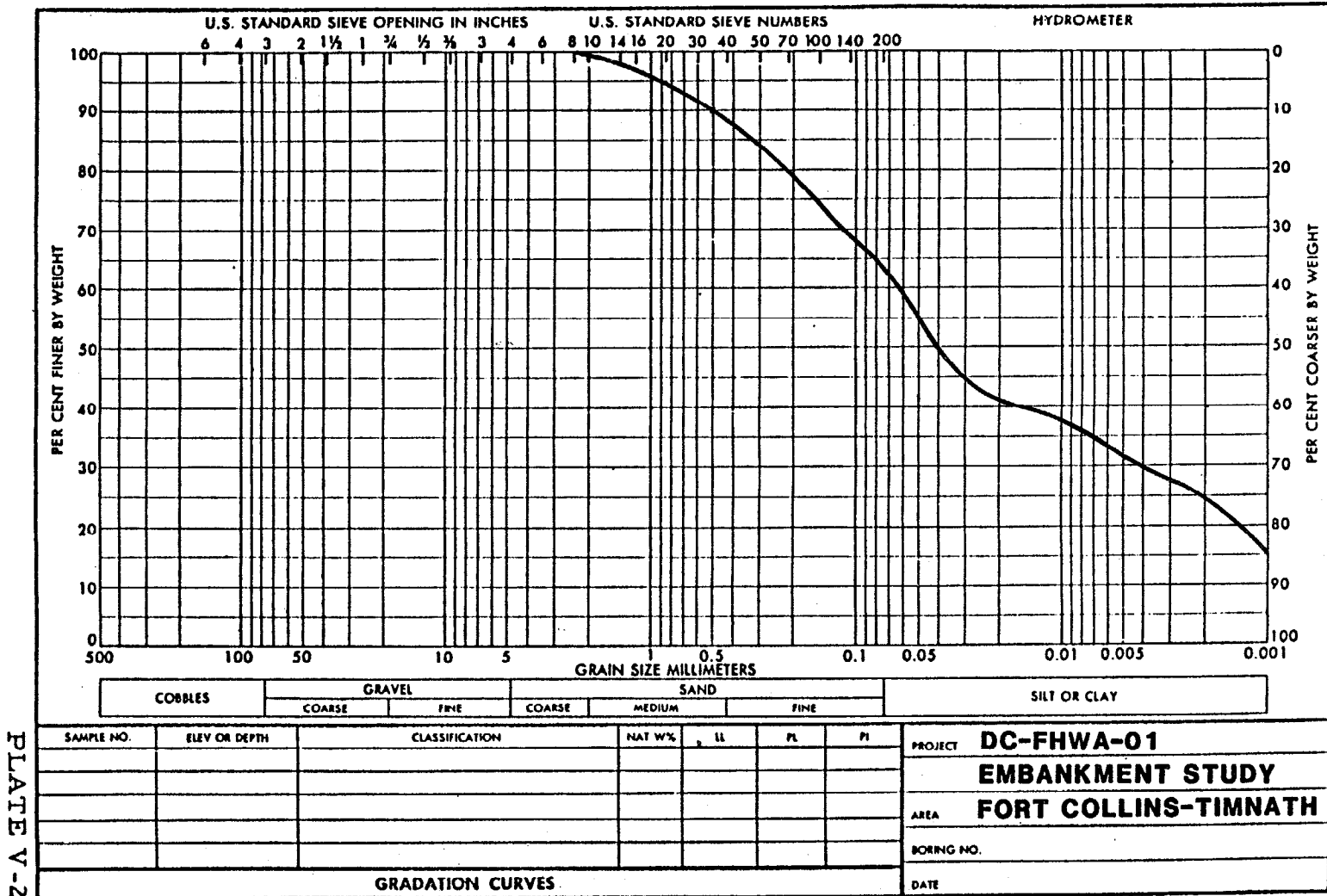
Table 4. Soil test results, soil type I.

Soil Property/Test	Results Before Construction	Results After Construction
Grain-size Distribution		
Percent Sand	40	40
Percent Passing #200 Sieve	60	60
Atterberg Limits		
Liquid Limit	32.8 to 47.8	32.7 to 35.1
Plastic Limit	20.7 to 23.2	19.3 to 22.3
Plasticity Index	11.6 to 24.6	11.7 to 15.7
AASHTO Classification	A-6	A-6
Unified Soil Classification	CL	CL
Specific Gravity	2.58 to 2.60	
Compaction		
Optimum Moisture Content	18 percent	13 to 19 percent
Maximum Dry Density	108 lb/ft^3	102 to 111 lb/ft^3
Hydraulic Conductivity	1.9×10^7 to 4.8×10^7 cm/s	
Dry Density	100.3 to 102.8 lb/ft^3	
Maximum Standard Proctor Density	92.7 to 95 percent	
Water Content	15.6 to 16.3 percent	
Torvane Shear Test		
Before Saturation	2.5 $tons/ft^2$	
After Saturation	0.1 to 3.2 $tons/ft^2$	
Pin-Hole Dispersion Test	ND_1 (no dispersive)	
Critical Shear, τ_c	0.078 lb/ft^2	

Figure 9. Size distribution curve for soil type II.

Table 5. Soil test results, soil type II.

Soil Property/Test	Test Result
Grain-size Distribution	
Percent Sand	59 percent
Percent Passing #200 Sieve	41 percent
Atterberg Limits	
Liquid Limit	24.4
Plastic Limit	18.7
Plasticity Index	5.7
AASHTO Classification	A-4(0)
Unified Soil Classification	SM-SC
Compaction	
Optimum Moisture Content	14.7
Maximum Dry Density	113.5

A detailed discussion of the testing procedures and soil test results is provided in a report entitled, "Report for Task D: Soil Tests," submitted to the Federal Highway Administration on January 28, 1985.

4. Embankment Construction Procedures

All embankment test sections were constructed to be 6 ft (1.8 m) high, and allow a top pavement width of 12 ft (3.7 m) and shoulder width of 10 ft (3.0 m). The sideslope of the embankments tested during this study varied from 2:1 (horizontal to vertical) to 3:1. Two types of soil were utilized as fill material and two roadway surfaces were tested along with five embankment protection measures. Table 6 presents the types of roadway surfaces and protection measures tested during this study.

The original proposal was to construct a long embankment, allow it to age, and test various conditions by moving the flume to various segments of the embankment where prescribed embankment conditions were set up. The effect of aging on the soil cohesion could be taken into account by this procedure. After several experiments, it was decided to move the flume for the grassed embankments only because the effects of the disturbed edges next to the flume walls were significant. More reliable data could be obtained by compacting the bare soil experiments in place rather than attempting to move the flume to the precompacted sections.

The procedures established for installing the embankment fill materials and embankment protection measures were an important aspect of this study. This is especially true for the tests which required the construction of the soil embankment within the flume. For these tests, the procedure consisted of mechanically mixing the individual soils composing the embankment fill material, followed by placement of the material in the flume with a Bobcat front-end loader. Water was carefully added during placement of the fill material to ensure that optimum moisture content (~18 percent) was obtained. Engineering technicians mechanically compacted the fill material in 6-inch

29

Table 6. Roadway surfaces and protection measures selected for testing.

Roadway Surface	Protection Measures Selected For Testing
Soil Surface	None
Paved Surface/Gravel Shoulder	None
Paved Surface/Gravel Shoulder	Grass
Soil Surface	Geoweb
Soil Surface	Enkamat
Soil Surface	Enkamat and Grass
Soil Surface	Gabion Mattress
Soil Surface	Soil Cement

(152-mm) lifts to obtain the compaction requirements (95 percent of maximum dry density, Standard Proctor). To the maximum extent possible, all test sections were constructed to meet Federal Highway Administration specifications. Figure 10 illustrates the installation and compaction of the embankment material. An illustration of the soil embankment following construction is provided in figure 11.

Tests of a paved roadway were also conducted within the flume. The soil embankment was constructed in accordance with the procedures previously described. A 12-inch (0.3-m) gravel base was placed on the surface of the soil embankment. The roadway was capped with a 4-inch (102-mm) thick bituminous pavement. The completed test section was 6 ft (1.8 m) high with a top pavement width of 12 ft (3.7 m) and a gravel shoulder width of 10 ft (3.0 m). Figure 12 illustrates a paved roadway test section ready for testing.

Testing an embankment slope vegetated with grass required the construction of a full-scale embankment. Consequently, a 300-foot (91.4-m) embankment was constructed to test the influence of a vegetated embankment slope under a variety of flow conditions. The embankment was constructed in accordance with Federal Highway Administration specifications. A gravel base and paved roadway surface were placed on top of the soil embankment. Figure 13 presents a sequence of photographs illustrating the construction procedure. Following construction of the road embankment, sideslopes were planted with a seed mixture accepted by the Federal Highway Administration. The seed mixture is presented in table 7.

The vegetated embankment was excavated for the movable flume tests using the following procedure. After adding sufficient sections of 36-inch (0.9-m) pipe to allow advancement of the flume, two 18-inch (0.5-m) trenches were excavated in the embankment. The embankment test section was approximately 32 inches (0.8 m) in width between the trenches. The trenches were lined with a bentonite mixture and a flume wall was placed in each trench. The headbox and
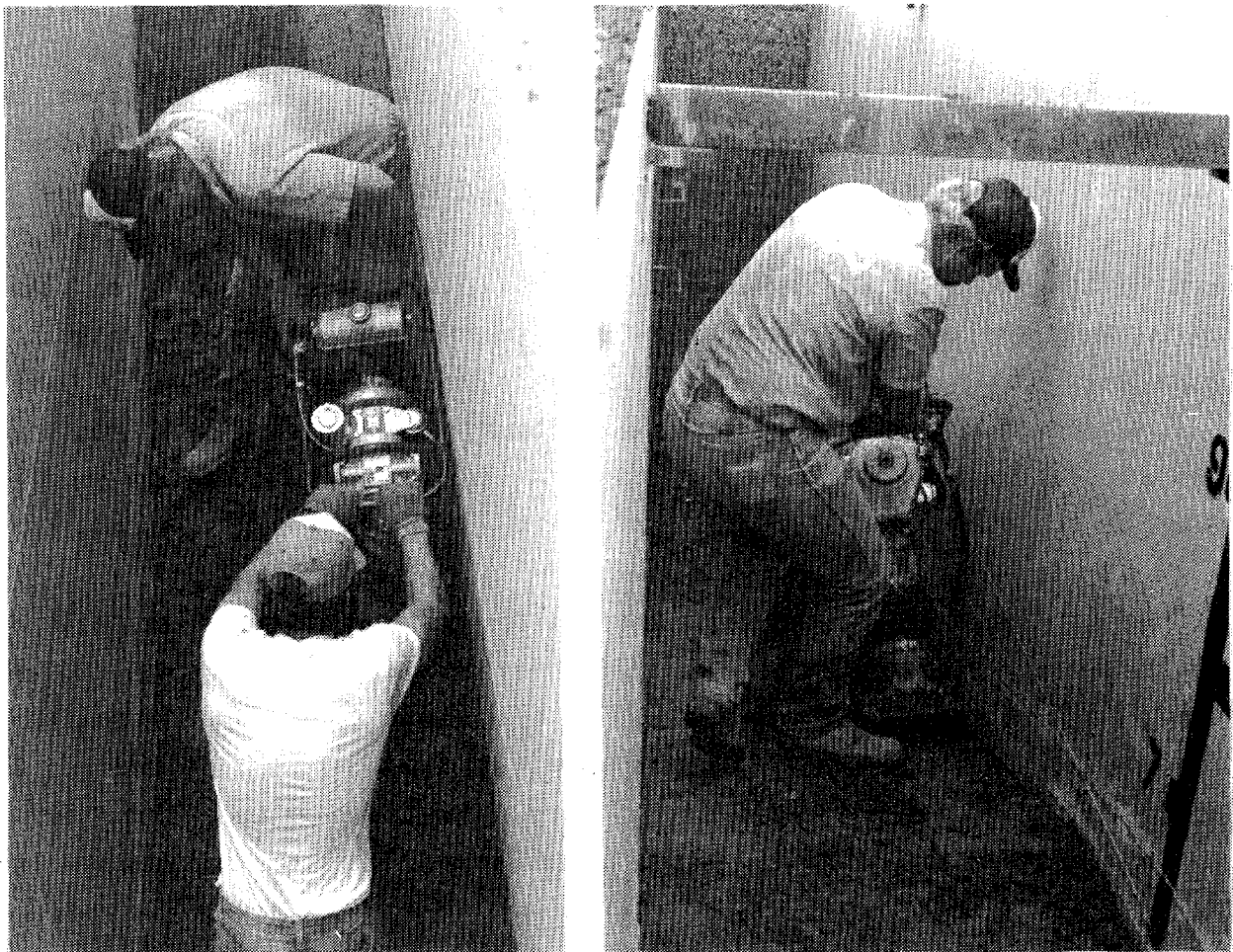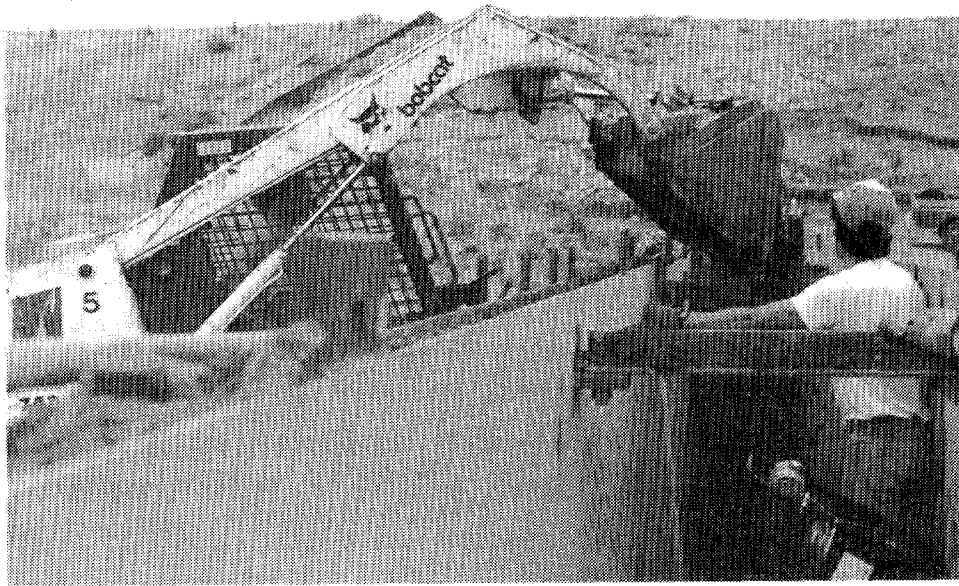
Figure 10. Installation and compaction of embankment.
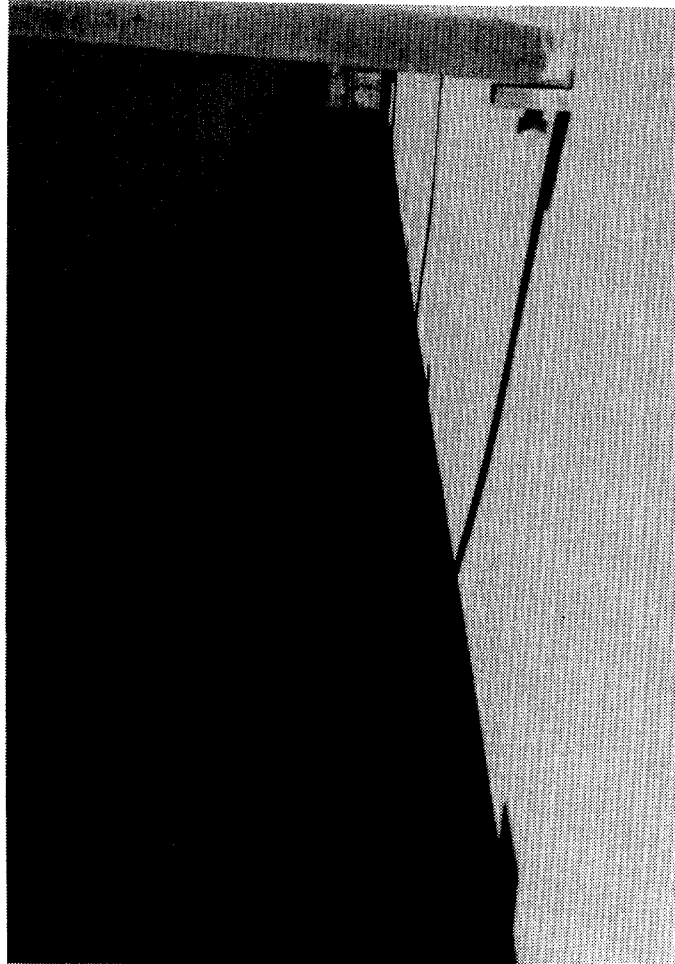
Figure 11. Illustration of the soil embankment following construction.

33
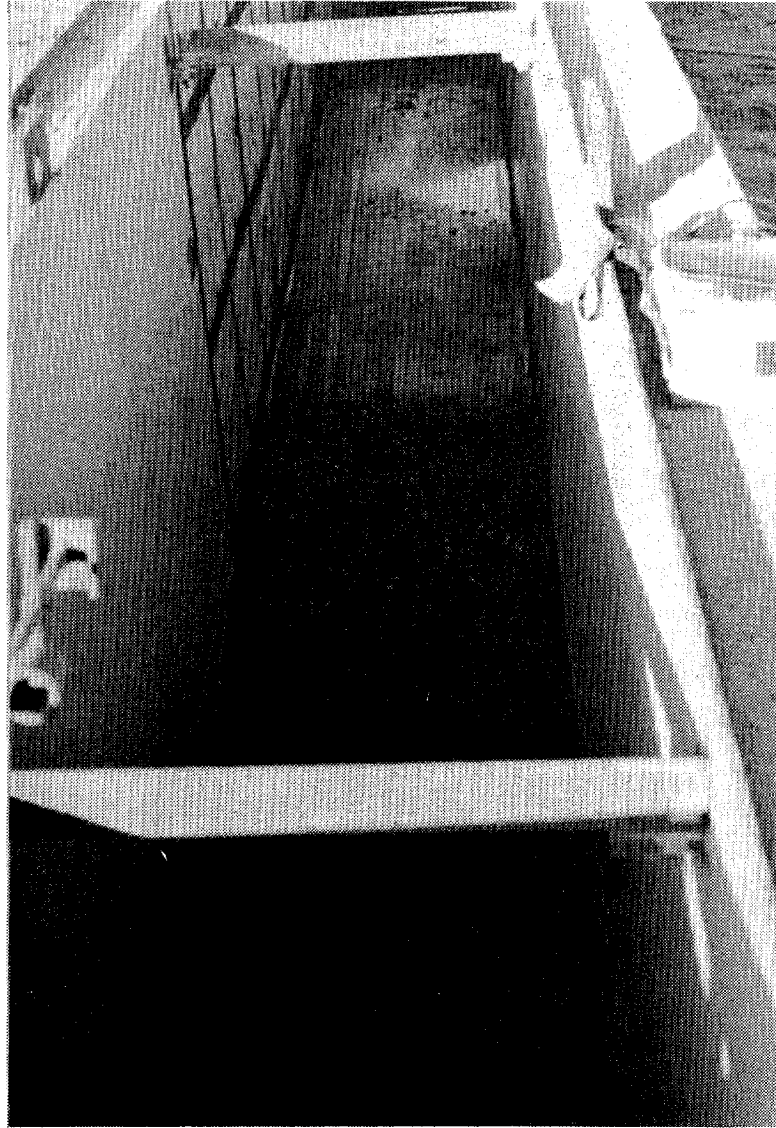
Figure 12. Illustration of a paved roadway test section.
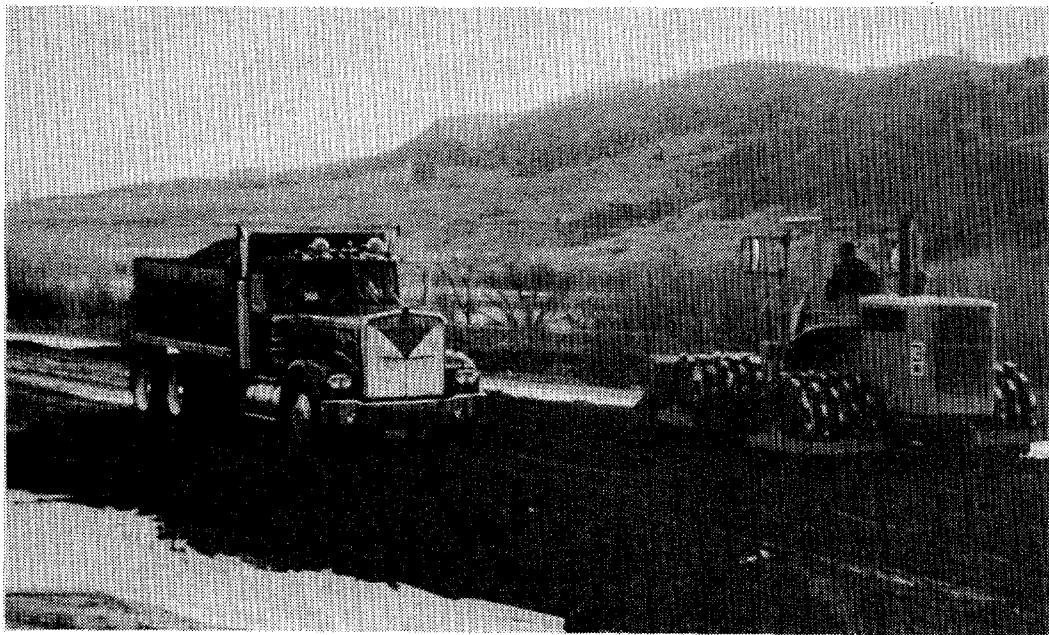
Figure 13. Construction of full-scale embankment.
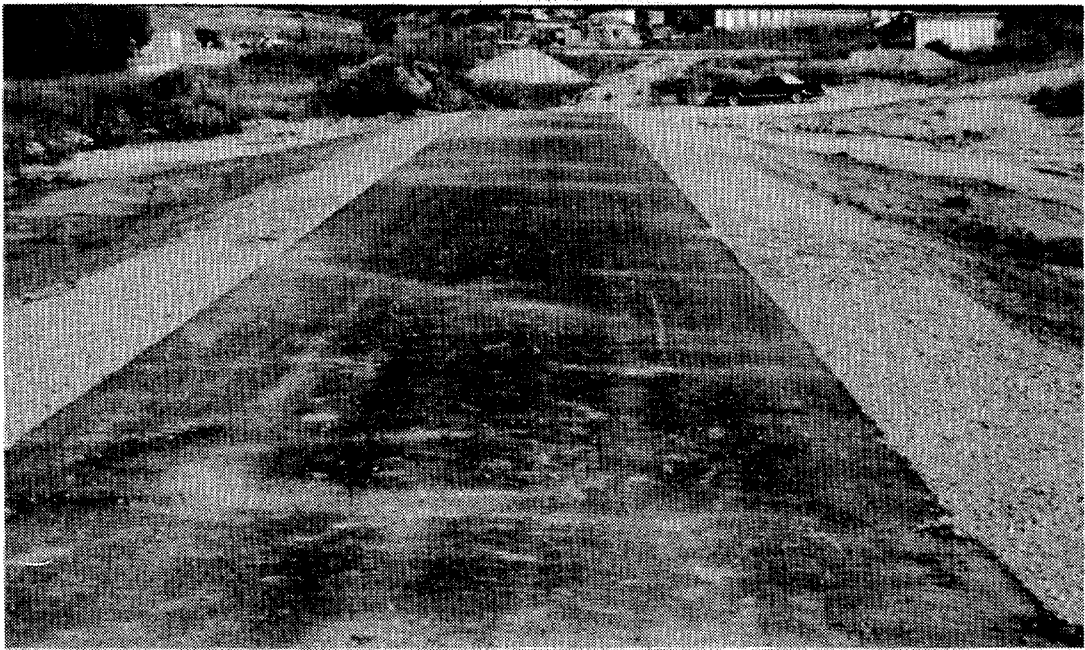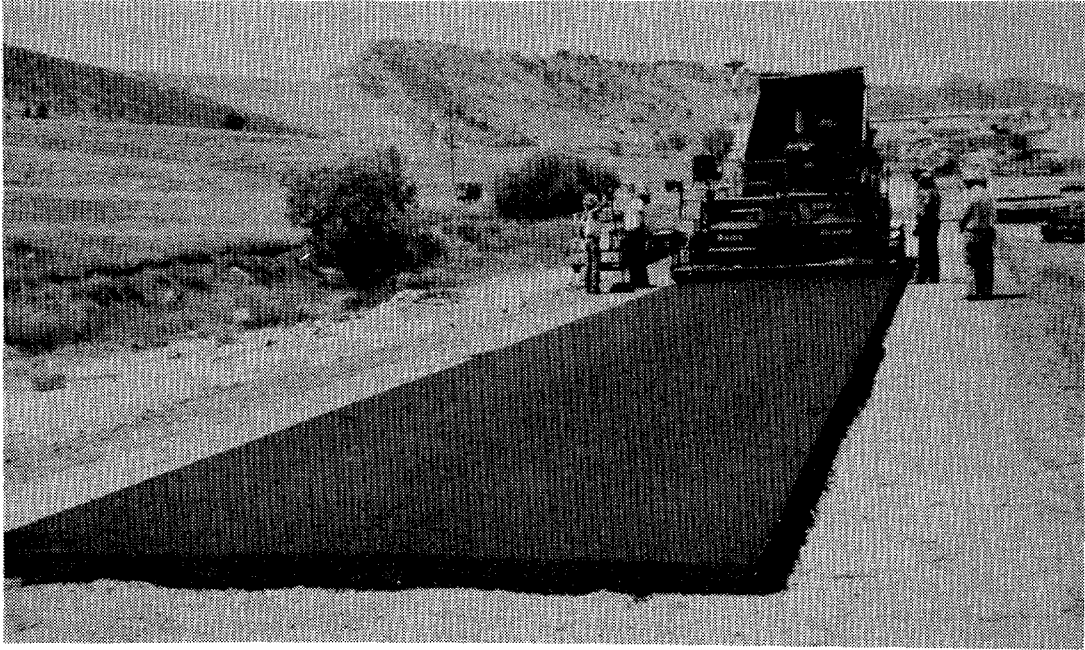
Figure 13. Construction of full-scale embankment (continued).

Table 7. Seed mixture.

Common Name	Lb/Ac[1]
Western Wheatgrass	7.0
Fairway Wheatgrass	5.0
Smooth Brome	4.5
Buffalo Grass	4.0
White Dutch Clover	1.0
	21.5

[1] Lb/Ac of live seed commonly abbreviated Pls/Ac.

tailwater control section were attached to the flume walls and the recirculating piping system was attached. Excess fill material was backfilled and compacted along the outside of the flume walls to minimize the bowing of the flume walls during the test. Bentonite gravel chips were obtained from a manufacturer in Casper, Wyoming, and placed along the flume walls next to the embankment test section. Mixing the bentonite with water allowed the bentonite mixture to swell and seal the void between the flume walls and the embankment. This procedure minimized the loss of water through the embankment test section when the flume was moved.

Several embankment protection measures were also tested. Included in the testing schedule were gabion mattresses, soil cement, geoweb, and enkamat. Testing the embankment protection measures did not necessitate movement of the flume; consequently, the procedures for construction of the soil embankment within the flume were followed.

The gabion mattresses were constructed to be 3 ft (0.9 m) wide, 8 ft (2.4 m) long, and 6 inches (152 mm) in depth. The wire mattresses, made from 19 gauge wire, were filled with 3- to 6-inch (76- to 152-mm) rock and placed on the top of the embankment and downstream sideslope. The mattresses were double wire wrapped at each mattress seam and single wire wrapped along each side of the mattress. A Dupont Typar 3401 nonwoven filter fabric was placed and pinned beneath the gabion mattresses. Figure 14 presents a cross-sectional view of the embankment protected by gabion mattresses. A view of the gabion mattresses within the flume is provided in figure 15.

The erosion protection afforded by soil cement was tested by placing a layer, 1 foot thick, along the top of the embankment and downstream sideslope (see figure 16). The soil cement was commercially produced by a local ready-mix contractor and delivered to the testing site. The specifications for the soil cement called for a cement content by weight of approximately 11 percent and a moisture content of approximately 10 percent. Plaster sand composed the remaining additive to the soil cement mixture. The test section protected by soil cement is depicted in figure 17.
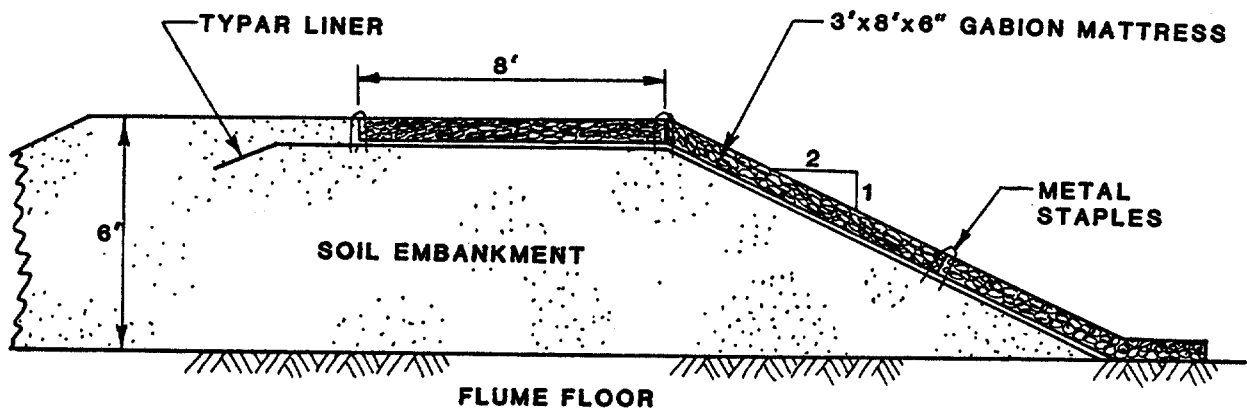
Figure 14. Cross- sectional view of gabion protection measure.
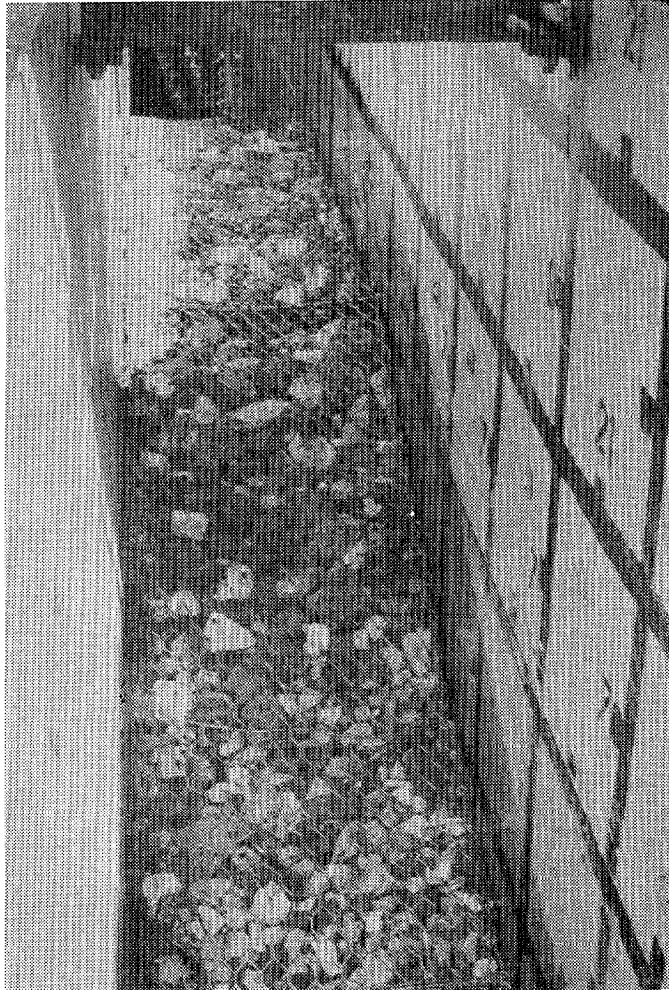
Figure 15. Illustration of mattress-protected embankment.
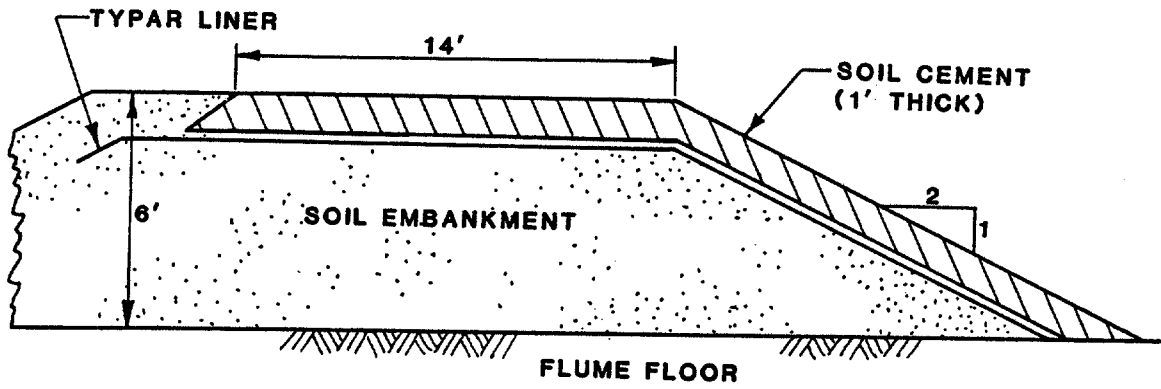
Figure 16. Cross-sectional view of soil cement protection measure.

41

Figure 17. Illustration of soil-cement protected embankment.

Geoweb is a grid confinement system made of high-density polyethylene. The geoweb system has been utilized for erosion control along lake shores and river banks, and for controlling embankment washouts due to surface water runoff. A standard geoweb section expands to a section 8 ft (2.4 m) wide and 20 ft (6.1 m) long and is 8 inches (203 mm) in depth. The nominal thickness of each grid wall is 0.047 inch (1.2 mm). For this study, the geoweb system was placed along the top of the embankment and downstream sideslopes in the manner indicated by figure 18. Wooden stakes, recommended by the manufacturer of geoweb, were initially utilized to secure the geoweb to the embankment. The individual grids or cells were filled with 1- to 2-inch (25- to 51-mm) rock. As with the gabion mattresses, a Dupont Typar 3401 nonwoven filter fabric was placed and pinned beneath the geoweb system. Figure 19 depicts the embankment protected by geoweb.

The final erosion protection measure tested was enkamat. Enkamat is a matting made from heavy nylon monofilaments fused at their intersections. The thickness of the tested material was 9 mm. During this study, the primary purpose of enkamat was to function as a permanent turf reinforcement. Previous applications have included the successful stabilization of natural and artificial embankments, steep excavated slopes, bridge and viaduct aprons, and drainage ditches. The enkamat was utilized in conjunction with a vegetated slope during the conduct of the testing program. On a 6-ft (1.8-m) wide section of the roadway embankment, enkamat was placed along the downstream shoulder and sideslope. Enkamat was installed with the peaked side down and the sections were overlapped by 3 inches (76 mm) and pinned with metal stakes every 3 ft (0.9 m). The upstream edge was buried not less than 12 inches (0.3 m). Figure 20 presents the cross-sectional view of the enkamat after installation. The entire embankment protected by enkamat was covered with 1 to 2 inches (25 to 51 mm) of soil and seeded with the grass mixture previously described. In addition to the installation of enkamat on the roadway embank-
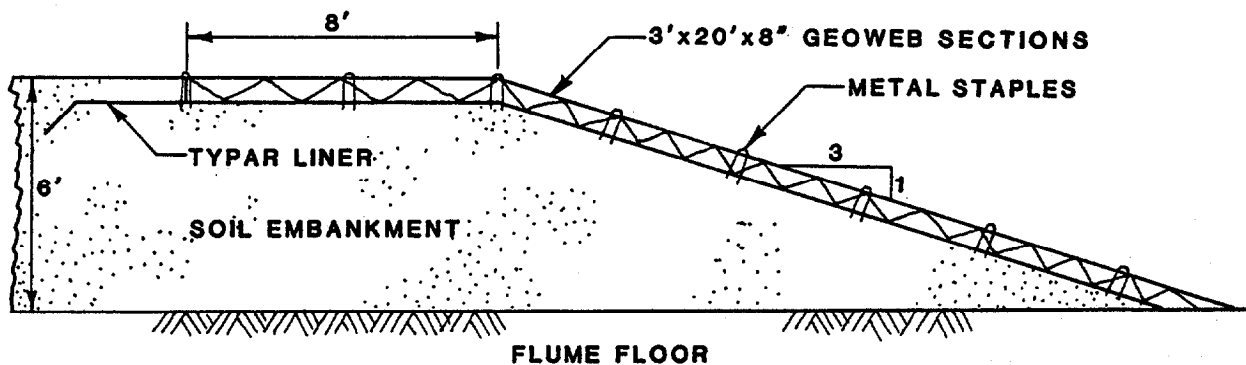
Figure 18. Cross-sectional view of geoweb protection measure.
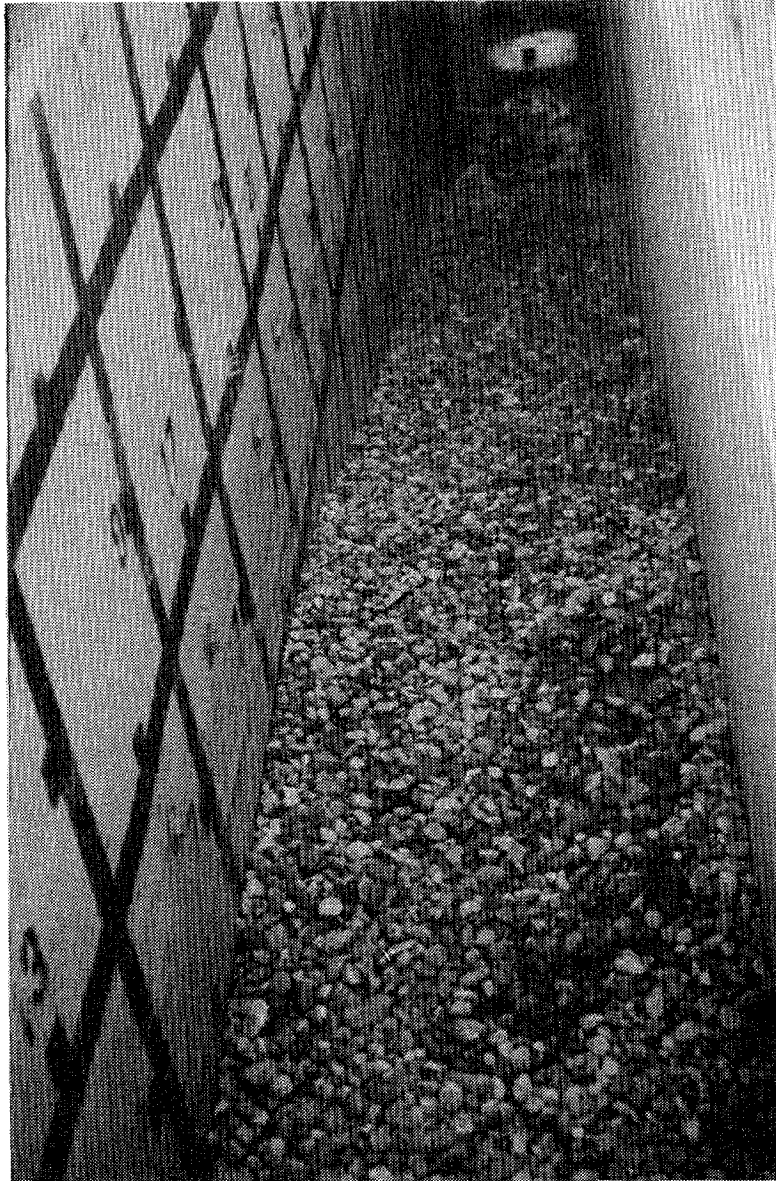
Figure 19. Illustration of geoweb-protected embankment.
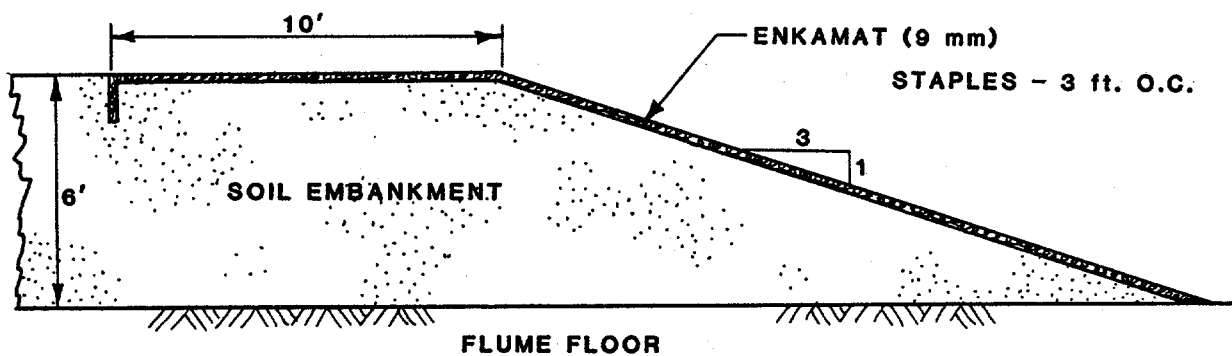
Figure 20. Cross-sectional view of enkamat protection measure.

ment, a separate section of level ground was isolated for placing the enkamat. In this instance, the enkamat material was placed in four adjacent strips with each strip overlapped by 3 inches (76 mm). The enkamat was covered with 1 to 2 inches (25 to 51 mm) of soil and seeded with the grass mixture. For this application and testing of enkamat, the material was cut and rolled after vegetation was established. The enkamat/vegetation material was placed on the soil embankment and pinned by metal stakes. Figure 21 provides an illustration of the enkamat material prior to testing.

5.   Embankment Test Program

Following the fabrication of the modeling facility and all construction at the testing site, rigid bed embankment tests were conducted to verify the hydraulics of the flow as described in section 2. Once completed, the hydraulic testing of the soil embankments was initiated. The flood overtopping tests included testing a variety of side slopes, overtopping depths, water-surface drops, overtopping durations, road surfaces, and embankment protection measures. The schedule of tests completed during this study is presented on table 8. Test data are presented in appendix B.

An integral part of the study involved the simulation of different tailwater conditions. The tailwater conditions were dictated by the overtopping depth and water-surface drop over the embankment. During the flood overtopping tests, a free-flow condition was simulated along with two levels of submerged flow. The purpose of testing different combinations of tailwater depth was to determine the impact of tailwater depth upon the location and magnitude of embankment erosion. Figure 22 provides an illustration of a high tailwater and a free-fall condition simulated during the testing program.

Tailwater conditions also influenced the discharge required to obtain the overtopping depth dictated by the test schedule. Testing a wide range of overtopping depths and consequently, discharges, allowed for assessing the relationship between discharge and erosion rate. The relationship between
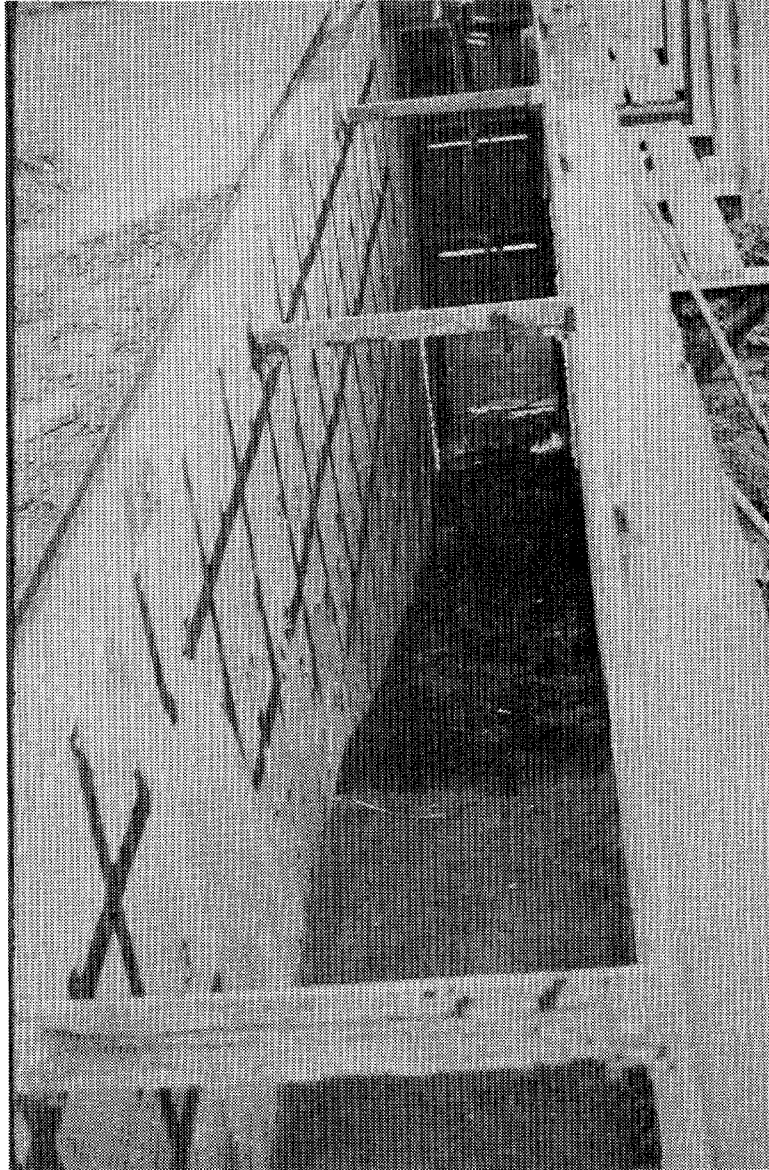
Figure 21. Illustration of enkamat-protected embankment.

48

Table 8. Schedule of tests.

Series	Description of Test	Soil Type	Slideslope	Overtopping Depth, ft (D_{ot})	Water Surface Drop Over Embankment (percent of D_{ot})	Testing Duration (hr)
FHWA I	Bare-Soil Surface; No Protection	I	3:1	0.5, 1, 2, 4	20, 70, Free Fall (FF)	1, 4, 10, 20
FHWA II	Bare-Soil Surface; No Protection	II	3:1	0.5, 1, 2, 4	70	1, 4, 10, 20
FHWA III	Paved Surface/ Gravel Shoulder; No Protection	II	3:1	0.5, 1, 2, 4	70	1, 4, 10, 20
FHWA IV	Paved Surface/ Gravel Shoulder; Grass	I	3:1	0.5, 2, 4	FF	1, 4, 10
FHWA V	Paved Surface/ Gravel Shoulder Grass	I	3:1	0.5, 2	70	1, 4, 10
USFS I	Bare-Soil Surface; Enkamat	II	3:1	0.5, 2	FF	1, 4, 10
USFS II	Bare-Soil Surface; Geoweb	II	3:1	1, 2, 4	FF	2
USFS III	Bare-Soil Surface; Enkamat/Grass	II	3:1	0.5, 1, 2, 4	FF	2
USFS IV	Bare-Soil Surface; Gabion Mattress	II	2:1	1, 2, 4	FF	2
USFS V	Bare-Soil Surface; Soil Cement	II	2:1	1, 2, 4	FF	2

49
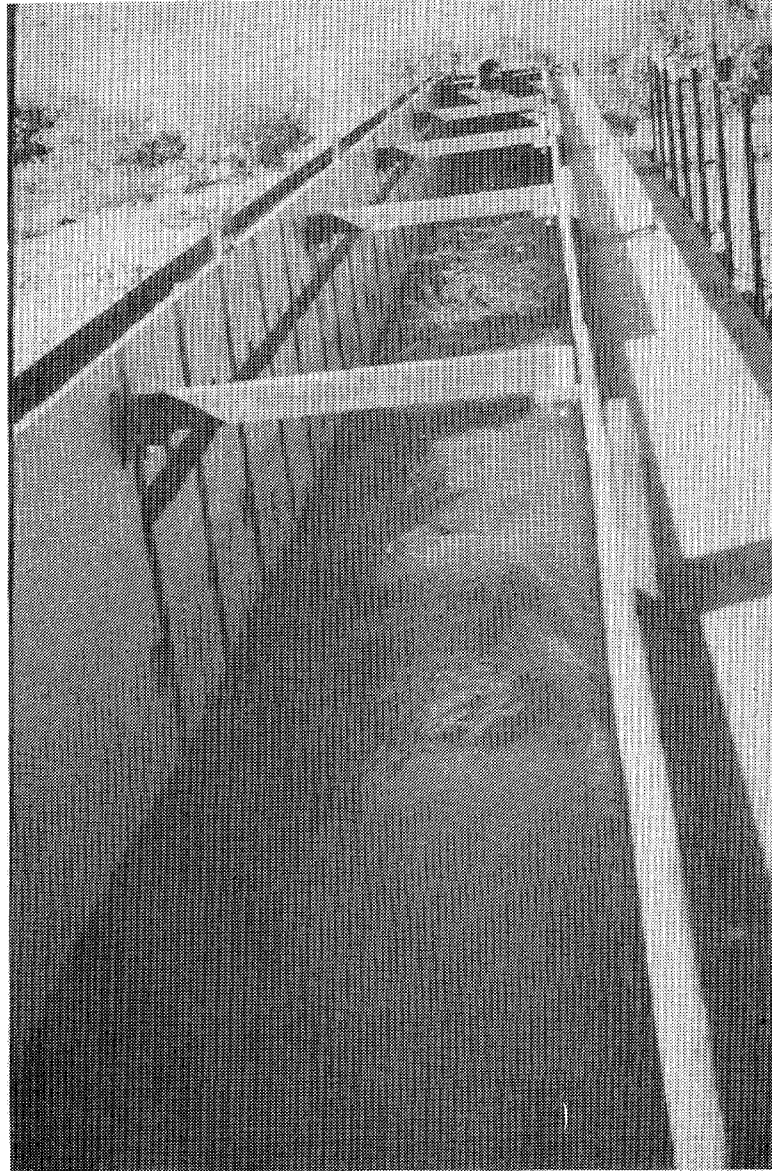
Figure 22. Illustration of embankment tests under high
tailwater and freefall conditions.
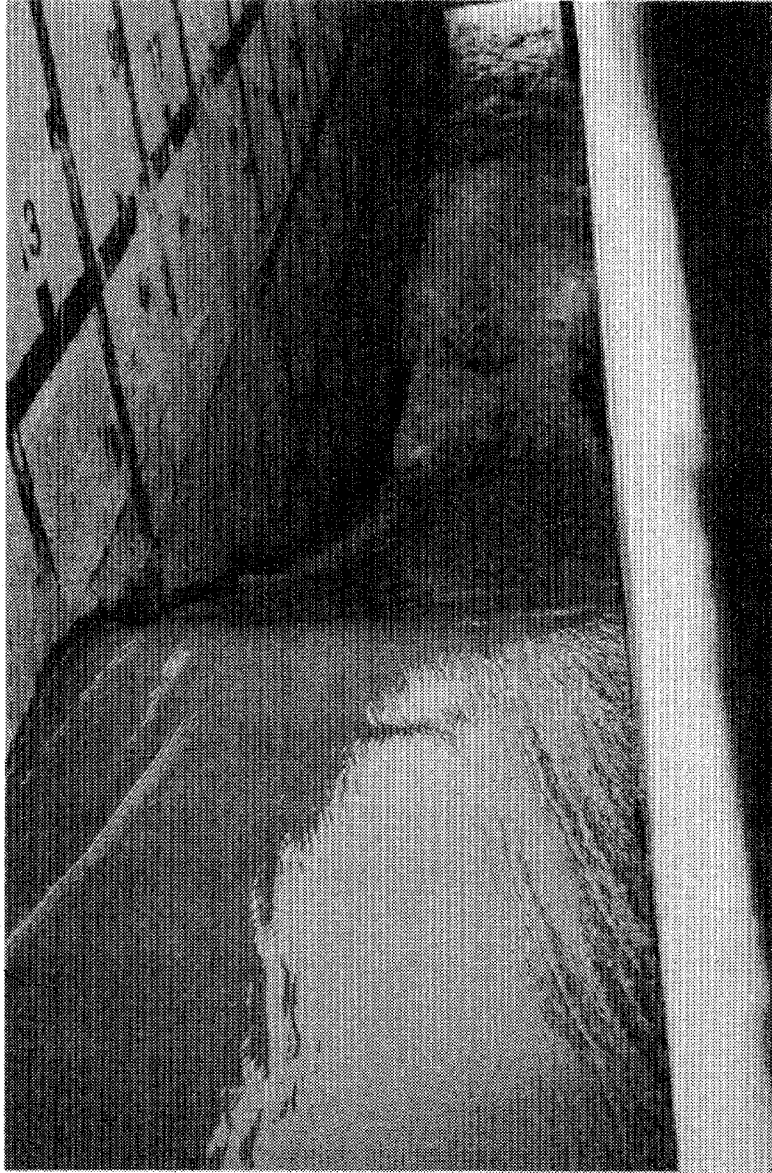
Figure 22. (continued)

51

tailwater depth, overtopping depth, and discharge varies depending upon the flow conditions, (i.e., submerged flow versus free flow). This relationship is explained in detail in "Hydraulics of Flow Over an Embankment."

The duration of the flood overtopping tests ranged from 1 hour to 20 hours. By systematically increasing the overtopping duration, the significance of overtopping duration and its impact on the magnitude and rate of erosion of the embankment or embankment protection measure could be ascertained.

Two series of tests were conducted over bare soil embankments. The information gained from these tests provided a basis for judging the erosion protection afforded by pavement, vegetation, and the other embankment protection measures.

As indicated by table 8, the embankment test program included fixed-flume tests and tests which necessitated the movement of the flume. In every instance, the movement of the flume coincided with tests conducted over slopes vegetated with grass. The test procedures followed in accomplishing the tests presented in table 8 are described in the following section.

a. Test Procedures

Essential to the embankment testing program was the development of a consistent and accurate testing procedure. Knowledge gained from the rigid embankment tests provided insight into the development of a procedure for establishing the appropriate flow conditions while minimizing the initial disturbance to the embankment. The testing procedure developed as part of this study consisted of four steps: filling, flow establishment, running the test, and draining. A detailed description of the four steps follows:

1. Filling: To initiate a test run, water was slowly fed into the flume through the upstream manifold. Except for zero tailwater cases, part of the water entered the downstream side of the embankment through a bypass. In this way, water at both sides of the embankment slowly raised to the same level. The initial disturbance in the embankment was a minimum. This filling was completed when the tailwater reached the desired level.

52

2. Flow Establishment: After the desired tailwater level had been reached, the water discharge was increased at a moderate rate to establish the desired discharge. Simultaneously, the tailwater-control device was adjusted to maintain the desired tailwater level. The flow establishment was not conducted quickly or initial surge damage would result, nor was it conducted too slowly or significant erosion would occur before the actual run.

3. Running: Once the flow was established, the discharge and tailwater levels were maintained throughout the duration of the run. If the erosion was so severe that the embankment was washed out before the test was completed, the run was stopped. The run was also stopped if failure of the protection measure was evident.

4. Draining: Immediately upon the completion of the run, the water discharge was stopped. The water remaining in both sides of the embankment was slowly drained, resulting in minimum disturbance to the postrun embankment.

A sequence of photographs illustrating the testing of various types of embankments and embankment protection measures is provided in appendix A.

b. Data Collection and Analysis

The data collected during each test included discharge, velocity, overtopping depth, water-surface profile, and embankment profile. The discharge for the test was measured by means of a calibrated flow meter and manometer tube. The overtopping depth was established by utilizing a staff gauge mounted to the flume wall. After the overtopping depth was set and the appropriate tailwater conditions established, the discharge was measured. The carriage mounted on top of the flume facilitated the measurement of the water surface elevation, velocity of flow, and bed elevation. Bed and water surface elevation measurements were taken at intervals of 2 ft (0.6 m) beginning with the upstream shoulder of the embankment. Flow velocity was measured once along the top of the embankment and at 3-ft (0.9-m) intervals from the downstream embankment shoulder. Still photographs of all tests were taken to assist in documenting the test condition and results.

The field data and laboratory test data collected in this study were analyzed to determine the hydraulic condition associated with embankment overtopping flow. This information was applied to erosion equations to facilitate the development of a methodology for quantitatively determining embankment damage due to flood overtopping and to assess effects of various protective measures. Specifically the following analyses were made:

- The fixed-bed embankment test data summarized in table 3 were analyzed to determine hydraulic conditions of overtopping flow including flow mode, discharge coefficients, local velocity, and shear stress immediately above embankment surface. A mathematical model was developed to determine the hydraulic conditions of overtopping flow and was verified using the test data. These hydraulic parameters are important factors affecting the flood conditions and embankment damage. The results of analysis are presented in "Hydraulics of Flow Over an Embankment."

- Data collected during FHWA test series I and II tests (refer to table 8) were analyzed to (1) determine the erosion patterns and critical shear stress of bare soil, (2) evaluate applicability of existing soil erosion equations, and (3) establish soil erosion equations that can be utilized to determine the rate of embankment soil erosion as a function of soil characteristics and hydraulics of overtopping flow. The results of analysis are presented in "Parameters and Equations Governing Erosion of Embankment."

- A mathematical model was developed by incorporating the erosion equations established in step two into the mathematical model developed in step one to determine embankment damage rate due to flood overtopping. This model was calibrated using the bare soil test results (FHWA test series I and II). The effects of pavement and grass were assessed by comparing the results of tests with and without pavement/grass (FHWA test series III, IV, and V with FHWA test series I, and II). The model was then applied to develop a set of nomographs for estimating embankment damages considering various flood conditions and embankment characteristics. These nomographs were verified using the field data described in "Collection of Field Embankment Damage Data." The results of analysis are presented in "Development of a Procedure for Determining Embankment Erosion Due to Flood Overtopping."

- Based on the results of USFS test series I to V, the effects of various protective measures on embankment stability were assessed. The critical conditions that would initiate the failure of these protective measures were determined and are discussed in "Evaluation of Embankment Protection Measures."

HYDRAULICS OF FLOW OVER AN EMBANKMENT

1. Flow Patterns

An understanding of the hydraulics of water flowing over an embankment provides a basis for understanding the erosion process. Several studies have been conducted in the past concerning this topic.[3,4,5] Perhaps the most comprehensive material is found in the USGS water supply paper by Kindsvater.[4] The purpose of his study was to determine the discharge characteristics of embankment-shaped weirs so the USGS could make more accurate estimates of flood discharges. The observations of laboratory tests are useful in understanding this phenomenon. Various flow patterns have been observed as water flows over an embankment. These flow patterns were classified in Kindsvater[4] as (1) free-plunging flow, (2) free surface flow, and (3) submerged flow.

For the low-tailwater condition known as free flow, critical flow control occurs on the roadway, and the discharge is determined by the upstream head. At higher tailwater levels, when the depth of flow over the roadway is greater than the critical depth, the discharge is controlled by the tailwater as well as the headwater. Under conditions of tailwater control, the flow is said to be submerged. With a rising tailwater level, the change from free flow to submerged flow occurs rather abruptly. The flow pattern antecedent to the change is described as incipient submergence.

Free flow is subclassified into plunging flow and surface flow. Plunging flow occurs when the jet plunges under the tailwater surface, producing a submerged hydraulic jump on the downstream slope. Surface flow occurs when the jet separates from the roadway surface at the downstream shoulder and "rides" over the tailwater surface. Whereas free flow can be either a plunging or a surface flow, submerged flow is always a surface flow.

The free-flow transition range is the range of tailwater levels within which a given discharge can produce either a plunging flow or a surface flow, depending on the antecedent conditions. Thus, if the tailwater is initially low and the flow plunging, this pattern persists as the tailwater level rises until it reaches the upper limit of the transition range, whereupon the plunging flow changes abruptly to a surface flow. However, if the tailwater is initially high and the flow is a surface flow, this pattern persists as the tailwater drops until it reaches the lower limit of the transition range, whereupon the flow pattern changes abruptly to plunging flow. The stability or persistence of the flow patterns within the transition range is related to the inertia of the large, horizontal-axis rollers which occur on the downstream side of the embankment.

The tailwater level limits of the transition range were recorded for all the models investigated by Kindsvater.[4] These transition range data are significant in the description of the characteristic flow pattern. Also these data are useful in determining the safety of the structure against destructive erosion. This conclusion is based on the observation that surface flows are doubtless less erosive than plunging flows.

Kindsvater[4] presented charts for determining flow patterns over embankments. Figure 23 defines variables utilized in the charts and figure 24 summarizes the limits of the incipient submergence and free-flow transition ranges for screen-wire roughness surface. Figure 24 can be utilized to determine the patterns of flow overtopping an embankment and ultimately provides a good indicator of embankment erosion patterns.

Figure 24 was checked using the data collected from fixed-bed embankment tests and evaluated to determine its applicability for large-scale embankments. The test results are also plotted on figure 24. These results indicate that figure 24 is applicable to determine the transition range between surface and plunging flow for large-scale embankments.
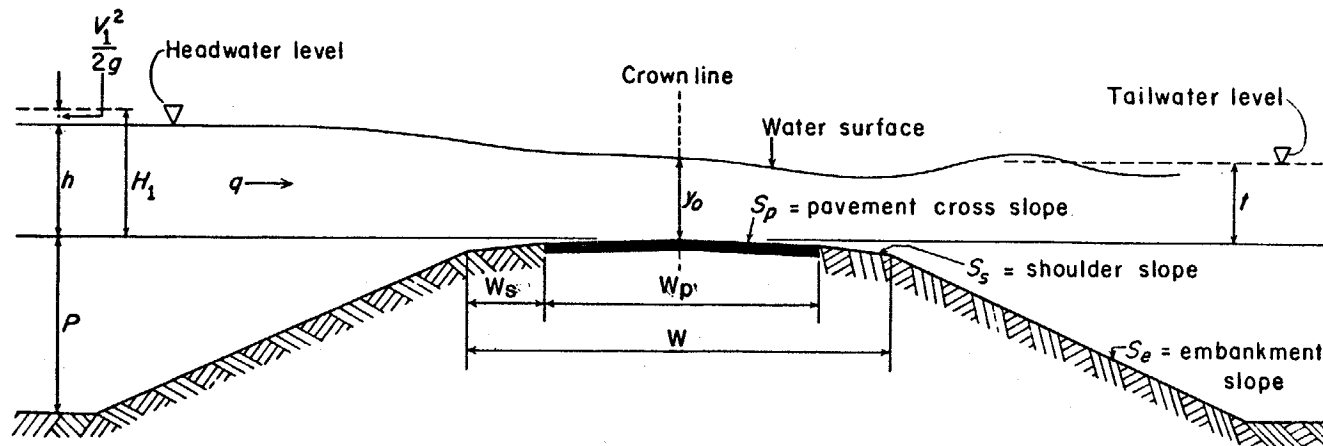
Figure 23. Principal variables needed to describe flow over an embankment.
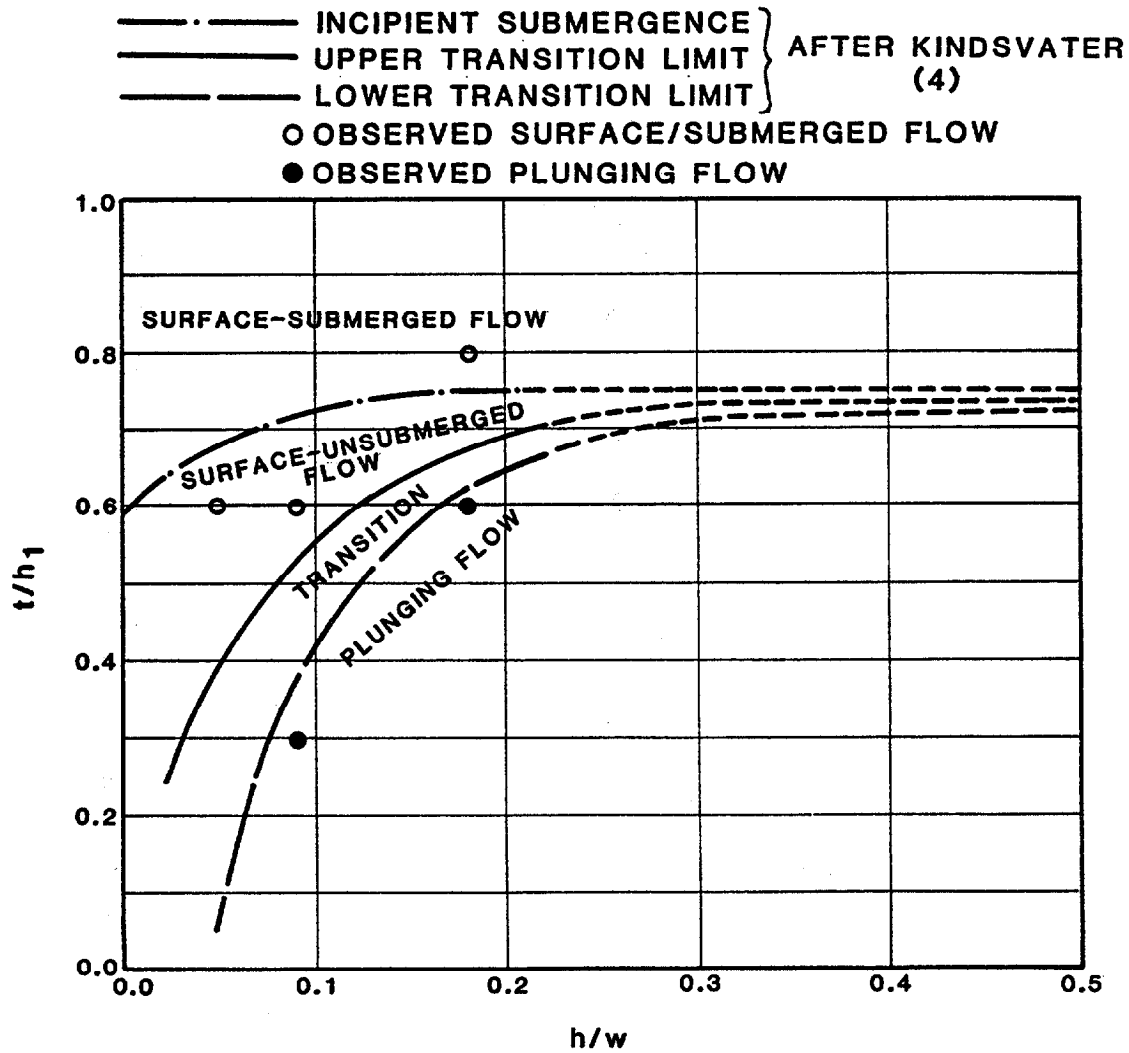
Figure 24. Summary of incipient submergence
and free flow transition ranges.

58

2. Discharge Equations for Flow Over an Embankment

The generally accepted form of the equation that computes discharge over an embankment for the free flow condition is

$$q = C H_1^{3/2} \qquad (1)$$

where q is the discharge per unit width, C is a coefficient that has been determined experimentally by a number of laboratory tests, and H_1 is the total head above the embankment crest as defined in figure 23. Using Kindsvater's data for a smooth roadway surface, Bradley[5] presented figure 25 to determine discharge coefficient. To determine the discharge flowing over a roadway, first enter curve B (figure 25) with H_1/W and obtain the free-flow coefficient of discharge C. Should the value of H_1/W be less than 0.15, it is suggested that C be read from curve A of the same figure. If submergence is present (i.e., if t/H_1 is larger than 0.7), enter curve C with the proper value of submergence in percent and read off the submergence factor C_s/C. The resulting discharge is obtained by substituting values in the expression:

$$Q = C L H^{3/2} \frac{C_s}{C} \qquad (2)$$

where L represents the length of inundated roadway, H_1 is the total upstream head measured above the crown of the roadway, and C and C_s are coefficients of discharge for free flow and with submergence, respectively. Where the depth of flow varies along the roadway, it is advisable to divide the inundated portion into reaches and compute the discharge over each reach separately. The process, of course, can be reversed to aid in determining backwater for a combination of bridge and roadway configurations.

Based on experimental results, it was found that the embankment side slope is insignificant in its effect on the flow except perhaps for the effect

59
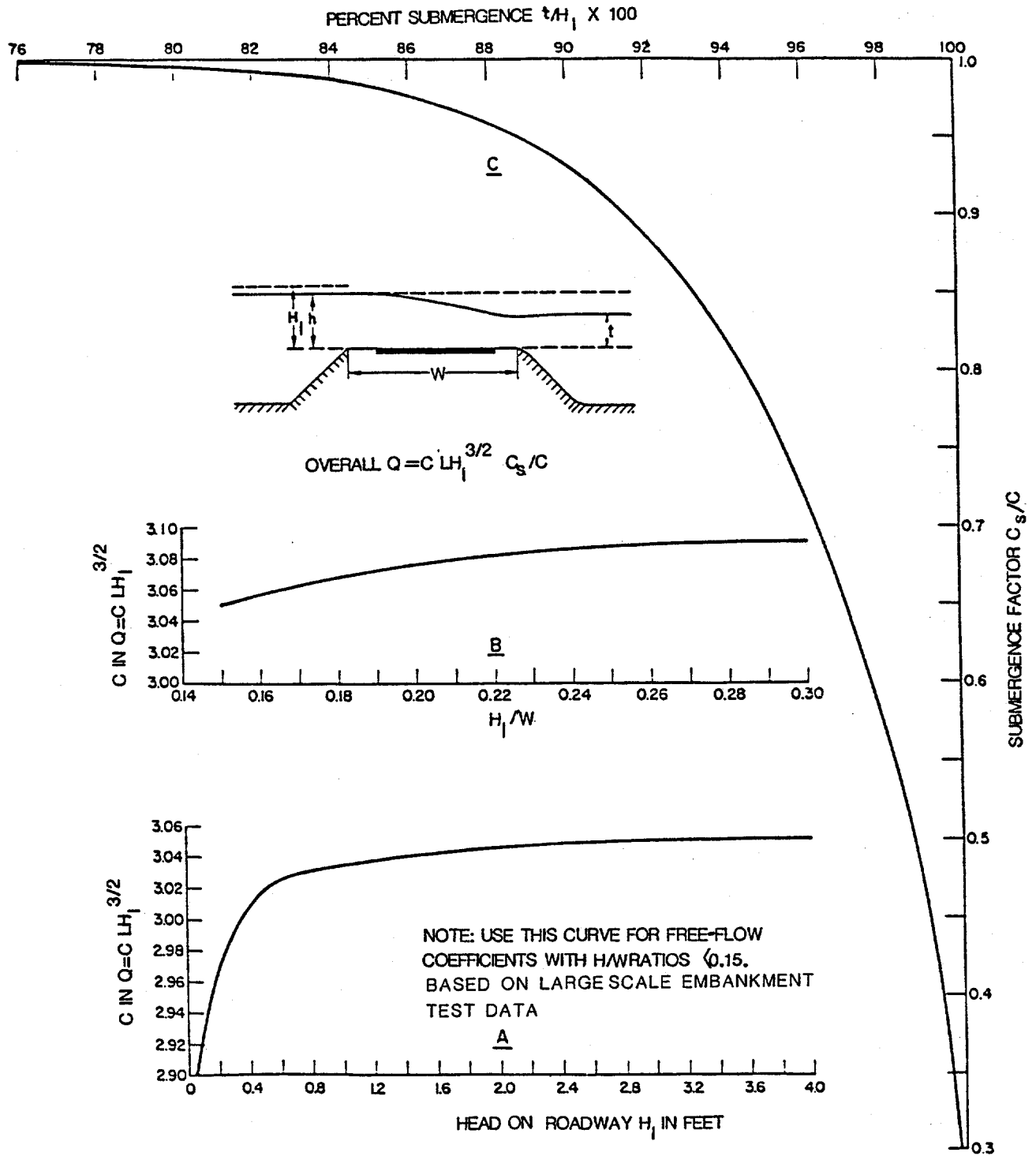
Figure 25. Discharge coefficients for flow over roadway embankment (after Bradley[5]).

on rolling waves on the downstream side. For the free-flow case, variation in embankment height, pavement, cross slope and shoulder slope do not affect the hydraulic conditions of flow on the embankment crest.

3. Method of Determining Hydraulic Variables

The physical processes governing the embankment erosion are closely related to flow-induced local velocity and effective shear stress adjacent to the embankment surface. At present, all of the hydraulic equations that have been presented relate the discharge to the head and tailwater conditions. No equations to determine the nonuniform velocity field and shear stress distribution over the embankment have been developed. All of these variables are highly nonuniform in this rapidly varied flow condition. Another complicating factor is the change of hydraulic conditions over time as erosion of embankment occurs. The experimental program conducted in this study provided useful data to evaluate these governing factors.

A concrete-bed embankment model was tested in this study. The flow conditions overtopping the embankment included:

- Overtopping depth, h = 0.5, 1, 2, and 4 ft.

- Tailwater drop, $(h-t)/h$ = 0.1, 0.2, 0.4, and 0.75 and free-fall conditions.

The data collected included water-surface profiles and velocity at selected stations as shown on figure 26. The flow conditions were summarized in table 3. These data were analyzed to determine velocity and shear stress of flow overtopping an embankment.

During the rigid embankment tests, the overtopping flow was either surface flow or plunging flow, depending on the tailwater conditions. This flow mode can be determined from figure 24 as a function of h/W and t/H_1. Examination of velocity data indicates that for surface flow the velocity over

61

WATER SURFACE DROP (%) = $\dfrac{DoT - t}{DoT}$ x 100

STA.	1	2	3	4	5	6
X	10	21	24	27	29	33

Figure 26.   Locations of measuring stations.

the downstream slope surface would be in reversed direction (e.g., figure 27). Its magnitude would be relatively constant down the slope, and generally less than the depth-averaged velocity. Therefore the actual embankment erosion would generally be less than the computed erosion if the average velocity was utilized for this determination. Examination of the rigid embankment test data as shown in figure 28 yields:

$$V_r = -0.15 \, V_u \tag{3}$$

where V_r is the flow velocity over the downstream slope surface and V_u is the average velocity at the upper edge of slope (station 2 on figure 26).

For plunging flow the velocity over the downstream slope surface would generally be larger than the depth-averaged velocity for with-tailwater condition and would be the same as the depth-averaged velocity for free-fall condition (e.g., figure 29). The following relation as shown in figure 30 was developed for plunging flow with tailwater condition.

$$V_r = 0.55 \, V_{uj} \tag{4}$$

where V_{uj} is the averaged flow velocity immediately upstream of a hydraulic jump, found by iteration in the computer program.

For plunging flow with no appreciable tailwater, the representative velocity v_r would be the average flow velocities at each grid point obtained from the standard step solution:

$$v_r = v_i \tag{5}$$

where v_i is the average velocity at a point i on the embankment.
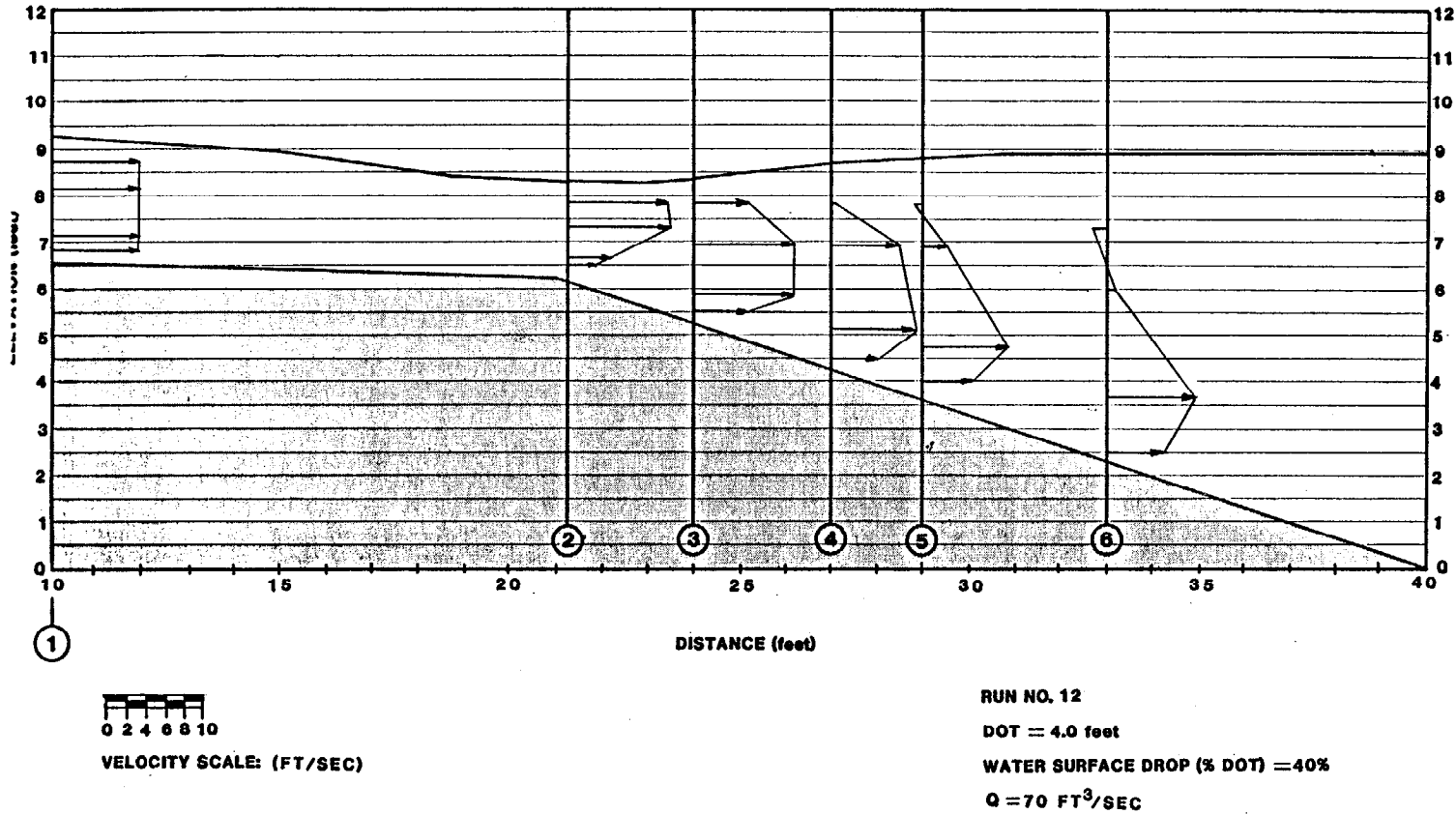
Figure 27. Water-surface and velocity profiles.
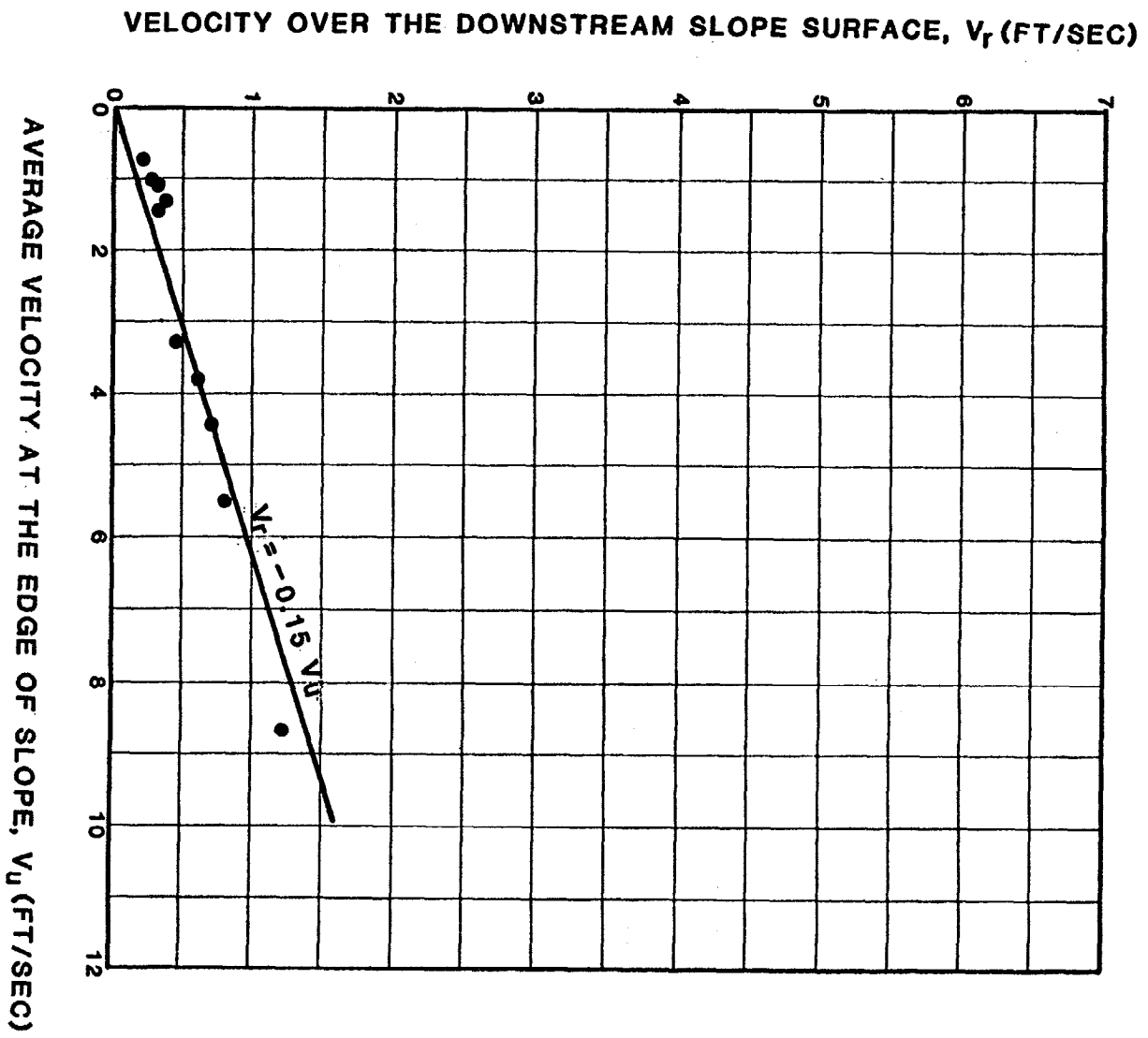
Figure 28. Downstream slope surface velocity for surface flow.

65
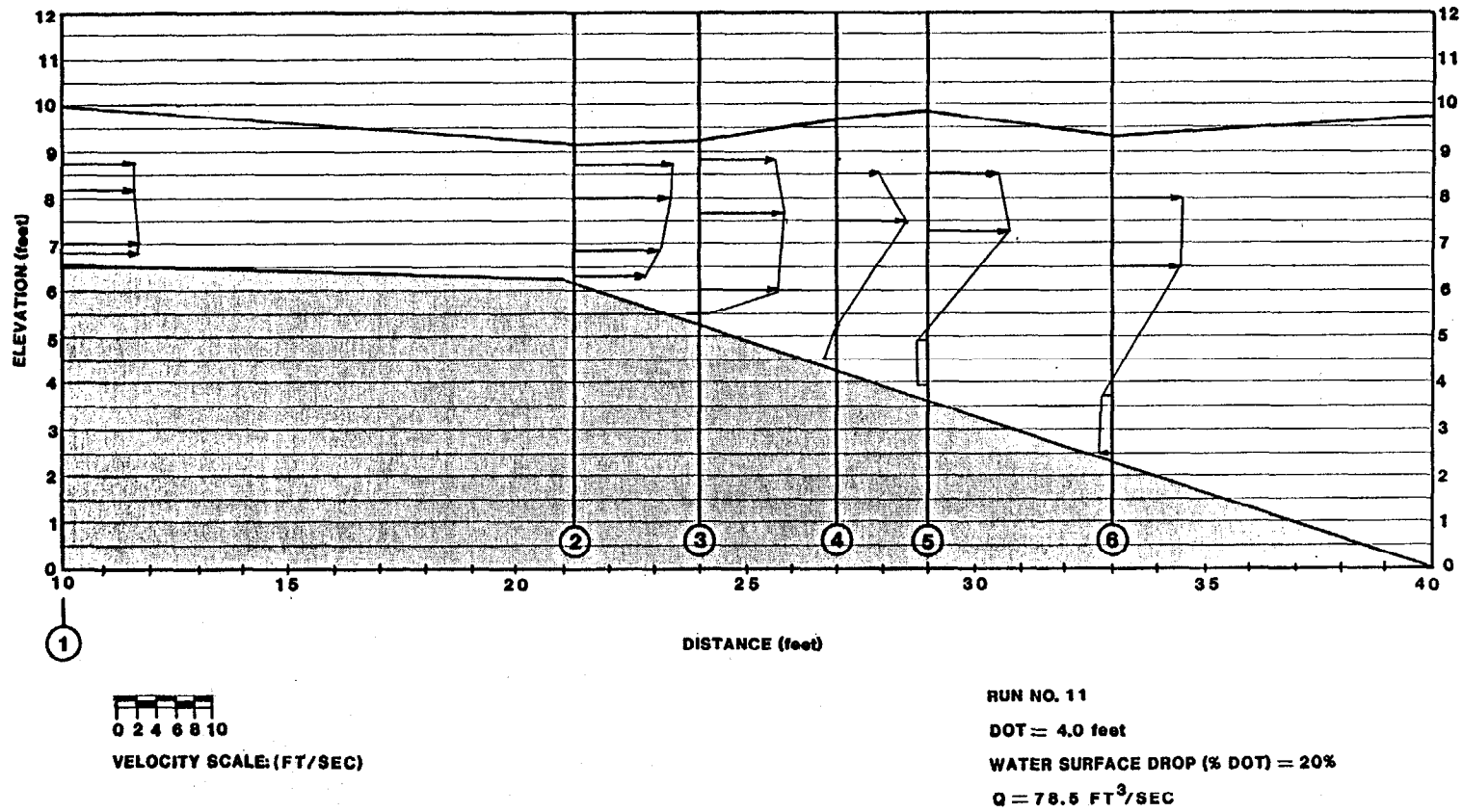
Figure 29. Water-surface and velocity profiles.

99

VELOCITY OVER THE DOWNSTREAM SLOPE SURFACE, V_r (FT/SEC)

AVERAGE VELOCITY IMMEDIATELY UPSTREAM
OF A HYDRAULIC JUMP, V_{uj} (FT/SEC)

$V_r = 0.55V_{uj}$
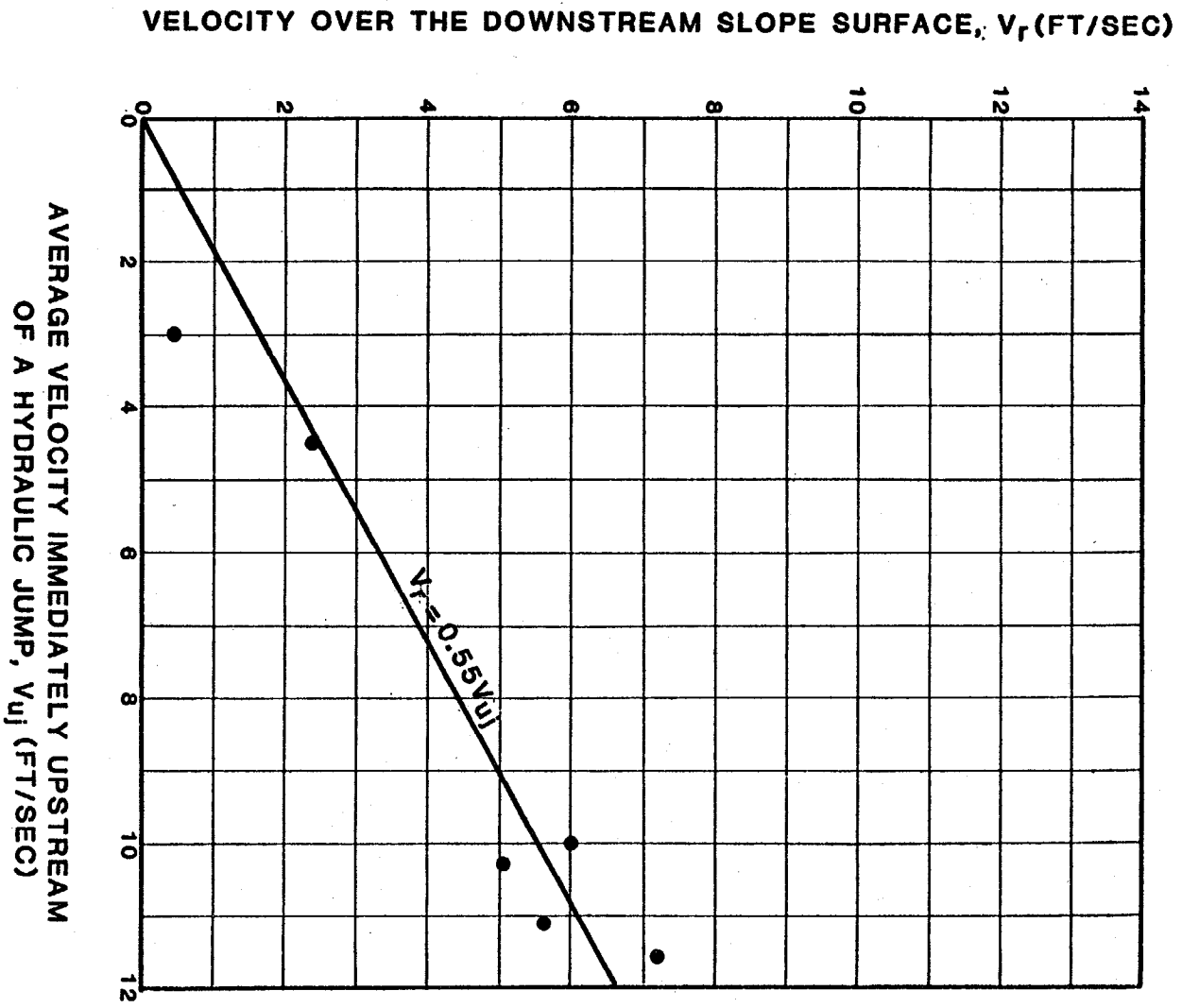
Figure 30. Downstream slope surface velocity for plunging
flow with tailwater.

67

The local shear stress can be related to local velocity by:

$$\tau = \frac{1}{8} f \rho V_r^2 \qquad\qquad (6)$$

where f is the Darcy-Weisbach coefficient, ρ is the water density, and V_r is a local reference velocity equal to depth-averaged velocity over the embankment crest and upstream slope, or equal to that determined from equations 3 or 4 for the downstream slope.

A computer model was developed to determine water-surface profile, velocity and shear stress of the embankment overtopping flow by solving the momentum equation and incorporating the following embankment hydraulic relations:

- Discharge coefficient, figure 25.

- Flow mode, figure 24.

- Hydraulic jump relations, Chow.[6]

- Velocity and shear stress relations,(equations 3 to 6).

Figure 31 shows a flow chart of this computer model. Steps 2, 13, and 14 are not required for determining flow conditions over rigid embankments, but are needed for determining embankment erosion due to flood overtopping. Detailed explanation of these computational steps will be given in "Development of a Procedure for Determining Embankment Erosion Due to Flood Overtopping."

The major steps for hydraulic computations are explained below:

Step 1. Divide the modeled embankment into computational sections. The geometry is then input as (x,z) pairs. Manning's n is input for each computational section. Figure 32 shows an example.

Step 2. Input embankment soil/structure coordinates and erosion equations (not used for rigid-bed version of model).

1. Input the embankment cross-section shape and Manning's n

2. Input embankment soil/structure characteristics and erosion equations

3. Input the hydrographs of headwater and tailwater

4.   J = 0

5. Determine the bed slope at each section

6. Determine overtopping discharge using figure 25

7. Compute critical depth and critical slope

8. Determine the control section, IC, using singular point method (Chow)

9. Compute water-surface profile upstream of the control section by solving momentum equation

10. Computer water-surface profile downstream of the control section by solving momentum equation

11. Compute jump condition considering tailwater depth

12. Determine velocity and shear stress using figure 24 and equations 3, 4, or 5 and 6

13. Determine erosion rate at each section

14. Determine embankment bed erosion at each section

15. Print computed results

16.   J = J + 1

17.   If J > ITIME

No

Yes

Stop

Figure 31. Flow chart of the computer model EMBANK.

69
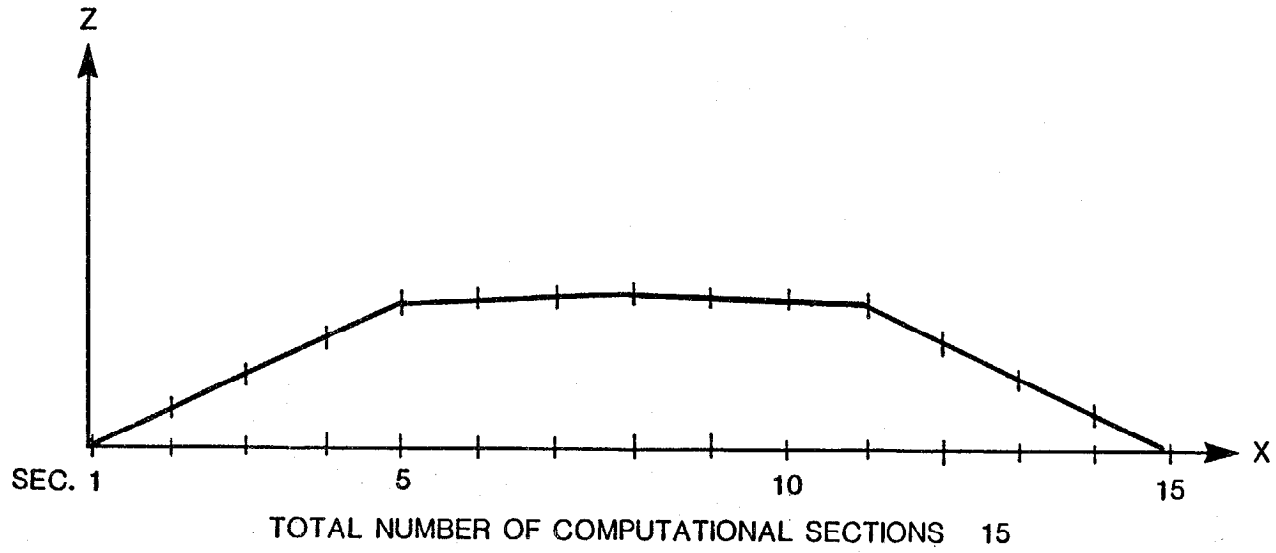
Figure 32. Embankment computational section.

Step 3. Input step hydrographs of headwater and tailwater. Figure 33 shows an example. For asumed steady flow, the hydrograph is a straight line.

Step 4. Initiate the computational step.

Step 5. Determine the bed slope at each section using the equation:

$$S_{o_i} = \frac{Z_{i-1} - Z_{i+1}}{X_{i+1} - X_{i-1}} \tag{7}$$

where i+1 and i-1 indicate the downstream and upstream sections of section i, respectively. For the most upstream section

$$S_{o_1} = \frac{Z_1 - Z_2}{X_2 - X_1} \tag{8}$$

For the most downstream section

$$S_{o_{NX}} = \frac{Z_{NX-1} - Z_{NX}}{X_{NX} - X_{NX-1}} \tag{9}$$

Step 6. Determine the discharge coefficient for a given headwater and tailwater elevation from figure 25 and then compute the flow discharge from equation 2.

Step 7. Compute critical depth y_c and critical slope S_c

$$y_c = (\frac{q^2}{g})^{1/3} \tag{10}$$

71
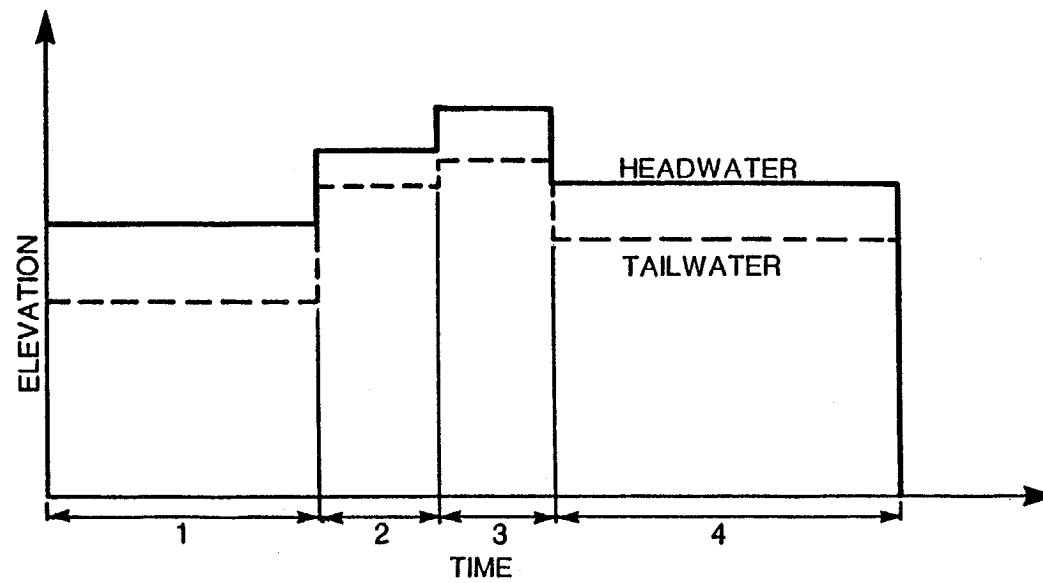
Figure 33. Headwater and tailwater step hydrographs.

72

$$S_c = \frac{g \, n^2}{2.2 \, y_c^{1/3}} \tag{11}$$

where q is the unit width discharge, g is the gravitational acceleration, and n is the Manning's roughness coefficient.

Step 8. Compare the bed slope with the critical slope at each section, starting from the upstream section, and determine the control sections, IC, at which the bed slope is just equal to or larger than the critical slope. Steps 5, 6, 7 and 8 are set up so that they will work for either the rigid embankment runs or the erosion runs. If the model were set up for rigid embankments only, these steps would be simplified.

Step 9. Compute water-surface profile upstream from the control sections by solving the momentum equation using the standard step method:

$$h_1 = h_2 + \frac{1}{2g} (V_1 + V_2)(V_2 - V_1) + \frac{\Delta x}{2}(S_{f1} + S_{f2}) \tag{12}$$

where h is the stage, V is the average velocity, Δx is the spatial increment, S_f is the friction slope, and subscripts 1 and 2 denote the upstream and downstream sections, respectively.

Step 10. Compute water-surface profile downstream of the control section by solving the momentum equation using the standard step method:

$$h_2 = h_1 + \frac{1}{2g} (V_1 + V_2)(V_1 - V_2) - \frac{\Delta x}{2}(S_{f1} + S_{f2}) \tag{13}$$

Step 11. Compute jump conditions considering tailwater effects as shown on figure 34. The following relations are utilized in this step and are based on the equations and figures developed by Bradley and Peterka.[7].

(1) Compute sequent depth assuming the jump will occur at computational section I

$$y_2 = \frac{y_1}{2\cos\theta} \left(\sqrt{\frac{8F_1^2 \cos^3\theta}{1 - 2K\tan\theta} + 1} - 1 \right) \tag{14}$$

in which y_1 is the depth before the jump, F_1 is the corresponding Froude number, θ is the angle of embankment slope ($\tan\theta = S_o$), and K is an empirical coefficient given by:

$$K = 21.98 \tan^2\theta - 14.40 \tan\theta + 3.74$$

(2) Compute jump length:

$$L_1 = y_2 (2.87 + 1.89 S_o) \sqrt{F_1} \tag{15}$$

(3) Compute water surface elevation at the end of jump:

$$TWH = y_2 (1 + 11.2 S_o^{3/2}) + Z_e \tag{16}$$

where: Z_e is the bed elevation at the end of the jump

The computed water surface elevation, TWH, is compared to the tailwater elevation, TW. The iteration to downstream sections continues until a section is found at which $TW \geq TWH$ or it can be concluded that a jump cannot occur on the slope.

I = IC + 1

Assume begin of jump is at section I. Compute sequent depth, y_2 using equation 14 ← Ⓐ

Compute jump length, L_1 using equation 15

Determine the location of end of jump

Determine the water-surface elevation at the end of jump, TWH, using equation 16

On the slope ← Is the end of jump on the slope or beyond? → Beyond the embankment

Yes

I = I + 1 ← Is I less than NX? ← No ← Is (TW $-Z_{NX}$) greater than y_2?

Ⓐ

No

No jump on slope

Return

Yes

Determine the distance between end of jump and the toe of embankment, L_2, using equation 17

Yes ← Is THW less than the tailwater elevation, TW and I equal to (IC+1)? → No

Flow is submerged. Compute water-surface profile using step procedure 8 (figure 31) from the downstream section with h_{NX} = TW

Return

Yes ← Is TWH greater than TW? → No

I=I+1

Ⓐ

Set stages at section downstream of the jump equal to TW

Approximate the stages at section within the jump by a parabolic curve

Return

Figure 34. Flow chart showing the computation of jump conditions.

75

(4) Determine the distance between the end of the jump and the edge of
    the embankment

For $(TW - Z_{NX})/y_2 \leq 1.3$,

$$L_2 = 2.05\ S_o^{-0.78}\ [(TW - Z_{NX}) - 0.9\ y_2] \tag{17a}$$

For $(TW - Z_{NX})/y_2 > 1.3$

$$L_2 = 0.82\ S_o^{-0.78}\ y_2 + [(TW - Z_{NX}) - 1.3\ y_2]/S_o \tag{17b}$$

where: TW is the tailwater elevation.

Step 12. Determine the flow mode (surface flow or plunging flow) from
figure 23 and compute local reference velocity using equations 3, 4, or 5 and
shear stress from equation 6.

Step 13. Determine erosion at each computational section (step used for
erosion runs only).

Step 14. Determine embankment bed erosion at each section during a time
step (step used for erosion runs only).

The developed computer model was verified using the water-surface data
collected for the rigid embankment runs. A comparison of the computed and
measured water-surface profiles is shown in figure 35. In general the agree-
ment is good. This model was later combined with a submodel for estimating
embankment erosion due to flood overtopping.
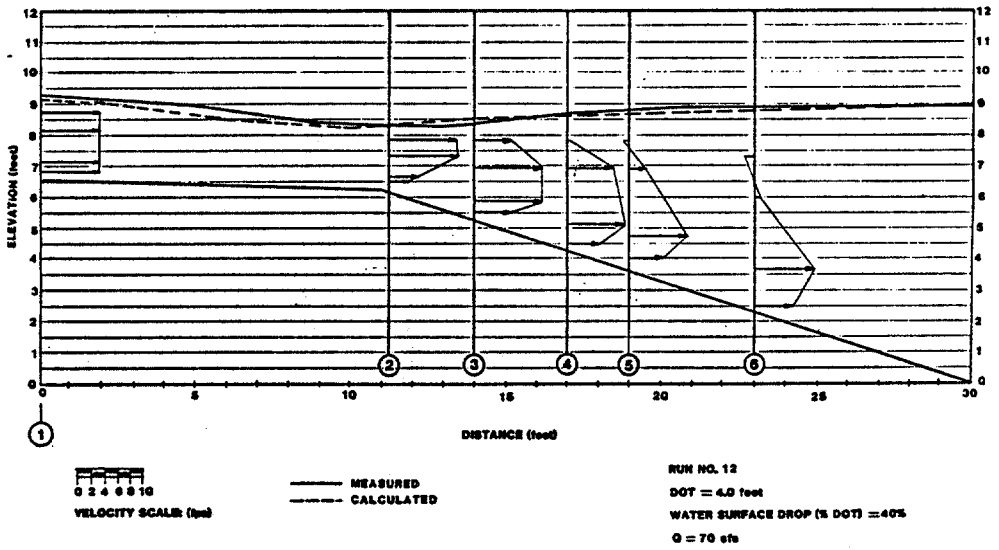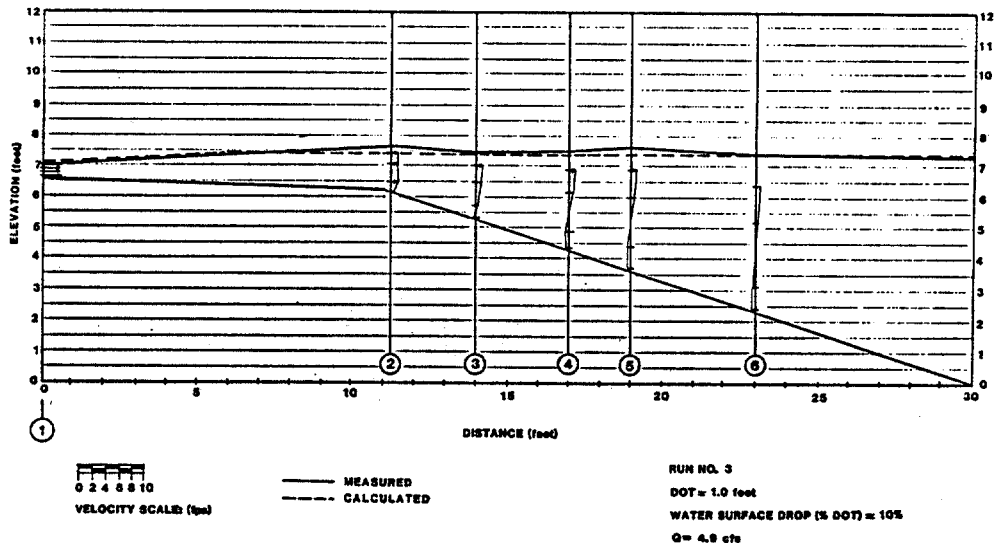
Figure 35. Comparison between measured and computed water-surface profile.

77

PARAMETERS AND EQUATIONS GOVERNING EROSION OF EMBANKMENT

1. General

Attempts to mathematically characterize embankment failure due to over-topping have relied on mathematical and physical models based on broad assumptions because performance data were lacking. In the following section, results of model studies and observational data are utilized to (1) demonstrate different approaches for characterizing overtopping erosion, and (2) demonstrate the role of shear stress and other parameters as related to embankment or dike design and construction. Embankment erosion equations are then developed using the laboratory test data conducted in this study.

2. Identification and Evaluation of Important Parameters

The erosion of soil, particularly cohesive soil, is complicated because many controlling parameters act interdependently. Principal factors involved are the physical and chemical properties of the soil itself, its behavior when partially and fully saturated, and the hydraulic properties of the flow. The following parameters are generally considered useful for evaluating the erodibility of cohesive soil: flow shear stress, critical shear stress of soil, percent clay, percent organic matter, cation exchange capacity, plasticity index, compaction, and temperature. Results of model studies which have monitored the role of these parameters more closely are given below.

Townsend and Goodings[8] performed several tests of waste embankment using centrifugal models to simulate embankment failure due to pore pressure changes and overtopping. Their results indicate that particle size distribution, and consequently permeability, are two important factors governing the failure of cohesionless materials in embankments. Permeable materials in embankments are subject to pore pressures due to seepage, which can cause mass instability. Less permeable embankments retard seepage and thus eliminate problems regarding throughflow erosion, but are susceptible to overtopping erosion. The mode of failure observed in embankments with intermediate per-

meabilities was mass instability (pore pressures) preceded by toe erosion. The nature of the foundation layers did not affect stability because the embankment was constructed such that the foundation strength was adequate for the embankment height. Hence, failure occurred in the embankment itself during the experiments.

The Waterways Experiment Station of the Corps of Engineers in Vicksburg, Mississippi, has drawn several conclusions about embankment performance when overtopping occurs. Their conclusions are based on case histories and documented in unpublished papers and reports. Their findings indicate:

* Low embankments constructed of cohesive or well-graded granular material with fines having good compaction can withstand limited overtopping depths for limited periods. Seepage through relatively clean rockfill is detrimental to stability and can lead to shallow slides which progress downhill.

* Two of the most important factors influencing durability of the embankment are the effects of concentration of flow at abutments or low areas along the crest and erosion resistance of the construction material at the downstream toe area. If downstream toe material is undercut and erosion progresses upslope, large rock, concrete or other measures can reduce scour in this area. Provision for tailwater can also reduce erosion.

* High embankments, i.e., over 75 feet, experience very high erosion forces on the downstream slope compared to low embankments.

* Other embankment failure modes, e.g., internal seepage and mass bank instability, can combine with the conditions of overtopping to cause breaching and failure of an embankment.

Researchers at the Waterways Experiment Station[9] suggested that if overtopping cannot be prevented, flow should be directed to more resistant and uniform areas of the embankment and abutments. They recommended that vegetation be used as protection, particularly on the crest and downstream slope.

In general, there are three major problems resulting from overtopping of highway embankments by floodwaters: destructive erosion, backwater impacts,

and magnitude of flood discharge. Kindsvater[4] studied the latter problem to determine the relationship of embankment form, roughness, and boundary layer conditions with discharge. Results of model tests indicated that discharge flow is virtually independent of embankment shape and height, and the influence of boundary resistance is appreciable only for small heads.

Tinney and Hsu[10] tested the erodibility of fuse plugs of spillways for dams. Fuse plugs are simply rockfill dams with clay cores surrounded by sand or other filtering materials designed to wash out at a certain flow discharge. The model study defined rates of erosion in terms of sediment transport characteristics (particle size), tractive force, and critical tractive force. The washout rate was found to be a function of grain size, i.e., the rate decreased as grain size increased. Also, by increasing the volume of rockfill (decrease the thickness of clay core), the washout rate decreased slightly. Scale modeling was conducted at laboratory scales of 1:20 and 1:40. Large-scale field model studies were conducted at 1:2 and prototype scales. Cohesionless material ranging from coarse to crushed rock was used in all studies. Using the DuBoys erosion rate equation, the Darcy-Weisbach friction factor critical shear stress equation, and geometry of the embankment, an equation was derived for the "rate of recession of the eroding face" in units of length per unit time. Based on a theoretical analysis, the ratio of the rate of recession between a physical model and its prototype was found to be the length ratio to the one-third power.

When embankments are overtopped by flood waters, erosion damage can be significant due to high velocities on the downstream side of the embankment. As the shear stress exerted by the flow exceeds the critical shear stress of the soil, erosion begins. The shear stress increases with the increase in velocity. Velocity depends on the headwater and tailwater conditions. Another important parameter is the erodibility of the soil. Cohesive soil or soil with larger particles is more resistant to erosion when compared to non-cohesive, fine-grained soils. Finally, the duration of overtopping affects the amount of damage.

Embankment failure due to piping and liquefaction depends mainly on the permeability of the soil, the head difference driving the water through the soil, and the duration of flood water allowing the soil to become saturated.

3. Critical Shear Stress

The critical or permissible shear stress and velocity are defined as the largest shear stress and velocity of flow that will not cause erosion. For noncohesive materials, the following equation can be utilized to determine the critical shear stress:[11]

$$\tau_c = 0.05 \ (\gamma_s - \gamma) \ d_{50} \tag{18}$$

where γ_s and γ are the unit weights of soil and water, respectively, and d_{50} is the median particle size of soil. Equation 18 is valid for a shear Reynolds number greater than 70. Fortier and Scobey[12] published the well-known table of "Permissible Canal Velocities" shown on table 9. This table can be utilized to estimate an average shear stress for noncohesive as well as cohesive soil.

Several relations for determining critical shear stress have been developed for cohesive soil. In the study of hydraulic erosive forces required to initiate motion of cohesive soils in open channels, Smerdon and Beasley[13,14] found that critical tractive force of cohesive soil correlated well with plasticity index. The relation developed for 11 uncompacted Missouri soils, ranging from a silty loam soil with little cohesion to a highly cohesive clay soil, was :

$$\tau_c = 0.0034 \ (PI)^{0.84} \tag{19}$$

81

Table 9. Maximum permissible velocities recommended by Fortier and Scobey and the corresponding unit-tractive-force values converted by the U.S. Bureau of Reclamation (for straight channels of small slope, after aging).

| | Clear Water | | Water Transporting colloidal silts | |
| | V_c | τ_c | V_c | τ_c |
Material	ft/s	lb/ft^2	ft/s	lb/ft^2
Fine sand, colloidal	1.50	0.027	2.50	0.075
Sandy loam, noncolloidal	1.75	0.037	2.50	0.075
Silt loam, noncolloidal	2.00	0.048	3.00	0.11
Alluvial silts, noncolloidal	2.00	0.048	3.50	0.15
Ordinary firm loam	2.50	0.075	3.50	0.15
Volcanic ash	2.50	0.075	3.50	0.15
Stiff clay, very colloidal	3.75	0.26	5.00	0.46
Alluvial silts, colloidal	3.75	0.26	5.00	0.46
Shales and hardpans	6.0	0.67	6.00	0.67
Fine gravel	2.50	0.075	5.00	0.32
Graded loam to cobbles when noncolloidal	3.75	0.38	5.00	0.66
Graded silts to cobbles when colloidal	4.00	0.43	5.50	0.80
Coarse gravel, noncolloidal	4.00	0.30	6.00	0.67
Cobbles and shingles	5.00	0.91	5.50	1.10

where PI is the plasticity index. Plasticity is defined as the ability of a material to change shape continuously under the influence of an applied stress and to retain the new shape after removal of the stress. The plasticity index is defined as the difference between the liquid limit and plastic limit. Values of plastic limit and liquid limit for different clays, obtained from Grissinger,[15] are given in table 10. Lyle and Smerdon[16] used a flume and Arumugam[17] used a rotating cylinder erosion test apparatus to study the relationships between critical shear stress and a variety of soil properties. They developed relations of the critical shear stress to the cation exchange capacity, percent organic matter, and other soil parameters.

Because the plasticity index is generally available or can be easily determined for different types of soils, it was decided that a power relation in the form of equation 19 be utilized in this study to determine critical shear stress. By using the data from McWhorter, et al.,[18] and soil data from this study, the following relation was obtained:

$$\tau_c = 0.019 \ (PI)^{0.58} \tag{20}$$

McWhorter, et al.,[18] conducted a comprehensive study for the design of open channels utilizing artificial lining materials. In the course of experimentation, 11 soils ranging from a noncohesive sand gravel to an inorganic clay were utilized in the tests. McWhorter conducted a series of tests to determine erosion rates of these soils by flow. In this study, the erosion rates were plotted versus shear stress for different soils. Regression lines were fit to the data points and then extended to zero erosion to determine the critical shear stress. These data are summarized on table 11, plotted on figure 36, and fitted by a power function (equation 20). The critical shear stress for type I soil was also plotted on figure 36. Equation 20 generally agrees with the values recommended by Chow.[6] However, it calculates higher critical shear stress than using equation 19. The reason could be that equation 20 was derived from tests of well compacted soils (dry density

Table 10. Liquid limit, plastic limit, and plasticity index values, Grissinger. [15]

Material	Liquid Limit	Plastic Limit	Plasticity Index
Grenada silt loam	31	20	11
Mixed with			
2 Percent Ca montmorillonite	32	21	11
5 Percent Ca montmorillonite	33	21	12
10 Percent Ca montmorillonite	41	24	17
2 Percent Na montmorillonite	32	21	11
5 Percent Na montmorillonite	40	24	16
10 Percent Na montmorillonite	62	27	35
2 Percent coarse kaolinite	28	21	7
5 Percent coarse kaolinite	29	22	7
10 Percent coarse kaolinite	30	20	10
15 Percent coarse kaolinite	30	20	10
20 Percent coarse kaolinite	32	22	10
2 Percent fine kaolinite	28	21	7
5 Percent fine kaolinite	31	19	12
10 Percent fine kaolinite	29	18	11

Table 11. Critical shear stress derived from McWhorter's data.

Soil Identification Number (after 18)	Unified Soil Classification	Liquid Limit	Plastic Limit	Plasticity Index	Critical Shear Stress (lb/ft^2)
1	SC	31	16	15	0.11
3	SM	28	24	4	0.04
6	CH	51	22	29	0.12
7	CL	28	16	12	0.06
8	CL	38	23	15	0.09
9	ML-CL	24	18	6	0.06
10	CH	76	29	47	0.17
11	CL	45	22	23	0.09
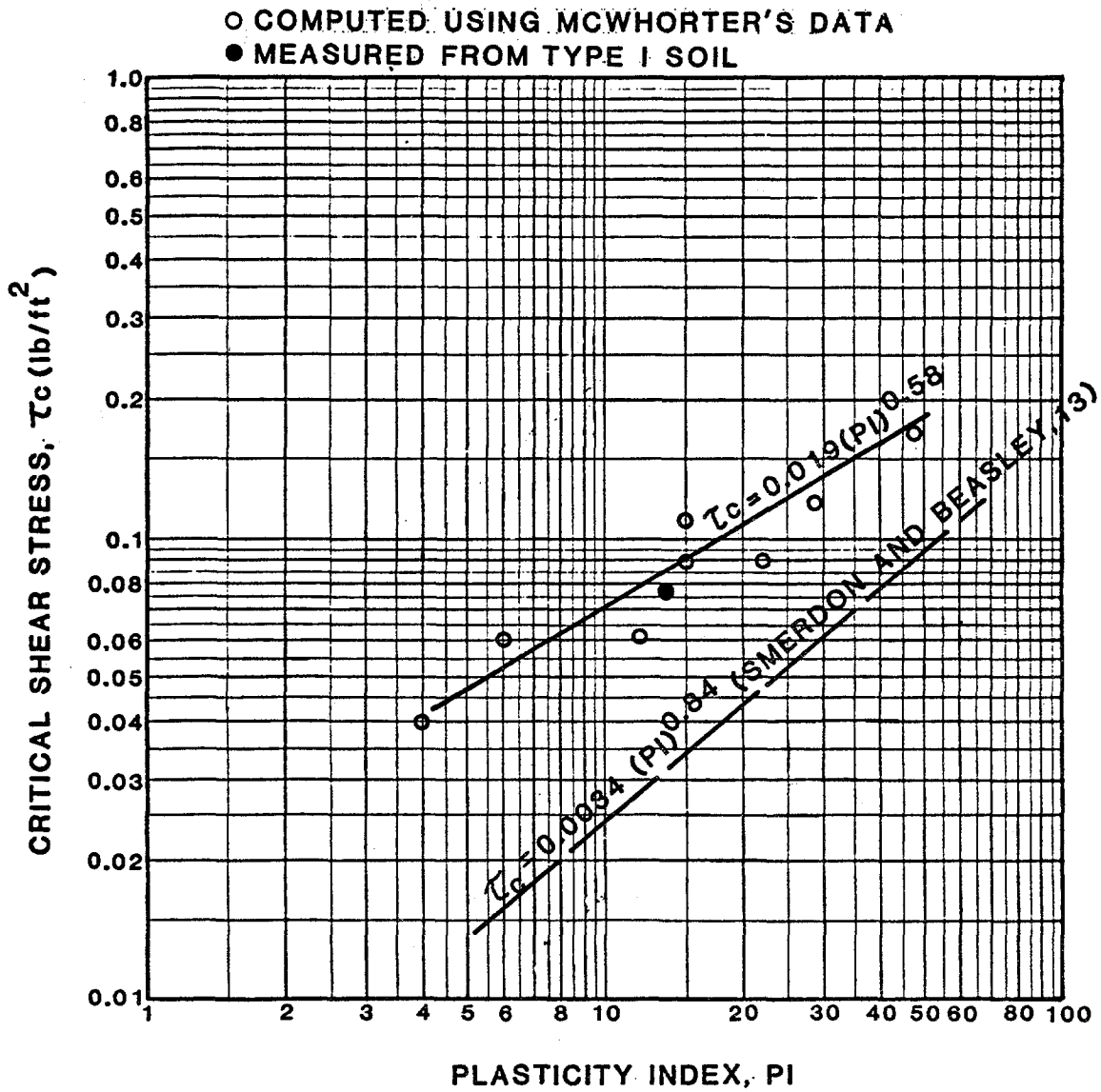
Figure 36.   Relation of critical shear stress
to plasticity index.

86

ranging from about 90 to 105 lbs/ft^3) (1,440 to 1,682 Kg/m^3), while equation 19 was derived from uncompacted soil tests (dry density ranging from about 60 to 75 lb/ft^3) (960 to 1,202 Kg/m^3). Compaction increases the strength of soil against erosion.

Stability of vegetated side slopes varies with flow velocities to different degrees, depending on the kind of vegetation present. Table 12 shows critical shear stress in channels lined with vegetation.[19] Classification of vegetal covers is defined by the USDA Soil Conservation Service.[20] These permissible velocities may be decreased somewhat when utilized to protect embankments with a slope up to 2H:1V.

4. Evaluation of Existing Equations for Estimating Erosive Rate

From the literature review several erosion equations related to embankment erosion were presented. These equations mainly relate the erosion rate to effective shear stress and velocity. Table 13 summarizes these equations. These equations were evaluated by comparing the erosion rates calculated by the equations versus the measured erosion rates from the laboratory tests. The results of the comparative analysis are provided in the following paragraphs.

Figure 37 compares the Wiggert and Contractor[21] equation with the measured erosion rate. The average velocity used in the comparison was determined as the average velocity at the middle point on the downstream slope of the embankment, and the measured erosion rate was the erosion amount during the first hour of the tests. Only results from FHWA test series I and II were utilized for the comparison. Figure 37 shows that, for most of the runs, the calculated erosion rates from the Wiggert and Contractor equation are larger than the measured values. While the erosion or transport rate is usually dependent on the velocity to the third to fifth power for a noncohesive soil embankment, the sensitivity of erosion rate to velocity is usually less, on the order of first to third power, for a cohesive soil embankment. Therefore,

Table 12. Critical shear stress for channels lined with vegetation.

Class	Cover	Condition	Critical Shear Stress (lb/ft^2)
A	Weeping lovegrass .... Yellow bluestem Ischaemum	Excellent stand, tall (average 30") (76 cm) Excellent stand, tall (average 36") (91 cm)	3.70

B	Kudzu ....
	Bermuda grass ....
	Native grass mixture
	  (little bluestem, blue-
	  stem, blue gamma, and
	  other long and short
	  midwest grasses).........
	Weeping lovegrass ....
	Lespedeza sericea ....
	
	Alfalfa ....
	Weeping lovegrass ....
	Kudzu ....
	Blue gamma ....
		Very dense growth, uncut
		Good stand, tall (average 12") (30 cm)
		
		Good stand, unmowed
		Good stand, tall (average 24") (61 cm)
		Good stand, not woody, tall (average 19")
		(48 cm)
		Good stand, uncut (average 11") (28 cm)
		Good stand, unmowed (average 13") (33 cm)
		Dense growth, uncut
		Good stand, uncut (average 13") (28 cm)
			2.10

C	Crabgrass ....
	Bermuda grass ....
	Common lespedeza ....
	Grass-legume mixture--
	  summer (orchard grass,
	  redtop, Italian ryegrass,
	  and common lespedeza)....
	
	Centipedegrass............
	Kentucky bluegrass........
		Fair stand, uncut (10 to 48") (25 to 120 cm)
		Good stand, mowed (average 6") (15 cm)
		Good stand, uncut (average 11") (28 cm)
		
		Good stand, uncut (6 to 8 inches) (15 to
		20 cm)
		Very dense cover (average 6 inches) (15 cm)
		Good stand, headed (6 to 12 inches (15 to
		30 cm)
			1.00

D	Bermuda grass..............
	Common lespedeza ....
	Buffalo grass ....
	
	Grass-legume mixture--
	  fall, spring (orchard
	  grass, redtop, Italian
	  ryegrass, and common
	  lespedeza)..............
	
	Lespedeza sericea ....
		Good stand, cut to 2.5-inch height (6 cm)
		Excellent stand, uncut (average 4.5") (11 cm)
		Good stand, uncut (3 to 6 inches (8 to
		15 cm)
		
		Good stand, uncut (4 to 5 inches) (10 to
		13 cm)
		After cutting to 2-inch height (5 cm)
		Very good stand before cutting
			0.60

E	Bermuda grass .... Bermuda grass	Good stand, cut to 1.5 inch height (4 cm) Burned stubble	0.35

Table 13. Existing embankment erosion equations.

Developer	Equation	Comments
1. Wiggert & Contractor [21]	$E = \alpha V^{\beta}$	This equation was derived specifically for embankment erosion due to flood overtopping, where E = the erosion rate in tons/day/ft of the roadway and V = mean flow velocity on the downstream slope in ft/s. The given values of $\alpha = 0.25$ and $\beta = 3.8$ represent a compromise between cohesive and noncohesive soils.
2. Cristofano [22]	$\dfrac{Q_s}{Q_w} = K\,e^{-x}$	This equation computes rate of erosion for earth dam failures due to overtopping, where Q_s = erosion rate, Q_w = overtopping flow discharge, K = constant, $x = (b/H)\tan\phi_d$, b = base length of the breach, H = hydraulic head and ϕ_d = angle of friction.
3. Ariathural and Arulanandan [23]	$E = M\left(\dfrac{\tau}{\tau_c} - 1\right)$	This equation computes erosion of cohesive soil, where M = erosion rate constant, ranging from 0.00012 to 0.0012 lb/ft²/s; τ = shear stress, and τ_c = critical shear stress.
4. Chee [24]	$\dfrac{q_s}{q_c} = \left(\dfrac{1}{60}\right) K_1 K_2 K_3 K_4 \left(g\,\dfrac{D-0.5H}{q_c^2}\right)^{1/20}$ $[1/(S_s -1)]^2 \,(D/d)^{1/8}$	This equation computes erosion rates for erodible fuse-plug dams, where q_s = erosion rate per unit width; D = water depth upstream of the dam; q_c = critical water discharge per unit width for D, height of dam, d = mean grain size, S_s = specific gravity of grain, and K = coefficients.
5. Agricultural Research Lab	$E = K\,(\tau - \tau_c)^a$	This equation computes detachment rate for erosion of cohesive soils.

89
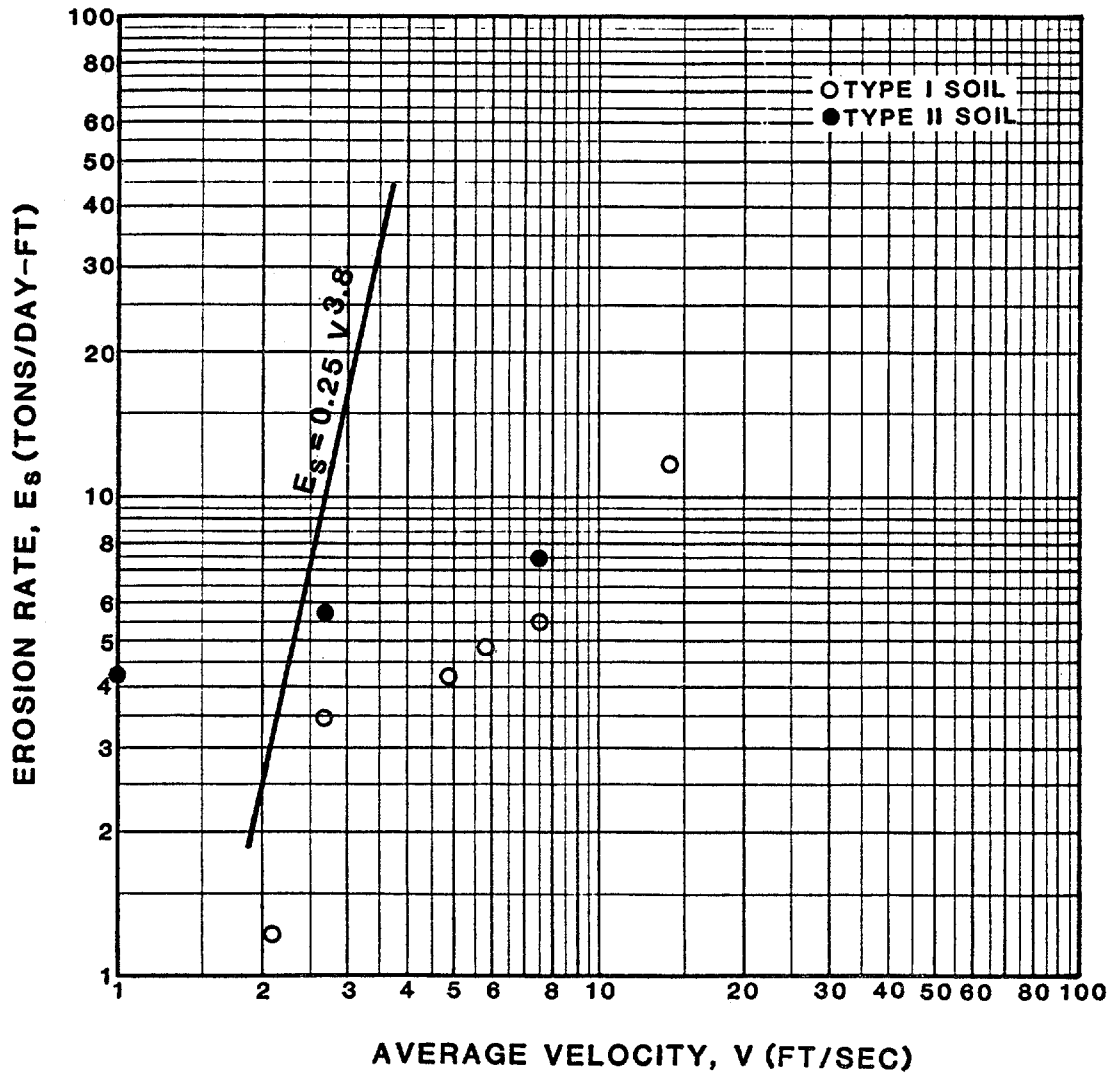
Figure 37. Comparison of measured erosion rate
with that computed by Wiggert and
Contractor equation.

90

the Wiggert and Contractor equation is more applicable to noncohesive soil embankments.

The Cristofano[22] equation was developed for estimating the rate of erosion in an earth dam failure due to overtopping. This equation shows that the erosion rate depends on overtopping depth exponentially. Figure 38 compares the Cristofano equation with the measured erosion rate. Only test runs with free-fall conditions were utilized for comparison. Again the Cristofano equation estimated larger erosion rates than those measured in the flume.

The equation developed by Ariathurai and Arulanandan[23] was plotted against measured erosion rates on figure 39. The agreement between the upper-band equation and the type I soil erosion rate is reasonable. This indicates that the form of the Ariathurai and Arulanandan equation is generally correct. However, the relation between the erosion rate and net shear stress rate may not always be linear. Therefore, a more general form, such as the one recommended by the Agricultural Research Laboratory

$$E = K (\tau - \tau_c)^a \tag{21}$$

may be more correct. Additional discussion of equation 21 is provided in section 5 on development of an erosion equation.

Chee's relation[24], as given in table 13, was developed for determining erosion rates of "fuse plug" dams which were formed by uniform size material ranging from 0.14 mm to 10 mm with clay core. This relation cannot be directly applied for estimating erosion of roadway embankments.

In 1980, the FHWA collected and analyzed data from highway agencies and work by Schneider and Wilson[25] to derive the relationships between overtopping depth and loss of pavement and embankments. The data were based on observations of roadway damage due to flood overtopping. The cumulative
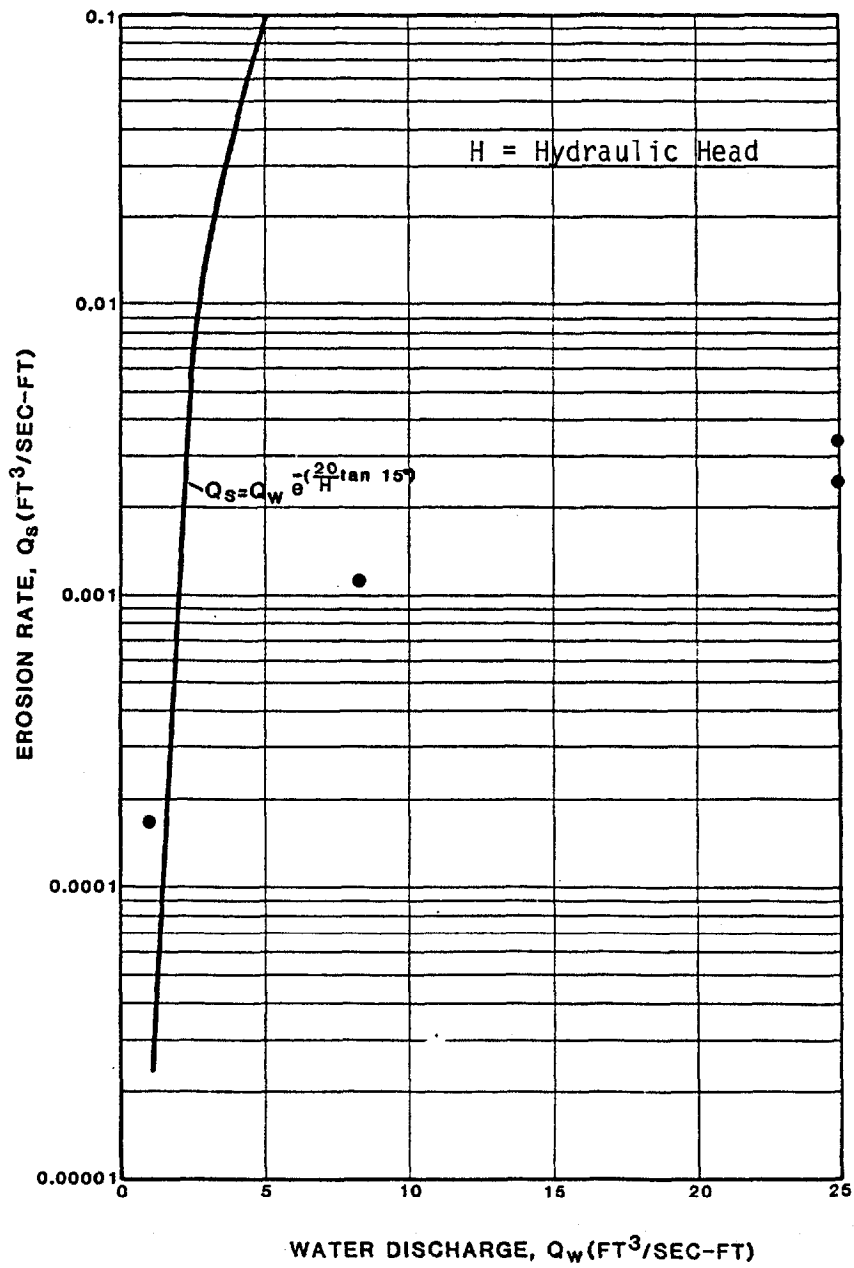
Figure 38. Comparison of measured erosion rate with that
computed by Cristofano equation.

92
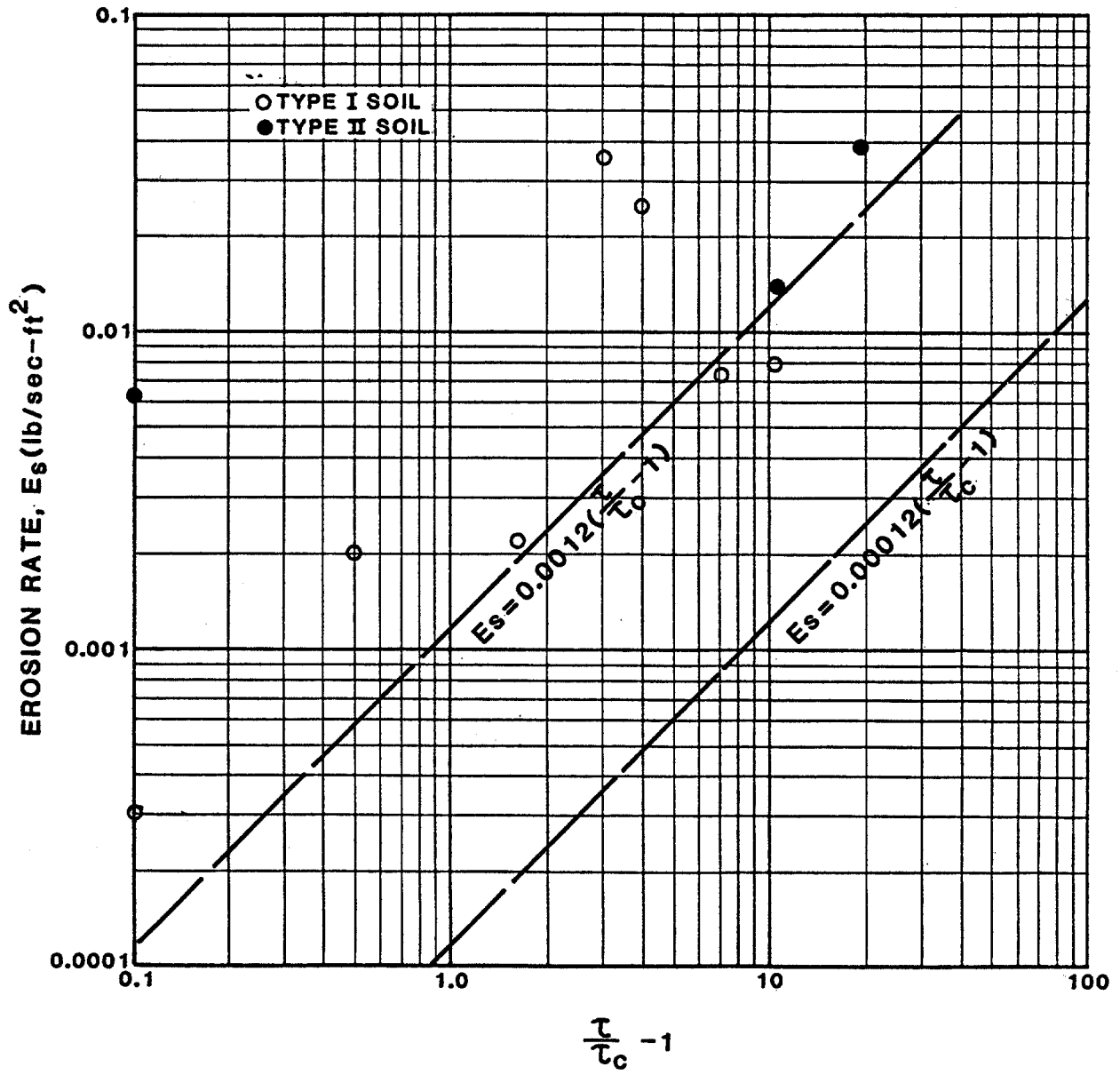
Figure 39. Comparison of measured erosion rate with that computed by Ariathurai and Arulanandan equation.

effects of overtopping over time based on these data and studies are illustrated by the relationship in figure 40. Data defining this relationship were obtained from highway sections 48 ft (14.6 m) wide, 40 ft (12.2 m) of asphalt, well vegetated 3:1 side slopes, and sandy-clay fill material. Additional hydraulic analysis of the observational data was done to determine time and depth of overtopping for various floods.

Embankment test data collected for this study were plotted on figure 40 for comparison with the 20-hour erosion curve. Type I soil embankment erosion data (with t/h = 0.3 conditions) showed good agreement with the curve, while the test data with free-fall conditions and the type II soil embankment erosion data showed higher erosion rates than the curve.

FHWA test series II to V tested paved embankments. During overtopping depths of 0.5, 1, and 2 ft (0.15, 0.3 and 0.6 m), the damage to the pavement was negligible. Only shoulder gravel was eroded. However, during the 4-ft (1.2-m) overtopping run, pavement was broken and lifted off the embankment surface. The entire pavement was eroded in four hours, as shown in figure 41. Similar situations have been observed in the field. The field situations, however, are more complicated and nonhomogeneous. Laboratory study of pavement damage and its effect on embankment erosion can be applied to field conditions only to a limited degree. Further discussion of the effect of pavement on embankment erosion is provided in "Development of a Procedure for Determining Embankment Erosion Due to Flood Overtopping."

5. Development of the Erosion Equation

Based on the evaluation of existing erosion equations and the literature review, a promising equation for estimating the embankment erosion rate is

$$E = K (\tau - \tau_c)^a \tag{22}$$

where E is the detachment rate per unit area, τ is the local effective
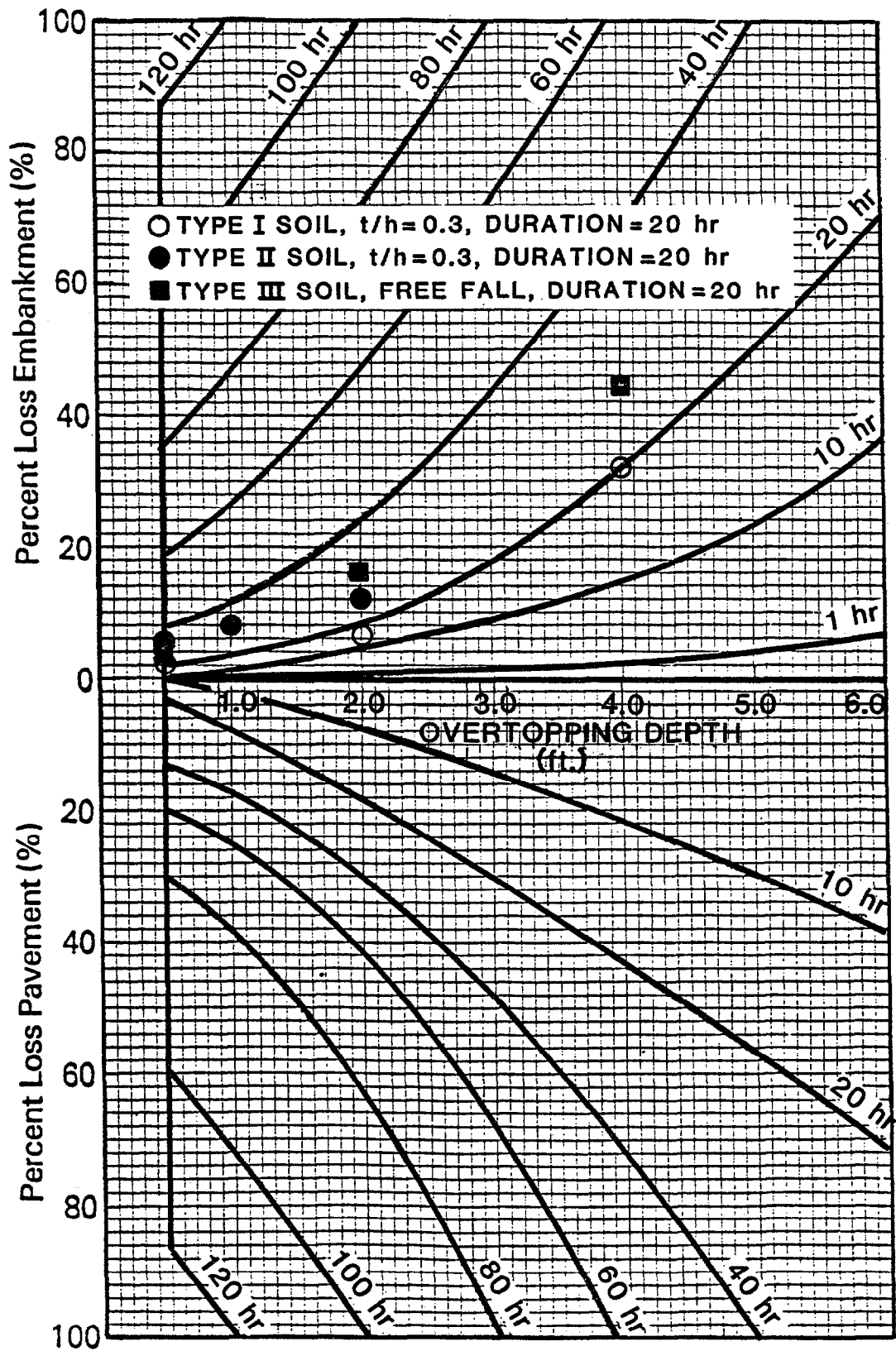
Figure 40. Embankment pavement losses (after Schneider and Wilson.[24])

95
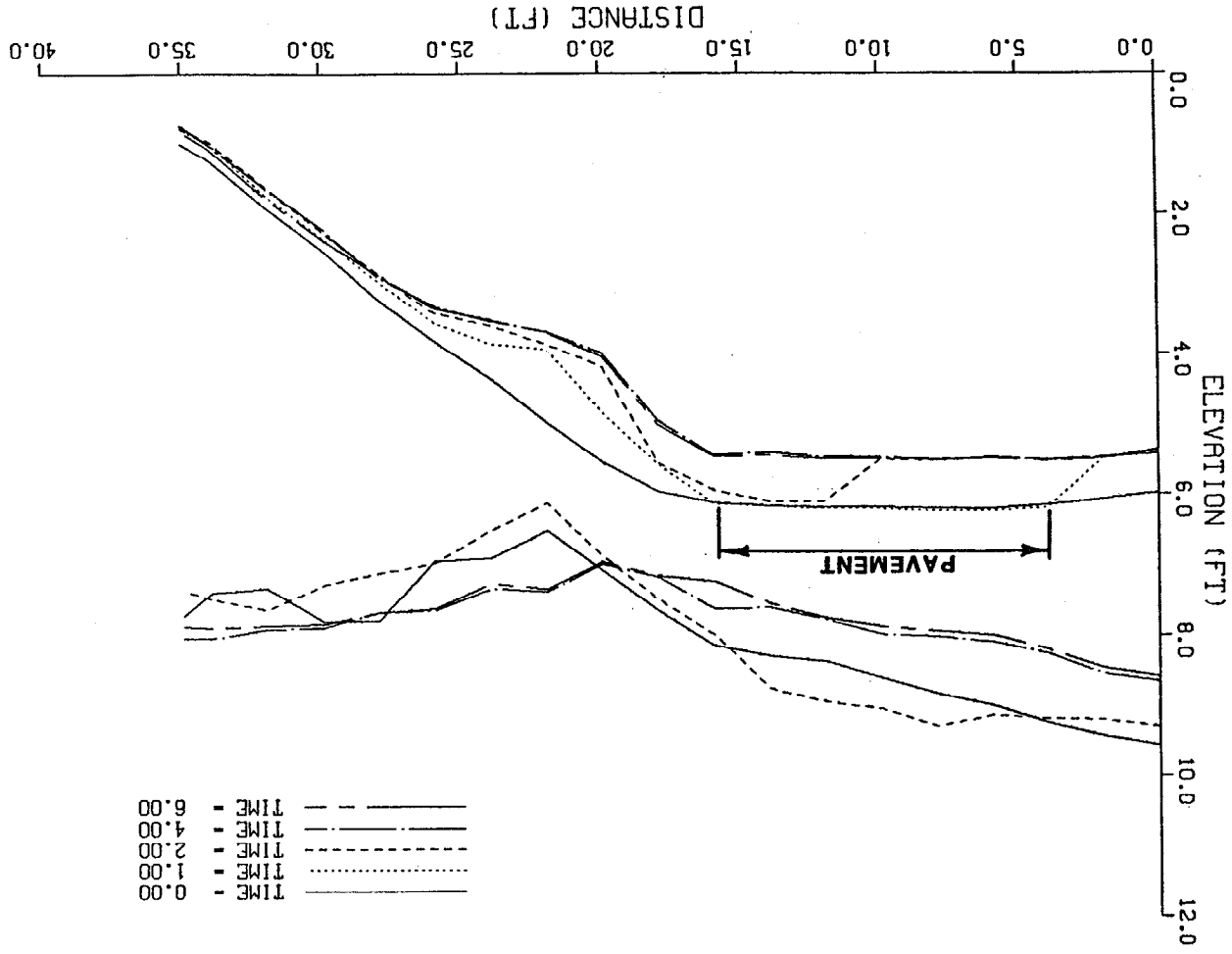
Figure 41. Water and bed surface profile of paved type II soil embankment.

shear stress based on hydraulic conditions, τ_c equals the critical shear stress of soil, and K and a are empirical coefficients dependent upon soil properties.

Erosion equations were developed for the two types of soils utilized for this study and a noncohesive soil tested by McWhorter et al.,[18] using the following procedure:

1. Determine the critical shear stress from equation 18 for noncohesive soils, and from equation 21 for cohesive soils. The critical shear stresses for type I soil, type II soil, and the noncohesive soil are 0.085, 0.053, and 0.050 lb/ft^2, respectively.

2. Determine the maximum local erosion rates during the first hour of the tests for FHWA test series I and II.

3. Determine the local shear stress based on

$$\tau = \frac{1}{8} f \rho V^2 \qquad (23)$$

   where V is the local velocity at the eroding site, f is the Darcy-Weisbach coefficient, and ρ is the water density. For the relatively smooth clay-soil surface, f = 0.02.

4. Plot the net shear stress $(\tau - \tau_c)$ versus the local erosion rate on figure 42 and determine the coefficients of K and a in equation 22 based on a linear regression method.

Three equations were thus developed:
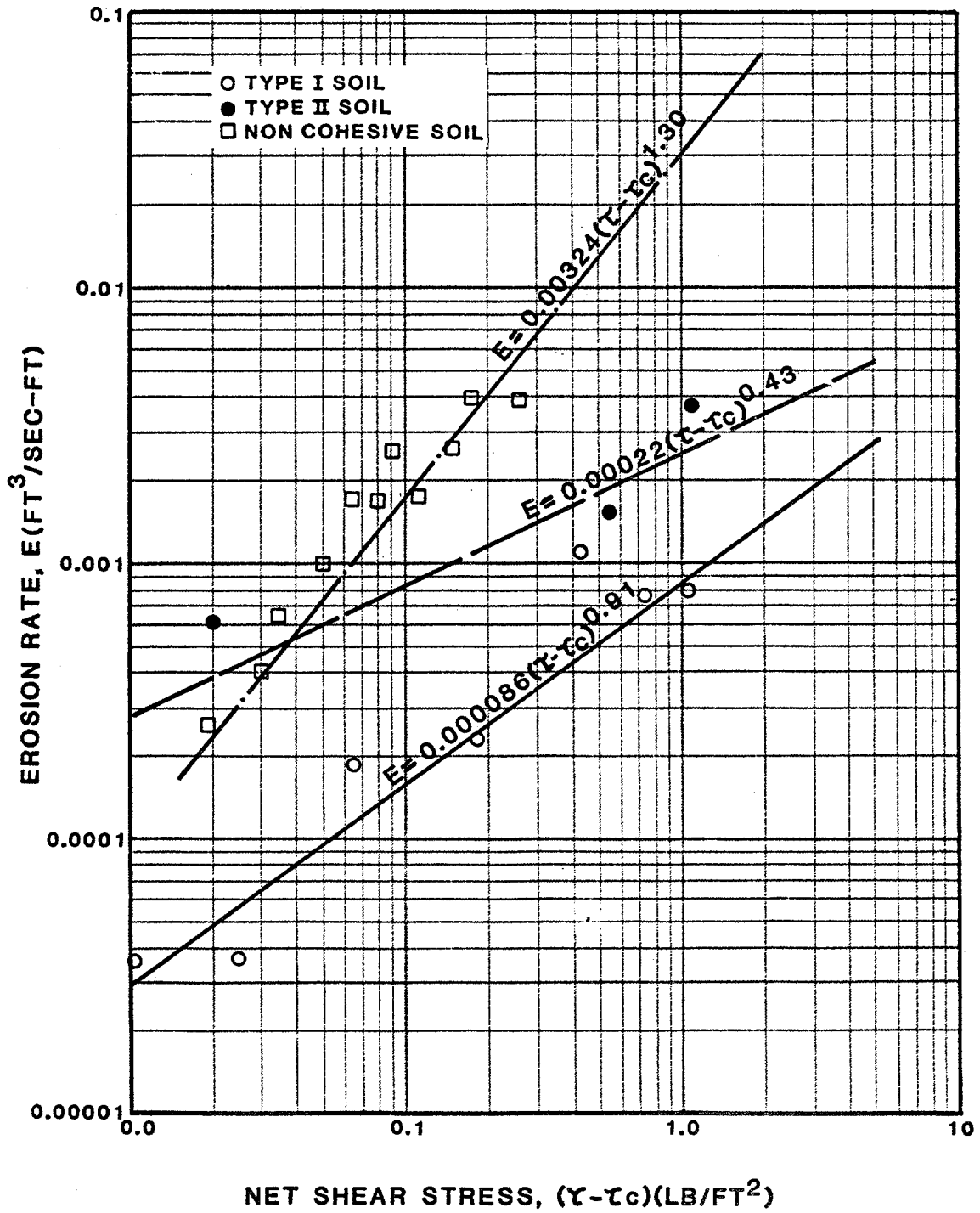
Figure 42. Embankment erosion equations.
98

1. For embankments made from highly cohesive soil such as clay (PI $\geq$ 10)

$$E = 0.000086 \ (\tau - \tau_c)^{0.91} \tag{24}$$

2. For embankments made from low-cohesive soil such as sandy clay (PI $\leq$ 5)

$$E = 0.00022 \ (\tau - \tau_c)^{0.43} \tag{25}$$

3. For embankments made from noncohesive sand/gravel soil

$$E = 0.00324 \ (\tau - \tau_c)^{1.3} \tag{26}$$

where E is the erosion rate in $ft^3/s\text{-}ft^2$.

Equations 24, 25 and 26 were utilized to generate design charts for estimating embankment damage due to flood overtopping as discussed in "Development of a Procedure for Determining Embankment Erosion Due to Flood Overtopping." The experiments for evaluating effects of grass covers on embankment erosion were inconclusive. All the tests were conducted with free-fall conditions. In tests with low overtopping depths [0.5 ft (0.15 m)], the grass-lined embankment appeared to perform well. In tests with high overtopping depths [2 and 4 ft (0.6 and 1.2 m)], pockets of grass were removed and induced the formation of local scour along the embankment. A partial explanation of this phenomenon could be the existence of weak spots along the embankment or area where the root system of the grass was not fully established. Severe toe erosion also occurred. It appeared that this spot and toe erosion was related to erodibility of underlying soil, therefore it is reasonable to assume that the erosion equation coefficients K and a for grass cover would be the same as for the underlying soil, and only the τ_c value would change.

DEVELOPMENT OF A PROCEDURE FOR DETERMINING EMBANKMENT EROSION DUE TO FLOOD OVERTOPPING

1. Development of a Computer Model for Determining Embankment Erosion

The computer model presented in "Hydraulics of Flow Over an Embankment" for determining embankment overtopping flow hydraulics was modified to compute embankment erosion. Figure 31 presented a flow chart of this model. Steps 2, 13, and 14 were added to the basic model for determining embankment erosion due to flood overtopping. These steps are explained below.

Step 2. Input embankment soil and structure characteristics and erosion equations. Figure 43 shows an example embankment with pavement and grass. This embankment was considered to contain four layers: pavement, gravel base, grass cover, and base soil. The critical shear stresses and Manning's n values for the four layers are input as data to the model. Also, the thickness of the layers at each computational section are input as data. Table 14 lists the example input data for the embankment shown on Figure 43. A user's manual and a listing of the computer program are provided in Appendix C. The developed model can also consider gravel or earth embankment with or without grass and with homogeneous or nonhomogeneous soil base. When one layer is eroded, the critical shear stress and Manning's n for the immediate lower layer are utilized for next time-step computation.

Considering the erosion equations developed by the various researchers referenced in "Parameters and Equations Governing Erosion of Embankment," the following equation form proposed by the Agricultural Research Laboratory was selected for the computer model:

$$E = K (\tau - \tau_c)^a \tag{27}$$

where E is the erosion rate in $ft^3/s\text{-}ft^2$, and τ and τ_c are effective shear and critical shear stress, respectively, in lb/ft^2.

100

Table 14. Sample input of embankment geometry and soil/structure characteristics for the embankment illustrated in figure 43.

Section	X (ft)	Z (ft)	Layer Thickness (ft)			
			Pavement	Gravel Base	Grass Depth	Base Soil
1	0	0.00	0.00	0.00	0.00	0.00
2	5	2.50	0.00	0.00	0.50	2.00
3	10	5.00	0.00	0.00	0.50	4.50
4	15	7.50	0.00	0.00	0.50	7.00
5	20	10.00	0.00	0.50	0.00	9.50
6	25	10.20	0.25	0.50	0.00	9.45
7	30	10.40	0.25	0.50	0.00	9.65
8	35	10.50	0.25	0.50	0.00	9.75
9	40	10.40	0.25	0.50	0.00	9.65
10	45	10.20	0.25	0.50	0.00	9.45
11	50	10.00	0.00	0.50	0.00	9.50
12	55	7.50	0.00	0.00	0.50	7.00
13	60	5.00	0.00	0.00	0.50	4.50
14	65	2.50	0.00	0.00	0.50	2.00
15	70	0.00	0.00	0.00	0.00	0.00
Manning's n			0.015	0.025	0.030	0.015
Critical shear stress			100.0	0.15	1.00	0.53
Erosion coefficient K			1.0	0.00324	0.000220	0.000220
Erosion coefficient a			1.0	1.300	0.43	0.43
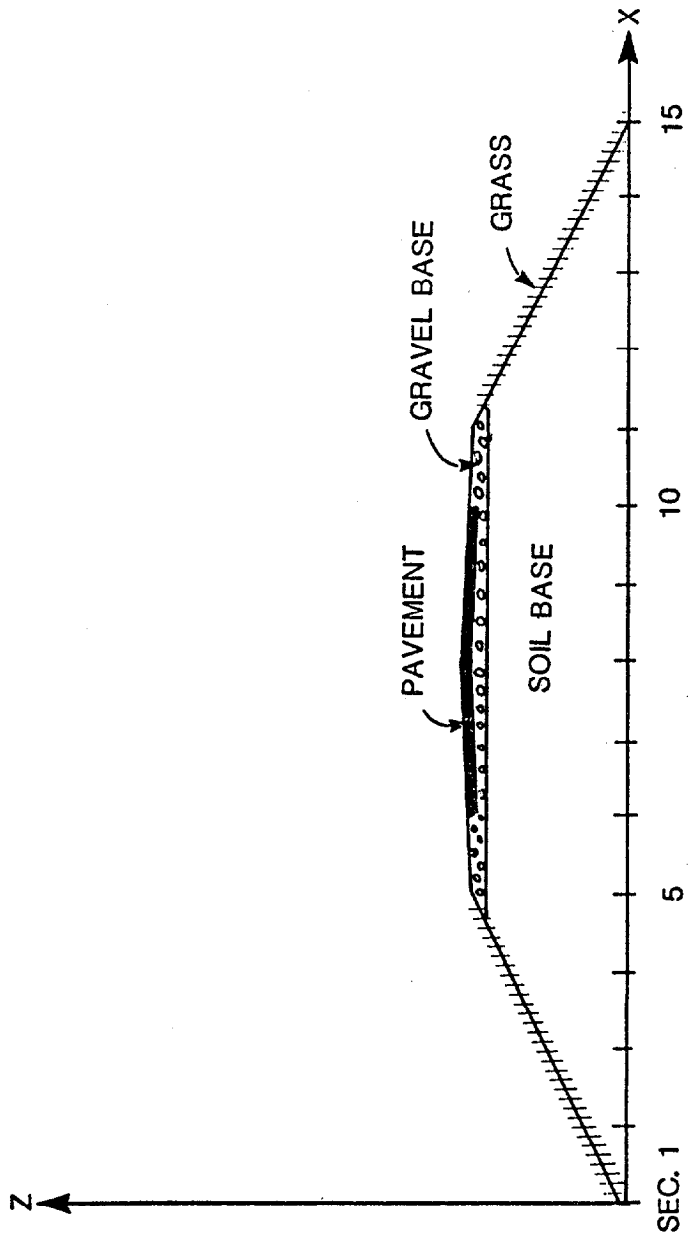
Figure 43. Example embankment.

As discussed in section 5 of "Parameters and Equations Governing Erosion Embankment," the following coefficients were utilized in the computer model for determining erosion of bare soil embankment:

- For highly cohesive soil with $PI \geq 10$, $K = 0.000086$ and $a = 0.91$

- For low cohesive soil with $PI \leq 5$, $K = 0.00022$ and $a = 0.43$

- For noncohesive soil $K = 0.00324$ and $a = 1.30$

Step 13. Determine erosion at each computational section from equation 27 using the critical shear stress of the surface layer. If the surface layer was eroded within a period shorter than a computational time step, then the critical shear stress of the immediate lower layer would be utilized for the computation for the remaining time period.

Step 14. Determine embankment bed erosion at each section during a time step. For grass, gravel, or soil surface, the bed erosion depth is:

$$\Delta Z = E \, \Delta t \tag{28}$$

where E is the erosion rate from equation 27 and Δt is the time step duration. For paved sections, it was assumed that damage to the pavement is not due to direct flow erosion, but instead to the erosion undermining the roadway base and cantilevering the pavement. Considering the condition illustrated by figure 44, the maximum normal stress of pavement due to flow is:

$$(\sigma_x)_{max} = \frac{M}{S_m} \tag{29}$$

where M is the bending movement induced by the weight of the pavement and water above point A, and S_m is the section modulus. Let D = the average depth of flow at the middle of undermined pavement, t = the thickness of
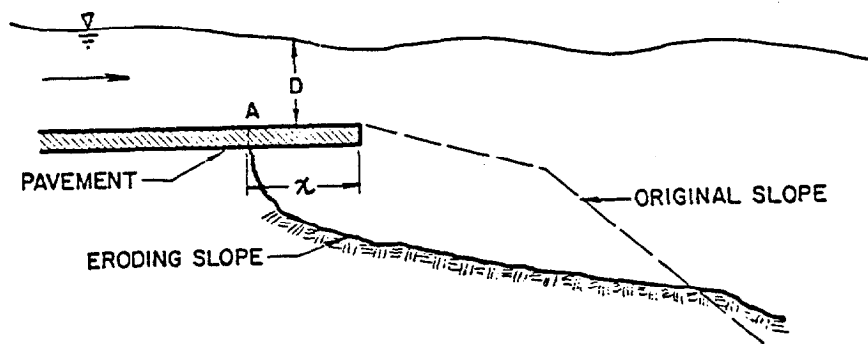
Figure 44. Undermining of embankment pavement.

pavement, γ_w = the unit weight of water and γ_a = the unit weight of pavement, then

$$M = (\gamma_w D + \gamma_a t) \, x^2/2 \qquad \text{and} \tag{30}$$

$$S_m = \frac{t^2}{6} \tag{31}$$

Substituting equations 30 and 31 into equation 29 yields

$$(\sigma_x)_{max} = \frac{3(\gamma_w D + \gamma_a t) \, x^2}{t^2} \tag{32}$$

For the computer model, the undermining length, x is assumed to be one-tenth of the eroded depth at the edge of pavement, D is the computed flow depth at the edge of pavement, and γ_w, γ_a, and t are known variables. By substituting these values into equation 32, $(\sigma_x)_{max}$ is computed. If $(\sigma_x)_{max}$ is larger than the allowable tension stress of the pavement σ_a, it is assumed that the pavement from the downstream edge to its immediately upstream computational section is eroded within one time step. Then this computation section becomes the downstream edge of the pavement for the next computational step.

2. Calibrations of the Computer Model

The bare-soil embankment test data from FHWA test series I and II were utilized to calibrate the computer model. The geometry and soil characteristics of these embankments and overtopping headwater and tailwater depths were input to the computer program to calculate the volume of material eroded during the first hour. Then the calculated values were compared with the measured volumes during the first hour of the tests and plotted on figure 45. The agreement is reasonable. The model was then utilized to develop nomographs for estimating embankment damages for various flow and embankment conditions.

105
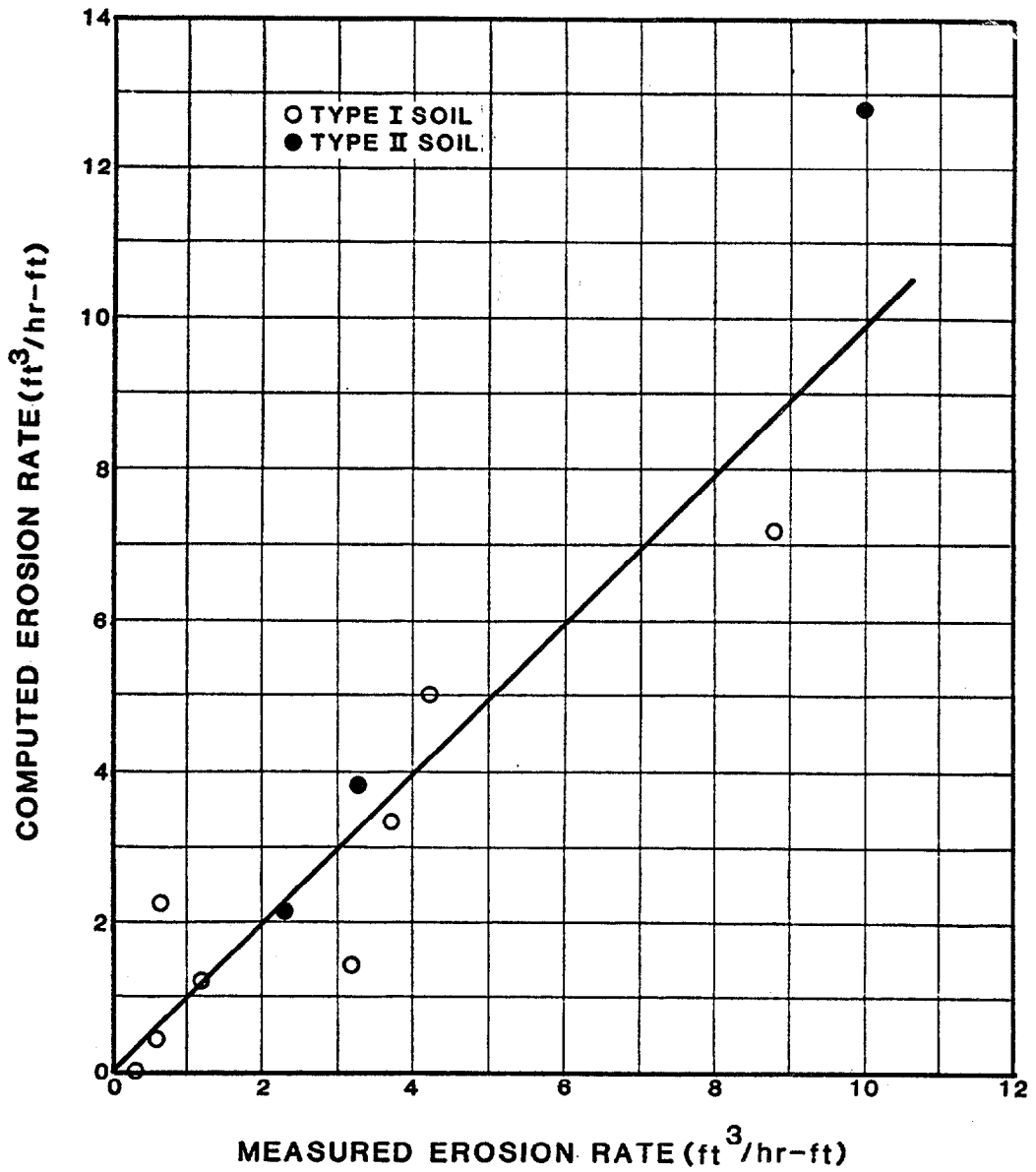
Figure 45. Computed versus measured erosion rate.

106

3.   Development of Nomographs for Determining Embankment Erosion Due to
     Flood Overtopping

The computer model calibrated in section 2 was applied to develop nomographs for estimating erosion of bare-soil embankment and paved embankment with and without vegetal cover under various conditions:

• Base soils consisting of high-cohesive material, low-cohesive material
  and noncohesive material.

• Paved embankment with and without class A, C, and E grass covers.

• Embankment heights ranging from 2.5 ft (0.8 m) to 15 ft (4.6 m).

• Overtopping depths ranging 1.0 ft (0.3 m) to ten ft (3.0 m).

• Ratio of tailwater depth to overtopping depth ranging from free fall to
  0.9.

The computed erosion rates (averaged over a four-hour period) were plotted on figure 46 for 5-foot (1.5-m) high-cohesive (PI = 13) and low-cohesive (PI = 5) bare soil embankments, and on figure 47 for 5-foot (1.5-m) noncohesive soil embankments $(d_{50}$ = 4 mm). These two figures can be utilized for estimating erosion rates of 5-foot (1.5-m) bare-soil embankments. Because critical shear stress is not a very sensitive parameter, it is suggested that figure 46 be applied to high-cohesive-soil embankment with PI $\geq$ 10, and to low-cohesive soil embankment with PI $\leq$ 5, and figure 47 be applied to noncohesive soil embankment with d_{50} < 8 mm. For the embankment soil with PI between 5 and 10, the erosion rate can be determined by interpolation.

Other factors considered in the procedure include the effects of pavement and grass, duration of overtopping, and embankment heights. Pavement and grass affect the embankment erosion rate. Figure 48 shows the embankment profiles eroded by a flow with a 2-foot (0.6-m) overtopping depth and 70 percent water-surface drop (t/h = 0.3) in two runs—one without and one with the roadway paved. As shown on figure 48, most erosion of the bare-soil embankment took place on the top and downstream shoulder. The pavement reduced the sur-

107
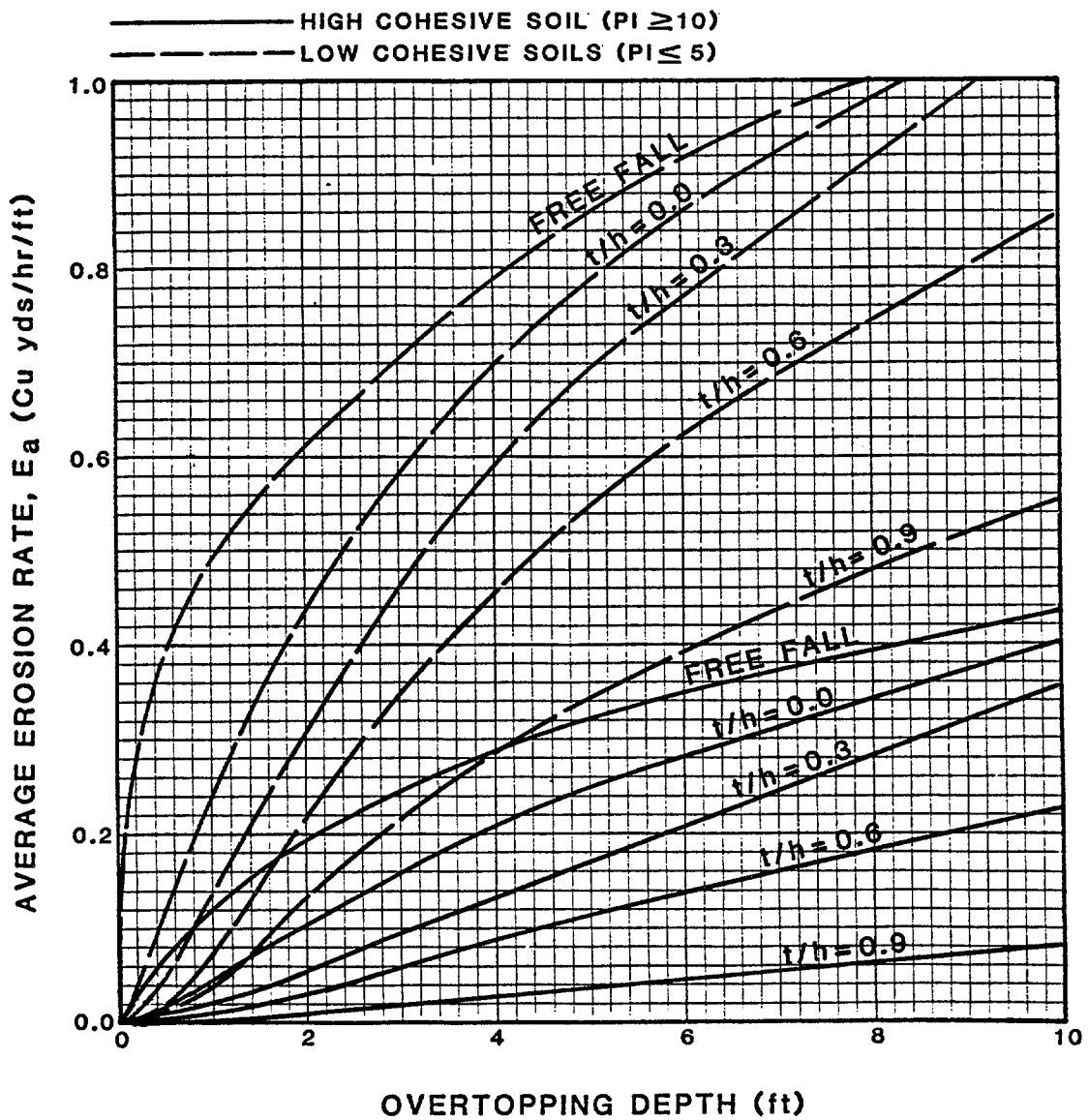
Figure 46. Average erosion rate during 4-hour flow overtopping
of 5-foot cohesive bare soil embankment.
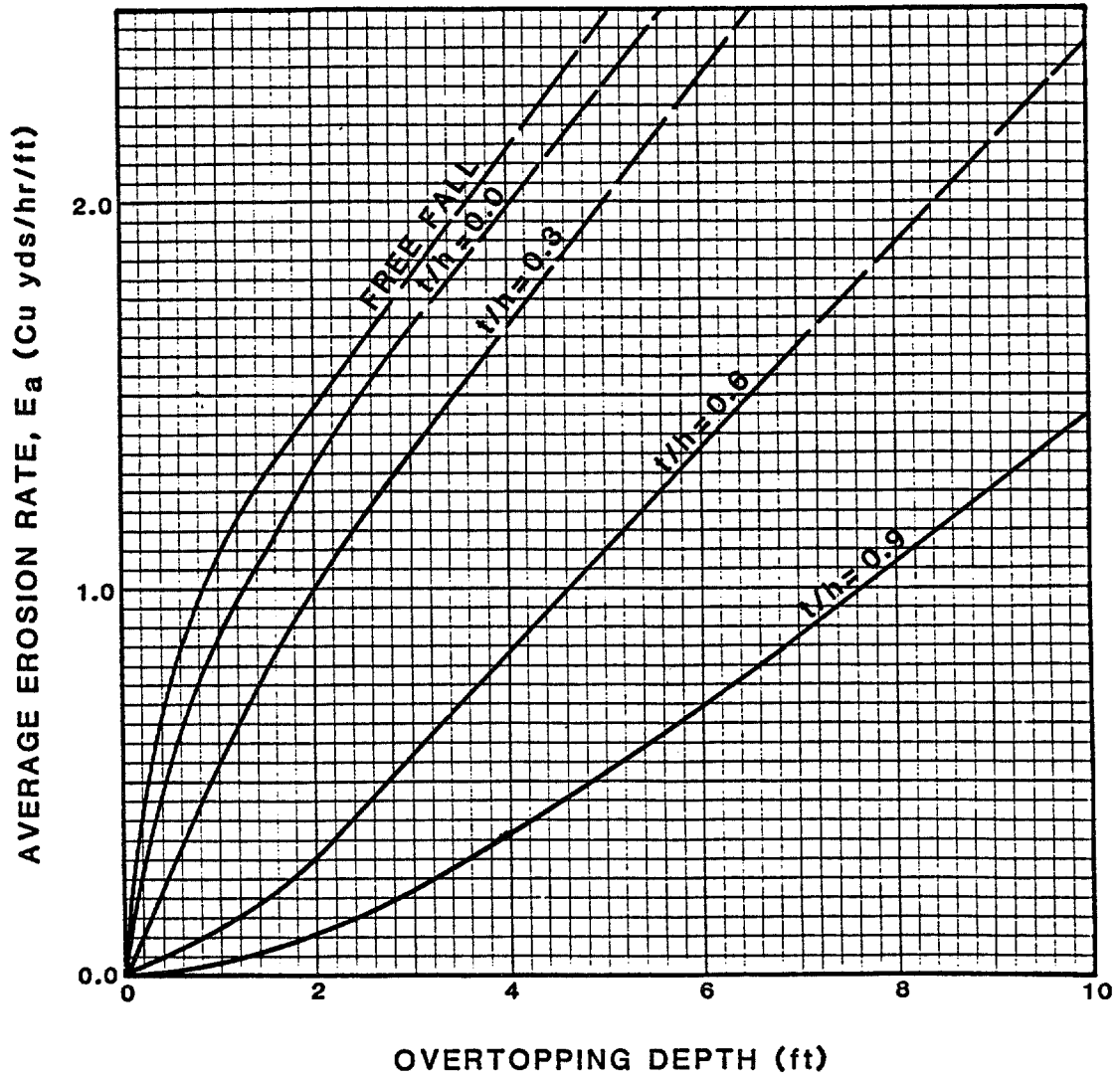
Figure 47. Average erosion rate during 4-hour overtopping
of 5-foot noncohesive bare soil embankment
(d_{50} less than 8 mm).
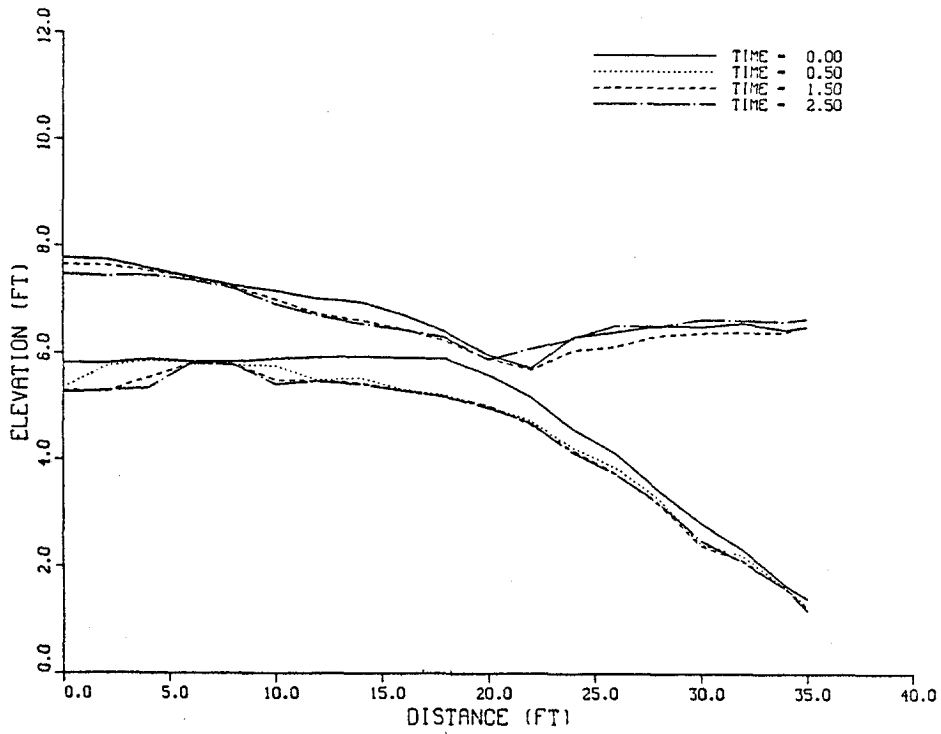
Bare-soil embankment.
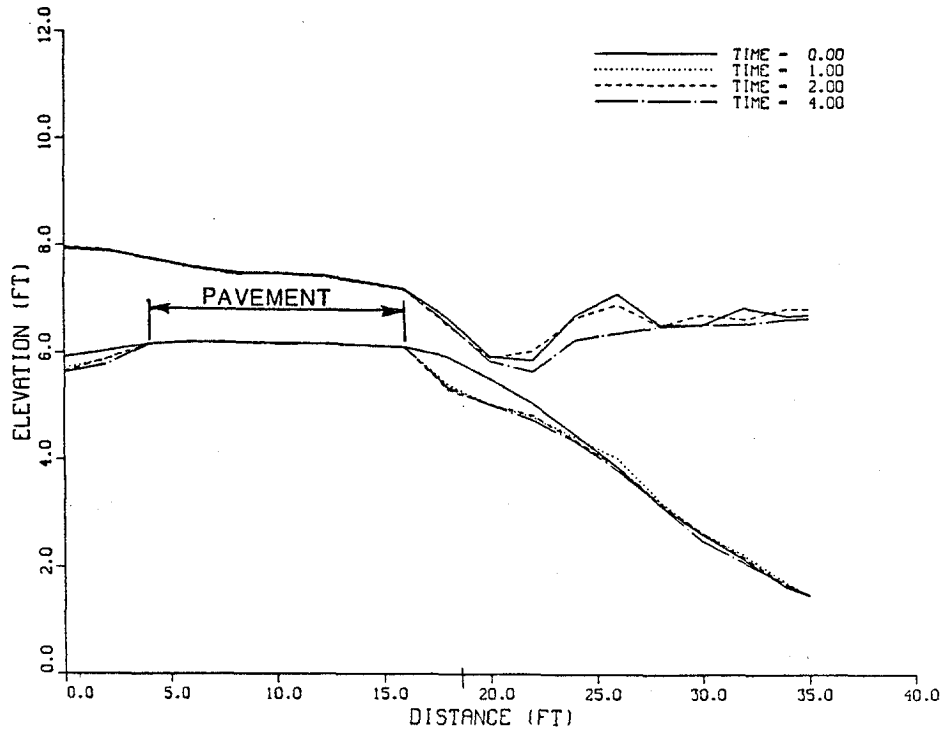
Paved embankment.

Figure 48.   Comparison of erosion rate between the bare soil
embankment with a paved roadway (h = 2 ft,
t/h = 0.3).

110

face area that would be eroded, as shown on figure 48. Figure 49 shows the average erosion rates versus time for these two runs. The pavement reduced the erosion by about 50 percent with t/h = 0.3. When tailwater is low, most erosion would occur near the downstream toe of the embankment and the effect of pavement on erosion is less. Figures 50 through 56 provide a series of nomographs for estimating average erosion rate of paved 5-foot high embankment without and with vegetal cover on embankment slopes during four-hour flood overtopping:

Figure	Base Soil	Vegetal Cover
50	Cohesive	None
51	Noncohesive	None
52	Cohesive	A
53	Cohesive	C
54	Cohesive	E
55	Noncohesive	C
56	Noncohesive	E

The classes of vegetal covers have been defined in table 12. Erosion rates for other conditions can be determined by interpolation.

The laboratory test data clearly showed that the erosion rate reduced with time. Figure 57 shows aproximated relations of $\overline{E}/E_a$ versus time, based on laboratory test data, where $\overline{E}$ is the average erosion rate over a test time period and E_a is the erosion rate during the first four hours. With high tailwater, the water-surface profile of overtopping flow is controlled by the tailwater and remains about the same during the erosion of embankment. Therefore, the velocity and shear stress generally decrease during the progress of embankment erosion and thereby reduce the erosion rate. With low tailwater and free-fall conditions, the reduction in erosion rate with time would be less. Figure 58 provides the adjustment factor when the embankment height is different from 5 feet (1.5 m). Embankment erosion increases with increases in embankment height.

111
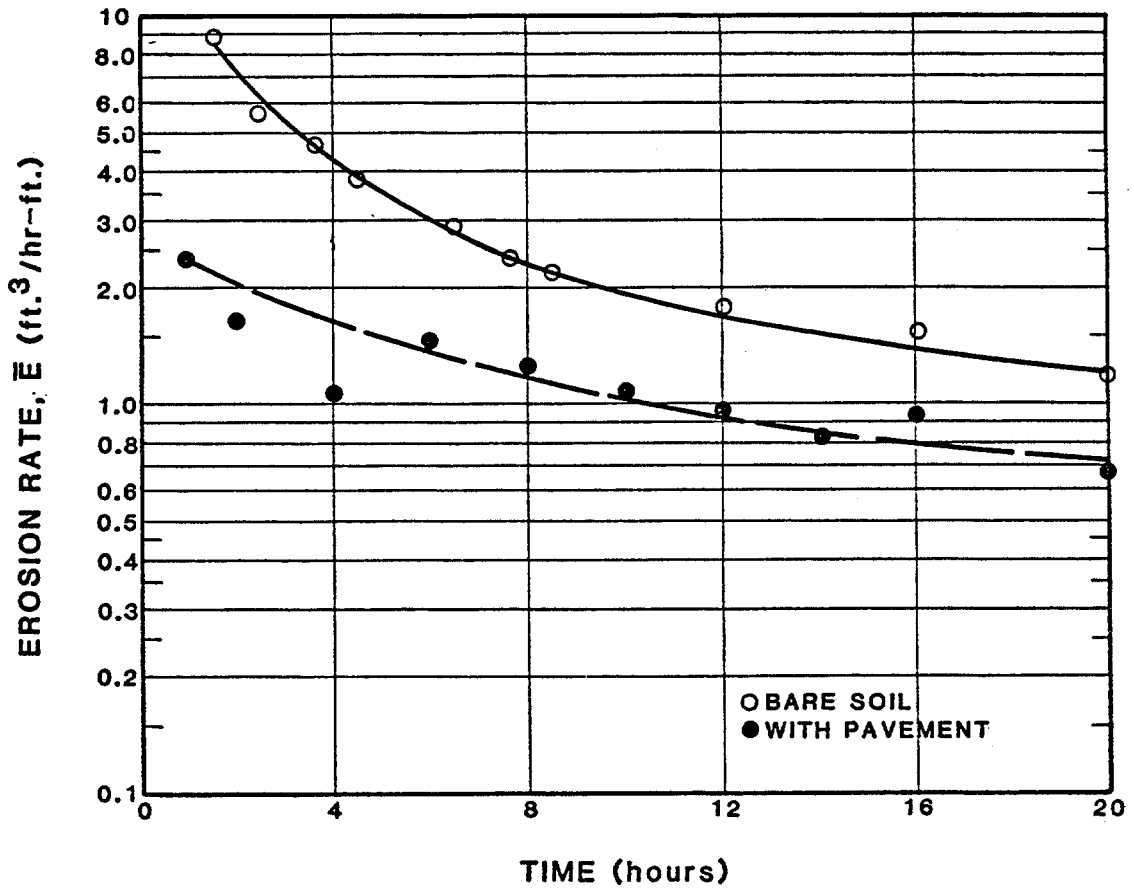
Figure 49. Comparison of erosion rate changes with time between the bare soil embankment and embankment with a paved roadway (h = 2 ft, t/h = 0.3).
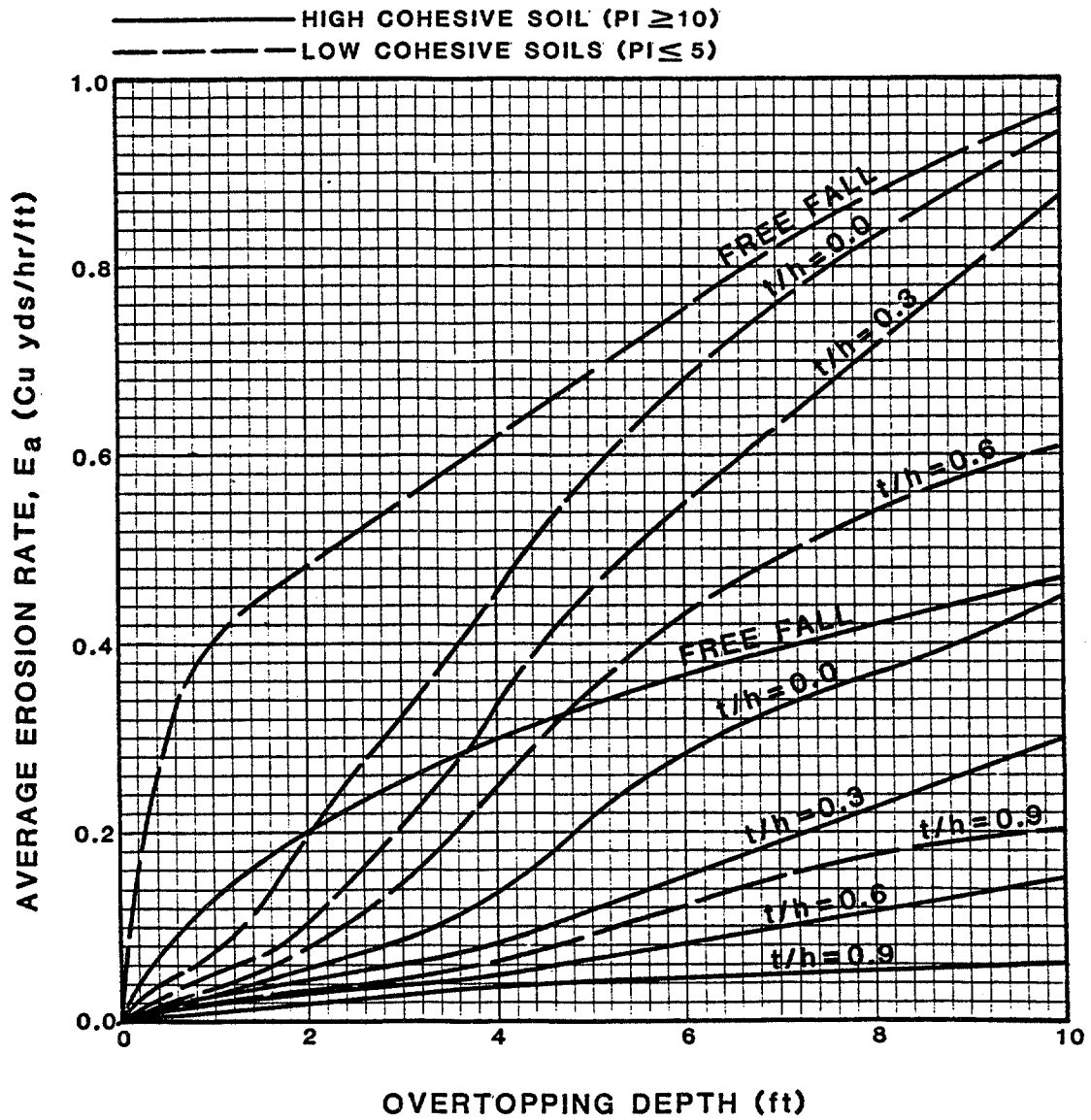
Figure 50. Average erosion rate during 4-hour flow overtopping for 5-foot paved cohesive soil embankment without vegtal cover.

113
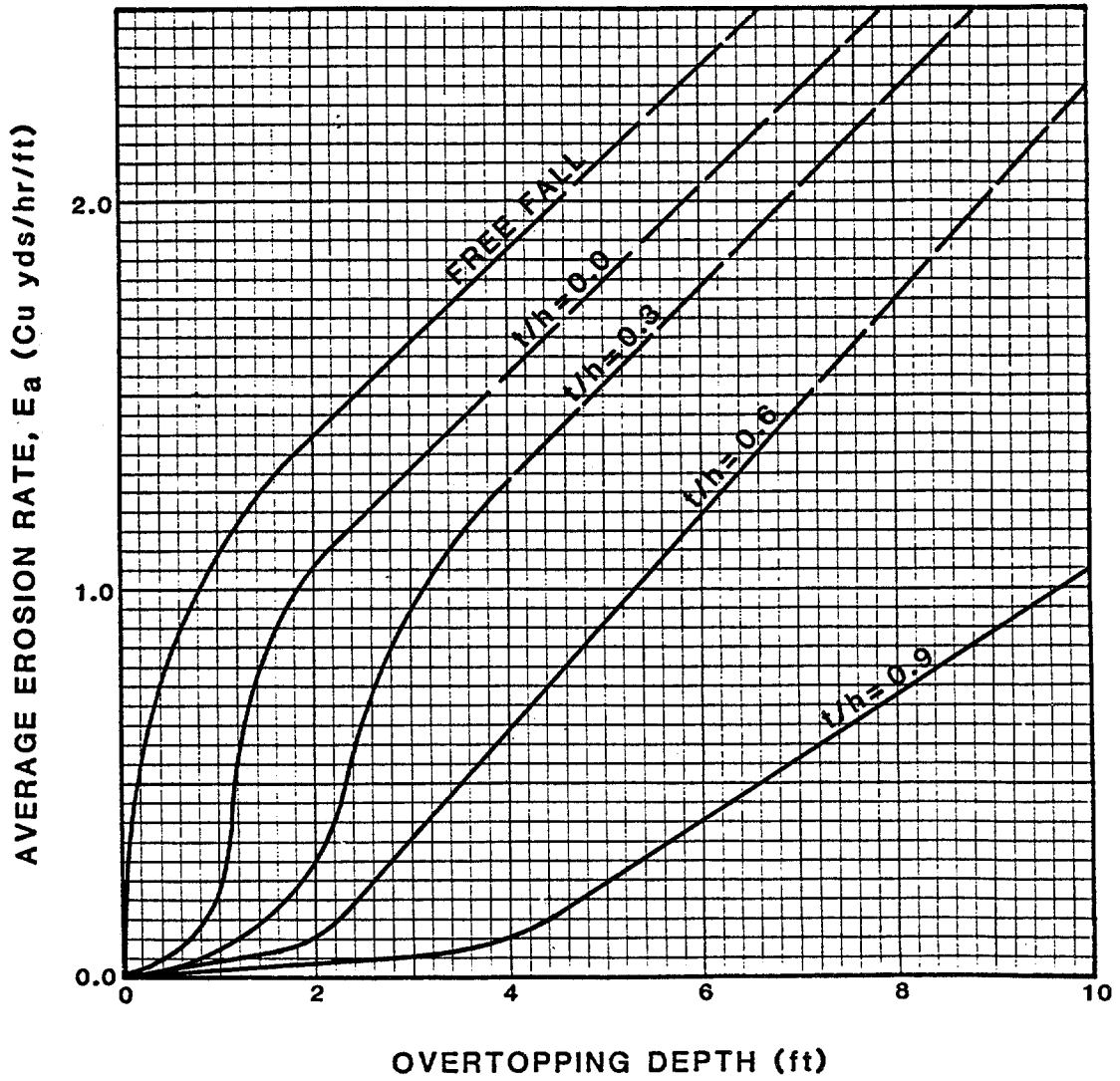
Figure 51. Average erosion rate during 4-hour flow
overtopping of 5-foot paved noncohesive
soil embankment without vegetal cover.

114
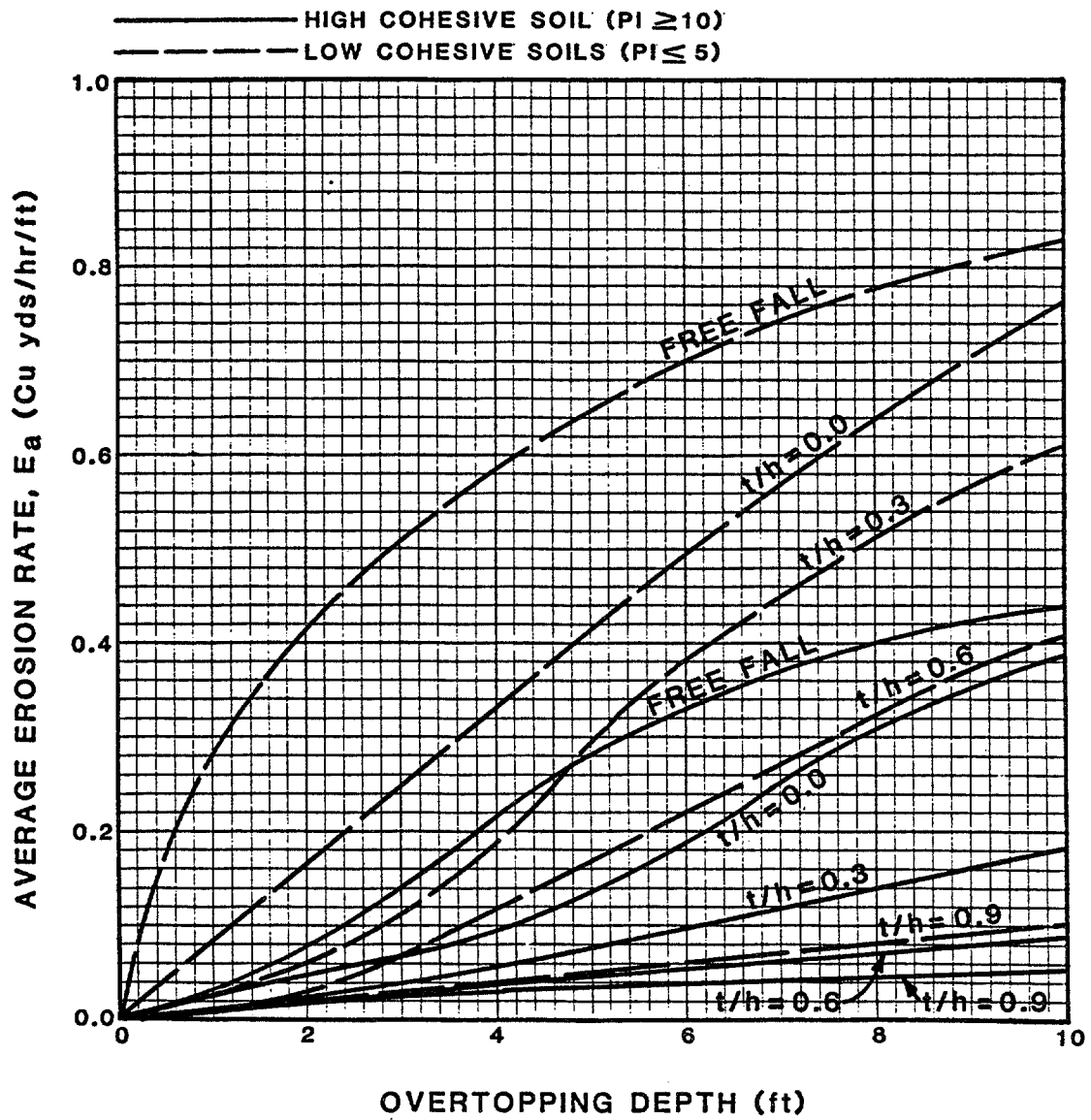
Figure 52. Average flow rate during 4-hour flow
overtopping of 5-foot paved cohesive soil
embankment with class A vegetal cover.
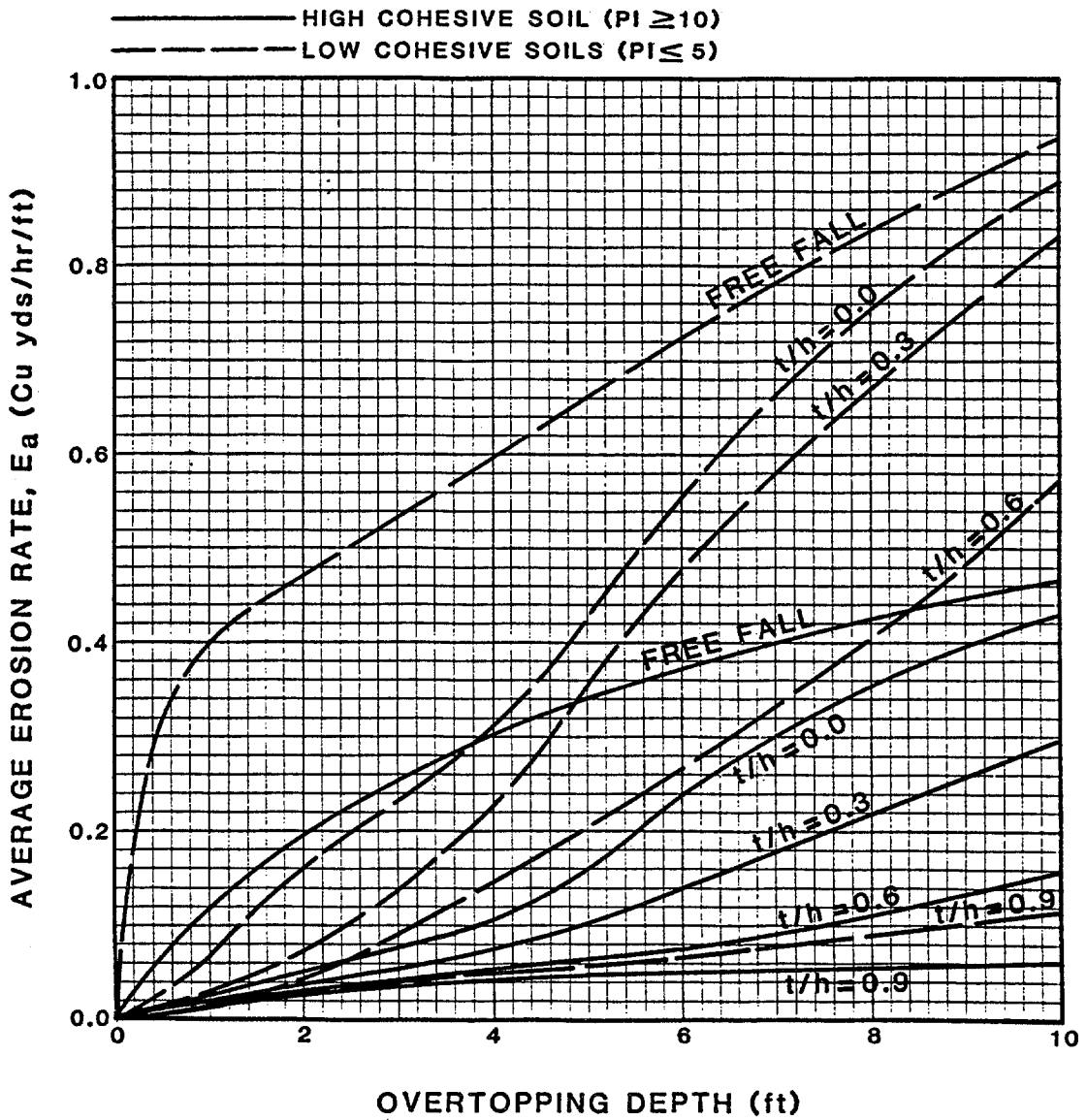
Figure 53. Average erosion rate during 4-hour flow overtopping of 5-foot paved cohesive soil embankment with class C vegetal cover.

116
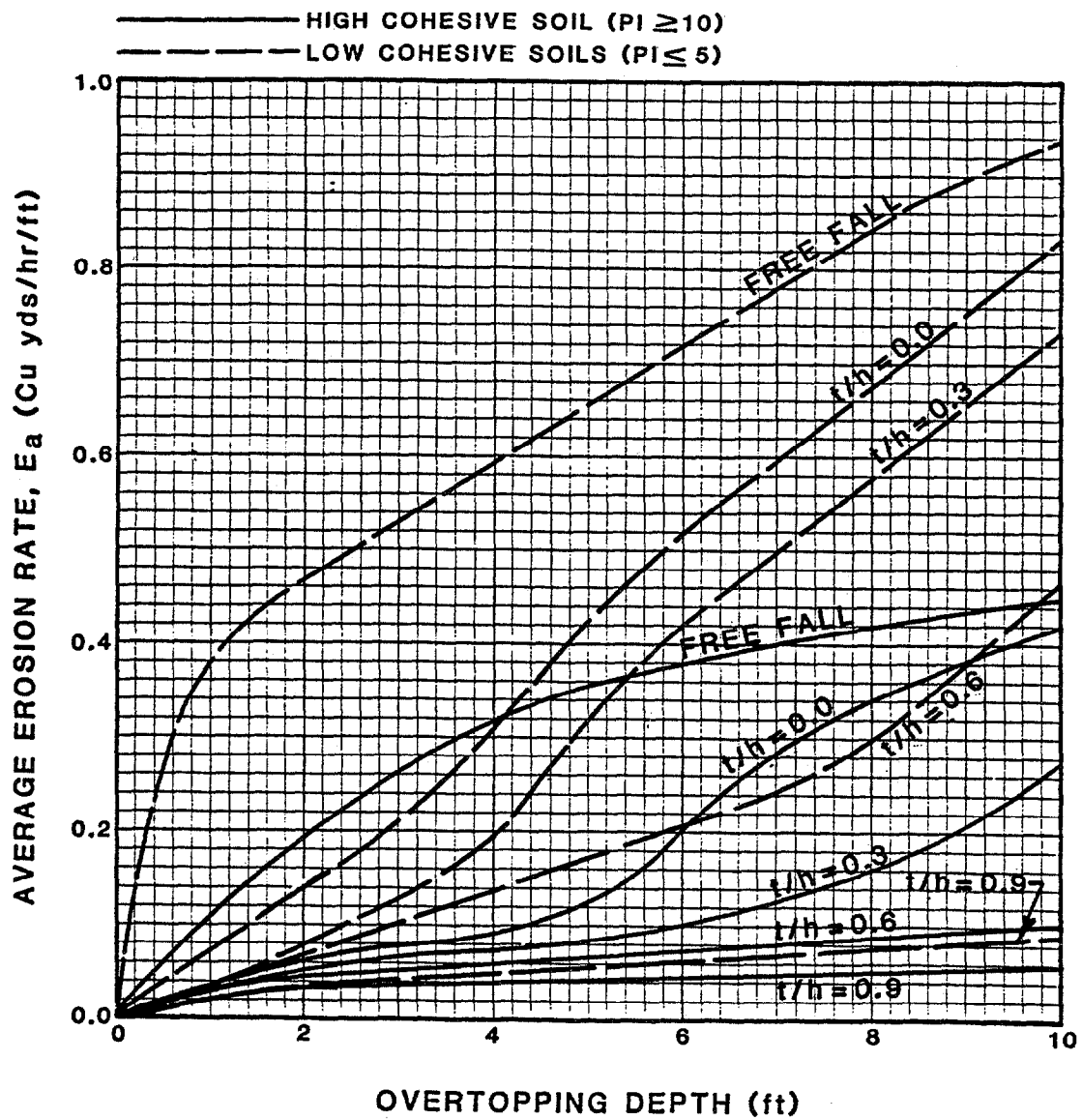
Figure 54. Average erosion rate during 4-hour flow overtopping of 5-foot paved cohesive soil embankment with class E vegetal cover.

117
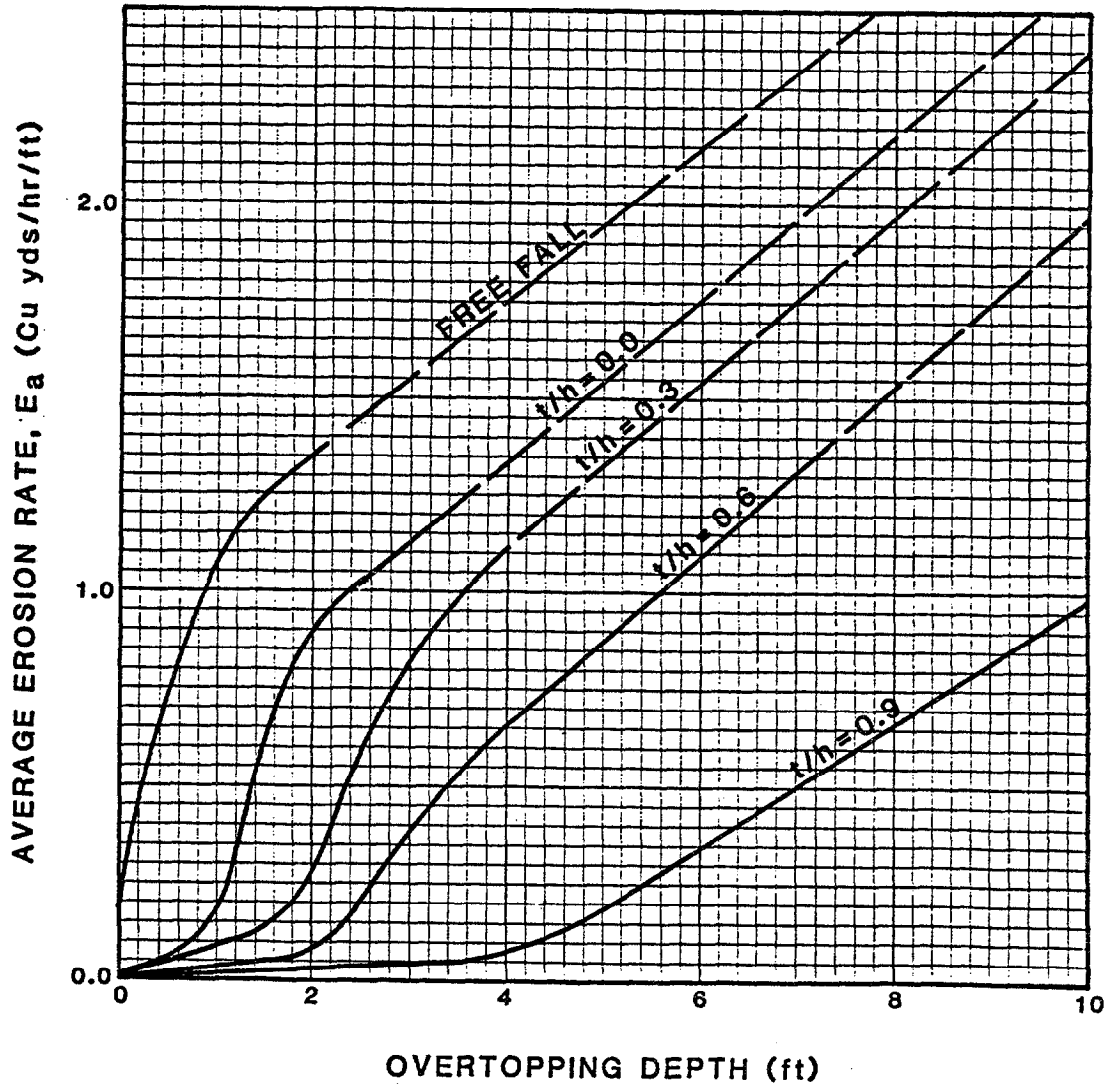
Figure 55. Average erosion rate during 4-hour flow overtopping of 5-foot paved noncohesive soil embankment with class C vegetal cover.

118
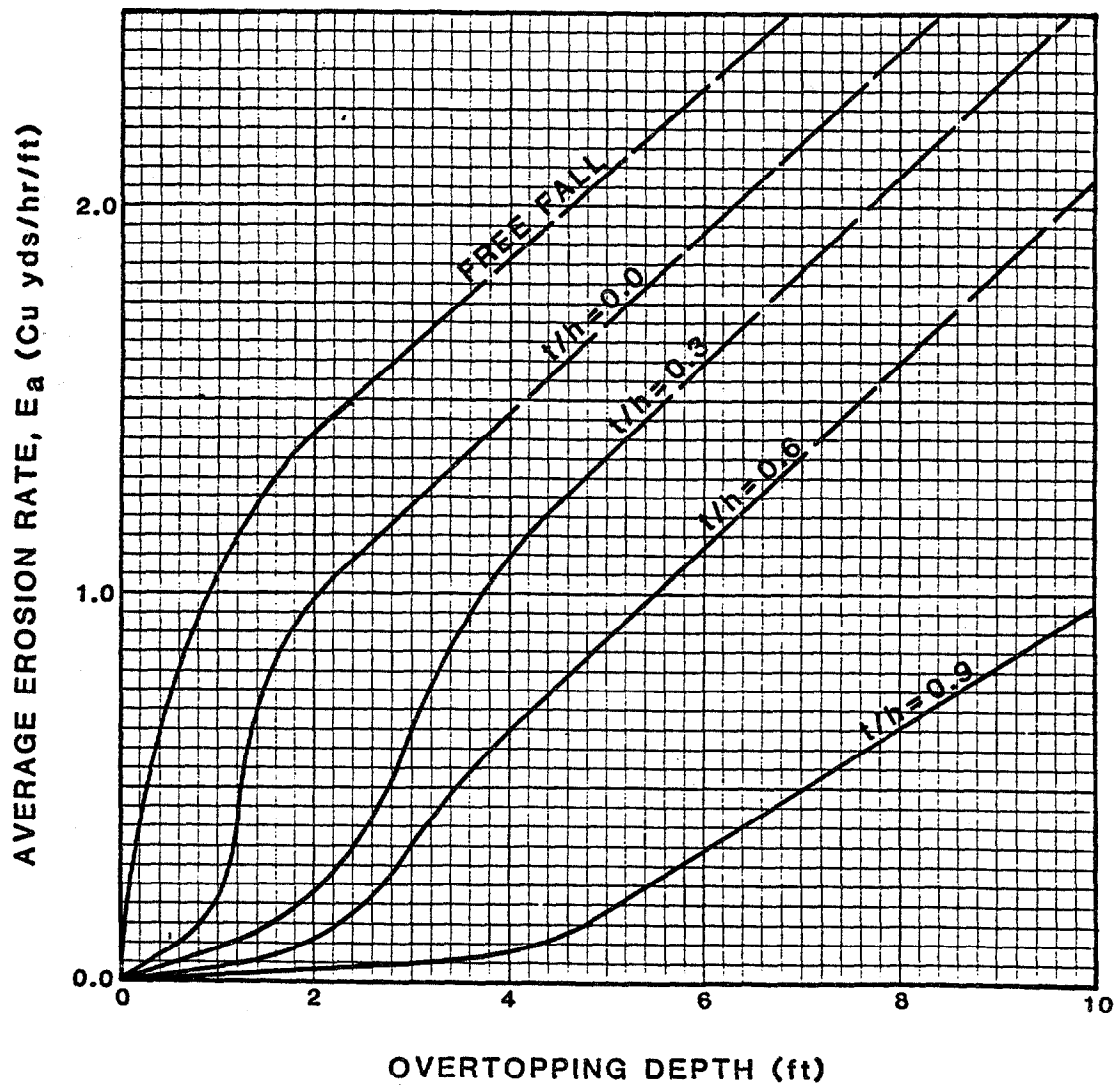
Figure 56. Average erosion rate during 4-hour flow overtopping of 5-foot paved noncohesive soil embankment with class E vegetal cover.
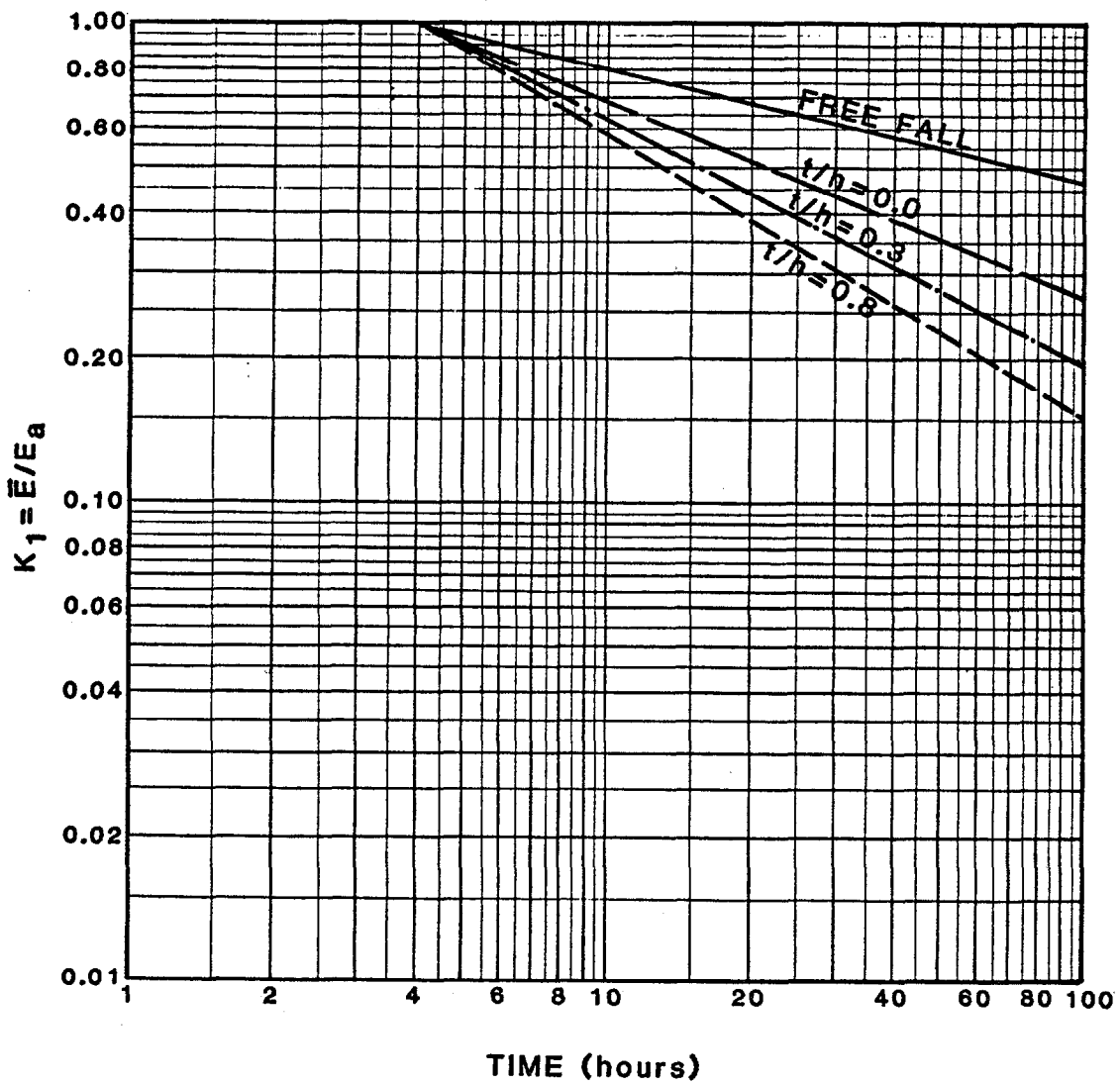
Figure 57. Average erosion rate change with
time duration.

120
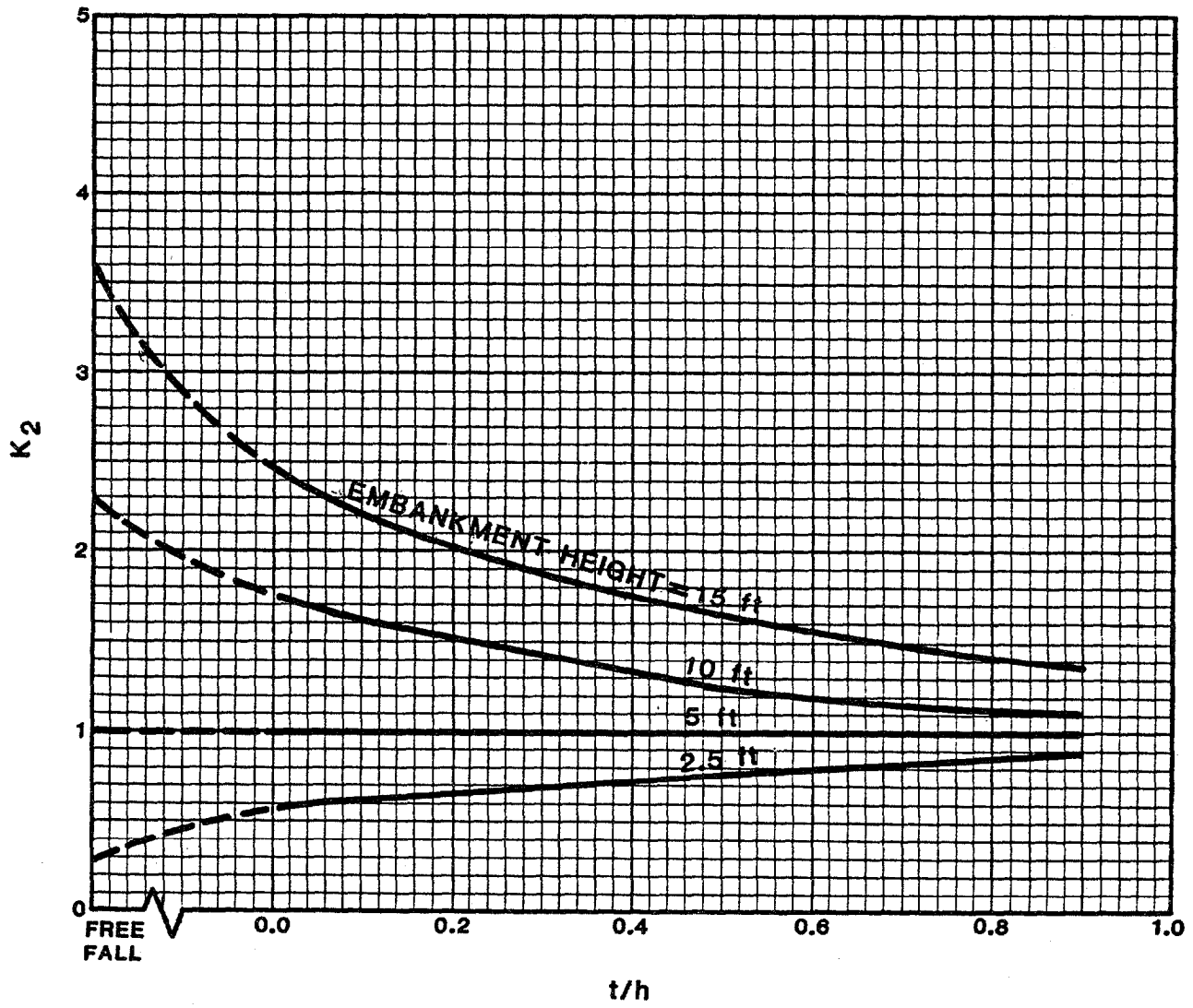
Figure 58. Adjustment factor considering embankment height.

Figures 46, 47, or 50 through 56, coupled with figures 57 and 58, can be applied for estimating embankment erosion rate using the following procedure:

1. Find out the type of embankment base soil (high-cohesive, low-cohesive, or noncohesive soils), embankment height, paved or nonpaved surface, and type of vegetal cover.

2. Select headwater depth, h, and tailwater depth, t, and duration for a design flood (see figure 23 for definition).

3. Compute t/h.

4. With h and t/h enter figure 46 (for cohesive bare soil), figure 47 (for non-cohesive bare soil), or figures 50 through 56 (for paved embankments) to determine erosion rate, E_a, for a 5-foot (1.5-m) embankment.

5. Determine adjustment factor K_1 from figure 57 considering design flood duration.

6. Determine K_2 from figure 50 if the embankment height is different from 5 ft (1.5 m).

7. Compute the average erosion rate over the design flood duration.

$$\bar{E} = K_1 \, K_2 \, E_a \tag{33}$$

The procedures described above were applied to laboratory test data (series FHWA I and II in table 8) and field cases listed on tables 1 and 2. The estimated results were compared to measured erosion rates in figure 59. The agreement is reasonably good. This indicates that the developed nomographs are useful for estimating embankment erosion rates with reasonable accuracy. However, only limited soil bases were considered in developing these nomographs and effects of pavement and grass were evaluated by using limited laboratory data. Therefore, for other types of embankments or for more detailed estimation of embankment erosion, the computer model developed earlier should be utilized. The nomographs and developed computer model should be verified and/or modified using additional field and experimental data.
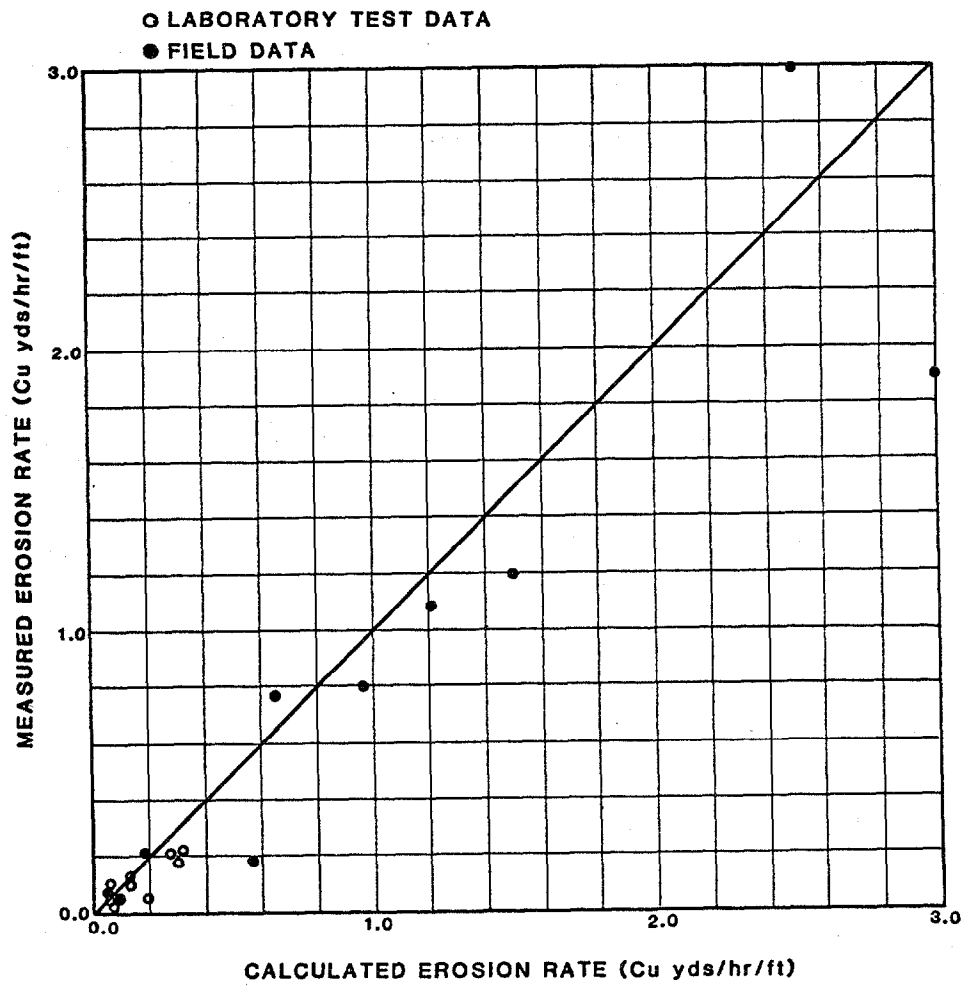
Figure 59. Comparison between calculated and measured embankment damage data.

123

4. Application Examples

Two examples were developed to demonstrate the application of the design nomographs.

a. Example 1. Erosion of a High-Cohesive Earth Road

The hydraulic conditions of overtopping flow are: (1) overtopping depth h = 3 feet (0.92 m), (2) tailwater depth t = 1.8 feet (0.55 m), (3) flood duration T = 20 hours, (4) earth embankment, 10 feet (3.0 m) in height with sparse grass on slope. The procedure follows:

1. Compute $\frac{t}{h} = \frac{1.8}{3.0} = 0.6$.

2. For high-cohesive base soil, find erosion rate E_a = 0.06 yd^3/hr/ft (0.15 m^3/hr/m) from figure 46 for h = 3 feet (0.92 m) and t/h = 0.6.

3. Determine the duration correction factor K_1 = 0.40 from figure 57 for a 20-hour flood and t/h = 0.6.

4. Determine the embankment height correction factor K_2 = 1.16 from figure 58 for t/h = 0.6 and an embankment height of 10 feet (3.0 m).

5. Compute the total erosion volume.

$$V_s = \overline{E}T = K_1\ K_2\ E_a\ T$$
$$= 0.40 \times 1.16 \times 0.06 \times 20$$
$$= 0.56\ \text{yd}^3/\text{ft}\ (1.39\ \text{m}^3/\text{m})$$

b. Example 2. Erosion of a Paved Road With a Low-Cohesive Soil Base

The hydraulic conditions of overtopping flow are: (1) overtopping depth h = 3 feet (0.92 m), (2) tailwater depth t = 0.0 feet, (3) flood duration T

= 20 hrs, (4) paved road, 10 feet (3.0 m) in height with class C grass on slope.

The procedure follows:

1. Compute $\frac{t}{h} = \frac{0.0}{3.0} = 0.0$.

2. For paved low-cohesive soil embankment with class C grass on slope, find erosion rate $E_a = 0.21 \text{ yd}^3/\text{hr}/\text{ft}$ ($0.53 \text{ m}^3/\text{hr}/\text{m}$) from figure 53 for h = 3 feet (0.92 m) and t/h = 0.0.

3. Determine the duration correction factor $K_1 = 0.52$ from figure 57 for a 20-hour flood and t/h = 0.0.

4. Determine the embankment height correction factor $K_2 = 1.76$ from figure 58 for t/h = 0.0 and an embankment height of 10 feet (3.0 m).

5. Compute the total erosion volume

$V_s = \overline{E}T = K_1 K_2 E_a T$

$= 0.52 \times 1.76 \times 0.21 \times 20$

$= 3.84 \text{ yd}^3/\text{ft}$ ($9.64 \text{ m}^3/\text{m}$)

EVALUATION OF EMBANKMENT PROTECTION MEASURES

As described in "Laboratory Embankment Test Program," this study also evaluated the effectiveness of several erosion protection measures. These measures included vegetated embankments and embankments protected with gabion mattresses, soil cement, geoweb, and enkamat. The protection measures were tested under the flow conditions indicated by table 8.

1.   Performance of Protection Measures

For each protection measure tested, a preliminary assessment of the failure mechanism or threshold conditions for failure of the protection measure was conducted. The failure signal was identified by a noticeable change in the water surface during the test or noticeable erosion of the protection measure or embankment material following the test.

The failure mechanism associated with the gabion mattresses appears to be related to the movement of the rocks within the mattress. As the rocks move to the downstream end of each mattress diaphragm, the liner installed beneath the mattress may become exposed. Although a properly installed liner still affords some erosion protection of the embankment material, the moment the liner becomes exposed was construed as the threshold condition for failure. During the tests conducted over the gabion mattresses, the liner did not become exposed. Under the most severe test conditions [4-ft (1.2-m) over-topping depth, free-fall condition], 10 to 20 percent of the rocks in the upstream end of the mattress migrated to the downstream end of the mattress. In general, the gabion mattresses performed very well and in no instance was the embankment in danger of erosion.

The potential failure mechanisms associated with soil cement were initially identified as the presence of surface cracks or the undermining of the layer of soil cement at the toe of the embankment. Due to the nature of the tests, neither failure mechanism was realized. A number of cycles involving

freezing and thawing or wetting and drying of the soil cement layer are the catalyst needed for surface cracks to form. The relatively short testing period prevented this effect. To undermine the toe of the embankment, a section of undisturbed ground is required downstream of the embankment. The concrete floor in the flume prevented the toe erosion from occurring. It is recommended, however, that some means of toe protection be afforded when placing soil cement as an embankment protection measure in the field. In general, the soil cement protective measure performed very well. After 10 hours of testing under the most severe conditions, no erosion was evident in either the soil cement or the embankment material.

For the geoweb grid confinement system, the failure mechanism appears to be associated with the boiling of rocks out of the cells of the geoweb. As the rocks are boiled out, the flow velocity directly impinges on the geoweb structure and creates an elongation of the geoweb section. The elongation effect, in turn, exposes the embankment material to direct erosion by the flowing water. Increased loss of rocks from the cells creates a void in the cells which is filled by the flowing water. Consequently, the water is directed toward the embankment and increases the rate of embankment erosion. In general, the geoweb performed poorly under the configuration tested by this study. Attempts were made to improve the stability of the protection measure by increasing the length and number of staples in the geoweb system. In addition, the configuration of the geoweb system was also changed. In the first series of tests, the geoweb was installed to expand down the sideslope. The second test series found the geoweb installed in a manner which would allow expansion across the sideslope. In all cases, the results were the same. The integrity of the geoweb grid confinement system was maintained for less than an hour during each test.

The failure mechanism associated with enkamat was related to ripping or stretching of the enkamat material or noticeable erosion of the embankment beneath the enkamat. The presence of grass in the enkamat had very little

effect. This resulted from an unsatisfactory stand of grass (density and length) during a growth period of only one year. Due to the relatively short growth period, the root system was not fully developed. The vegetation intermingled with the enkamat was quickly removed during the tests of the enkamat/grass protection measure. For overtopping depths less than or equal to 1 ft (0.3 m), the enkamat material caused a noticeable decrease in flow velocity near the embankment and afforded reasonably good erosion protection. As the flow velocity increased with the increase in overtopping depth, however, the enkamat sustained severe damage from stretching and ripping, and unusually high local scour occurred near the staples. In the initial stapling pattern, the staples were installed perpendicular to the flow at 3-ft (0.9-m) intervals along the embankment. The local scour near the staples was evident to a minor degree during the 0.5 ft (0.15 m) overtopping tests, while ripping and severe stretching of the enkamat occurred at overtopping depths greater than 1 ft (0.3 m). A second stapling pattern was tested in which the staples were installed along the path of the flow. In this case, the local scour near the staples was minimized and only minor stretching/ripping of the enkamat occurred at overtopping depths greater than 1 ft (0.3 m). In all cases, regardless of stapling pattern, minor erosion of the embankment material occurred as the flow velocity increased with overtopping depths greater than 1 ft (0.3 m). In general, enkamat afforded reasonably good erosion protection during the tests of low overtopping depths. As the overtopping depths increased beyond 1 ft (0.3 m), erosion of the embankment appeared to be accelerated by the presence of the enkamat.

For embankments vegetated with grass, the failure mechanism was associated with the direct erosion or loss of grass. In tests with low velocities and overtopping depths [0.5 ft (0.15 m)], the grass-lined embankment appeared to perform well. In tests with overtopping depths greater than 0.5 ft (0.15 m), pockets of grass were removed and induced the formation of local scour along the embankment. A partial explanation of this phenomenon may be the existence of weak spots along the embankment or areas where the root system of

the grass was not fully established. In addition to the local scour, severe toe erosion occurred during the tests involving overtopping depths of 2 and 4 ft (0.6 and 1.2 m). Although grass-lined slopes usually retard the flow velocity and reduce erosion, these tests did not confirm those results.

2. Comparison of Protection Measures

Based on the results of the flood overtopping tests, a comparison of erosion protection measures can be made. If comparison is based solely on the test results, soil cement and gabion mattresses performed very well in protecting the embankment from erosion. Enkamat, grass, and geoweb accelerated embankment erosion in some cases. Additional factors must also be taken into account, however, in the evaluation process. These factors are discussed in the paragraphs that follow.

Soil cement performed the best of all erosion protection measures. No erosion of the soil cement or embankment material was evident in any of the tests conducted. It must be noted, however, that these were short-term tests. The failure mechanism associated with soil cement involves long-term weathering processes. In addition, placement of soil cement is subject to the local availability of suitable soil material for mixing with the cement. Finally, a form of toe protection is recommended with the soil cement protection measure. Based on the results of this study, additional testing of soil cement as a protection measure should include:

1. Develop a technique, such as rotating cylinders, to measure the rate of wear of soil cement (with various proportions of cement) due to flow erosion and weathering, and thereby determine proper thickness and cement ratio.

2. Investigate the long-term weathering process for failure of the soil cement, i.e., subject the protection measure to a winter weathering process before testing.

3. Vary the slope at which the protective measure is tested.

4. Test a different configuration of the protection measure, such as a stairstep configuration or placement in 6-inch (0.15-m) lifts.

Gabion mattresses performed very well during the flood overtopping tests. Minimal failure of the gabion mattress occurred, and when failure was evident, it appeared only during the most severe flow condition. No erosion of the embankment material occurred in any test. An important aspect of the gabion mattress, however, is the deterioration of the wire basket with time. For mattresses which sustain periodic wetting and drying, the deterioration will occur much faster. The installation of gabion mattresses is also the most labor intensive of all the protection measures tested by this study. As with soil cement, toe protection is recommended with the installation of gabion mattresses. Additional testing of this protection measure may include:

● Variation in the thickness of the gabion mattresses and the size of rock-fill material.

● Variation in the slopes at which the protective measure is tested.

Enkamat performed well during tests involving the low overtopping depths. Minimal, if any, erosion of the embankment was observed and the enkamat maintained its structural integrity. For overtopping depths greater than 1 ft (0.3 m), however, enkamat accelerated the erosion of the embankment. Enkamat was the least labor intensive of all the protective measures, but its effectiveness depended greatly upon the type and pattern of the staples. Toe protection is also required with enkamat. Enkamat has potential to be an effective protective measure if properly installed. Proper installation would include a liner beneath the enkamat, an appropriate stapling pattern, and a well-established growth of vegetation combined with the enkamat material. Additional testing of enkamat is recommended, and should include:

● Testing an installation involving a liner and enkamat.

130

- Testing a well-established growth of vegetation in place on the enkamat material. This type of test would require a long term (maybe two years), but the results would be very enlightening.

- Testing the enkamat with an improved stapling pattern and an asphalt mixture on top of the enkamat.

- Varying of the slope at which the protection is tested.

- Testing a well established sod on the enkamat material. The sod could be established under ideal growth conditions, rolled onto the test embankment, and stapled properly.

The geoweb grid confinement system geoweb performed poorly in comparison with the other protective measures. The main problem with the geoweb was the boiling of rocks from the cells of the system. As this occurred, the embankment was subject to direct erosion by the flowing water, and in most cases, erosion of the embankment was accelerated by the geoweb. As with enkamat, toe protection will be required. In spite of the test results, geoweb may have potential to be an effective protective measure. Additional testing of the geoweb is recommended, and should include:

- Testing a variety of measures which prevent boiling of rocks from the cells of the geoweb, (e.g., cap the geoweb with asphalt, soil cement, or a wire netting).

- Varying the slope at which the protection measures are tested.

The results of the tests over grass-protected embankments were inconsistent with previous tests results. For flows with low overtopping depths, the grass-lined embankment performed reasonably well. Higher overtopping depths, however, indicated an increase in erosion with a grass-lined embankment. The nature of the increase in erosion is attributable to the occurrence of local scour following the removal of a pocket of vegetation. These results are inconclusive and additional tests are recommended.

3. Hydraulic Stability of Protection Measures

Table 15 shows the hydraulic conditions of flow overtopping the protection measures before significant failure occurred. The velocity and shear

131

Table 15. Evaluation of critical conditions for the protection measures.

Protection Measure	Overtopping Depth (ft)	Discharge (ft³/s-ft)	Average Flow Depth (ft)	Average Velocity (ft/s)	Maximum Velocity (ft/s)	Energy Slope	Manning's n	Shear* Stress (lb²/ft²)	Remarks
Geoweb	1.0	3.0	0.38	7.9	8.3	0.27	0.051	1.0	Significant toe erosion occurred after 9 hours of test.
Gabion	1.0	3.0	0.42	7.1	7.9	0.34	0.068	1.0	Stable
Gabion	2.0	8.4	0.82	10.2	10.9	0.27	0.066	2.0	Stable
Gabion	4.0	25.0	1.59	15.7	17.2	0.22	0.060	5.0	Some rock migrated, but gabion remained stable.
Soil Cement	1.0	3.0	0.32	9.4	11.5	0.21	0.034	0.6	Stable
Soil Cement	2.0	8.4	0.55	15.3	18.0	0.11	0.022	1.6	Stable
Soil Cement	4.0	25.0	1.48	16.9	20.0	0.022	0.017	1.9	Stable
Enkamat	1.0	3.0	0.38	7.9	8.0	0.28	0.051	1.0	Stable
Enkamat	2.0	8.4	0.80	10.5	12.0	0.15	0.047	2.5	Some erosion
Grass	0.5	3.0	0.17	5.9	6.1	0.33	0.044	0.4	Stable

*Note: Shear stress $\tau = \frac{1}{8}\rho f V^2$, where ρ is the water density, f is Darcy-Weisbach coefficient and V is the velocity.

Based on Information by Chow,[6] f = 0.02 (soil cement), 0.04 (grass), 0.06 (geoweb), 0.07 (enkamat and gabion).

stress of flow given in table 15 provide indications of stability and roughness of the protection measures. In general, erosion of the geoweb system started when the flow velocity exceeded 8.0 ft/s (2.4 m/s). Rocks within each gabion were observed to migrate as the flow velocity exceeded 15 ft/s (4.6 m/s). However, gabion still provided sufficient protection during the 15-hour testing period. Even at velocities in excess of 20 ft/s (6.1 m/s), no failure of soil cement was observed. Damage to the enkamat material was observed when the flow velocities exceeded 10 ft/s (3 m/s). Based on the tests conducted, the critical velocities associated with the various protection measures are given in table 16. Table 16 also includes critical shear stress recommended by Chen and Cotton[19] for gabion, enkamat, and grass.

Table 16. Critical velocity associated with protection measures.

Protection Measures	Critical Velocity (ft/s)	Critical Shear Stress (lb/ft^2)
Geoweb	6.0	0.7
Gabion	15.0	4.0
Soil Cement	>20.0	---
Enkamat	10.0	2.0
Grass	Varies (see table 12)	Varies

SUMMARY AND CONCLUSIONS

The objectives of this project were to perform a review of literature, collect field data, and conduct laboratory tests to develop a methodology to quantitatively determine embankment damages due to flood overtopping and to assess protection measures. A comprehensive literature review was conducted to identify existing research works and data pertinent to embankment damage due to flood overtopping and protection measures. Seventy-nine reports and papers were identified as potentially useful to the study. These reports and papers were reviewed to identify important parameters that control embankment damage, investigate the failure mode of embankments, and assess effects of protection measures on the embankment due to flood overtopping and other factors. Very limited data are available for quantitatively estimating embankment damage due to flood overtopping.

Field data of roadway erosion caused by flood overtopping were collected at five sites in Arkansas, three sites in Missouri, seven sites in Wyoming, one site in Colorado, and five sites in Arizona. These field data were analyzed and utilized to evaluate the methodology developed for determining the embankment damage due to flood overtopping.

Embankment overtopping tests were conducted in a large flume. The embankments tested in this study were 6 ft (1.8 m) high, 10 to 22 ft (3.0 to 6.7 m) in crest width, and 3 ft (0.9 m) in length, with slopes varying from 2:1 to 3:1. The embankment surfaces which were tested included various combinations of two surface materials (bare soil and pavement), along with five protective measures (grass, rock-filled mattresses, geoweb, soil cement, and enkamat). Two base soils forming the embankments were tested, including soils classified as a clay of low plasticity (CL) and a sandy clay (SM-SC) by the Unified Soil Classification. The flood overtopping conditions include overtopping depths ranging from 0.5 to 4 ft (0.15 to 1.2 m), discharges ranging from 1 to 25 ft^3/s-ft (0.031 to 0.77 m^3/s-m), and tailwater conditions ranging

from 10 percent water surface drop to free fall. The embankment test program included fixed-flume tests and tests which necessitated the movement of the flume. For the tests that did not involve grass, embankments were constructed inside the flume by filling material in 6-inch (0.15-m) lifts and mechanically compacted to obtain the compaction required (95 percent of maximum dry density, Standard Proctor). For the tests involving grass, the flume was moved to an embankment slope constructed in accordance with Federal Highway Administration specifications and vegetated with grass.

Also a series of fixed-bed embankment tests were conducted to determine the hydraulic conditions of overtopping flow. This set of data was analyzed along with small-scale model data conducted by Kindsvater[4] to determine discharge coefficients, flow patterns, velocity distribution, and shear stress over an embankment. It was found that flow patterns and discharge coefficients determined from the small-scale model tests are applicable to the prototype conditions. When tailwater was high, free surface flow or submerged flow occurred with the flow jet separating from the roadway at the downstream shoulder and "rides" over the tailwater surface. Flow velocity near the downstream slope surface became reversed. When tailwater was low, free plunging flow occurred when the jet plunged under the tailwater surface, producing a submerged hydraulic jump on the downstream slope. The plunging flow causes more erosion of embankment than the surface flow for the same overtopping depth. A mathematical model was established to determine the hydraulic conditions of overtopping flow.

Bare-soil embankment tests were analyzed to evaluate existing embankment erosion equations. The results of the evaluation indicate that in general the erosion rate can be related to a net shear stress by a power relation. A relation was then developed to determine the critical shear stress as a function of plasticity index. Three equations were established to determine embankment erosion rate for high-cohesive, low-cohesive, and noncohesive soils.

A mathematical model was then developed by integrating the hydraulic model with the soil erosion equations to determine embankment erosion due to flood overtopping. This model was calibrated using the bare-soil test data (FHWA test series I and II). The calibrated model was utilized to generate three sets of nomographs for determining the embankment erosion rates for high-cohesive (PI $\geq$ 10), low-cohesive (1 < PI $\leq$ 5) and noncohesive soils. The effects of embankment heights, flood duration, pavement and grass are considered in the procedure. The developed procedure was evaluated using field data with reasonable agreement. Two examples were developed to explain the applications of this procedure. It should be pointed out that only limited soil bases were considered in developing these nomographs, and effects of pavement and grass were assessed by using limited laboratory data. For embankment with soil significantly different from those analyzed, or for more detailed estimation of embankment erosion, the computer model developed should be utilized. These nomographs and the computer model should be verified and/or modified when additional field and experimental data become available.

The effectiveness of five erosion protection measures was evaluated: gabion mattresses, soil cement, geoweb, enkamat, and grass. Critical velocities that initiate the erosion of these protection materials were estimated. It was found that gabion mattresses and soil cement performed very well during the flood overtopping tests. Some rock movement was observed during the gabion tests. However, no erosion of the embankment material occurred in the tests. An important aspect of the gabion mattress, however, is the deterioration of the wire basket with time. Additional testing of gabion mattresses may include:

● Variation in thickness of the gabion mattresses and the size of rock-fill material.

● Variation in the slopes at which the protective measure is tested.

Soil cement performed the best of all erosion protection measures tested in the study. No erosion of the soil cement or embankment material was evi-

136

dent in the tests. However, the long-term weathering effects and potential toe erosion were not evaluated in the study. Additional testing of soil cement may include:

- Develop a technique to measure the rate of wear due to flow erosion and weathering and thereby to determine proper thickness and cement content.

- Investigate the long-term weathering process for failure of the soil cement.

- Vary the slope at which the protective measure is tested.

- Test a different configuration of the protection measure.

Enkamat performed well during tests involving the low overtopping depth. For overtopping depths greater than 1 ft (0.3 m), however, enkamat accelerated the erosion of the embankment because of additional turbulence generated at the staples and ripped enkamat. Enkamat has the potential to be an effective protective measure if properly installed. Proper installation would include a liner beneath the enkamat, an appropriate stapling pattern, and a well-established growth of vegetation combined with the enkamat material. Additional testing is recommended:

- Test an installation involving a liner and enkamat.

- Test a well-established growth of vegetation on the enkamat material.

- Test the enkamat with an improved stapling pattern and an asphalt mixture on top of the enkamat.

- Varying the slope at which the protection is tested.

The geoweb grid confinement system with geoweb filled with 1- to 2-inch (25- to 51-mm) gravel performed poorly in comparison with the other protective measures. The main problem with the geoweb focused upon the boiling of rocks from the cells of the system. As this occurred, the embankment was subject to direct erosion by the flowing water, and in most cases erosion of the embankment was accelerated by the geoweb. In spite of the test results, geoweb may

137

also have potential to be an effective protective measure. Additional testing of the geoweb is recommended.

- Test measures which prevent boiling of rocks from the cells of the geoweb.

- Vary the slope at which the protection measures are tested.

The results of the tests over grass-protected embankments indicated results inconsistent with previous tests results. For flow with low over-topping depths, the grass-lined embankment performed reasonably well. Higher overtopping depths, however, caused an increase in erosion with a grass-lined embankment. The nature of the increase in erosion is attributable to the occurrence of local scour following the removal of a pocket of vegetation. These results are inconclusive, and additional tests are recommended.

APPENDIX A - PHOTOGRAPHS ILLUSTRATING LABRATORY TESTS CONDUCTED IN THIS STUDY

The following series of photographs depict the embankment following the laboratory tests. Photographs are not provided for every test conducted during this study. In particular, no photographs are provided for the soil cement tests. Erosion of the soil cement embankment protection measure was not evident following the completion of testing. For an illustration of the soil cement embankment protection measure, refer to figure 17 in the main report.

The first series of photographs illustrate the erosion of the bare-soil embankment (figures 60 to 62). Erosion of the paved embankment with and without vegetation is provided in figures 63 to 66. The erosion protection afforded by gabion protection measure is illustrated in figures 67 to 69. Figures 70 to 73 depict the erosion of the geoweb material. Finally, the erosion of the embankment sustained during the utilization of enkamat is illustrated in figures 74 to 76.

Figure 60. Bare-soil surface (Type I Soil) following overtopping depth of 0.5 feet and 20 percent water surface drop.

Figure 61. Bare-soil surface (Type II Soil) following overtopping depth of
1 foot and 70 percent water surface drop.
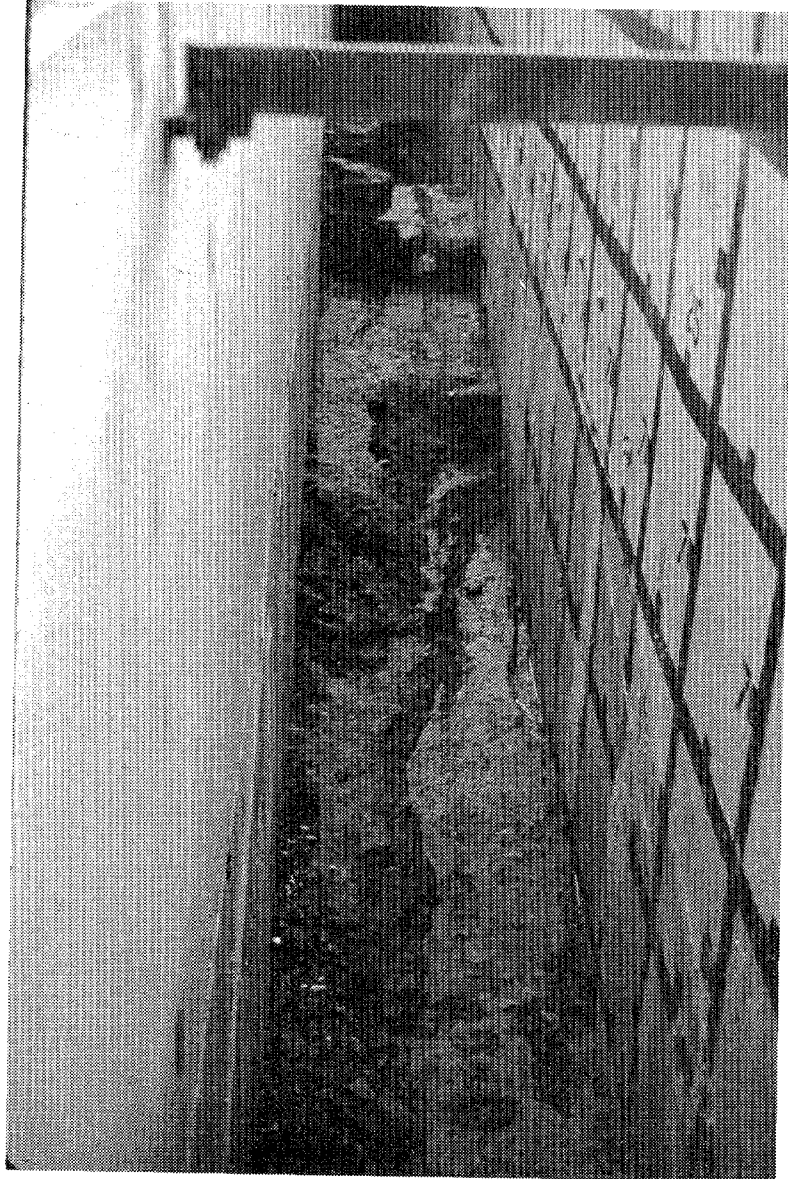
Figure 62. Bare-soil surface (Type II Soil) following overtopping depth of
2 feet and freefall conditions.
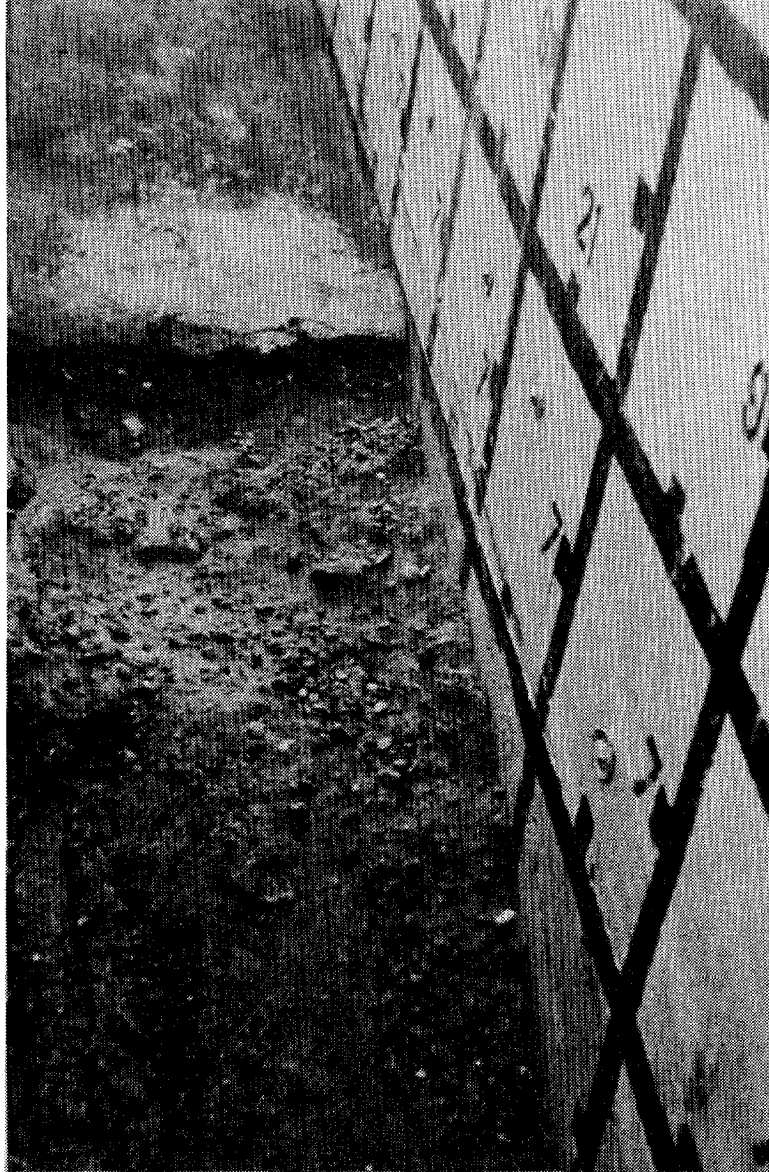
Figure 63. Paved embankment (Type II Soil) without vegetation following overtopping depth of 0.5 feet and 70 percent water surface drop.

143

Figure 64. Paved embankment (Type I Soil) with vegetation following
overtopping depth of 0.5 feet and 70 percent
water surface drop.

144
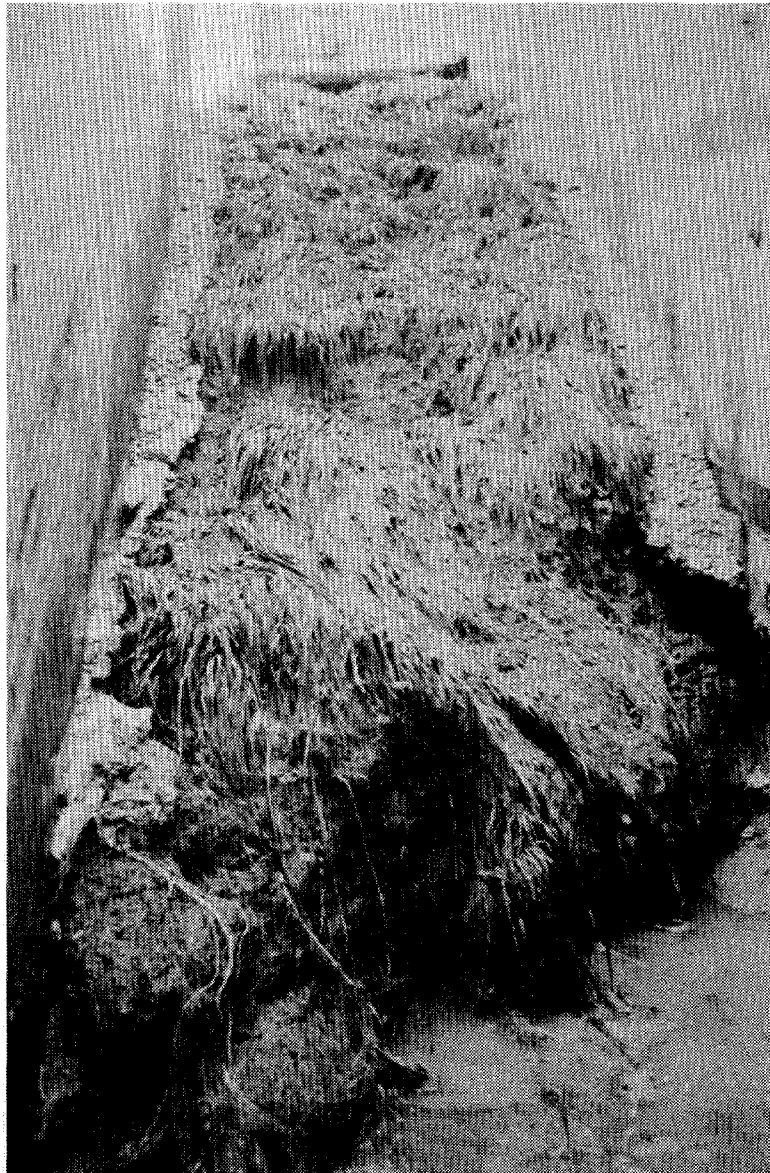
Figure 65. Paved embankment (Type I Soil) with vegetation following overtopping depth of 1 foot and 70 percent water surface drop.

145
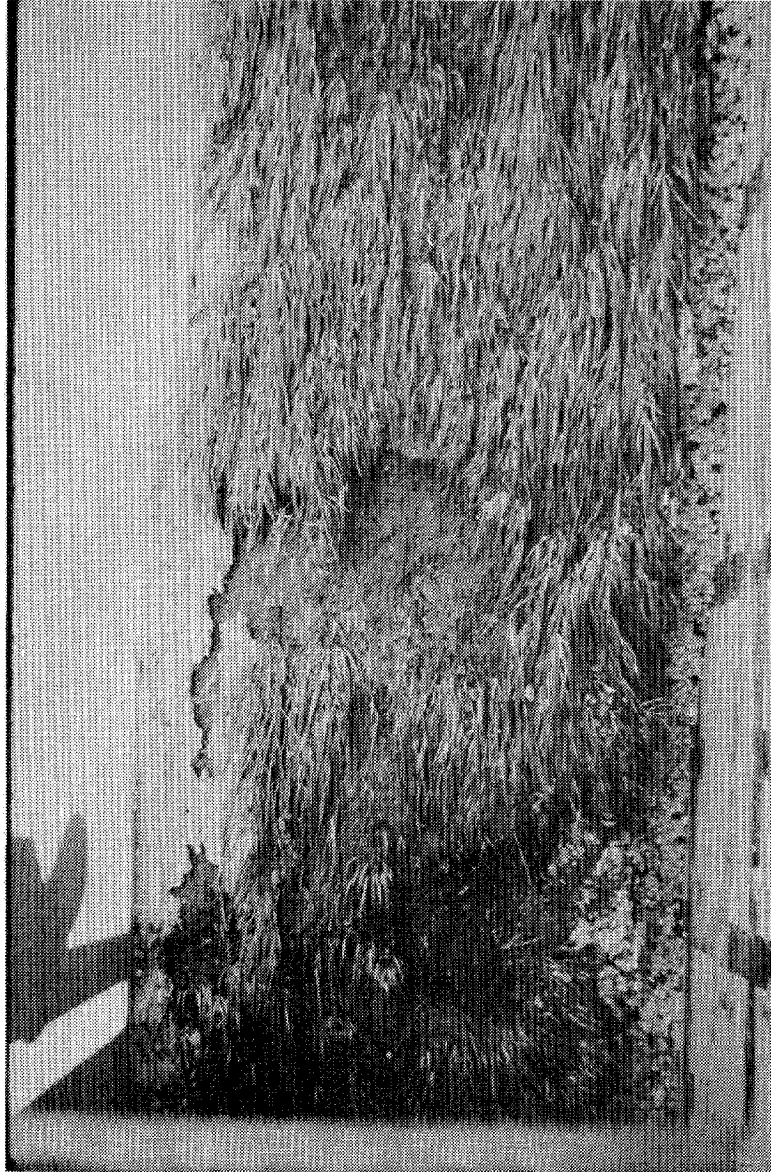
Figure 66. Paved embankment (Type I Soil) with vegetation following overtopping depth of 0.5 feet and freefall conditions.

146
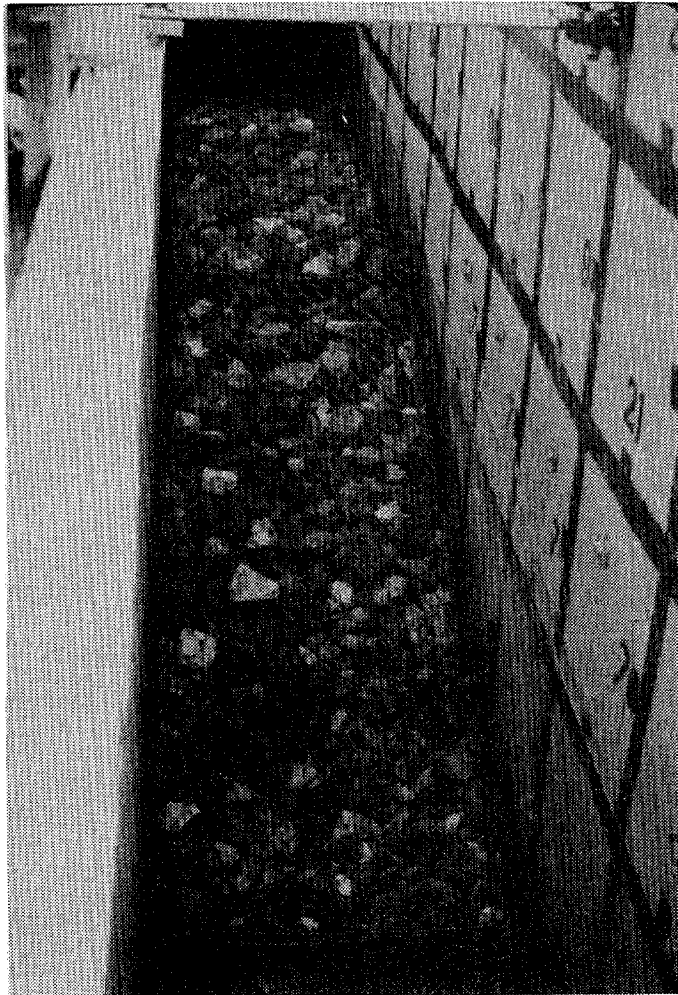
Figure 67. Gabion protection following overtopping depth of 1 foot and free fall conditions.

147
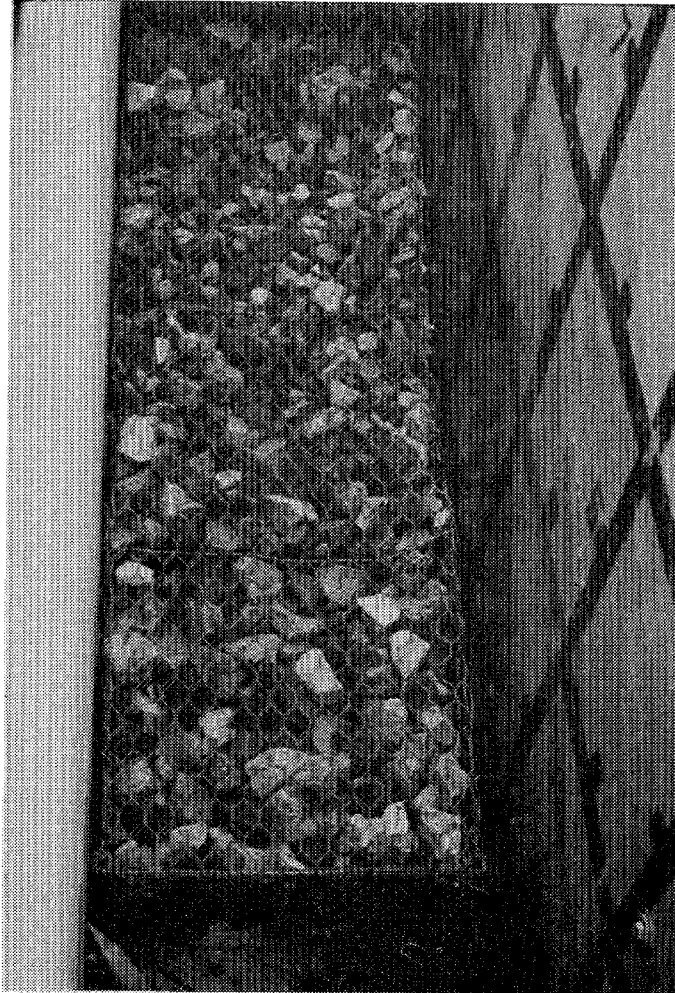
Figure 68. Gabion protection following overtopping depth of 2 feet and freefall conditions.

Figure 69. Gabion protection following overtopping depth of 4 feet and freefall conditions.
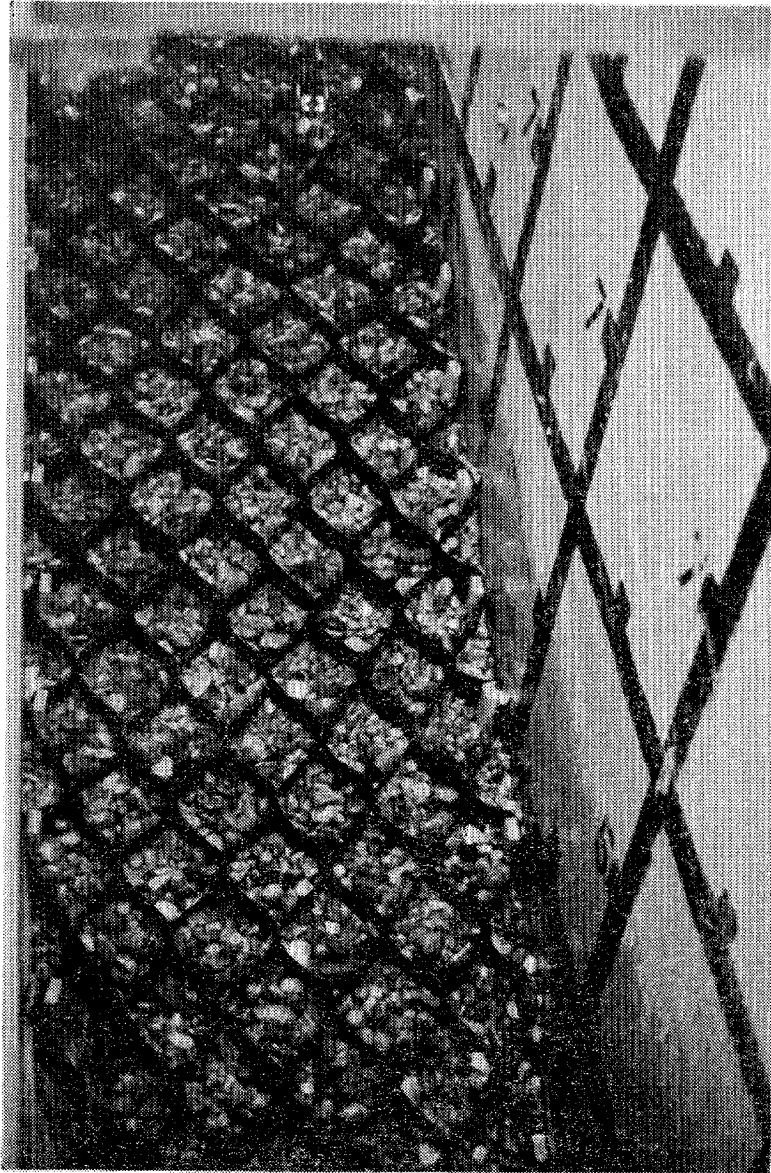
Figure 70. Geoweb protection following overtopping depth of 1 foot, free-
fall conditions, and testing duration of 30 minutes.

150
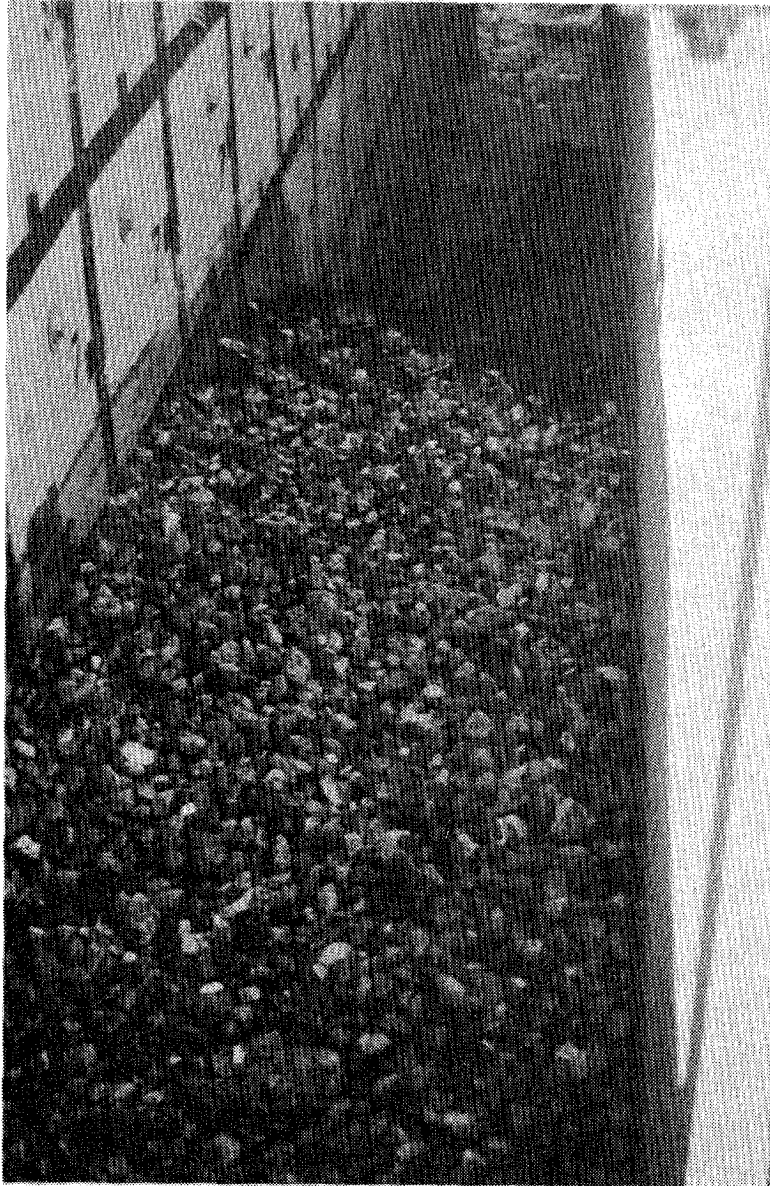
Figure 71. Geoweb protection following overtopping depth of 1 foot, free-fall conditions and testing duration of 1 hour.
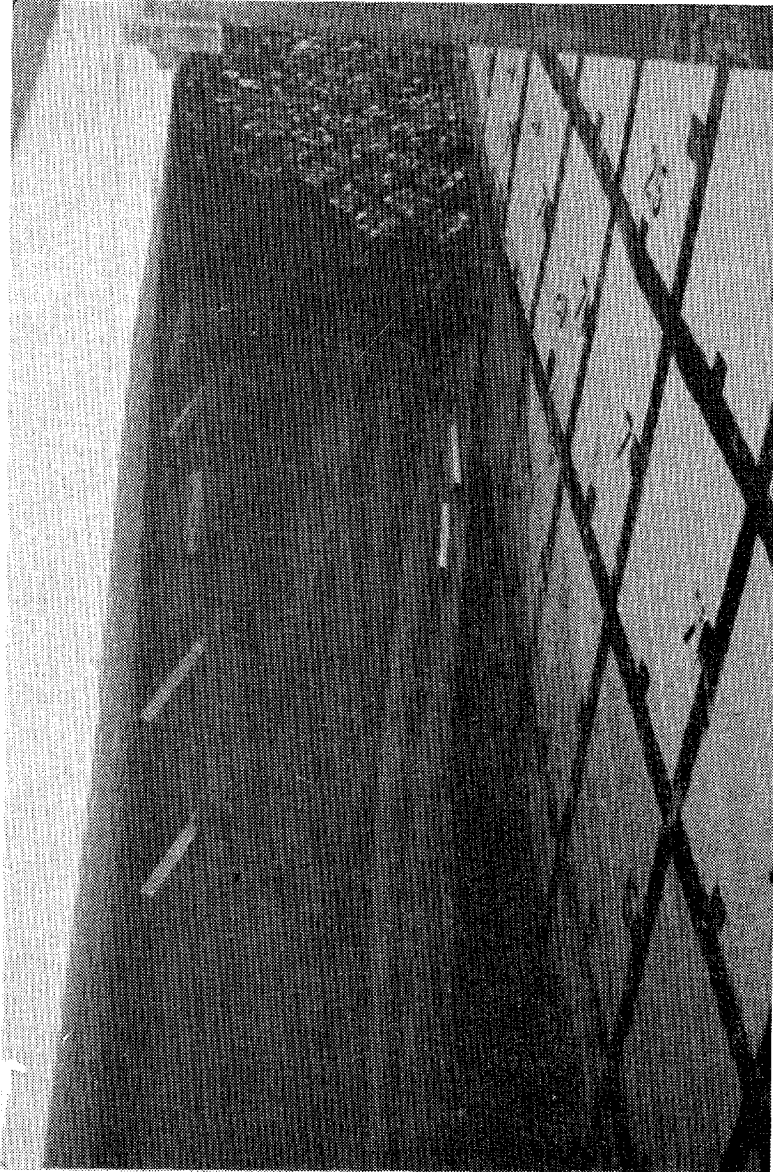
Figure 72. Geoweb protection following overtopping depth of 2 feet, freefall
conditions and testing duration of 1 hour.
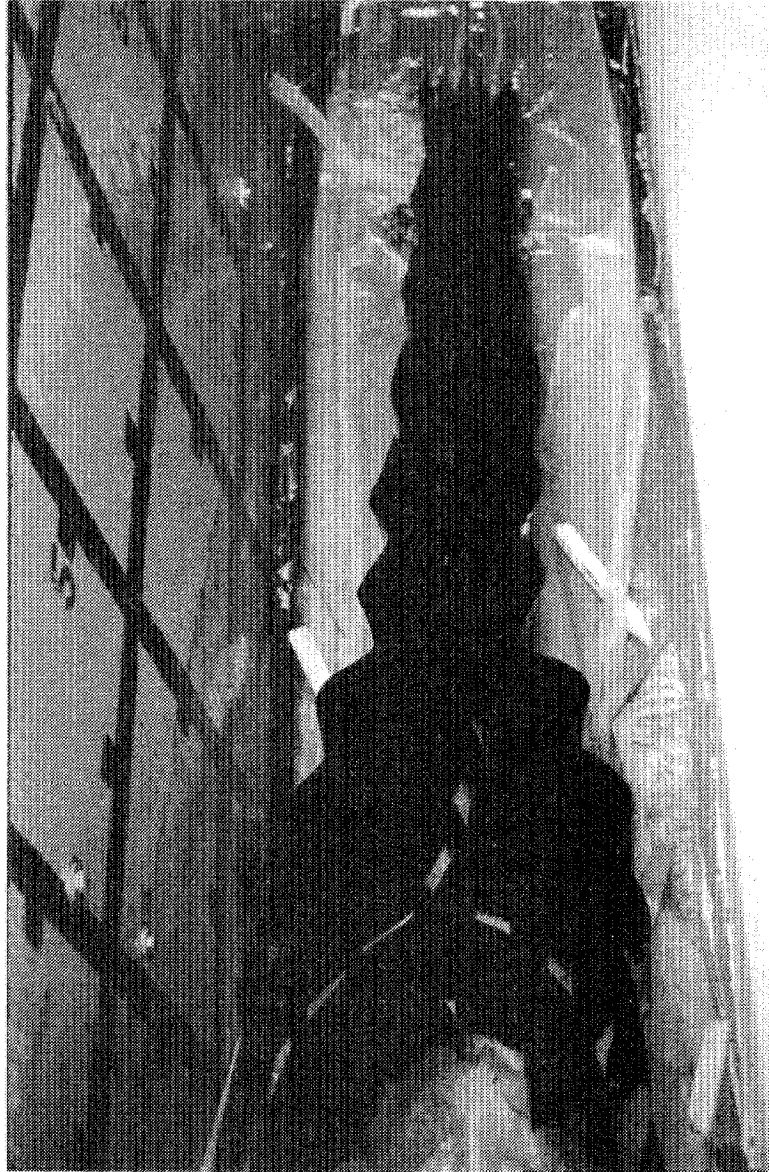
Figure 73. Geoweb protection following overtopping depth of 2 feet, freefall conditions and testing duration of 2 hours.

Figure 74. Enkamat protection following overtopping depth of 0.5 feet, free-fall conditions and testing duration of 1 hour.

Figure 75. Enkamat protection following overtopping depth of 2 feet, free-fall conditions and testing duration of 1 hour.
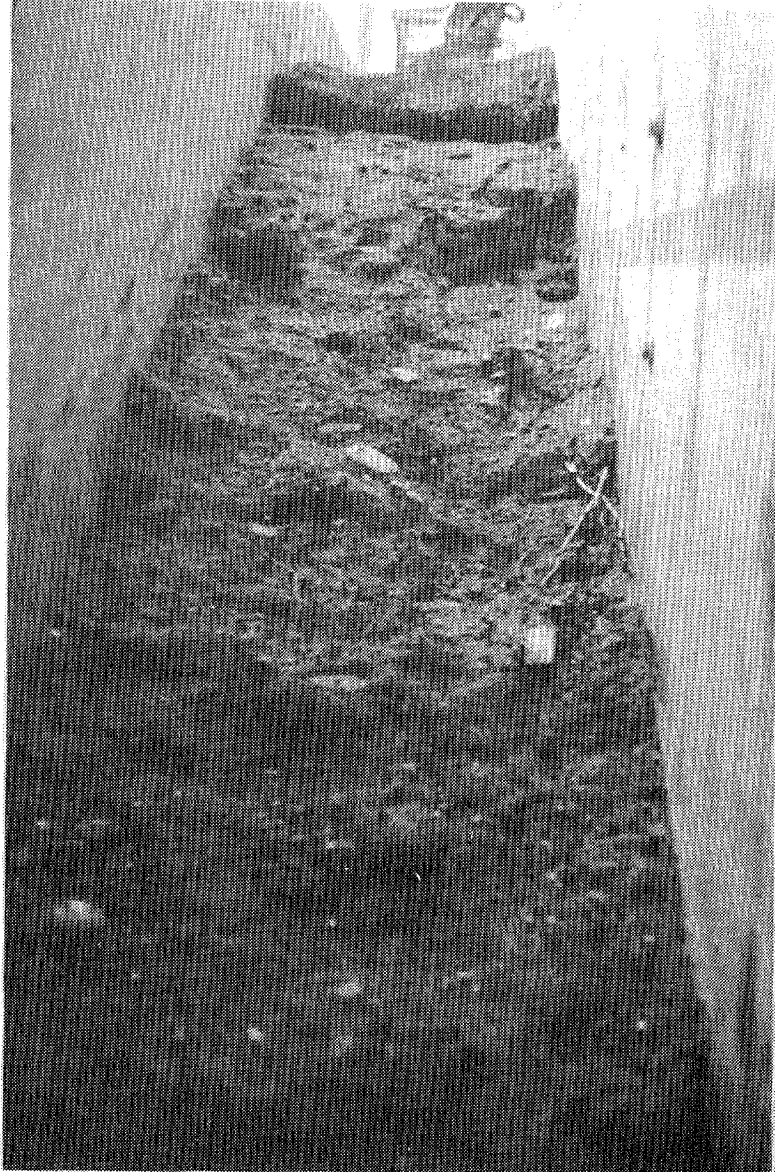
Figure 76. Embankment (Type II Soil) beneath enkamat protection following overtopping depth of 2 feet, freefall conditions and testing duration of 1 hour.

APPENDIX B - DATA SUMMARY

Table 17 lists a schedule of tests. Totally there were 35 runs conducted in this study. Table 18 tabulates the water-surface and bed-surface profile changes with time. Table 19 tabulates the velocity measurements.

Table 17. Schedule of tests.

Run No.	Series	Description of Test	Soil Type	Side Slope	Discharge (cfs)	Overtopping Depth, ft (D_{ot})	Water Surface Drop (% of D_{ot})
1	FHWA I	Bare-Soil Surface; No Protection	I	3:1	3.0	0.5	70
2	FHWA I	Bare-Soil Surface; No Protection	I	3:1	3.2	0.5	Free Fall (FF)
3	FHWA I	Bare-Soil Surface; No Protection	I	3:1	9.0	1.0	20
4	FHWA I	Bare-Soil Surface; No Protection	I	3:1	28.0	2.0	20
5	FHWA I	Bare-Soil Surface; No Protection	I	3:1	28.5	2.0	70
6	FHWA I	Bare-Soil Surface; No Protection	I	3:1	28.0	2.0	FF
7	FHWA I	Bare-Soil Surface; No Protection	I	3:1	72.6	4.0	20
8	FHWA I	Bare-Soil Surface; No Protection	I	3:1	70.0	4.0	70
9	FHWA I	Bare-Soil Surface; No Protection	I	3:1	70.0	4.0	FF

158

Table 17. Schedule of tests. (continued)

Run No.	Series	Description of Test	Soil Type	Side Slope	Discharge (cfs)	Overtopping Depth, ft (D_{ot})	Water Surface Drop (% of D_{ot})
10	FHWA II	Bare Soil Surface; No Protection	II	3:1	3.0	0.5	70
11	FHWA II	Bare-Soil Surface; No Protection	II	3:1	9.0	1.0	70
12	FHWA II	Bare-Soil Surface; No Protection	II	3:1	30.0	2.0	70
13	FHWA II	Bare-Soil Surface; No Protection	II	3:1	70.0	4.0	70
14	FHWA III	Paved Surface/ Gravel Shoulder; No Protection	II	3:1	3.0	0.5	70
15	FHWA III	Paved Surface/ Gravel Shoulder; No Protection	II	3:1	9.0	1.0	70
16	FHWA III	Paved Surface/ Gravel Shoulder; No Protection	II	3:1	30.0	2.0	70

159

Table 17. Schedule of tests. (continued)

Run No.	Series	Description of Test	Soil Type	Side Slope	Discharge (cfs)	Overtopping Depth, ft (D_{ot})	Water Surface Drop (% of D_{ot})
17	FHWA III	Paved Surface/ Gravel Shoulder; No Protection	II	3:1	70.0	4.0	70
18	USFS II	Bare-Soil Surface; Geoweb	II	3:1	9.0	1.0	FF
19	USFS II	Bare-Soil Surface; Geoweb	II	3:1	30.0	2.0	FF
20	USFS IV	Bare-Soil Surface; Gabion	II	2:1	9.0	1.0	FF
21	USFS IV	Bare-Soil Surface; Gabion	II	2:1	30.0	2.0	FF
22	USFS IV	Bare-Soil Surface; Gabion	II	2:1	70.0	4.0	FF
23	USFS V	Bare-Soil Surface; Soil Cement	II	2:1	9.0	1.0	FF
24	USFS V	Bare-Soil Surface; Soil Cement	II	2:1	30.0	2.0	FF

160

Table 17. (continued)

Run No.	Series	Description of Test	Soil Type	Side Slope	Discharge (cfs)	Overtopping Depth, ft (D_{ot})	Water Surface Drop (% of D_{ot})
25	USFS V	Bare-Soil Surface; Soil Cement	II	2:1	70.0	4.0	FF
26	FHWA IV	Paved Surface/ Gravel Shoulder; Grass	I	3:1	3.0	0.5	FF
27	FHWA IV	Paved Surface/ Gravel Shoulder; Grass	I	3:1	30.0	2.0	FF
28	FHWA IV	Paved Surface/ Gravel Shoulder; Grass	I	3:1	70.0	4.0	FF
29	FHWA V	Paved Surface/ Gravel Shoulder; Grass	I	3:1	3.0	0.5	70
30	FHWA V	Paved Surface/ Gravel Shoulder; Grass	I	3:1	30.0	2.0	70
31	USFS I	Bare-Soil Surface; Enkamat	II	3:1	3.0	0.5	FF

Table 17. Schedule of tests. (continued)

Run No.	Series	Description of Test	Soil Type	Side Slope	Discharge (cfs)	Overtopping Depth, ft (D_{ot})	Water Surface Drop (% of D_{ot})
32	USFS I	Bare-Soil Surface; Enkamat	II	3:1	30.0	2.0	FF
33	USFS III	Bare-Soil Surface; Enkamat/Grass	II	3:1	3.0	0.5	FF
34	USFS III	Bare-Soil Surface; Enkamat/Grass	II	3:1	9.0	1.0	FF
35	USFS III	Bare-Soil Surface; Enkamat/Grass	II	3:1	70.0	4.0	FF

Table 18. Water surface (WS) and bed surface (BS) elevations.

Run Number	Time (hrs)		Distance Along Embankment (ft.) *																	
			0	2	4	6	8	10	12	14	16	18	20	22	24	26	28	30	32	34	35
1	0.00	WS	6.53	6.50	6.48	6.46	6.44	6.43	6.39	6.37	6.36	6.30	6.06	6.14	6.19	6.16	6.16	6.15	6.16	6.18	6.19
		BS	5.77	5.88	5.91	5.97	5.96	5.97	5.96	5.94	5.91	5.96	5.83	5.40	4.61	4.04	3.39	2.67	2.14	1.51	1.19
1	0.75	WS	6.53	6.50	6.48	6.46	6.44	6.43	6.39	6.37	6.36	6.30	6.06	6.14	6.19	6.16	6.16	6.15	6.16	6.18	6.19
		BS	5.80	5.89	5.91	5.97	5.95	5.90	5.93	5.96	5.89	5.95	5.82	5.44	4.73	4.03	3.43	2.68	2.13	1.51	1.21
1	4.00	WS	6.60	6.54	6.50	6.49	6.44	6.44	6.43	6.41	6.37	6.32	5.97	6.17	6.18	6.13	6.11	6.13	6.14	6.16	6.16
		BS	5.81	5.90	5.91	5.93	5.95	5.90	5.90	5.89	5.84	5.85	5.59	5.40	4.58	3.93	3.40	2.69	2.15	1.45	1.22
1	10.00	WS	6.59	6.54	6.50	6.50	6.47	6.45	6.44	6.41	6.38	6.33	5.93	6.13	6.17	6.14	6.12	6.13	6.14	6.16	6.16
		BS	5.80	5.88	5.90	5.92	5.94	5.92	5.90	5.88	5.80	5.80	5.45	5.35	4.55	3.90	3.35	2.67	2.15	1.44	1.18
1	20.00	WS	6.61	6.56	6.51	6.50	6.45	6.44	6.43	6.41	6.37	6.34	5.85	6.10	6.16	6.13	6.12	6.13	6.14	6.16	6.16
		BS	5.80	5.89	5.89	5.90	5.93	5.90	5.90	5.88	5.82	5.70	5.40	5.31	4.50	3.84	3.36	2.68	2.15	1.42	1.17
2	0.00	WS	6.58	6.54	6.52	6.50	6.49	6.48	6.43	6.31	6.33	6.30	6.07	5.68	5.01	4.40	3.74	3.11	2.52	2.03	1.80
		BS	5.98	6.15	6.12	6.17	6.12	6.12	6.12	6.11	6.04	6.12	5.87	5.54	4.87	4.29	3.62	2.99	2.40	1.86	1.61
2	1.75	WS	6.57	6.53	6.51	6.50	6.49	6.48	6.43	6.31	6.33	6.30	6.05	5.67	5.00	4.34	3.80	3.08	2.49	2.02	1.78
		BS	5.99	6.13	6.11	6.10	6.10	6.10	6.11	6.09	6.05	6.07	5.85	5.45	4.85	4.24	3.67	2.96	2.36	1.86	1.61
2	5.00	WS	6.52	6.49	6.46	6.41	6.43	6.45	6.39	6.33	6.39	6.37	6.04	5.65	5.02	4.34	3.72	3.01	2.48	1.95	1.72
		BS	5.95	6.03	6.09	6.08	6.08	6.05	6.04	6.00	6.04	6.05	5.83	5.42	4.84	4.18	3.54	2.89	2.39	1.84	1.57
2	10.00	WS	6.56	6.52	6.47	6.42	6.44	6.40	6.39	6.44	6.40	6.35	6.04	5.54	4.95	4.28	3.73	3.01	2.45	1.98	1.80
		BS	5.92	6.01	6.07	6.06	6.08	6.03	6.01	5.99	5.98	6.01	5.83	5.37	4.76	4.13	3.53	2.86	2.36	1.81	1.54
2	20.00	WS	6.55	6.53	6.47	6.43	6.43	6.40	6.44	6.38	6.15	6.09	5.96	5.44	4.79	4.21	3.54	2.98	2.39	1.82	1.74
		BS	5.90	6.02	6.06	6.04	6.02	6.01	5.99	5.94	5.80	5.75	5.68	5.25	4.66	4.10	3.43	2.80	2.24	1.65	1.50

*See figure 26 for the measurement locations.

Table 18. Water surface (WS) and bed surface (BS) elevations. (continued)

Run Number	Time (hrs)		Distance Along Embankment (ft.)																		
			0	2	4	6	8	10	12	14	16	18	20	22	24	26	28	30	32	34	35
3	0.00	WS	6.98	6.95	6.90	6.82	6.73	6.65	6.73	6.85	6.94	7.05	7.10	7.12	7.15	7.07	6.92	7.00	6.85	6.88	6.90
		BS	5.77	5.85	5.91	5.99	5.99	5.94	6.00	5.99	6.00	5.99	5.85	5.49	4.71	4.08	3.46	2.68	2.18	1.50	1.18
3	1.00	WS	6.96	6.93	6.90	6.85	6.77	6.70	6.73	6.85	6.94	7.00	7.07	7.10	7.13	7.06	6.95	7.01	6.85	6.85	6.87
		BS	5.76	5.85	5.91	5.99	5.97	5.94	6.00	6.00	6.00	5.97	5.82	5.47	4.70	4.05	3.45	2.70	2.19	1.49	1.19
3	4.50	WS	6.97	6.95	6.90	6.88	6.74	6.70	6.73	6.83	6.91	6.98	7.00	7.08	7.11	7.08	6.98	6.99	6.90	6.85	6.88
		BS	5.77	5.88	5.91	5.94	5.96	5.96	5.96	5.94	5.91	5.96	5.83	5.40	4.61	4.04	3.39	2.67	2.14	1.51	1.19
3	10.00	WS	6.99	6.95	6.92	6.90	6.77	6.71	6.75	6.81	6.92	6.98	6.97	7.05	7.10	7.08	6.99	6.94	6.88	6.90	6.90
		BS	5.76	5.88	5.90	5.95	5.96	5.96	5.97	5.95	5.90	5.93	5.79	5.30	4.55	4.03	3.37	2.66	2.13	1.50	1.18
3	20.00	WS	6.97	6.94	6.93	6.90	6.80	6.75	6.74	6.82	6.92	6.97	6.99	7.03	7.08	7.07	7.00	6.93	6.87	6.88	6.87
		BS	5.77	5.87	5.89	5.94	5.95	5.96	5.94	5.94	5.88	5.91	5.77	5.27	4.50	3.98	3.35	2.63	2.13	1.50	1.18
4	0.00	WS	7.85	7.79	7.69	7.64	7.60	7.62	7.61	7.60	7.63	7.61	7.43	7.62	7.57	7.65	7.55	7.80	7.65	7.72	7.62
		BS	5.82	5.91	5.92	5.95	5.95	5.90	5.90	5.89	5.85	5.92	5.69	5.45	4.62	3.98	3.41	2.68	2.11	1.44	1.21
4	1.00	WS	7.81	7.75	7.66	7.63	7.58	7.61	7.57	7.54	7.59	7.59	7.42	7.71	7.59	7.73	7.55	7.78	7.65	7.71	7.60
		BS	5.77	5.88	5.91	5.94	5.91	5.78	5.80	5.79	5.76	5.85	5.68	5.41	4.76	4.11	3.41	2.68	2.21	1.52	1.20
4	10.00	WS	7.75	7.69	7.64	7.61	7.58	7.61	7.53	7.60	7.61	7.60	7.58	7.66	7.70	7.70	7.63	7.71	7.74	7.71	7.65
		BS	5.77	5.85	5.87	5.85	5.80	5.85	5.69	5.71	5.60	5.69	5.57	5.37	4.51	4.00	3.38	2.42	2.06	1.46	1.17
4	20.00	WS	7.74	7.68	7.63	7.58	7.56	7.60	7.50	7.58	7.60	7.60	7.56	7.63	7.67	7.66	7.60	7.70	7.72	7.71	7.63
		BS	5.76	5.83	5.85	5.80	5.79	5.78	5.55	5.66	5.48	5.58	5.50	5.31	4.40	3.95	3.30	2.35	2.01	1.35	1.13

Table 18. (continued).

Run Number	Time (hrs)		Distance Along Embankment (ft.)																		
			0	2	4	6	8	10	12	14	16	18	20	22	24	26	28	30	32	34	35
5	0.00	WS	7.73	7.62	7.49	7.39	7.31	7.19	7.05	6.86	6.87	7.00	6.91	6.65	6.40	6.51	6.53	6.65	6.66	6.61	6.73
		BS	5.77	5.85	5.87	5.86	5.84	5.87	5.75	5.73	5.65	5.75	5.63	5.39	4.71	4.03	3.43	2.52	2.10	1.51	1.19
5	0.75	WS	7.73	7.62	7.49	7.39	7.29	7.17	7.03	6.82	6.83	7.01	6.87	6.42	6.36	6.49	6.50	6.62	6.65	6.58	6.71
		BS	5.76	5.87	5.85	5.81	5.77	5.84	5.57	5.56	5.52	5.58	5.57	5.35	4.63	4.01	3.36	2.66	2.13	1.45	1.17
5	3.75	WS	7.62	7.50	7.36	7.25	7.14	6.97	6.82	6.64	6.52	6.72	6.79	6.44	6.27	6.41	6.54	6.58	6.61	6.61	6.68
		BS	5.74	5.81	5.80	5.71	5.74	5.82	5.52	5.39	5.33	5.47	5.49	5.26	4.63	4.02	3.27	2.63	2.08	1.39	1.11
5	9.75	WS	7.58	7.47	7.29	7.18	7.09	6.87	6.70	6.46	6.33	6.51	6.65	6.32	6.34	6.45	6.56	6.66	6.66	6.72	6.71
		BS	5.69	5.79	5.74	5.68	5.72	5.68	5.43	5.15	5.13	5.21	5.38	5.12	4.43	3.83	3.23	2.51	1.93	1.31	0.57
5	19.50	WS	7.61	7.50	7.33	7.19	7.09	6.86	6.68	6.43	6.30	6.51	6.66	6.30	6.33	6.42	6.51	6.58	6.62	6.65	6.67
		BS	5.68	5.78	5.73	5.68	5.68	5.46	5.22	5.00	5.01	5.08	5.18	4.80	4.25	3.68	3.10	2.38	1.82	1.28	0.50
6	0.00	WS	7.85	7.74	7.65	7.55	7.44	7.65	7.68	7.46	7.41	7.37	6.95	6.46	5.87	5.26	4.55	3.70	3.23	2.57	2.21
		BS	5.89	6.00	6.06	6.04	6.03	6.00	6.01	5.98	5.97	6.08	5.86	5.45	4.94	4.46	3.78	3.01	2.61	1.98	1.66
6	1.00	WS	7.84	7.71	7.63	7.52	7.41	7.62	7.64	7.46	7.40	7.31	6.93	6.41	5.54	4.65	4.27	3.76	3.23	2.45	2.15
		BS	5.89	5.99	6.05	6.03	5.98	6.00	5.99	5.97	5.97	6.07	5.86	5.45	4.77	3.96	3.50	2.98	2.48	1.86	1.61
6	3.50	WS	7.82	7.71	7.61	7.49	7.39	7.56	7.66	7.41	7.35	7.25	6.87	6.36	5.19	4.46	3.97	3.34	2.93	2.61	2.23
		BS	5.89	5.97	6.05	6.02	5.95	5.92	5.96	5.98	5.96	6.01	5.80	5.42	4.31	3.86	3.44	2.65	2.37	1.80	1.50
6	9.50	WS	7.81	7.69	7.56	7.43	7.23	7.43	7.83	7.31	7.19	7.13	6.74	6.19	5.02	4.06	3.37	2.82	2.15	1.73	1.73
		BS	5.87	5.93	5.96	5.97	5.94	5.79	5.97	5.91	5.93	5.92	5.74	5.14	4.17	3.34	2.68	2.06	0.57	0.52	0.52
6	20.00	WS	7.75	7.61	7.49	7.31	7.03	7.08	7.63	7.39	7.15	7.04	6.58	5.96	4.70	3.27	1.30	1.30	1.30	1.30	1.30
		BS	5.83	5.91	5.89	5.87	5.77	5.66	5.81	5.80	5.88	5.80	5.67	4.95	3.80	0.68	0.31	0.00	0.00	0.00	0.00

Table 18. Water surface (WS) and bed surface (BS) elevations. (continued)

Run Number	Time (hrs)		Distance Along Embankment (ft.)																		
			0	2	4	6	8	10	12	14	16	18	20	22	24	26	28	30	32	34	35
7	0.00	WS	9.10	8.85	8.61	8.42	8.30	8.01	7.77	7.68	7.72	8.50	8.93	8.94	8.63	8.71	8.81	8.82	8.60	8.65	9.05
		BS	5.86	5.94	5.97	6.01	5.93	5.87	5.95	5.95	5.96	5.99	5.79	5.16	4.28	3.44	2.81	2.33	1.72	0.61	0.52
7	0.75	WS	9.05	8.80	8.56	8.41	8.28	7.99	7.74	7.61	7.68	8.46	8.91	8.91	8.61	8.71	8.81	8.81	8.51	8.56	8.91
		BS	5.66	5.76	5.70	5.66	5.69	5.66	5.39	4.99	5.06	5.12	5.33	5.06	4.48	3.83	3.24	2.56	2.10	1.38	0.81
7	3.25	WS	8.88	8.70	8.49	8.36	8.21	7.92	7.69	7.56	7.58	7.78	8.58	8.55	8.43	8.26	8.78	8.63	8.45	8.47	8.45
		BS	5.65	5.76	5.70	5.67	5.72	5.67	5.42	5.01	5.04	5.18	5.39	5.14	4.57	3.88	3.24	2.59	2.15	1.41	0.73
7	10.00	WS	8.87	8.71	8.48	8.34	8.17	7.90	7.51	7.42	7.47	7.71	8.42	8.44	8.37	8.27	8.80	8.62	8.44	8.47	8.47
		BS	5.64	5.71	5.68	5.65	5.67	5.60	5.21	4.85	4.80	5.05	5.11	5.05	4.45	3.80	3.20	2.47	2.01	1.32	0.53
7	20.00	WS	8.90	8.73	8.51	8.39	8.11	7.85	7.38	7.25	7.19	7.37	8.21	8.35	8.36	8.25	8.70	8.59	8.45	8.46	8.68
		BS	5.61	5.69	5.65	5.61	5.60	5.41	4.95	4.44	4.35	4.71	4.89	4.90	4.31	3.68	3.11	2.41	1.95	1.30	0.48
8	0.00	WS	9.10	8.92	8.71	8.51	8.48	8.46	8.35	8.33	8.12	8.05	7.44	7.50	7.54	7.62	7.71	7.80	7.67	7.32	7.23
		BS	5.86	5.96	5.94	6.01	5.91	5.87	5.92	5.96	5.89	5.84	5.81	5.16	4.24	3.46	2.82	2.32	1.74	0.63	0.56
8	4.00	WS	8.74	8.54	8.30	8.08	7.82	7.45	7.22	7.04	6.83	6.67	6.53	6.60	6.61	7.08	7.71	7.90	7.72	7.31	7.25
		BS	5.56	5.69	5.58	5.52	5.28	5.18	5.18	4.93	4.65	4.72	4.72	4.65	4.26	3.72	3.17	2.33	2.01	1.15	0.51
8	10.00	WS	8.61	8.43	8.12	7.81	7.46	7.06	7.01	6.43	6.35	6.91	7.35	6.61	7.22	7.20	7.38	7.56	7.48	7.32	7.21
		BS	5.41	5.42	5.37	5.02	4.77	4.56	4.50	4.54	4.35	4.20	4.03	3.94	3.70	3.47	2.45	2.16	1.54	1.21	0.76
8	20.00	WS	8.59	8.33	8.21	7.86	7.55	7.13	6.81	6.18	6.39	6.50	6.59	6.63	6.56	6.87	6.80	7.10	7.16	7.19	7.20
		BS	4.81	5.02	4.80	3.34	3.40	3.22	2.95	2.79	2.82	2.13	1.82	1.76	1.59	1.41	1.62	1.49	1.52	1.44	1.39

166

Table 18. (continued).

Run Number	Time (hrs)		Distance Along Embankment (ft.)																		
			0	2	4	6	8	10	12	14	16	18	20	22	24	26	28	30	32	34	35
9	0.00	WS	9.09	8.93	8.75	8.70	8.67	8.67	8.70	8.57	8.43	8.12	7.72	7.25	6.36	5.71	5.05	4.38	4.01	3.21	3.03
		BS	5.81	5.83	5.82	5.86	5.84	5.81	5.90	5.98	5.99	5.88	5.75	5.41	4.78	4.20	3.62	2.87	2.47	1.95	1.67
9	1.00	WS	9.09	8.93	8.75	8.55	8.53	8.67	8.80	8.57	8.43	8.12	7.39	6.81	6.06	5.45	4.85	4.28	3.73	3.06	2.93
		BS	5.75	5.77	5.87	5.80	5.62	5.61	5.85	5.90	5.93	5.77	5.35	4.90	4.40	3.92	3.38	2.75	2.18	1.75	1.56
9	4.00	WS	9.01	8.78	8.58	8.31	8.28	8.34	8.43	8.47	8.25	7.89	7.07	6.34	5.61	5.07	4.77	4.23	3.63	3.06	2.82
		BS	5.75	5.74	5.76	5.76	5.54	5.71	5.79	5.93	5.86	5.76	5.01	4.51	4.06	3.41	3.29	2.65	2.16	1.69	1.44
9	10.00	WS	8.93	8.78	8.46	8.27	8.03	7.84	7.95	8.21	8.19	7.73	6.58	5.56	4.11	2.76	1.75	1.56	1.56	1.56	1.56
		BS	5.63	5.67	5.67	5.63	5.45	5.35	5.59	5.75	5.76	5.69	4.33	3.47	1.49	0.24	0.21	0.00	0.00	0.00	0.00
9	20.00	WS	8.61	8.43	8.12	7.81	7.46	7.06	7.01	7.08	6.86	6.35	5.35	4.01	2.76	1.56	1.56	1.56	1.56	1.56	1.56
		BS	5.36	5.44	5.43	5.15	4.89	4.46	4.40	4.46	4.16	3.72	2.65	1.12	0.00	0.00	0.00	0.00	0.00	0.00	0.00
10	0.00	WS	6.62	6.59	6.55	6.53	6.47	6.42	6.39	6.30	6.26	6.20	6.30	6.39	6.40	6.45	6.49	6.38	6.20	6.19	6.20
		BS	5.98	6.03	6.06	6.11	6.09	6.00	6.02	5.99	6.01	5.93	5.78	5.42	4.82	4.18	3.59	2.81	2.27	1.76	1.55
10	1.50	WS	6.58	6.54	6.50	6.48	6.43	6.40	6.32	6.28	6.21	6.15	5.90	6.29	6.28	6.17	6.17	6.23	6.28	6.28	6.27
		BS	5.66	5.76	5.75	5.83	5.77	5.78	5.79	5.73	5.71	5.67	5.41	5.29	4.66	3.93	3.33	2.75	2.32	1.81	1.52
10	4.50	WS	6.46	6.47	6.41	6.46	6.43	6.46	6.39	6.33	6.24	6.23	6.10	6.31	6.41	6.45	6.57	6.64	6.21	6.31	6.36
		BS	5.44	5.65	5.75	5.37	5.44	5.46	5.48	5.43	5.31	5.31	5.29	5.28	4.65	3.95	3.36	2.78	2.33	1.85	1.56
10	10.50	WS	6.47	6.47	6.47	6.43	6.41	6.39	6.41	6.40	6.40	6.41	6.36	6.39	6.41	6.42	6.39	6.40	6.36	6.38	6.36
		BS	5.36	5.42	5.47	5.40	5.46	5.48	5.47	5.44	5.35	5.27	5.27	5.07	4.62	4.27	3.61	2.81	2.42	1.82	1.53
10	20.00	WS	6.45	6.43	6.40	6.29	6.26	6.33	6.33	6.26	6.30	6.31	6.30	6.29	6.32	6.33	6.31	6.30	6.29	6.28	6.27
		BS	5.37	5.41	5.44	5.34	5.31	5.33	5.41	5.19	5.17	4.91	4.91	5.04	4.62	3.68	3.36	2.54	2.32	1.73	1.53

Table 18. Water surface (WS) and bed surface (BS) elevations. (continued)

Run Number	Time (hrs)		Distance Along Embankment (ft.)																		
			0	2	4	6	8	10	12	14	16	18	20	22	24	26	28	30	32	34	35
11	0.00	WS	7.06	7.00	6.94	6.91	6.91	6.86	6.79	6.71	6.89	6.67	6.90	7.01	6.92	6.81	6.46	6.41	6.40	6.41	6.42
		BS	5.74	5.91	6.01	5.94	5.92	5.99	6.01	6.00	5.94	5.92	5.62	5.19	4.61	4.07	3.42	2.79	2.31	1.71	1.41
11	2.00	WS	6.86	6.85	6.79	6.76	6.74	6.61	6.59	6.41	6.21	6.47	6.51	6.46	6.52	6.57	6.57	6.61	6.61	6.56	6.53
		BS	5.60	5.69	5.74	5.92	5.80	5.97	6.01	6.00	5.56	5.57	5.26	4.83	4.61	4.01	3.21	2.70	2.19	1.59	1.26
11	4.00	WS	6.71	6.67	6.61	6.57	6.56	6.53	6.47	6.41	6.50	6.50	6.59	6.51	6.50	6.52	6.57	6.61	6.61	6.59	6.57
		BS	5.51	5.59	5.52	5.56	5.59	5.61	5.51	5.47	5.26	5.17	5.01	4.89	4.57	4.10	3.37	2.76	2.26	1.66	1.31
11	10.00	WS	6.63	6.56	6.51	6.48	6.42	6.27	6.23	6.30	6.41	6.38	6.45	6.52	6.49	6.52	6.51	6.51	6.49	6.48	6.47
		BS	5.39	5.44	5.49	5.49	5.56	5.53	5.47	5.42	5.26	5.16	4.91	4.57	4.33	3.81	3.33	2.82	2.49	1.59	1.40
11	20.00	WS	6.60	6.57	6.52	6.46	6.41	6.23	6.35	6.49	6.50	6.41	6.43	6.43	6.48	6.51	6.51	6.47	6.46	6.49	6.49
		BS	5.36	5.43	5.40	5.46	5.54	5.43	5.45	5.30	5.13	4.95	4.61	4.50	4.26	3.80	3.22	2.80	2.39	1.57	1.40
12	0.00	WS	7.74	7.73	7.58	7.45	7.39	7.32	7.25	7.20	6.95	6.79	6.55	6.20	6.49	6.48	6.52	6.53	6.56	6.46	6.53
		BS	5.81	5.80	5.88	5.83	5.83	5.89	5.92	5.93	5.91	5.90	5.59	5.18	4.59	4.12	3.44	2.83	2.33	1.65	1.41
12	1.50	WS	7.65	7.63	7.53	7.41	7.23	7.00	6.73	6.61	6.45	6.24	5.90	5.69	6.06	6.13	6.34	6.39	6.41	6.41	6.53
		BS	5.29	5.27	5.53	5.79	5.78	5.48	5.47	5.43	5.29	5.18	5.02	4.67	4.17	3.74	3.19	2.40	2.11	1.59	1.23
12	4.50	WS	7.22	7.24	7.29	7.11	7.03	6.95	6.81	6.71	6.50	6.32	5.81	6.09	6.33	6.31	6.49	6.41	6.57	6.54	6.62
		BS	5.25	5.26	5.26	5.33	5.38	5.31	5.47	5.42	5.29	5.19	4.68	4.48	4.19	3.84	3.21	2.40	2.09	1.45	1.09
12	9.00	WS	7.18	7.15	7.19	7.05	6.95	6.76	6.61	6.49	6.39	6.13	5.71	6.15	6.31	6.48	6.55	6.55	6.57	6.58	6.63
		BS	5.24	5.22	5.24	5.28	5.34	5.28	5.42	5.35	5.20	5.18	4.62	4.42	4.01	3.59	2.91	2.41	2.03	1.33	1.10
12	20.00	WS	7.20	7.18	7.22	7.07	6.97	6.85	6.74	6.60	6.43	6.20	5.78	6.10	6.25	6.35	6.49	6.59	6.64	6.65	6.65
		BS	5.22	5.18	5.20	5.23	5.30	5.23	5.36	5.10	5.14	5.15	4.54	4.36	3.88	3.40	2.60	2.25	1.93	1.21	1.02

168

Table 18. (continued).

Run Number	Time (hrs)		0	2	4	6	8	10	12	14	16	18	20	22	24	26	28	30	32	34	35
13	0.00	WS	9.04	8.93	8.83	8.66	8.50	8.18	8.14	7.99	7.81	7.70	7.35	6.90	6.71	7.01	7.10	7.18	7.22	7.28	7.28
		BS	5.85	5.98	6.04	6.02	6.01	6.00	6.01	5.96	5.90	5.91	5.62	5.22	4.67	4.03	3.47	2.78	2.33	1.87	1.46
13	1.00	WS	9.02	8.91	8.81	8.64	8.48	8.15	8.14	7.97	7.79	7.63	7.31	6.75	6.51	6.88	7.08	7.16	7.21	7.29	7.26
		BS	5.44	5.86	5.91	5.91	5.98	5.95	5.95	5.91	5.87	5.86	5.61	4.86	4.43	3.77	3.20	2.57	1.99	1.48	1.41
13	4.50	WS	8.98	8.81	8.73	8.64	8.52	8.39	8.31	8.07	7.79	7.47	6.76	6.31	6.80	6.93	7.05	7.17	7.31	7.41	7.31
		BS	5.39	5.65	5.62	5.71	5.73	5.69	5.89	5.88	5.76	5.56	4.85	4.54	4.02	3.66	3.11	2.41	1.90	1.34	1.23
13	10.50	WS	8.77	8.60	8.43	8.31	8.13	7.91	7.82	7.67	7.32	6.87	6.32	6.17	6.71	6.91	7.03	7.18	7.26	7.28	7.31
		BS	5.31	5.60	5.61	5.69	5.70	5.68	5.63	5.57	5.51	5.17	4.68	4.33	3.96	3.51	3.01	2.32	1.76	1.15	1.00
13	20.00	WS	8.76	8.58	8.41	8.27	8.10	7.87	7.77	7.60	7.25	6.81	6.24	6.09	6.58	6.81	6.94	7.11	7.24	7.27	7.30
		BS	5.21	5.56	5.57	5.65	5.67	5.58	5.37	5.27	5.21	4.45	4.40	4.09	3.88	3.27	2.85	2.20	1.52	0.95	0.80
14	0.00	WS	6.60	6.59	6.58	6.53	6.50	6.49	6.48	6.39	6.34	6.26	6.30	6.28	6.25	6.24	6.26	6.28	6.27	6.26	6.27
		BS	5.91	5.98	6.16	6.20	6.19	6.17	6.18	6.14	6.11	5.94	5.56	5.15	4.44	3.86	3.21	2.53	2.19	1.59	1.41
14	1.00	WS	6.59	6.59	6.59	6.53	6.50	6.49	6.48	6.39	6.34	6.24	6.30	6.28	6.24	6.24	6.26	6.27	6.27	6.25	6.28
		BS	5.91	6.02	6.16	6.19	6.19	6.17	6.17	6.13	6.11	5.37	5.32	5.04	4.41	3.79	3.18	2.49	2.08	1.54	1.48
14	5.00	WS	6.59	6.59	6.55	6.53	6.50	6.49	6.46	6.35	6.35	6.39	6.27	6.28	6.29	6.26	6.27	6.28	6.25	6.26	6.23
		BS	5.89	5.99	6.15	6.20	6.19	6.18	6.18	6.13	6.11	5.32	5.22	4.98	4.36	3.81	3.25	2.57	2.11	1.51	1.45
14	9.00	WS	6.59	6.59	6.56	6.55	6.51	6.50	6.49	6.39	6.36	6.19	6.18	6.21	6.15	6.19	6.25	6.29	6.26	6.25	6.24
		BS	5.90	6.00	6.15	6.19	6.19	6.18	6.18	6.14	6.11	5.21	5.13	4.81	4.42	3.85	3.21	2.53	2.07	1.56	1.40
14	20.00	WS	6.60	6.60	6.56	6.55	6.51	6.54	6.47	6.38	6.33	6.29	6.27	6.28	6.27	6.26	6.27	6.28	6.26	6.25	6.23
		BS	5.88	5.97	6.15	6.19	6.19	6.18	6.18	6.13	6.11	5.02	4.97	4.51	4.36	3.81	3.14	2.45	1.98	1.51	1.38

169

Table 18. Water surface (WS) and bed surface (BS) elevations. (continued)

Run Number	Time (hrs)		Distance Along Embankment (ft.)																		
			0	2	4	6	8	10	12	14	16	18	20	22	24	26	28	30	32	34	35
15	0.00	WS	7.13	7.12	7.07	7.01	6.94	6.91	6.87	6.75	6.67	6.65	6.30	6.40	6.41	6.45	6.48	6.66	6.45	6.43	6.42
		BS	5.96	6.05	6.14	6.19	6.19	6.16	6.17	6.14	6.12	5.98	5.61	5.07	4.45	3.81	3.19	2.54	2.08	1.51	1.01
15	1.00	WS	7.12	7.12	7.07	7.09	6.94	6.94	6.87	6.75	6.67	6.23	6.27	6.48	6.41	6.45	6.48	6.45	6.44	6.43	6.41
		BS	5.92	6.03	6.19	6.21	6.21	6.18	6.17	6.13	6.11	5.51	5.23	4.81	4.39	3.80	3.21	2.43	2.05	1.29	1.03
15	4.00	WS	7.12	7.09	7.03	6.97	6.92	6.90	6.89	6.76	6.68	6.30	6.33	6.35	6.47	6.45	6.45	6.45	6.46	6.46	6.44
		BS	5.89	6.03	6.15	6.19	6.19	6.19	6.18	6.14	6.12	5.45	4.59	4.25	3.99	4.19	3.15	2.54	1.53	1.53	1.08
15	9.00	WS	7.22	7.17	7.11	7.03	6.99	6.95	6.99	6.85	6.76	6.31	6.39	6.39	6.40	6.38	6.44	6.50	6.49	6.48	6.47
		BS	5.91	5.98	6.13	6.19	6.19	6.18	6.18	6.15	6.12	5.30	4.51	4.20	3.85	3.63	3.11	2.99	2.61	1.49	1.05
15	20.00	WS	7.20	7.16	7.08	7.03	6.97	6.97	6.96	6.88	6.71	6.31	6.32	6.33	6.35	6.47	6.46	6.44	6.46	6.46	6.47
		BS	5.88	5.95	6.13	6.19	6.19	6.17	6.17	6.14	6.11	5.13	4.31	4.18	3.81	3.35	3.05	2.75	2.60	1.45	1.02
16	0.00	WS	7.96	7.91	7.76	7.61	7.51	7.48	7.45	7.33	7.19	6.89	6.40	6.01	6.69	6.80	6.53	6.62	6.81	6.70	6.73
		BS	5.92	6.03	6.16	6.20	6.19	6.18	6.17	6.14	6.11	5.93	5.52	5.07	4.49	3.87	3.16	2.61	2.13	1.60	1.47
16	1.00	WS	7.95	7.90	7.76	7.61	7.51	7.48	7.45	7.33	7.19	6.65	5.94	5.86	6.69	7.10	6.53	6.52	6.85	6.69	6.71
		BS	5.71	5.87	6.16	6.20	6.19	6.18	6.17	6.14	6.10	5.41	5.04	4.81	4.44	4.03	3.23	2.63	2.21	1.68	1.45
16	4.00	WS	7.93	7.89	7.75	7.60	7.47	7.49	7.43	7.31	7.18	6.55	5.85	5.65	6.24	6.36	6.49	6.53	6.54	6.63	6.64
		BS	5.63	5.78	6.15	6.20	6.19	6.16	6.17	6.14	6.11	5.36	5.04	4.75	4.36	3.81	3.16	2.49	2.07	1.65	1.47
16	10.00	WS	7.96	7.93	7.75	7.65	7.51	7.49	7.45	7.31	7.18	6.47	6.05	6.07	6.28	6.31	6.47	6.49	6.51	6.53	6.52
		BS	5.58	5.77	6.15	6.19	6.19	6.16	6.16	6.12	6.10	5.17	4.51	4.04	3.68	3.58	3.05	2.41	1.84	1.31	0.87
16	20.00	WS	7.96	7.91	7.76	7.61	7.49	7.49	7.45	7.31	7.15	6.55	5.78	6.04	6.05	6.23	6.36	6.37	6.51	6.53	6.53
		BS	5.57	5.73	6.15	6.19	6.19	6.15	6.16	6.13	6.10	5.10	4.03	3.95	3.67	3.30	2.98	2.29	1.78	1.15	0.81

Table 18. (continued).

Run Number	Time (hrs)		0	2	4	6	8	10	12	14	16	18	20	22	24	26	28	30	32	34	35
			Distance Along Embankment (ft.)																		
17	0.00	WS	9.60	9.46	9.27	9.04	8.90	8.68	8.47	8.36	8.20	7.94	7.55	7.05	7.17	7.20	7.70	7.77	7.50	7.65	7.71
		BS	5.98	6.07	6.15	6.20	6.19	6.17	6.17	6.15	6.10	5.94	5.51	4.95	4.32	3.77	3.18	2.48	1.88	1.22	0.99
17	1.00	WS	9.57	9.43	9.24	8.99	8.82	8.59	8.36	8.28	8.13	7.63	7.05	6.48	6.87	6.91	7.76	7.77	7.30	7.36	7.69
		BS	5.41	5.48	6.19	6.23	6.23	6.19	6.19	6.15	6.11	5.55	4.81	3.90	3.82	3.51	2.92	2.31	1.71	0.97	0.78
17	4.00	WS	8.66	8.55	8.26	8.09	8.01	7.97	7.76	7.59	7.60	7.15	6.96	7.35	7.30	7.61	7.64	7.86	7.88	8.01	8.01
		BS	5.43	5.47	5.51	5.47	5.50	5.46	5.45	5.39	5.42	4.93	3.96	3.65	3.50	3.28	2.87	2.18	1.61	1.00	0.73
17	10.00	WS	8.68	8.47	8.30	8.01	7.93	7.84	7.63	7.51	7.43	6.94	6.17	6.31	6.81	6.67	6.97	7.17	7.17	7.41	7.40
		BS	5.34	5.47	5.43	5.49	5.49	5.49	5.46	5.36	5.38	5.01	3.95	3.63	3.36	3.25	2.81	2.17	1.62	0.89	0.70
17	20.00	WS	8.61	8.51	8.32	8.03	8.00	7.85	7.71	7.60	7.34	6.90	6.21	6.29	6.71	6.82	6.97	7.16	7.21	7.31	7.35
		BS	5.20	5.43	5.41	5.32	5.34	5.34	5.43	5.28	5.32	3.98	1.05	0.93	0.92	0.53	0.52	0.71	0.82	0.51	0.20
18	0.00	WS	7.08	7.07	7.06	7.05	7.05	6.90	6.81	6.79	6.75	6.52	6.19	5.69	4.96	4.57	4.01	3.51	3.00	2.63	2.40
		BS	6.01	6.01	6.01	6.01	6.01	6.19	6.15	6.16	6.18	6.17	5.81	5.37	4.64	4.08	3.61	3.11	2.65	2.14	2.01
18	2.00	WS	7.06	7.06	7.06	7.06	7.06	6.89	6.81	6.79	6.75	6.51	6.19	5.69	4.95	4.42	3.89	3.49	3.01	2.59	2.38
		BS	5.99	5.99	5.99	5.99	5.99	6.21	6.16	6.09	6.17	6.09	5.59	5.27	4.47	3.93	3.41	2.99	2.71	1.99	1.93
18	4.00	WS	7.03	7.03	7.03	7.03	7.03	6.89	6.81	6.72	6.71	6.52	6.19	5.63	4.93	4.43	3.95	3.41	3.05	2.49	2.37
		BS	5.93	5.93	5.93	5.93	5.93	6.19	6.15	6.13	6.11	5.97	5.75	5.29	4.41	3.91	3.55	3.01	2.61	2.11	1.97
19	0.00	WS	7.97	7.95	7.64	7.55	7.50	7.11	6.69	6.51	5.70	5.14	4.43	3.87	3.40	2.82	2.43	2.11	2.10	2.10	2.10
		BS	6.10	6.31	6.30	6.31	6.22	6.17	5.94	5.42	4.81	4.25	3.64	3.08	2.51	2.02	1.64	0.00	0.00	0.00	0.00
19	2.50	WS	7.94	7.93	7.59	7.51	7.48	7.10	6.66	5.81	4.85	4.40	3.40	3.09	3.01	2.11	2.11	2.11	2.11	2.11	2.11
		BS	5.49	6.05	6.30	6.32	6.24	6.12	5.98	4.42	3.95	3.56	2.66	2.14	1.65	0.00	0.00	0.00	0.00	0.00	0.00

171

Table 18. Water surface (WS) and bed surface (BS) elevations. (continued)

Run Number	Time (hrs)		0	2	4	6	8	10	12	14	16	18	20	22	24	26	28	30	32	34	35
									Distance Along Embankment (ft.)												
20	0.00	WS	7.15	7.14	6.90	6.94	6.81	6.59	6.30	5.92	4.79	4.30	3.79	2.92	2.35	2.11	1.90	1.90	1.90	1.90	1.90
		BS	6.33	6.33	6.22	6.22	6.24	6.14	5.86	5.52	4.38	3.74	2.88	2.31	1.85	1.64	1.51	0.00	0.00	0.00	0.00
20	2.17	WS	7.09	7.09	6.74	6.81	6.76	6.48	6.29	5.58	4.91	4.15	3.64	3.01	2.38	2.06	1.89	1.89	1.89	1.89	1.89
		BS	6.33	6.33	6.22	6.21	6.20	6.18	5.88	5.20	4.54	3.82	2.87	2.44	1.88	1.65	1.54	0.00	0.00	0.00	0.00
21	0.00	WS	7.95	7.95	7.59	7.27	7.29	7.07	6.78	6.09	5.31	4.60	3.76	3.09	2.71	2.44	2.34	2.34	2.34	2.34	2.34
		BS	6.33	6.33	6.28	6.22	6.23	6.14	5.90	5.35	4.59	3.76	2.96	2.45	1.90	1.65	1.53	0.00	0.00	0.00	0.00
21	2.00	WS	7.95	7.95	7.56	7.25	7.27	7.11	6.71	6.13	5.31	4.53	3.75	3.12	2.80	2.37	2.27	2.27	2.27	2.27	2.27
		BS	6.35	6.35	6.27	6.22	6.21	6.16	5.85	5.34	4.69	3.80	2.89	2.53	1.87	1.62	1.54	0.00	0.00	0.00	0.00
22	0.00	WS	9.55	9.55	9.55	8.80	8.34	8.11	7.81	7.15	6.29	5.53	4.56	4.01	3.31	3.03	2.90	2.90	2.90	2.90	2.90
		BS	6.31	6.21	6.21	6.19	6.23	6.13	5.92	5.23	4.57	3.79	2.87	2.57	1.83	1.65	1.69	0.00	0.00	0.00	0.00
22	2.00	WS	9.38	9.38	9.24	8.61	8.44	8.01	7.73	7.12	6.31	5.57	4.51	3.95	3.27	2.96	2.84	2.84	2.84	2.84	2.84
		BS	6.26	6.26	6.25	6.22	6.23	6.14	5.93	5.17	4.63	3.89	2.87	2.50	1.85	1.65	1.65	0.00	0.00	0.00	0.00
22	6.00	WS	9.43	9.43	9.22	8.76	8.38	8.13	7.81	7.10	6.43	5.61	4.57	3.92	3.30	3.00	2.93	2.93	2.93	2.93	2.93
		BS	6.22	6.22	6.25	6.20	6.20	6.13	5.95	5.18	4.70	3.87	2.91	2.50	1.87	1.64	1.52	0.00	0.00	0.00	0.00
23	0.00	WS	7.07	7.06	6.95	6.91	6.89	6.81	6.57	5.67	4.65	3.80	2.70	2.01	1.35	0.91	0.91	0.91	0.91	0.91	0.91
		BS	6.17	6.17	6.22	6.22	6.23	6.21	6.18	5.35	4.38	3.54	2.42	1.73	1.13	0.85	0.00	0.00	0.00	0.00	0.00
23	2.00	WS	7.05	7.05	6.95	6.91	6.91	6.81	6.57	5.67	4.63	3.75	2.69	1.95	1.32	0.91	0.91	0.91	0.91	0.91	0.91
		BS	6.14	6.14	6.21	6.23	6.25	6.22	6.17	5.35	4.36	3.48	2.41	1.68	1.10	0.69	0.00	0.00	0.00	0.00	0.00
24	0.00	WS	7.83	7.82	7.63	7.56	7.55	7.39	7.11	6.15	5.06	4.13	3.01	2.29	1.58	1.17	1.17	1.17	1.17	1.17	1.17
		BS	6.18	6.18	6.21	6.23	6.25	6.22	6.18	5.34	4.36	3.49	2.41	1.68	1.07	0.71	0.00	0.00	0.00	0.00	0.00
24	2.00	WS	7.82	7.82	7.63	7.56	7.53	7.39	7.11	6.15	5.06	4.09	2.97	2.29	1.58	1.17	1.17	1.17	1.17	1.17	1.17
		BS	6.18	6.18	6.21	6.23	6.23	6.22	6.18	5.32	4.37	3.41	2.34	1.75	1.07	0.71	0.00	0.00	0.00	0.00	0.00

Table 18. (continued).

Run Number	Time (hrs)		Distance Along Embankment (ft.)																		
			0	2	4	6	8	10	12	14	16	18	20	22	24	26	28	30	32	34	35
25	0.00	WS	9.35	9.34	9.09	8.84	8.51	8.18	7.94	7.21	6.16	4.93	3.83	3.06	2.39	1.92	1.92	1.92	1.92	1.92	1.92
		BS	6.16	6.16	6.21	6.22	6.24	6.22	6.18	5.35	4.36	3.48	2.37	1.64	1.08	0.71	0.00	0.00	0.00	0.00	0.00
25	2.00	WS	9.34	9.34	9.09	8.84	8.51	8.18	7.94	7.11	6.16	4.83	3.63	3.05	2.29	1.92	1.92	1.92	1.92	1.92	1.92
		BS	6.13	6.13	6.21	6.23	6.24	6.22	6.17	5.21	4.35	3.27	2.17	1.63	0.95	0.69	0.00	0.00	0.00	0.00	0.00
26	0.00	WS	6.58	6.56	6.51	6.47	6.42	6.34	6.22	6.14	6.02	5.70	5.56	5.62	4.17	3.60	3.07	2.62	2.03	1.56	1.41
		BS	5.93	6.04	6.01	6.04	6.06	6.09	6.01	5.95	5.83	5.69	5.17	4.67	4.00	3.41	2.68	2.27	1.68	1.26	0.91
26	1.00	WS	6.59	6.55	6.51	6.47	6.42	6.32	6.22	6.14	5.97	5.44	5.46	5.63	4.14	3.55	3.04	2.39	1.85	1.55	1.41
		BS	5.93	6.03	6.01	6.04	6.07	6.05	6.01	5.94	5.79	5.31	5.05	4.89	3.97	3.35	2.65	1.98	1.45	1.14	0.91
26	3.50	WS	6.43	6.40	6.37	6.33	6.31	6.23	6.13	6.08	5.35	5.32	5.39	4.83	4.07	3.52	2.84	2.16	1.90	1.93	1.19
		BS	5.89	6.01	6.01	6.07	6.08	6.05	6.00	5.94	5.20	5.18	5.16	4.64	3.95	3.34	2.51	1.88	1.73	1.10	0.90
26	10.00	WS	6.40	6.36	6.39	6.33	6.32	6.25	6.15	6.11	5.34	5.37	5.35	4.83	4.11	3.49	2.54	2.37	1.86	1.41	1.13
		BS	5.87	6.00	6.01	6.09	6.08	6.05	6.01	5.95	5.05	5.17	5.15	4.59	3.85	3.17	2.16	1.80	1.44	1.01	0.80
27	0.00	WS	7.80	7.71	7.67	7.57	7.42	7.35	7.14	6.97	6.61	6.13	5.87	5.41	4.75	4.11	3.52	3.01	2.31	2.01	1.98
		BS	5.81	6.03	6.01	6.07	6.08	6.05	6.01	5.94	5.80	5.47	5.13	4.53	3.95	3.33	2.37	1.90	1.70	1.06	0.88
27	1.25	WS	7.81	7.71	7.67	7.55	7.42	7.35	7.14	6.96	6.59	6.03	5.77	5.31	4.67	4.05	3.48	2.51	2.03	1.85	1.31
		BS	5.86	6.03	6.01	6.05	6.08	6.05	6.01	5.95	5.21	5.16	5.01	4.48	3.84	3.25	2.31	1.39	1.35	0.05	0.09
27	3.50	WS	7.81	7.71	7.67	7.55	7.42	6.96	6.86	6.56	6.62	6.24	5.60	5.15	4.22	3.40	1.58	1.35	1.30	1.07	1.07
		BS	5.86	6.03	6.01	6.05	6.08	6.05	6.01	5.95	5.10	5.05	4.99	4.45	3.80	3.15	1.23	0.53	0.41	0.27	0.00
27	10.00	WS	7.82	7.70	7.66	7.54	7.43	6.95	6.88	6.15	5.74	5.65	5.40	4.89	4.08	2.75	1.51	1.06	1.06	1.06	1.06
		BS	5.85	6.03	6.01	6.05	6.08	6.05	6.01	5.26	4.87	4.75	4.70	4.35	3.66	2.35	0.71	0.15	0.00	0.00	0.00

173

Table 18. Water surface (WS) and bed surface (BS) elevations. (continued)

Run Number	Time (hrs)		Distance Along Embankment (ft.)																		
			0	2	4	6	8	10	12	14	16	18	20	22	24	26	28	30	32	34	35
28	0.00	WS	9.56	9.54	9.53	9.52	9.50	9.49	9.25	8.80	8.43	7.83	6.69	6.20	5.59	4.81	3.93	3.21	2.85	2.56	2.16
		BS	5.35	5.67	5.95	5.93	5.94	5.93	5.92	5.93	5.85	5.63	4.81	4.49	3.83	3.15	2.31	1.79	1.49	1.03	0.67
28	1.00	WS	9.54	9.54	9.53	9.53	9.50	9.49	9.25	8.73	7.04	6.93	6.19	5.87	5.39	4.71	3.93	3.11	2.71	2.34	2.06
		BS	5.35	5.67	5.95	5.93	5.94	5.93	5.92	5.93	4.84	4.73	4.43	4.15	3.59	3.05	2.29	1.98	1.16	0.67	0.43
28	4.00	WS	8.63	8.61	8.62	8.63	8.45	8.37	8.12	7.55	6.96	6.74	6.23	5.64	5.51	4.67	3.29	2.37	1.73	1.71	1.71
		BS	4.92	4.90	4.91	4.90	4.91	4.81	4.79	4.77	4.61	4.57	4.26	3.83	3.58	2.78	1.64	0.61	0.00	0.00	0.00
28	10.00	WS	8.61	8.60	8.57	8.55	8.38	8.29	8.05	7.45	6.86	6.59	6.08	5.33	5.25	4.54	2.58	1.73	1.73	1.73	1.73
		BS	4.88	4.85	4.80	4.83	4.80	4.71	4.69	4.58	4.50	4.37	4.06	3.43	3.20	2.61	0.81	0.00	0.00	0.00	0.00
29	0.00	WS	6.61	6.60	6.52	6.35	6.25	6.24	6.20	6.09	5.86	5.86	5.80	5.39	5.32	5.01	5.12	5.40	5.39	5.70	5.68
		BS	5.93	5.93	5.93	5.93	5.93	5.93	5.85	5.82	5.59	5.41	5.07	4.17	3.51	2.53	2.09	1.63	1.23	0.95	0.90
29	1.00	WS	6.61	6.61	6.50	6.34	6.25	6.24	6.19	6.10	5.85	5.86	5.74	5.29	5.32	5.01	5.16	5.41	5.37	5.68	5.66
		BS	5.93	5.93	5.93	5.93	5.93	5.93	5.86	5.82	5.61	4.99	4.75	4.08	3.50	2.57	2.11	1.62	1.19	0.97	0.88
29	4.00	WS	6.61	6.55	6.34	6.25	6.22	6.23	6.12	6.02	5.91	6.01	5.92	5.41	5.53	5.11	5.27	5.31	5.49	5.80	5.84
		BS	5.93	5.93	5.93	5.93	5.93	5.93	5.84	5.82	5.64	4.94	4.71	4.00	3.46	2.54	2.07	1.64	1.16	0.94	0.88
29	10.00	WS	6.61	6.56	6.33	6.24	6.23	6.21	6.08	5.95	5.88	5.90	5.84	5.37	5.49	5.13	5.22	5.32	5.49	5.70	5.66
		BS	5.93	5.93	5.92	5.92	5.91	5.90	5.80	5.77	5.61	4.82	4.61	3.95	3.41	2.48	2.03	1.63	1.15	0.92	0.85
30	0.00	WS	7.95	7.94	7.60	7.35	7.27	7.23	7.05	6.96	6.66	6.63	5.87	5.18	5.37	5.59	5.38	5.52	5.84	5.90	6.11
		BS	5.93	5.93	5.93	5.93	5.93	5.93	5.85	5.82	5.59	5.41	5.07	4.17	3.51	2.53	2.09	1.63	1.23	0.95	0.90
30	1.00	WS	7.95	7.95	7.55	7.34	7.27	7.22	7.10	7.01	6.66	6.62	5.91	5.18	5.33	5.59	5.37	5.49	5.81	5.91	6.10
		BS	5.93	5.93	5.93	5.93	5.93	5.93	5.84	5.81	5.59	5.40	5.01	4.15	3.48	2.54	2.11	1.59	1.20	0.91	0.88
30	4.00	WS	7.95	7.95	7.59	7.34	7.22	7.24	7.09	6.94	6.62	6.57	6.64	5.91	5.86	5.35	5.44	5.58	5.74	6.02	6.11
		BS	5.93	5.93	5.93	5.93	5.93	5.93	5.82	5.80	5.57	5.39	5.04	4.10	3.47	2.53	1.97	1.59	1.18	0.88	0.87
30	10.00	WS	7.94	7.94	7.53	7.35	7.22	7.24	7.08	6.91	6.55	6.57	6.40	5.88	5.81	5.33	5.40	5.57	5.74	6.04	6.12
		BS	5.93	5.93	5.93	5.93	5.93	5.93	5.77	5.76	5.53	5.29	5.00	4.05	3.45	2.49	1.67	1.51	1.10	0.87	0.83

174

Table 18. (continued).

Run Number	Time (hrs)		Distance Along Embankment (ft.)																		
			0	2	4	6	8	10	12	14	16	18	20	22	24	26	28	30	32	34	35
31	0.00	WS	6.65	6.65	6.58	6.55	6.53	6.50	6.48	6.43	6.39	6.34	5.85	5.46	4.75	4.20	3.45	2.62	1.96	1.30	1.20
		BS	5.49	5.83	6.08	6.04	6.00	6.12	6.13	6.16	6.10	6.08	5.73	5.21	4.66	3.82	3.16	2.26	1.66	1.12	0.92
31	1.00	WS	6.63	6.59	6.56	6.57	6.51	6.48	6.48	6.42	6.37	6.32	5.44	5.26	4.47	4.05	2.64	2.61	1.77	1.11	1.11
		BS	5.43	5.79	5.99	6.01	6.01	6.08	6.08	6.11	6.13	6.05	5.24	4.93	4.38	3.67	2.32	2.21	1.44	0.89	0.78
32	0.00	WS	7.85	7.73	7.67	7.58	7.44	7.65	7.50	7.48	7.43	7.39	6.53	5.99	5.65	4.49	3.67	2.98	2.25	1.60	1.31
		BS	5.36	5.83	6.03	6.08	6.03	6.05	6.03	6.08	6.03	5.81	5.36	4.99	4.45	3.85	3.07	2.34	1.65	0.98	0.72
33	0.00	WS	6.68	6.60	6.58	6.57	6.57	6.56	6.54	6.43	6.35	6.28	5.70	5.42	5.25	4.48	3.61	2.82	1.95	1.42	1.34
		BS	5.46	5.85	6.09	6.05	6.08	6.10	6.07	6.14	6.07	5.95	5.45	5.23	4.79	4.05	3.26	2.39	1.47	1.12	0.89
33	1.00	WS	6.67	6.59	6.58	6.57	6.57	6.57	6.53	6.41	6.34	6.23	5.60	5.28	4.90	4.10	3.47	2.64	1.99	1.28	1.26
		BS	5.33	5.81	6.07	6.01	6.05	6.08	6.09	6.11	6.05	5.89	5.33	5.00	4.41	3.65	3.10	2.21	1.56	0.95	0.81
33	2.00	WS	6.60	6.61	6.69	6.55	6.57	6.53	6.51	6.37	6.34	6.21	5.71	5.21	5.01	3.81	3.53	2.46	1.65	1.19	1.01
		BS	5.43	5.81	6.07	6.01	6.03	6.06	6.07	6.10	6.07	5.88	5.24	4.84	4.43	3.60	3.13	2.15	1.36	0.98	0.76
33	4.00	WS	6.62	6.61	6.57	6.61	6.51	6.49	6.51	6.37	6.35	6.19	5.63	5.11	4.82	3.81	3.39	2.45	1.99	1.11	1.10
		BS	5.45	5.81	6.02	6.01	6.03	6.09	6.09	6.16	6.07	5.86	5.17	4.83	4.45	3.58	3.12	2.11	1.51	0.93	0.71
34	0.00	WS	7.06	7.05	6.97	6.96	6.88	6.86	6.82	6.75	6.62	6.44	5.94	5.52	4.86	4.20	3.59	2.61	2.17	1.43	1.27
		BS	5.37	5.81	6.03	6.01	6.07	6.08	6.03	6.11	6.04	5.86	5.41	5.16	4.49	3.81	3.25	2.26	1.59	1.00	0.75
34	1.00	WS	7.06	7.05	6.96	6.96	6.90	6.84	6.82	6.72	6.61	6.42	5.91	5.43	4.87	4.18	3.59	2.58	2.14	1.40	1.27
		BS	5.37	5.81	6.01	6.01	6.01	6.05	6.07	6.07	6.02	5.84	5.34	5.04	4.58	3.79	3.10	2.21	1.53	0.96	0.74
34	2.00	WS	7.07	7.06	6.93	6.94	6.90	6.84	6.88	6.71	6.60	6.39	5.98	5.45	4.83	4.17	3.65	2.69	1.90	1.47	1.70
		BS	5.34	5.80	6.05	6.00	6.02	6.03	6.02	6.08	6.03	5.83	5.35	5.03	4.48	3.81	3.20	2.27	1.51	0.98	0.73
35	0.00	WS	9.79	9.70	9.48	9.23	9.11	8.92	8.77	8.44	8.20	7.91	7.70	6.96	6.25	5.70	4.98	4.18	3.36	2.62	2.23
		BS	5.39	5.84	6.02	5.98	6.04	6.06	6.03	6.06	5.92	5.80	5.54	5.05	4.54	3.97	3.76	2.46	1.79	1.05	0.80
35	1.00	WS	9.75	9.64	9.48	9.21	9.04	8.89	8.73	8.41	8.18	7.92	7.40	6.95	6.21	5.71	4.79	3.88	3.30	2.46	2.18
		BS	5.34	5.76	6.01	5.95	5.92	6.01	5.97	6.02	5.90	5.81	5.19	5.02	4.48	4.01	3.07	2.12	1.72	0.88	0.74

Table 19. Velocity measurements.

Distance Along Embankment (ft.)

Run No	Time (hrs)	10.0 Va (ft/s)	10.0 Vr (ft/s)	21.2 Va (ft/s)	21.2 Vr (ft/s)	24.0 Va (ft/s)	24.0 Vr (ft/s)	27.0 Va (ft/s)	27.0 Vr (ft/s)	29.0 Va (ft/s)	29.0 Vr (ft/s)	33.0 Va (ft/s)	33.0 Vr (ft/s)
1	0.0	2.3	2.3	2.2	1.3	0.7	0.4	0.4	0.1	0.3	0.1	0.2	0.1
1	10.0	2.0	2.2	1.7	1.0	0.7	0.3	0.4	0.1	0.3	0.1	0.2	0.1
2	0.0	3.0	2.9	6.3	5.1	7.7	6.1	9.4	6.6	9.0	6.6	7.4	5.5
2	10.0	2.9	2.5	5.7	4.5	5.7	4.3	6.2	4.9	6.2	4.8	8.3	5.8
3	0.0	4.1	3.8	2.1	1.1	1.2	-0.5	0.9	-0.3	0.8	-0.2	0.6	-0.3
3	10.0	4.0	3.9	2.0	1.1	1.2	-0.4	0.9	-0.2	0.8	-0.2	0.6	-0.3
4	0.0	5.4	4.9	4.8	1.4	3.1	-0.6	2.4	-0.6	2.0	-0.5	1.6	-0.6
4	10.0	5.3	4.7	4.3	1.3	2.9	-0.5	2.3	-0.5	1.9	-0.5	1.5	-0.6
5	0.0	7.2	5.8	7.5	5.5	5.6	4.6	3.8	4.3	2.6	4.3	1.9	4.4
5	9.7	8.0	6.1	7.7	5.6	5.0	4.5	3.2	4.2	2.5	4.2	1.8	3.7
6	0.0	5.6	4.9	8.8	5.3	10.0	6.1	11.9	7.5	12.7	8.2	15.4	10.3
6	9.5	5.7	5.2	9.1	5.4	10.9	6.9	13.2	8.3	12.8	8.3	9.4	7.5
7	0.0	11.3	10.5	7.0	3.6	5.5	1.2	4.3	-1.2	3.9	-1.3	3.2	-1.5
7	10.0	10.5	10.1	7.2	3.7	6.2	1.3	4.8	-1.2	4.1	-1.3	3.5	-1.5
8	0.0	9.0	7.7	11.8	6.8	7.8	7.2	5.2	5.5	4.5	6.0	3.7	5.5
8	10.0	9.3	7.8	7.8	7.7	6.6	5.1	5.4	4.7	4.5	5.0	3.9	5.2
9	0.0	8.2	7.8	12.2	6.7	14.8	8.5	15.8	9.5	15.9	9.5	16.7	9.7
9	10.0	9.4	8.0	10.8	8.9	8.9	6.9	11.5	6.9	15.0	8.3	15.0	8.5
10	0.0	2.4	2.3	1.3	1.5	0.6	0.4	0.4	0.3	0.3	0.2	0.2	0.2
10	10.5	1.1	1.0	0.8	0.7	0.5	0.3	0.4	0.3	0.3	0.2	0.2	0.2
11	0.0	3.4	3.3	1.9	1.3	1.3	0.7	1.0	-0.4	0.9	-0.6	0.7	-0.5
11	10.0	4.1	3.9	1.7	1.5	1.4	0.7	1.0	-0.4	0.9	-0.6	0.7	-0.4
12	0.0	7.0	6.7	10.1	7.9	5.3	4.8	3.9	4.7	2.9	4.8	2.2	5.0
12	9.0	6.8	6.6	7.1	5.0	4.3	4.7	3.1	4.6	2.6	4.8	2.0	4.9
13	0.0	10.7	10.0	13.7	7.1	11.4	7.9	7.1	6.7	5.8	6.9	4.5	7.2
13	10.5	10.5	10.7	13.4	6.9	8.5	6.4	6.3	6.7	5.3	6.8	4.0	6.9

V_a = averaged velocity, V_r = local velocity at about 0.5" above the bed surface.
See figure 26 for the measurement locations.
Detailed velocity information is available upon formal request.

Table 19. (continued).

Distance Along Embankment (ft.)

Run No	Time (hrs)	10.0 Va (ft/s)	10.0 Vr (ft/s)	21.2 Va (ft/s)	21.2 Vr (ft/s)	24.0 Va (ft/s)	24.0 Vr (ft/s)	27.0 Va (ft/s)	27.0 Vr (ft/s)	29.0 Va (ft/s)	29.0 Vr (ft/s)	33.0 Va (ft/s)	33.0 Vr (ft/s)
14	0.0	3.4	3.0	1.2	0.7	0.6	0.3	0.4	0.3	0.3	0.1	0.2	0.1
14	0.0	3.4	3.0	0.9	0.1	0.6	0.3	0.4	0.3	0.3	0.1	0.2	0.1
15	0.0	4.0	3.5	3.0	1.7	1.5	1.0	1.0	-0.3	0.8	-0.5	0.6	-0.5
15	0.0	3.9	3.5	1.5	0.9	1.2	0.3	1.0	-0.2	0.9	-0.4	0.7	-0.4
16	0.0	7.7	7.0	11.0	6.0	4.5	4.5	3.2	4.7	2.7	4.8	2.0	5.0
16	10.0	7.5	5.8	5.6	*	3.8	4.6	3.2	4.7	2.7	4.9	2.0	4.9
17	0.0	9.3	7.5	11.3	8.5	8.2	6.5	5.9	5.2	4.8	5.2	3.9	4.4
17	10.0	9.9	7.8	9.5	*	6.8	5.2	6.2	5.0	5.1	4.8	3.9	4.2
18	0.0	4.2	3.4	8.6	6.0	9.4	6.0	6.7	5.2	7.5	2.4	7.1	4.4
18	2.0	4.4	3.8	5.9	5.0	6.3	4.8	6.2	5.6	6.1	8.2	6.7	4.2
19	0.0	10.2	9.8	12.7	10.2	11.2	8.2	12.6	7.9	12.7	*	*	*
19	2.5	10.2	9.5	11.8	6.7	7.4	3.5	*	*	*	*	*	*
20	0.0	8.5	7.9	3.9	3.5	6.0	3.5	7.0	4.3	7.7	4.0	*	*
20	2.2	10.0	8.5	4.5	4.0	6.0	3.2	7.3	4.4	8.6	4.3	*	*
21	0.0	10.8	9.8	13.9	8.2	12.3	7.5	12.5	7.3	12.3	7.4	*	*
21	2.0	10.5	10.0	13.8	8.4	10.8	7.3	13.5	7.3	13.7	7.4	*	*
22	0.0	11.8	10.7	14.9	8.5	15.8	8.3	18.0	8.1	19.3	9.6	*	*
22	2.0	12.4	11.0	15.1	8.5	16.4	8.5	18.7	8.2	19.6	9.8	*	*
23	0.0	5.0	4.5	10.7	10.5	13.6	13.6	15.0	15.0	*	*	*	*
23	2.0	5.1	4.5	10.9	10.5	13.6	13.6	13.6	13.6	*	*	*	*
24	0.0	8.5	7.5	16.5	15.2	19.6	18.0	21.7	19.5	*	*	*	*
24	2.0	8.5	7.5	17.1	15.3	19.6	18.0	21.7	19.5	*	*	*	*
25	0.0	11.9	10.5	16.2	15.2	17.8	17.5	19.3	18.0	*	*	*	*
25	2.0	11.9	10.5	16.2	15.0	17.4	17.5	19.3	17.5	*	*	*	*
26	0.0	4.0	3.8	1.5	2.0	5.9	5.9	3.4	1.5	2.7	1.5	3.1	1.6
26	3.5	5.6	4.5	4.8	3.5	8.3	8.3	3.9	1.7	3.3	1.6	3.3	1.8
27	0.0	7.4	6.8	12.3	10.0	12.5	8.3	10.4	7.0	8.8	6.0	12.8	7.0
28	0.0	6.6	5.1	13.0	8.9	13.3	8.0	14.2	8.0	15.4	8.0	16.1	8.2
28	4.0	6.6	5.1	12.3	7.8	12.1	7.8	13.2	8.1	13.7	8.2	*	*

*Measurement location was off embankment or was in vortex region.

177

Table 19. Velocity measurements. (continued)

Distance Along Embankment (ft.)

Run No	Time (hrs)	10.0		21.2		24.0		27.0		29.0		33.0	
		Va (ft/s)	Vr (ft/s)	Va (ft/s)	Vr (ft/s)	Va (ft/s)	Vr (ft/s)	Va (ft/s)	Vr (ft/s)	Va (ft/s)	Vr (ft/s)	Va (ft/s)	Vr (ft/s)
29	0.0	3.2	3.0	1.0	1.3	1.2	0.6	0.4	0.1	0.3	0.1	0.2	0.0
29	4.0	3.3	3.0	0.8	0.8	0.9	0.5	0.3	0.1	0.3	0.1	0.2	0.1
30	0.0	7.7	5.9	11.0	8.2	5.4	5.6	3.1	4.6	2.8	4.7	2.1	5.0
30	4.0	7.6	5.7	5.9	4.0	4.2	4.5	3.2	4.6	2.7	4.7	2.1	5.0
31	0.0	2.6	2.0	5.1	5.0	11.1	11.0	3.0	3.0	3.1	3.0	4.2	2.0
31	1.0	2.5	1.8	3.8	3.5	11.0	11.0	2.9	2.7	2.8	2.7	3.6	3.0
32	0.0	6.3	5.5	9.2	10.0	8.3	10.0	15.8	8.0	15.8	7.0	16.0	7.0
33	0.0	2.2	2.0	4.5	4.5	2.2	2.0	2.6	2.6	2.6	2.6	2.6	2.6
33	2.0	2.1	2.0	2.4	2.4	1.7	2.0	3.3	3.0	2.8	2.5	4.0	3.0
34	0.0	3.9	4.1	6.7	4.5	8.1	7.8	8.2	5.5	8.7	4.8	5.9	4.0
34	2.0	3.7	3.6	5.7	4.2	8.6	7.7	7.4	4.5	6.9	4.3	6.8	4.1
35	0.0	12.5	11.5	11.5	12.0	13.6	14.0	15.8	11.5	15.8	11.5	14.9	12.0
35	1.0	12.4	11.8	11.3	11.0	13.5	13.0	13.6	11.0	13.4	11.0	14.8	12.0

APPENDIX C - USER'S MANUAL AND LIST OF COMPUTER PROGRAMS

1. Introduction

A computer model "EMBANK" has been developed to determine unit-width embankment damage due to flood overtopping. The input data required to apply the model are:

-   Number of computational points and composition layers of the embankment studied.

-   Digitized cross-sectional shapes of the embankment.

-   Critical shear stresses and erosion equations.

-   Manning's roughness coefficients.

-   Thickness of composition layers.

-   Headwater hydrograph.

-   Tailwater hydrograph.

Section 2 of this appendix describes the procedure for preparing input data, section 3 presents an example of an output file, and section 4 presents a listing of the computer program.

2. Description of Input Data

The example shown on tables 20 and 21 is utilized to demonstrate the procedures for preparing the input data file. Table 20 shows an example of an input data file.

3. Description of Output Results

Table 22 shows an example of output results. The variables on table 22 are explained below:

J = Computational time step.

TIMEP = Time in hours after beginning of flood overtopping.

HW = Headwater elevation in feet.

TW = Tailwater elevation in feet.

Q = QO.

179

YC = Critical depth at control piont.

SC = Critical slope.

IC = Location of control point.

LAYER = Identification of surface layer. For example, if the pavement layer remains on the embankment surface points, LAYER = 1. But if the pavement layer is removed and the gravel layer is exposed, then LAYER becomes 2, and so on.

X = Horizontal distance of computational points in feet.

Y = Flow depths in feet.

Z = Embankment elevations in feet.

H = Water surface elevation in feet.

V = Velocity in ft/s.

F = Froude number.

SF = Friction slope.

SO = Bed slope.

QE = Erosion rate in ft^3/s-ft.

SH = Shear stress in lb/ft^2.

TL = Remaining thickness of surface layer in feet.

DZTL = Cumulative embankment elevation change in feet.

4. Listing of Computer Program
    The listing of the computer program is provided in table 23.

180

Table 20. Example input file.

```
Card
Number

 1   EXAMPLE EMBANKMENT WITH PAVEMENT & C VEGETAL COVER, TYPE 1 SOIL
 2     1        1        4        1        1        1        1
 3    15
 4     0.     0.00     5.     2.50    10.     5.00    15.     7.50
 5    20.    10.00    25.    10.20    30.    10.40    35.    10.50
 6    40.    10.40    45.    10.20    50.    10.00    55.     7.50
 7    60.     5.00    65.    12.50    70.    10.00
 8     5       11
 9   100.0    0.15     1.00    0.053
10     0.015   0.025    0.030   0.015
11     1.94
12     1.6
13     1.0     1.0     1.300    1.300   0.000220  0.000220   0.43   0.43
14   142.      10
15     0.25    0.000    0.000    0.000    0.25     0.25
16     0.000   0.25     0.000    0.000    0.000    0.000
17     0.000   0.000    0.000    0.500    0.500    0.500
18     0.50    0.50     0.500    0.000    0.000    0.000
19     0.50    0.50     0.50     0.50     0.50     0.50
20     0.00    0.00     0.00     0.00     0.00     0.00
21     8
22     1.5     1.5      0.8      0.8      1.0      1.0      1.0      1.0
23     9.5    11.5     13.0     14.0     12.0     12.0     12.0     12.0
24     0.0     5.0     10.0     12.5     10.5     10.5     10.5     10.5
25     0.0     5.8     15.9     24.5      8.7      8.7      8.7      8.7
```

181

Table 21. Input file description.

Card Number	Variable	Format	Description
1	NCASE	I10	Number of study cases.
2	TITLE	--	Title description.
3	NX	I10	Number of digitized computational points. NX should be less than or equal to 50.
	IPAV	I10	= 1, paved embankment = 0, earth embankment
	NLAYER	I10	Number of composition layers. In the example shown on figure 43 and table 20, NLAYER = 4, indicating there are 4 layers: pavement, gravel, grass, and soil. NLAYER should be less than or equal to 10.
	IEOS	I10	= 1, erodible embankment, = 0, rigid embankment.
	IPRINT	I10	Output control to print out the calculated results once every IPRINT step.
	ITM	I10	= 0, overtopping flood hydrographs are single-step hydrographs with a constant headwater and tailwater. = 1, overtopping flood hydrographs are multiple-step hydrographs.
4 - 7	[x(I),Z0(I) I =1, NX]	8F10.0	Coordinates of computational points, X(I) = horizontal distance, Z(I) = elevation in feet.
8	[IP(I), I = 1,2]	2I10	Upstream and downstream edges of embankment surface.
9	[SHCI(I), I = 1, NLAYER]	4F10.0	Critical shear stresses for individual composition layers in lbs/ft^2.

Table 21. (continued).

Card Number	Variable	Format	Description
10	[RNI(I), I = 1, NLAYER]	4F10.0	Manning's roughness coefficient for individual composition layers.
11	P	F10.0	Density of flow fluid.
12	[SCI(I), BCI(I), I = 1, NLAYER]	8F10.0	Coefficients of erosion equations for each composition layer: $QS(J) = ACI(I) * (SH(J) - SHCI(I)) ** BCI(I)$ where $QS(J)$ is the erosion rate in $ft^3/ft/s$, and $SH(J)$ is the flow shear stress in lb/ft^2, at each computational point J.
13	[LPAV(I), I = 1,2]	2I10	Upstream and downstream edges of paved section. This card should be deleted if IPAV = 0.
14	PS	F10.0	Unit weight of pavement in lb/ft^3.
	TS	F10.0	Thickness of pavement in feet.
	SA	F10.0	Allowable tension stress of pavement in lb/ft^2. This card should be deleted if IPAV = 0.
15 - 20	[TL (I, J), I = 1, NX J = 1, NLAYER -1]	8F10.0	Thickness of individual composition layers from Layer 1 to Layer (NLAYER - 1). These cards should be deleted if NLAYER = 1.
21	ITIME	I10	Number of time steps for overtopping flow hydrographs.
22	[DT(J), J = 1, ITIME]	8F10.0	Duration of each time step in hours (ITM = 1). ITM = 0 indicates a constant DT and only a single DT value has to be input.
23	[HW(J), J =1, ITIME]	8F10.0	Headwater elevation of each step hydrograph in feet (ITM = 1). ITM = 0 indicates a constant HW and only a single HW value has to be input.

Table 21. Input file description. (continued)

Card Number	Variable	Format	Description
24	[TW(J), J = 1, ITIME]	8F10.0	Tailwater elevation of each step hydrograph in feet (ITM = 1). For free-fall condition, let TW = 0. ITM = 0 indicates a constant TW and only a single TW value has to be input.
25	[QO(J), J = 1, ITIME]	8F10.0	Maximum overtopping flow discharge for each step hydrograph in ft^3/s-ft. QO = C * (HW - ZMAX) ** 1.5, where C is the discharge coefficient, and ZMAX is the crest elevation of embankment. ITM = 0 indicates a constant QO and only a single QO value has to be input.

Table 22. Example output file.

EXAMPLE EMBANKMENT WITH PAVEMENT & C VEGETAL COVER, TYPE 1 SOIL

J,TIMEP,HW,TW,Q,YC,SC,IC   2 0.3000E+01 0.1150E+02 0.5000E+01 0.3032E+01 0.6595E+00 0.1051E-01   9

I	LAYER	X	Y	Z	H	V	F	SF	SO	QE	SH	TL	DZTL
1	4	0.000E+00	0.115E+02	0.000E+00	0.115E+02	0.264E+00	0.137E-01	0.276E-06	-0.500E+00	0.000E+00	0.197E-03	0.000E+00	0.000E+00
2	3	0.500E+01	0.900E+01	0.250E+01	0.115E+02	0.337E+00	0.198E-01	0.250E-05	-0.500E+00	0.000E+00	0.826E-03	0.500E+00	0.000E+00
3	3	0.100E+02	0.650E+01	0.500E+01	0.115E+02	0.466E+00	0.322E-01	0.738E-05	-0.500E+00	0.000E+00	0.158E-02	0.500E+00	0.000E+00
4	3	0.150E+02	0.400E+01	0.750E+01	0.115E+02	0.758E+00	0.668E-01	0.372E-04	-0.500E+00	0.000E+00	0.418E-02	0.500E+00	0.000E+00
5	2	0.200E+02	0.148E+01	0.100E+02	0.115E+02	0.205E+01	0.297E+00	0.709E-03	-0.270E+00	0.000E+00	0.331E-01	0.500E+00	0.000E+00
6	1	0.250E+02	0.125E+01	0.102E+02	0.115E+02	0.242E+01	0.382E+00	0.447E-03	-0.400E-01	0.000E+00	0.214E-01	0.250E+00	0.000E+00
7	1	0.300E+02	0.993E+00	0.104E+02	0.114E+02	0.305E+01	0.540E+00	0.962E-03	-0.300E-01	0.000E+00	0.339E-01	0.250E+00	0.000E+00
8	1	0.350E+02	0.559E+00	0.105E+02	0.111E+02	0.542E+01	0.128E+01	0.650E-02	0.000E+00	0.000E+00	0.107E+00	0.250E+00	0.000E+00
9	1	0.400E+02	0.659E+00	0.104E+02	0.111E+02	0.460E+01	0.998E+00	0.376E-02	0.553E-01	0.000E+00	0.769E-01	0.250E+00	0.000E+00
10	2	0.450E+02	0.451E+00	0.995E+01	0.107E+02	0.673E+01	0.177E+01	0.133E-01	0.152E+00	0.000E+00	0.165E+00	0.497E+00	0.253E+00
11	4	0.500E+02	0.425E+00	0.888E+01	0.104E+02	0.713E+01	0.193E+01	0.451E-01	0.294E+00	0.140E-03	0.401E+00	0.888E+01	0.112E+01
12	3	0.550E+02	0.244E+00	0.701E+01	0.774E+01	0.124E+02	0.444E+01	0.414E+00	0.388E+00	0.905E-04	0.113E+01	0.113E-01	0.489E+00
13	3	0.600E+02	0.116E+01	0.500E+01	0.616E+01	0.261E+01	0.428E+00	0.230E-02	0.451E+00	0.000E+00	0.282E+00	0.500E+00	0.000E+00
14	3	0.650E+02	0.300E+01	0.250E+01	0.550E+01	0.101E+01	0.103E+00	0.966E-04	0.500E+00	0.000E+00	0.282E+00	0.500E+00	0.000E+00
15	4	0.700E+02	0.500E+01	0.000E+00	0.500E+01	0.606E+00	0.478E-01	0.442E-05	0.500E+00	0.788E-04	0.145E+00	0.000E+00	0.000E+00

CASE 1 TIME(HRS)= 3.00 TOT EROSION(FT**3/FT)= 0.9327E+01   AVG EROSION RATE(YD**3/FT/HR)= 0.1151E+00

J,TIMEP,HW,TW,Q,YC,SC,IC   3 0.3800E+01 0.1300E+02 0.1000E+02 0.1204E+02 0.1654E+01 0.7736E-02   9

I	LAYER	X	Y	Z	H	V	F	SF	SO	QE	SH	TL	DZTL
1	4	0.000E+00	0.130E+02	0.000E+00	0.130E+02	0.926E+00	0.453E-01	0.289E-05	-0.500E+00	0.000E+00	0.233E-02	0.000E+00	0.000E+00
2	3	0.500E+01	0.105E+02	0.250E+01	0.130E+02	0.115E+01	0.625E-01	0.237E-04	-0.500E+00	0.000E+00	0.959E-02	0.500E+00	0.000E+00
3	3	0.100E+02	0.797E+01	0.500E+01	0.130E+02	0.151E+01	0.943E-01	0.590E-04	-0.500E+00	0.000E+00	0.166E-01	0.500E+00	0.000E+00
4	3	0.150E+02	0.543E+01	0.750E+01	0.129E+02	0.222E+01	0.168E+00	0.212E-03	-0.498E+00	0.000E+00	0.358E-01	0.500E+00	0.000E+00
5	2	0.200E+02	0.269E+01	0.998E+01	0.127E+02	0.448E+01	0.481E+00	0.153E-02	-0.270E+00	0.602E-05	0.158E+00	0.483E+00	0.173E-01
6	1	0.250E+02	0.241E+01	0.102E+02	0.126E+02	0.500E+01	0.569E+00	0.797E-03	-0.417E-01	0.000E+00	0.911E-01	0.250E+00	0.000E+00
7	1	0.300E+02	0.206E+01	0.104E+02	0.125E+02	0.585E+01	0.719E+00	0.134E-02	-0.300E-01	0.000E+00	0.125E+00	0.250E+00	0.000E+00
8	1	0.350E+02	0.165E+01	0.105E+02	0.122E+02	0.728E+01	0.997E+00	0.277E-02	0.000E+00	0.000E+00	0.193E+00	0.250E+00	0.000E+00
9	1	0.400E+02	0.165E+01	0.104E+02	0.121E+02	0.728E+01	0.997E+00	0.277E-02	0.159E+00	0.000E+00	0.193E+00	0.250E+00	0.000E+00
10	4	0.450E+02	0.114E+01	0.891E+01	0.111E+02	0.105E+02	0.174E+01	0.265E-01	0.212E+00	0.202E-03	0.877E+00	0.891E+01	0.129E+01
11	4	0.500E+02	0.868E+00	0.828E+01	0.974E+01	0.139E+02	0.262E+01	0.237E-01	0.190E+00	0.206E-03	0.908E+00	0.828E+01	0.172E+01
12	3	0.550E+02	0.286E+01	0.701E+01	0.987E+01	0.421E+01	0.438E+00	0.179E-02	0.328E+00	0.000E+00	0.349E+00	0.113E-01	0.489E+00
13	3	0.600E+02	0.493E+01	0.500E+01	0.993E+01	0.244E+01	0.194E+00	0.293E-03	0.451E+00	0.000E+00	0.349E+00	0.500E+00	0.000E+00
14	3	0.650E+02	0.747E+01	0.250E+01	0.997E+01	0.161E+01	0.104E+00	0.734E-04	0.500E+00	0.000E+00	0.349E+00	0.500E+00	0.000E+00
15	4	0.700E+02	0.100E+02	0.000E+00	0.100E+02	0.120E+01	0.671E-01	0.693E-05	0.500E+00	0.779E-04	0.143E+00	0.000E+00	0.000E+00

CASE 1 TIME(HRS)= 3.80 TOT EROSION(FT**3/FT)= 0.1754E+02   AVG EROSION RATE(YD**3/FT/HR)= 0.1710E+00

Table 23. Listing of computer program.

```
      PROGRAM EMBANK
C *** THIS PROGRAM IS FOR COMPUTING HYDRAULICS OF
C     EMBANKMENT OVERTOPPING FLOW
      CHARACTER*80 TITLE
      COMMON/GEOM/X(50),Z(50),IT(50),RN(50),SO(50),TCS(50),
     1TCB(50),IP(2),RL,NX,SMAX,IS,ZMAX,LPAV(2),ZO(50),DZTL(50)
      COMMON/HYDRO/TIME(50),HW(50),TW(50),Q(50),YN,ITIME,DT(50),QO(50)
      COMMON/YSC/YC,SC,IC,G
      COMMON/WS/H(50),SF(50),V(50),Y(50),F(50),IJUMP
      COMMON/EROS/IPAV,NLAYER,TL(50,10),IEOS,SHCI(10),RNI(10),SH(50),
     1ILAYER(50),QE(50),DZT(50),DZ(50),P,PS,AC(50),BC(50),
     2SA,EL,SHC(50),TS,ACI(10),BCI(10),XB(50),DEC,IPRINT,TIMEP,ITM
      OPEN(UNIT=5,FILE='INPUT',STATUS='OLD')
      OPEN(UNIT=6,FILE='OUTPUT',STATUS='NEW')
C     OPEN(UNIT=7,FILE='TEMP',STATUS='UNKNOWN')
C     OPEN(UNIT=8,FILE='OUTEROS',STATUS='NEW')
C *** INPUT THE EMBANKMENT CHARTERISTICS AND HYDROGRAPH
      READ(5,1)NCASE
    1 FORMAT(I10)
      DO 200 NC=1,NCASE
      TVOL=0.
      DEC=0.
      CALL INP(TITLE)
      IF(IPRINT.EQ.0)IPRINT=1
      WRITE(6, 300)TITLE
C     WRITE(7,300)TITLE
C     WRITE(8,300)TITLE
  300 FORMAT(///2X,A80)
      CALL LAYER
      TIMEP=0.
      DO 100 J=1,ITIME
C *** COMPUTE OVERTOPPING DISCHARGE
      TIMEP=TIMEP+DT(J)/3600.
      CALL DISCH(J)
      IF(Q(J).LT.0.01)GO TO 100
      YN=(Q(J)*RN(IS)/(1.486*SQRT(SMAX)))**0.6
C *** COMPUTE CRITICAL DEPTH AND CONTROL SECTION
      CALL CRICT(J)
C *** COMPUTE UPSTREAM STAGE4 FROM THE CONTROL SECTION
      IF(IC.EQ.1)GO TO 10
      I=IC
      ID=I-1
      DO 11 K=1,ID
      K1=I-K+1
      CALL USWS(K1,J)
   11 CONTINUE
   10 CONTINUE
C *** COMPUTE DOWNSTREAM STAGE FROM THE CONTROL SECTION
      IF(IC.EQ.NX)GO TO 20
      I=IC
      NX1=NX-1
      DO 21 K=I,NX1
      CALL DSWS(K,J)
   21 CONTINUE
   20 CONTINUE
C *** COMPUTE FLOW PROFILE UPSTREAM FROM THE TAILWATER
C     DEPTH AND DETERMINE JUMP LOCATION
      CALL JUMP(J)
C *** DETERMINE EROSION OF EMBANKMENT
      IF(IEOS.EQ.0)GO TO 101
      CALL SHEAR(J)
```

186

Table 23. (continued).

```
      CALL SEDQ
      CALL SEDZ(J)
      IF(IPAV.NE.0)CALL PAVZ
      CALL NEWSO
101 CONTINUE
C *** OUTPUT
      IJ=(J-1)/IPRINT*IPRINT
      IF(IJ.EQ.(J-1))CALL OUTP(J)
      TVOL=0.
      DO 210 I=1,NX
210 DZTL(I)=ZO(I)-Z(I)
      DO 102 I=1,NX1
102 TVOL=TVOL+(DZTL(I)+DZTL(I+1))*(X(I+1)-X(I))/2.
      ERATE=TVOL/TIMEP/27.
      WRITE(6,103)NC,TIMEP,TVOL,ERATE
100 CONTINUE
103 FORMAT(/' CASE',I3,'  TIME(HRS)=',F6.2,'  TOT EROSION(FT**3/FT)='
     1,E11.4,'     AVG EROSION RATE(YD**3/FT/HR)=',E11.4)
200 CONTINUE
      CALL EXIT
      END
      SUBROUTINE INP(TITLE)
C *** INPUT THE EMBANKMENT CHARACTERISTICS AND HYDROGRAPH
      CHARACTER*80 TITLE
      COMMON/GEOM/X(50),Z(50),IT(50),RN(50),SO(50),TCS(50),
     1TCB(50),IP(2),RL,NX,SMAX,IS,ZMAX,LPAV(2),ZO(50),DZTL(50)
      COMMON/HYDRO/TIME(50),HW(50),TW(50),Q(50),YN,ITIME,DT(50),QO(50)
      COMMON/EROS/IPAV,NLAYER,TL(50,10),IEOS,SHCI(10),RNI(10),SH(50),
     1ILAYER(50),QE(50),DZT(50),DZ(50),P,PS,AC(50),BC(50),
     2SA,EL,SHC(50),TS,ACI(10),BCI(10),XB(50),DEC,IPRINT,TIMEP,ITM
      DIMENSION TLT(50)
      READ(5,1)TITLE
  1 FORMAT(A80)
      READ(5,2)NX,IPAV,NLAYER,IEOS,IPRINT,ITM
  2 FORMAT(8I10)
      READ(5,4)(X(I),ZO(I),I=1,NX)
      DO 10 I=1,NX
      Z(I)=ZO(I)
      DZ(I)=0.
      TLT(I)=0.
      DZT(I)=0.
  3 FORMAT(I10,7F10.0)
 10 CONTINUE
      READ(5,2)(IP(I),I=1,2)
      READ(5,4)(SHCI(I),I=1,NLAYER)
      READ(5,4)(RNI(I),I=1,NLAYER)
      IF(IEOS.EQ.0)GO TO 21
      READ(5,4)P
      READ(5,4)(ACI(I),BCI(I),I=1,NLAYER)
      IF(IPAV.EQ.1)READ(5,2)(LPAV(I),I=1,2)
      IF(IPAV.EQ.1)READ(5,4)PS,TS,SA
      NL=NLAYER-1
      IF(NL.EQ.0)GO TO 40
      DO 41 J=1,NL
      READ(5,4)(TL(I,J),I=1,NX)
 41 CONTINUE
      DO 42 I=1,NX
      TLT(I)=0.
      DO 43 J=1,NL
      TLT(I)=TLT(I)+TL(I,J)
 43 CONTINUE
 42 CONTINUE
```

Table 23. Listing of computer program. (continued)

```
40 DO 44 I=1,NX
44 TL(I,NLAYER)=Z(I)-TLT(I)
21 CONTINUE
   NX1=NX-1
   SO(1)=(Z(1)-Z(2))/(X(2)-X(1))
   SO(NX)=(Z(NX-1)-Z(NX))/(X(NX)-X(NX-1))
   DO 11 I=2,NX1
   SO(I)=(Z(I-1)-Z(I+1))/(X(I+1)-X(I-1))
11 CONTINUE
   DO 50 I=1,NX
   I1=IP(1)
   XB(I)=X(I)-X(I1)
50 CONTINUE
   SMAX=SO(1)
   DO 13 I=2,NX
   IF(SMAX.GT.SO(I))GO TO 13
   SMAX=SO(I)
   IS=I
   IF(SMAX.LT.1.0E-6) SMAX=1.0E-6
13 CONTINUE
   READ(5,2)ITIME
   IF (ITM.NE.0) GO TO 60
   READ(5,4) DTM
   READ(5,4) HWM
   READ(5,4) TWM
   READ(5,4) QOM
   DO 61 J=1,ITIME
   DT(J)=DTM
   HW(J)=HWM
   TW(J)=TWM
   QO(J)=QOM
61 CONTINUE
   GO TO 62
60 CONTINUE
   READ(5,4)(DT(J),J=1,ITIME)
   READ(5,4)(HW(J),J=1,ITIME)
   READ(5,4)(TW(J),J=1,ITIME)
   READ(5,4)(QO(J),J=1,ITIME)
62 CONTINUE
   DO 12 J=1,ITIME
   DT(J)=DT(J)*3600.
 4 FORMAT(8F10.0)
12 CONTINUE
   RETURN
   END
   SUBROUTINE LAYER
   CHARACTER*80 TITLE
   COMMON/GEOM/X(50),Z(50),IT(50),RN(50),SO(50),TCS(50),
  1TCB(50),IP(2),RL,NX,SMAX,IS,ZMAX,LPAV(2),ZO(50),DZTL(50)
   COMMON/EROS/IPAV,NLAYER,TL(50,10),IEOS,SHCI(10),RNI(10),SH(50),
  1ILAYER(50),QE(50),DZT(50),DZ(50),P,PS,AC(50),BC(50),
  2SA,EL,SHC(50),TS,ACI(10),BCI(10),XB(50),DEC,IPRINT,TIMEP,ITM
   DO 22 I=1,NX
   ILAYER(I)=1
   RN(I)=RNI(1)
   SHC(I)=SHCI(1)
   AC(I)=ACI(1)
   BC(I)=BCI(1)
   IF(NLAYER.LE.1)GO TO 22
   NLA=NLAYER-1
   DO 23 K=1,NLA
   IF(IEOS.EQ.0)TL(I,K)=Z(I)
```

Table 23. (continued).

```
      IF(TL(I,K).GE.0.01)GO TO 24
      ILAYER(I)=K+1
      RN(I)=RNI(K+1)
      SHC(I)=SHCI(K+1)
      AC(I)=ACI(K+1)
      BC(I)=BCI(K+1)
   23 CONTINUE
   24 CONTINUE
C     WRITE(7,1)I,ILAYER(I),RN(I),SHC(I),TL(I,K),AC(I),BC(I)
    1 FORMAT('  LAYER  I,ILAYER,RN,SHC,TC,AC,BC',2I5,5E11.4)
   22 CONTINUE
      RETURN
      END
      SUBROUTINE DISCH(J)
C *** COMPUTE OVERTOPPING DISCHARGE USING EMPIRICAL RELATION
      CHARACTER*80 TITLE
      COMMON/GEOM/X(50),Z(50),IT(50),RN(50),SO(50),TCS(50),
     1TCB(50),IP(2),RL,NX,SMAX,IS,ZMAX,LPAV(2),ZO(50),DZTL(50)
      COMMON/HYDRO/TIME(50),HW(50),TW(50),Q(50),YN,ITIME,DT(50),QO(50)
C *** COMPUTE ZMAX
      ZMAX=Z(1)
      DO 10 I=2,NX
      IF(ZMAX.GT.Z(I))GO TO 10
      ZMAX=Z(I)
   10 CONTINUE
      I1=IP(1)
      I2=IP(2)
      RL=X(I2)-X(I1)
      IF(RL.LT.0.01)RL=0.01
C *** COMPUTE OVERTOPPING HEADWATER AND TAILWATER DEPTH
      HM=HW(J)-ZMAX
      IF(HM.GT.0.)GO TO 100
      Q(J)=0.
      RETURN
  100 CONTINUE
      TM=TW(J)-ZMAX
C *** COMPUTE OVERTOPPING DISCHARGE
      HL=HM/RL
      IF(HL.LT.0.15)GO TO 11
      CF=-1.809*HL**2+1.074*HL+2.930
      IF(HL.GT.0.30)CF=3.09
      GO TO 16
   11 IF(HM-2.7)14,15,15
   15 CF=3.05
      GO TO 16
   14 IF(HM-0.05)17,17,18
   17 CF=2.90
      GO TO 16
   18 IF(HM.LE.0.6)GO TO 19
      CF=3.032*HM**0.0046
      GO TO 16
   19 CF=3.052*HM**0.0176
   16 TH=TM/HM
      CSF=1.0
      IF(TM.LT.0.)GO TO 12
      IF(TH.LE.0.92)GO TO 20
      CSF=-63.830*TH**2+115.838*TH-51.666
      GO TO 12
   20 IF(TH.GE.0.80)GO TO 21
      CSF=1.0
      GO TO 12
   21 CSF=-9.722*TH**2+15.806*TH-5.432
```

Table 23. Listing of computer program. (continued)

```
   12 Q(J)=CF*HM**1.5*CSF
      IF(Q(J).GT.QO(J))Q(J)=QO(J)
      RETURN
      END
      SUBROUTINE CRICT(J)
C *** COMPUTE CRITICAL DEPTH YC, SLOPE SC, AND SECTION IC
      CHARACTER*80 TITLE
      COMMON/GEOM/X(50),Z(50),IT(50),RN(50),SO(50),TCS(50),
     1TCB(50),IP(2),RL,NX,SMAX,IS,ZMAX,LPAV(2),ZO(50),DZTL(50)
      COMMON/HYDRO/TIME(50),HW(50),TW(50),Q(50),YN,ITIME,DT(50),QO(50)
      COMMON/YSC/YC,SC,IC,G
      COMMON/WS/H(50),SF(50),V(50),Y(50),F(50),IJUMP
      G=32.2
      I=IP(1)
      YC=Q(J)**0.667/G**0.333
      SC=G*RN(I)**2/(2.2*YC**0.333)
      DO 10 I=1,NX
      IF(SO(I).GT.SC)GO TO 11
   10 CONTINUE
   11 IC=I
      IF(IC.GT.NX)IC=NX
      Y(I)=YC
      H(I)=YC+Z(I)
      V(I)=Q(J)/YC
      F(I)=V(I)/SQRT(Y(I)*G)
      SF(I)=(RN(I)*V(I))**2/(2.2*Y(I)**1.33)
      RETURN
      END
      SUBROUTINE USWS(I,J)
C *** COMPUTE UPSTREAM STAGE AT SECTION I-1
      CHARACTER*80 TITLE
      COMMON/GEOM/X(50),Z(50),IT(50),RN(50),SO(50),TCS(50),
     1TCB(50),IP(2),RL,NX,SMAX,IS,ZMAX,LPAV(2),ZO(50),DZTL(50)
      COMMON/HYDRO/TIME(50),HW(50),TW(50),Q(50),YN,ITIME,DT(50),QO(50)
      COMMON/YSC/YC,SC,IC,G
      COMMON/WS/H(50),SF(50),V(50),Y(50),F(50),IJUMP
      HTRY=H(I)*1.1
      ITRY=0
      ID=I-1
      IF(I.EQ.1)RETURN
      DX=X(I)-X(ID)
   11 YTRY=HTRY-Z(ID)
      ITRY=ITRY+1
      IF(YTRY.LT.YN)YTRY=YN
      HTRY=YTRY+Z(ID)
      IF(HTRY.LE.HW(J))GO TO 110
      HTRY=HW(J)
      YTRY=HTRY-Z(ID)
  110 CONTINUE
      IF(HTRY.GT.H(I))GO TO 200
      HTRY=H(I)
      YTRY=HTRY-Z(ID)
  200 CONTINUE
      VTRY=Q(J)/YTRY
      SFTRY=(RN(ID)*VTRY)**2/(2.2*YTRY**1.33)
      FRO=VTRY/SQRT(G*YTRY)
      IF(ITRY.GE.1)GO TO 10
      HTRY=H(I)+(V(I)+VTRY)*(V(I)-VTRY)/(2.*G)
     1+(SF(I)+SFTRY)*DX/2.
      GO TO 11
   10 FUNC=G*DX*(SF(I)+SFTRY)+(V(I)+VTRY)*(V(I)-VTRY)
     1+2.*G*(H(I)-HTRY)
```

Table 23. (continued).

```
      FP=-G*DX*3.33*SFTRY/YTRY+2.*VTRY**2/YTRY-2.*G
      HTRYN=HTRY-FUNC/FP
C     WRITE(7,2)ID,J,ITRY,HTRY,HTRYN,FUNC,FP,VTRY,SFTRY,FRO
    2 FORMAT('  USWS',3I4,7E11.4)
      IF(ABS(HTRYN-HTRY).LT.0.01)GO TO 12
      IF(ITRY.GT.10)GO TO 13
      HTRY=HTRYN
      GO TO 11
   13 CONTINUE
C     WRITE(7,1)ID,J,ITRY,HTRY,HTRYN,FUNC,FP
    1 FORMAT('      SECTION I, TIME J',2I3,
     1/'  THE USWS IS NOT CONVERGED AFTER STEP',I3,
     2/'  HTRY,HTRYN,FUNC,FP=',4E12.4/)
   12 V(ID)=VTRY
      SF(ID)=SFTRY
      Y(ID)=YTRY
      H(ID)=YTRY+Z(ID)
      F(ID)=V(ID)/SQRT(G*Y(ID))
      RETURN
      END
      SUBROUTINE DSWS(I,J)
C *** COMPUTE DOWNSTREAM STAGE AT SECTION I+1
      CHARACTER*80 TITLE
      COMMON/GEOM/X(50),Z(50),IT(50),RN(50),SO(50),TCS(50),
     1TCB(50),IP(2),RL,NX,SMAX,IS,ZMAX,LPAV(2),ZO(50),DZTL(50)
      COMMON/HYDRO/TIME(50),HW(50),TW(50),Q(50),YN,ITIME,DT(50),QO(50)
      COMMON/YSC/YC,SC,IC,G
      COMMON/WS/H(50),SF(50),V(50),Y(50),F(50),IJUMP
      YTRY=Y(I)*0.9
      ITRY=0
      ID=I+1
      IF(I.EQ.NX)RETURN
      DX=X(ID)-X(I)
      HTRY=YTRY+Z(ID)
   11 CONTINUE
      YTRY=HTRY-Z(ID)
      ITRY=ITRY+1
      IF(YTRY.LT.YN)YTRY=YN
      IF(YTRY.GT.Y(I))YTRY=Y(I)
      HTRY=YTRY+Z(ID)
      VTRY=Q(J)/YTRY
      SFTRY=(RN(ID)*VTRY)**2/(2.2*YTRY**1.33)
      FRO=VTRY/SQRT(G*YTRY)
      IF(ITRY.GE.1)GO TO 10
      HTRY=H(I)-(V(I)+VTRY)*(VTRY-V(I))/(2.*G)
     1-DX/2.*(SF(I)+SFTRY)
      GO TO 11
   10 FUNC=G*DX*(SF(I)+SFTRY)+(V(I)+VTRY)*(VTRY-V(I))
     1+2.*G*(HTRY-H(I))
      FP=-G*DX*3.33*SFTRY/YTRY-2.*VTRY**2/YTRY+2.*G
      HTRYN=HTRY-FUNC/FP
C     WRITE(7,2)ID,J,ITRY,HTRY,HTRYN,FUNC,FP,VTRY,SFTRY,FRO
    2 FORMAT('  DSWS',3I4,7E11.4)
      IF(ABS(HTRYN-HTRY).LT.0.01)GO TO 12
      IF(ITRY.GT.10)GO TO 13
      HTRY=HTRYN
      GO TO 11
   13 CONTINUE
C     WRITE(7,1)ID,J,ITRY,HTRY,HTRYN,FUNC,FP
    1 FORMAT('      SECTION I,TIME J',2I3,
     1/'  THE DSWS IS NOT CONVERGED AFTER STEP',I3,
     2/'  HTRY,HTRYN,FUNC,FP=',4E12.4/)
```

Table 23. Listing of computer program. (continued)

```
   12 V(ID)=VTRY
      SF(ID)=SFTRY
      Y(ID)=YTRY
      H(ID)=YTRY+Z(ID)
      F(ID)=V(ID)/SQRT(G*Y(ID))
      RETURN
      END
      SUBROUTINE JUMP(J)
C *** COMPUTE FLOW PROFILE UPSTREAM FROM THE TAILWATER DEPTH
C     AND DETERMINE JUMP LOCATION
      CHARACTER*80 TITLE
      COMMON/GEOM/X(50),Z(50),IT(50),RN(50),SO(50),TCS(50),
     1TCB(50),IP(2),RL,NX,SMAX,IS,ZMAX,LPAV(2),ZO(50),DZTL(50)
      COMMON/HYDRO/TIME(50),HW(50),TW(50),Q(50),YN,ITIME,DT(50),QO(50)
      COMMON/YSC/YC,SC,IC,G
      COMMON/WS/H(50),SF(50),V(50),Y(50),F(50),IJUMP
C *** DETERMINE EFFECT OF TAILWATER ON WATER SURFACE PROFILE AND JUMP
C *** COMPUTE D2
      I=IC
      HJUMP=H(I)
  101 IF(SO(I).GT.0.)GO TO 100
      I=I+1
      IJUMP=I
      IF(I.GE.NX)RETURN
      GO TO 101
  100 Y1=H(I)-Z(I)
      IF (I.EQ.1)RETURN
      SOI=(SO(I)*2.+SO(I-1))/3.
      IF(SOI.LT.0.)SOI=1.0E-10
      PHI=ATAN(SOI)
      D1=Y1*COS(PHI)
      V1=Q(J)/D1
      F1=V1/SQRT(G*D1)
      RK=21.978*SOI**2-14.396*SOI+3.740
      RK1=1.-2.*RK*SOI
      IF(RK1.LT.0.15)RK1=0.15
      D2=D1/2./COS(PHI)*(SQRT(8.*F1**2*COS(PHI)**3/(RK1)
     1+1.)-1.)
C     WRITE(7,2)I,Y1,PHI,D1,V1,F1,RK,D2
    2 FORMAT(/'  JUMP    I,Y1,PHI,D1,V1,F1,RK,D2',I4,7E11.4)
C *** COMPUTE JUMP LENGTH ON SLOPE & LOCATION
      RL1=D2*(2.89+1.89*SOI)*SQRT(F1)
      XX=RL1+X(I)
      DO 10 K=I,NX
      IF(XX.GE.X(K))GO TO 10
      IK=K-1
      GO TO 11
   10 CONTINUE
      IK=NX-1
   11 CONTINUE
      IF(IK.LT.IC)IK=IC
C *** COMPUTE THE JUMP WATER SURFACE PROFILE ON SLOPE
      CC=(XX-X(IK))/(X(IK+1)-X(IK))
      ZZ=Z(IK)+(Z(IK+1)-Z(IK))*(XX-X(IK))/(X(IK+1)-X(IK))
      SS=SOI
      IF(SS.LT.0.)SS=0.
      TWX=D2*(1.+11.2*SS**1.5)
      TWH=TWX+ZZ
C     WRITE(7,3)IK,RL1,XX,TWX,ZZ,TWH
    3 FORMAT('  IK,RL1,XX,TWX,ZZ,TWH',I5,5E11.4)
      IF(XX.GT.X(NX))GO TO 20
      IF(HJUMP.LE.TW(J)+.21.AND.TWH.GE.TW(J)-.21)GO TO 44
```

Table 23.   (continued).

```
      IF(HJUMP.GE.TW(J)-.21.AND.TWH.LE.TW(J)+.21)GO TO 44
      GO TO 22
   44 IJ=I-1
      IJUMP=IJ
C *** ASSUME HORIZONTAL SURFACE DOWNSTREAM OF THE JUMP
      IF(IK.LT.(IC+1))IK=IC+1
      DO 23 K=IK,NX
      H(K)=TW(J)
      Y(K)=H(K)-Z(K)
      IF(Y(K).LT.0.2)Y(K)=0.2
      V(K)=Q(J)/Y(K)
      SF(K)=(RN(K)*V(K))**2/(2.2*Y(K)**1.33)
      F(K)=V(K)/SQRT(G*Y(K))
C     WRITE(7,4)K,H(K),Y(K),V(K),SF(K),F(K)
    4 FORMAT('    JUMP1   K,H,Y,V,SF,F',I5,5E11.4)
   23 CONTINUE
C *** APPROXIMATE THE JUMP PROFILE BY A PARABOLIC
      IF(IJ.EQ.IK)IK=IJ+1
      DO 24 K=IJ,IK
      DIST=(X(K)-X(IJ))/(X(IK)-X(IJ))
      IF(DIST.LT.0.)DIST=0.
      H(K)=H(IJ)+(H(IK)-H(IJ))*SQRT(DIST)
      Y(K)=H(K)-Z(K)
      IF(Y(K).LT.0.2)Y(K)=0.2
      V(K)=Q(J)/Y(K)
      SF(K)=(RN(K)*V(K))**2/(2.2*Y(K)**1.33)
      F(K)=V(K)/SQRT(G*Y(K))
C     WRITE(7,5)K,DIST,H(K),Y(K),V(K),SF(K),F(K)
    5 FORMAT('    JUMP2   K,DIST,H,Y,V,SF,F',I5,6E11.4)
   24 CONTINUE
      RETURN
   22 I=I+1
      IF(I.GT.NX)I=NX
      IJUMP=I
      HJUMP=TWH
      IF(TWH.LT.TW(J).AND.I.EQ.(IC+1))GO TO 21
      IF(TWH.LT.TW(J))GO TO 44
      GO TO 100
C *** FLOW BECOMES SUBMERGED
   21 H(NX)=TW(J)
      Y(NX)=H(NX)-Z(NX)
      V(NX)=Q(J)/Y(NX)
      SF(NX)=(RN(NX)*V(NX))**2/(2.2*Y(NX)**1.33)
      F(NX)=V(NX)/SQRT(G*Y(NX))
      NX1=NX-1
      IF((TW(J)-Z(IC)).LT.1.4*YC)NX1=IC-2
      DO 25 K=1,NX1
      K1=NX-K+1
      CALL USWS(K1,J)
   25 CONTINUE
      RETURN
   20 IF(TW(J).GT.H(IC))GO TO 21
      IF((TW(J)-Z(NX)).GT.(D2*0.7))GO TO 30
      IF(I.LT.NX)GO TO 22
C     WRITE(7,1)
    1 FORMAT('    THERE IS NO JUMP OCCURRING ON SLOPE')
      RETURN
C *** DETERMINE JUMP LENGTH ON THE SLOPE/HORIZONTAL REACH
   30 DTW=TW(J)-Z(NX)
      RD=DTW/D2
      XXL=X(NX)-X(I)
      IF(XXL.LT.0.01)XXL=0.01
```

Table 23. Listing of computer program. (continued)

```
      SS=(Z(I)-Z(NX))/XXL
      IF(SS.LT.0.01)SS=0.01
      IF(RD.LE.1.3)GO TO 31
      RL2=D2*0.82*SS**(-0.78)+(RD-1.3)/SS*D2
      GO TO 32
   31 RL2=D2*2.05*SS**(-0.78)*(RD-0.9)
   32 CONTINUE
      IF(RD.LT.1.01)RL2=0.
      IF(RL2.GT.RL1)RL2=RL1
      XX=X(NX)-RL2
C     WRITE(7,6)DTW,RD,RL1,RL2,XX
    6 FORMAT('  JUMP3  DTW,RD,RL1,RL2,XX',5E11.4)
      DO 43 K=I,NX
      IF(XX.GE.X(K))GO TO 43
      IJ=K-1
      GO TO 45
   43 CONTINUE
   45 XX=X(NX)
      IJ=I
      IJUMP=IJ
      DO 46 K=IJ,NX
      XXL=XX-X(IJ)
      IF(XXL.LT.0.01)XXL=0.01
      DIST=(X(K)-X(IJ))/XXL
      IF(DIST.LT.0.)DIST=0.
      H(K)=H(IJ)+(TW(J)-H(IJ))*SQRT(DIST)
      Y(K)=H(K)-Z(K)
      IF(Y(K).LT.YN)Y(K)=YN
      V(K)=Q(J)/Y(K)
      SF(K)=(RN(K)*V(K))**2/(2.2*Y(K)**1.33)
      F(K)=V(K)/SQRT(G*Y(K))
C     WRITE(7,7)K,DIST,H(K),Y(K),V(K),SF(K),F(K)
    7 FORMAT('  JUMP4  K,DIST,H,Y,V,SF,F',I5,6E11.4)
   46 CONTINUE
      RETURN
      END
      SUBROUTINE OUTP(J)
C *** PRINT OUT THE COMPUTED RESULTS
      CHARACTER*80 TITLE
      COMMON/GEOM/X(50),Z(50),IT(50),RN(50),SO(50),TCS(50),
     1TCB(50),IP(2),RL,NX,SMAX,IS,ZMAX,LPAV(2),ZO(50),DZTL(50)
      COMMON/HYDRO/TIME(50),HW(50),TW(50),Q(50),YN,ITIME,DT(50),QO(50)
      COMMON/YSC/YC,SC,IC,G
      COMMON/WS/H(50),SF(50),V(50),Y(50),F(50),IJUMP
      COMMON/EROS/IPAV,NLAYER,TL(50,10),IEOS,SHCI(10),RNI(10),SH(50),
     1ILAYER(50),QE(50),DZT(50),DZ(50),P,PS,AC(50),BC(50),
     2SA,EL,SHC(50),TS,ACI(10),BCI(10),XB(50),DEC,IPRINT,TIMEP,ITM
      DIMENSION DA(50),DE(50)
C     WRITE(6,1)TITLE
    1 FORMAT(/8A10)
      WRITE(6,2)J,TIMEP,HW(J),TW(J),Q(J),YC,SC,IC
    2 FORMAT(///2X,'  J,TIMEP,HW,TW,Q,YC,SC,IC',I5,6E11.4,I4)
      WRITE(6,4)
    4 FORMAT(/2X,'I',1X,'LAYER',4X,'X',9X,'Y',9X,'Z',9X,'H',9X,1HV,
     19X,'F',9X,'SF',8X,'SO',8X,'QE',8X,'SH',8X,'TL',8X,'DZTL'/)
      DO 10 I=1,NX
      NL=ILAYER(I)
      DZTL(I)=ZO(I)-Z(I)
      WRITE(6,3)I,ILAYER(I),X(I),Y(I),Z(I),H(I),V(I),F(I),SF(I),SO(I)
     1,QE(I),SH(I),TL(I,NL),DZTL(I)
   10 CONTINUE
    3 FORMAT(2I4,12E10.3)
```

Table 23.   (continued).

```
      RETURN
      END
      SUBROUTINE SHEAR(J)
      CHARACTER*80 TITLE
      COMMON/GEOM/X(50),Z(50),IT(50),RN(50),SO(50),TCS(50),
     1TCB(50),IP(2),RL,NX,SMAX,IS,ZMAX,LPAV(2),ZO(50),DZTL(50)
      COMMON/HYDRO/TIME(50),HW(50),TW(50),Q(50),YN,ITIME,DT(50),QO(50)
      COMMON/YSC/YC,SC,IC,G
      COMMON/WS/H(50),SF(50),V(50),Y(50),F(50),IJUMP
      COMMON/EROS/IPAV,NLAYER,TL(50,10),IEOS,SHCI(10),RNI(10),SH(50),
     1ILAYER(50),QE(50),DZT(50),DZ(50),P,PS,AC(50),BC(50),
     2SA,EL,SHC(50),TS,ACI(10),BCI(10),XB(50),DEC,IPRINT,TIMEP,ITM
C *** DETERMINE SHEAR STRESS BASED ON FLOW HYDRAULICS
      ISG=IC
      IS=1
      DO 10 I=1,NX
      YI=Y(I)
      IF(YI.LT.1.0)YI=1.0
      FC=8.*G*RN(I)**2/(2.2*YI**0.333)
      IF(FC.GT.(1.3*RN(I)))FC=1.3*RN(I)
      IF(FC.GT.RN(I).AND.SHC(I).GT.0.3) FC=RN(I)
C*** CONSIDER FLOW MODE (SURFACE OF PLUNGING FLOW)
      HM=HW(J)-ZMAX
      TM=TW(J)-ZMAX
      HL=HM/RL
      THMC=1.914*HL**0.558
      IF(THMC.GT.0.65)THMC=0.65
      THM=TM/HM
      IF(THM.GT.THMC)GO TO 20
C *** PLUNGING FLOW
      IF(I.LE.IJUMP)GO TO 21
      VL=0.5*V(IJUMP)
      IF(VL.LT.V(I))VL=V(I)
C     WRITE(7,2)I,IJUMP,HM,TM,HL,THMC,THM,VL
    2 FORMAT('  PLUNGING FLOW   I,IJUMP,HM,TM,HL,THMC,THM,VL',
     12I4,6E10.3)
      GO TO 23
   21 VL=V(I)
      GO TO 23
C *** SURFACE FLOW
   20 IF(I.LE.IC)GO TO 21
      IF(IS.EQ.1.AND.SO(I).GT.0.15)GO TO 30
      GO TO 31
   30 IS=IS+1
      ISG=I
      GO TO 32
   31 IF(IS.EQ.1)GO TO 32
      VL=0.2*V(ISG)
      GO TO 33
   32 VL=V(I)
   33 CONTINUE
C     WRITE(7,3)I,ISG,IS,HM,TM,HL,THMC,THM,VL
    3 FORMAT('  SURFACE FLOW   I,ISG,IS,HM,TM,THMC,THM,VL',
     13I4,6E10.3)
   23 SH(I)=P*FC*VL**2/8.
C     WRITE(7,1)I,FC,RN(I),Y(I),SH(I)
    1 FORMAT('  SHEAR I,FC,RN,Y,SH',I5,4E11.4)
   10 CONTINUE
      RETURN
      END
      SUBROUTINE SEDQ
      CHARACTER*80 TITLE
```

195

Table 23. Listing of computer program. (continued)

```
      COMMON/GEOM/X(50),Z(50),IT(50),RN(50),SO(50),TCS(50),
     1TCB(50),IP(2),RL,NX,SMAX,IS,ZMAX,LPAV(2),ZO(50),DZTL(50)
      COMMON/HYDRO/TIME(50),HW(50),TW(50),Q(50),YN,ITIME,DT(50),QO(50)
      COMMON/YSC/YC,SC,IC,G
      COMMON/WS/H(50),SF(50),V(50),Y(50),F(50),IJUMP
      COMMON/EROS/IPAV,NLAYER,TL(50,10),IEOS,SHCI(10),RNI(10),SH(50),
     1ILAYER(50),QE(50),TS,ACI(10),RCI(10),XB(50),DEC,IPRINT,TIMEP,ITM
     2SA,EL,SHC(50),DZT(50),DZ(50),P,PS,AC(50),BC(50),
C ***  COMPUTE EROSION RATE
      DO 10 I=1,NX
      IF(SH(I).LE.SHC(I))GO TO 11
      QE(I)=AC(I)*(SH(I)-SHC(I))**BC(I)
      GO TO 12
11    QE(I)=0.
12    CONTINUE
      WRITE(7,1)I,AC(I),BC(I),SHC(I),QE(I)
1     FORMAT('   ',SEDQ   I,AC,BC,SHC,QE',I5,4E11.4)
10    CONTINUE
      RETURN
      END
      SUBROUTINE SEDZ(J)
      CHARACTER*80 TITLE
      COMMON/GEOM/X(50),Z(50),IT(50),RN(50),SO(50),TCS(50),
     1TCB(50),IP(2),RL,NX,SMAX,IS,ZMAX,LPAV(2),ZO(50),DZTL(50)
      COMMON/HYDRO/TIME(50),HW(50),TW(50),Q(50),YN,ITIME,DT(50),QO(50)
      COMMON/YSC/YC,SC,IC,G
      COMMON/WS/H(50),SF(50),V(50),Y(50),F(50),IJUMP
      COMMON/EROS/IPAV,NLAYER,TL(50,10),IEOS,SHCI(10),RNI(10),SH(50),
     1ILAYER(50),QE(50),TS,ACI(10),RCI(10),XB(50),DEC,IPRINT,TIMEP,ITM
     2SA,EL,SHC(50),DZT(50),DZ(50),P,PS,AC(50),BC(50),
C ***  COMPUTE BED ELEVATION CHANGES FOR FLEXIBLE SURFACE (SOIL,GRASS,ETC.)
      DO 10 I=1,NX
      DT1=DT(J)
13    DZ(I)=QE(I)*DT1
      NL=ILAYER(I)
      IF(QE(I).LT.1.E-20)GO TO 30
      IF(TL(I,NL).LT.DZ(I))GO TO 30
      TL(I,NL)=TL(I,NL)-DZ(I)
      Z(I)=Z(I)-DZ(I)
      DZT(I)=DZT(I)+DZ(I)
      WRITE(7,2)I,ILAYER(I),QE(I),DZ(I),Z(I),TL(I,NL),SHC(I),DZT(I),DT1
2     FORMAT('   ',SEDZ1 I,ILAYER,QE,DZ,Z,TL,SHC,DZT,DT1',2I4,7E11.4)
      GO TO 30
11    DZZ=DZ(I)-TL(I,NL)
      DTT=TL(I,NL)/QE(I)
      Z(I)=Z(I)-TL(I,NL)
      TL(I,NL)=0.
      DZT(I)=DZT(I)+TL(I,NL)
      NL=NL+1
      IF(NL.GT.NLAYER)GO TO 30
      DO 40 INL=NL,NLAYER
      IF(TL(I,INL).GT.0.01)GO TO 31
40    CONTINUE
31    CONTINUE
      NL=INL
      IF(NL.GT.NLAYER)GO TO 30
      DT1=DT1-DTT
      ILAYER(I)=NL
      SHC(I)=SHCI(NL)
      AC(I)=ACI(NL)
      BC(I)=BCI(NL)
```

Table 23.   (continued).

```
      IF(SHC(I).GT.SH(I))GO TO 20
      QE(I)=AC(I)*(SH(I)-SHC(I))**BC(I)
      GO TO 21
   20 QE(I)=0.
   21 RN(I)=RNI(NL)
C     WRITE(7,3)I,ILAYER(I),QE(I),DZ(I),Z(I),TL(I,NL),DTT,DZT(I),DT1
    3 FORMAT('   SEDZ2 I,ILAYER,QE,DZ,Z,TL,DTT,DZT,DT1',2I4,7E11.4)
      GO TO 13
   30 CONTINUE
C     WRITE(7,1)I,ILAYER(I),QE(I),DZ(I),Z(I),TL(I,NL),SHC(I),DZT(I),DT1
    1 FORMAT('   SEDZ3 I,ILAYER,QE,DZ,Z,TL,SHC,DZT,DT1',2I4,7E11.4)
   10 CONTINUE
      RETURN
      END
      SUBROUTINE PAVZ
      CHARACTER*80 TITLE
      COMMON/GEOM/X(50),Z(50),IT(50),RN(50),S0(50),TCS(50),
     1TCB(50),IP(2),RL,NX,SMAX,IS,ZMAX,LPAV(2),Z0(50),DZTL(50)
      COMMON/HYDRO/TIME(50),HW(50),TW(50),Q(50),YN,ITIME,DT(50),Q0(50)
      COMMON/YSC/YC,SC,IC,G
      COMMON/WS/H(50),SF(50),V(50),Y(50),F(50),IJUMP
      COMMON/EROS/IPAV,NLAYER,TL(50,10),IEOS,SHCI(10),RNI(10),SH(50),
     1ILAYER(50),QE(50),DZT(50),DZ(50),P,PS,AC(50),BC(50),
     2SA,EL,SHC(50),TS,ACI(10),BCI(10),XB(50),DEC,IPRINT,TIMEP,ITM
C *** DETERMINE EROSION OF PAVEMENT
      IF(LPAV(2).LT.LPAV(1))RETURN
      KK=LPAV(2)
      EZ=DZT(KK+1)
      EL=EZ*0.125
      RM=(P*G*Y(KK)+PS*G*TS)*EL**2/2.
      SM=TS**2/6.
      STM=RM/SM
C     WRITE(7,1)KK,EZ,EL,RM,SM,STM,SA
    1 FORMAT('   PAVZ1   KK,EZ,EL,RM,SM,STM,SA',I5,6E11.4)
      IF(STM.LT.SA)RETURN
      IK=1
   11 IF(EL.LT.(X(KK)-X(KK-IK)))GO TO 10
      IK=IK+1
      IF((KK-IK).LT.1)GO TO 10
      GO TO 11
   10 DO 12 K=1,IK
      K1=KK-K+1
      DZ(K1)=DZT(KK+1)*(EL-X(KK)+X(K1))/(EL+X(KK+1)-X(K))
      Z(K1)=Z(K1)-DZ(K1)-TS
      DZT(K1)=DZ(K1)+DZT(K1)
C     WRITE(7,2)K1,DZ(K1),Z(K1),DZT(K1)
    2 FORMAT('   PAVZ2,K1,DZ,Z,DZT',I5,3E11.4)
   12 CONTINUE
      DO 20 K=1,IK
      K1=KK-K+1
      NL=ILAYER(K1)+1
   22 IF(TL(K1,NL).LT.DZ(K1))GO TO 21
      IF(NL.GT.NLAYER)NL=NLAYER
      TL(K1,NL)=TL(K1,NL)-DZ(K1)
      ILAYER(K1)=NL
      SHC(K1)=SHCI(NL)
      AC(K1)=ACI(NL)
      BC(K1)=BCI(NL)
      RN(K1)=RNI(NL)
      GO TO 30
   21 DZZ=DZ(K1)-TL(K1,NL)
      TL(K1,NL)=0.
```

Table 23. Listing of computer program. (continued)

```
        NL=NL+1
        IF(NL.GT.NLAYER)GO TO 30
        ILAYER(K1)=NL
        SHC(K1)=SHCI(NL)
        AC(K1)=ACI(NL)
        BC(K1)=BCI(NL)
        DZ(K1)=DZZ
        RN(K1)=RNI(NL)
        GO TO 22
   30 CONTINUE
C       WRITE(7,3)K1,NL,ILAYER(K1),TL(K1,NL),SHC(K1),RN(K1),DZ(K1)
    3 FORMAT('  PAVZ3  K1,NL,ILAYER,TL,SHC,RN,DZ',3I4,4E11.4)
   20 CONTINUE
        LPAV(2)=LPAV(2)-IK
C       WRITE(7,4)LPAV(1),LPAV(2)
    4 FORMAT('  PAVZ4  LPAV1,LPAV2',2I5)
        RETURN
        END
        SUBROUTINE NEWSO
        CHARACTER*80 TITLE
        COMMON/EROS/IPAV,NLAYER,TL(50,10),IEOS,SHCI(10),RNI(10),SH(50),
      1ILAYER(50),QE(50),DZT(50),DZ(50),P,PS,AC(50),BC(50),
      2SA,EL,SHC(50),TS,ACI(10),BCI(10),XB(50),DEC,IPRINT,TIMEP,ITM
        COMMON/GEOM/X(50),Z(50),IT(50),RN(50),SO(50),TCS(50),
      1TCB(50),IP(2),RL,NX,SMAX,IS,ZMAX,LPAV(2),ZO(50),DZTL(50)
C *** COMPUTE NEW BED SLOPE
        NX1=NX-1
        DO 10 I=2,NX1
        SO(I)=(Z(I-1)-Z(I+1))/(X(I+1)-X(I-1))
   10 CONTINUE
        SO(1)=(Z(1)-Z(2))/(X(2)-X(1))
        SO(NX)=(Z(NX1)-Z(NX))/(X(NX)-X(NX1))
        SMAX=SO(I)
        DO 11 I=2,NX
        IF(SMAX.GT.SO(I))GO TO 11
        SMAX=SO(I)
        IF(SMAX.LT.1.0E-6) SMAX=1.0E-6
   11 CONTINUE
C *** DETERMINE THE CHANGE IN THE ROADWAY WIDTH
        I1=IP(1)
        I2=IP(2)
   21 IF(DZT(I1).LT.0.5)GO TO 20
        I1=I1+1
        IP(1)=I1
        IF(I1.GE.I2)GO TO 22
        GO TO 21
   20 IF(DZT(I2).LT.0.5)GO TO 23
        I2=I2-1
        IP(2)=I2
        IF(I2.LE.I1)GO TO 22
        GO TO 20
   22 IP(1)=I1
        IP(2)=I1
   23 RETURN
        END
$
```

198

REFERENCES

(1) Simons, Li & Associates, Inc., "Presentation of Field Data on Embankment Damage Due to Flood Overtopping," Progress Report for Task A, Prepared for U.S. Department of Transportation, Federal Highway Administration, January 1984.

(2) H. W. Hjalmarson, "FLood Characteristics and Highway Damage at Five Arizona Sites, Flood of October 1983," U.S. Geological Survey prepared in cooperation with the U.S. Department of Transportation, Federal Highway Administration, Tucson, September 1984.

(3) D. L. Yarnell, and F. A. Nagler, "Flow of Flood Water Over Railway and Highway Embankments," Public Roads, Vol. II, No. 2, 30-34, 1930.

(4) C. E. Kindsvater, "Discharge Characteristics of Embankment-Shaped Weirs," Studies of Flow of Water Over Weirs and Dams, USGS Water-Supply Paper 1617-A, 1964.

(5) J. N. Bradley, "Hydraulics of Bridge Waterways," Hydraulic Design Series No. 1, U.S. Department of Transportation, Federal Highway Administration, 1973.

(6) V. T. Chow, Open-Channel Hydraulics, McGraw-Hill Book Company, New York, 1959.

(7) J. N. Bradley, and A. J. Peterka, "Hydraulic Design of Stilling Basins: Stilling Basin with Sloping Apron (Basin V), Journal of Hydraulics Division, ASCE, Vol.83, No. HY5, October 1957.

(8) F. C. Townsend, and D. J. Goodings, "Centrifugal Model Analysis of Coal Waste Embankment Stability," U.S. Army Engineer Waterways Experiment Station for Bureau of Mines, Open File Report, 1979.

(9) P. Miller, Personal Communication, U.S. Army Engineer Waterways Experiment Station, 1983.

(10) E. R. Tinney, and H. Y. Hsu, "Mechanics of Washout of an Erodible Fuse Plug," Trans. ASCE, Paper No. 3283, Vol. 127, Part 1, 1962, pp. 31-59. Library Reference.

(11) J. Gessler, "Beginning and Ceasing of Sediment Motion," River Mechanics, Chapter 7, edited by H.W. Shen, 1971.

(12) S. Fortier and F. C. Scobey, "Permissible Canal Velocities," Trans. ASCE, Vol. 89, 1926, pp. 940-956.

(13) E. T. Smerdon, and R. P. Beasley, "Relation of Compaction and Other Soil Properties to Erosion Resistance of Soils," Trans. ASCE, Vol. 8, 1959.

REFERENCES (continued)

(14) E. T. Smerdon, and R. P. Beasley, "The Tractive Force Theory Applied to Stability of Open Channels in Cohesive Soils," Research Bulletin 715, University of Missouri, College of Agriculture, Agr. Exp. Station, October, 1959.

(15) E. H. Grissinger, "Resistance of Selected Clay Systems to Erosion by Water," Water Resources Research, Vol. 2, No. 1, 1966, pp. 131-138.

(16) W. Lyle, and E. Smerdon, "Relation of Compaction and Other Soil Properties to the Erosion Resistance of Soils," Trans. ASAE, 1965.

(17) A. Arumugam, "Fundamental Aspect of Surface Erosion of Cohesive Soils," Ph.D. Dissertation, University of California, Davis, 1974.

(18) J. C. McWhorter, T. G. Carpenter, and R. N. Clark, "Erosion Control Criteria for Drainage Channels," prepared for the Mississippi State Highway Department in Cooperation with U.S. Department of Transporation, Federal Highway Administration, by Agricultural Experiment Station, Mississippi State University, State College, Mississippi, March 1968.

(19) Y. H. Chen and G. K. Cotton, "Design of Roadside Channels with Flexible Linings," Hydraulic Engineering Circular No. 15, Federal Highway Administration, February 1986.

(20) USDA Soil Conservation Service, Handbook of Channel Design for Soil and Water Conservation, 1954.

(21) J. M. Wiggert, and D. N. Contractor, "A Methodology for Estimating Embankment Failure," an unpublished paper presented to Water Resources Engineers, Inc., Springfield, VA, Department of Civil Engineering, Virginia Polytechnic Institute and State University, Blacksburg, VA 24060, no date, written around 1969.

(22) E. A. Cristofano, "Method of Computing Erosion Rate for Failure of Earthfill Dams," unpublished memorandum, Engineering and Research Center, Bureau of Reclamation, Department of the Interior, Denver, CO, April 1965.

(23) R. Ariathurai, and K. Arulanandan, "Erosion Rates of Cohesive Soils," Journal of Hydraulics Division, ASCE, Vol. 104, No. HY2, February 1978, pp. 279-283.

(24) S. P. Chee, "Design of Erodible Dams," in Proceedings of International Conference of Water Resources Engineerings, Asian Institute of Technology, Bankok AIT, V. 1, 105-113, 1978.

(25) V. R. Schneider, and K. V. Wilson, "Hydraulic Design of Bridges with Risk Analysis," U.S. Geological Survey for FHWA Office of Development, Report FHWA-TS-80-226, FHWA HDV-21, March 1980.

BIBLIOGRAPHY

(1) J. O. Abreu-Lima, and W. B. Morgan, "Protection of Earth Embankments by Riprap of Uniform Size," M.S. Thesis, Univ. Iowa, Iowa City, 1951.

(2) K. Arnulanandan, P. Logannathan, and R. B. Kron, "Pore and Eroding Fluid Influences on Surface Erosion of Soil," Journal of Geotechnical Engineering Division, ASCE, Vol. 101, No. GT1, January 1975, pp. 51-65.

(3) D. T. Babbit, (Chrmn), "Specialty Session of Slopes and Embankments," Proceedings of Conference on Earthquake Engineering and Soil Dynamics, ASCE, 1386, 1978.

(4) N. J. Brogdon, and V. L. Grace, "Stability of Riprap and Discharge Characteristics, Overflow Embankment, Arkansas River, Arkansas," Army Engineering Waterway Experiment Station, Vicksburg, 94 p, June 1964.

(5) J. Davidian, and D. I. Cahal, "Distribution of Shear in Rectangular Channels," Article 113, U.S. Geological Survey Professional Paper 475-C, 1963.

(6) Federal Highway Administration, "The Design of Encroachments on Flood Plains Using Risk Analysis," Hydraulic Engineering Circular No. 17, FHWA HNG-31, Washington, D.C. 20590, 1980.

(7) J. Fowler, "Design Construction and Analysis of Fabric-Reinforced Embankment Test Section of Pinto Pass, Mobile Alabama," Rpt. EL-81-7, U.S. Army Engineering Waterways Experiment Station, Vicksburg, MS; 225 p, 1981.

(8) J. Fowler, "Synthetic Fabrics for Reinforced Embankments," Civil Engineering, ASCE, 51(10), 48-51, 1981.

(9) S. Fortier, and F. C. Scobey, "Permissible Canal Velocities," Transactions, ASCE, Vol. 89, pp. 940-956, 1926.

(10) H. P. Greenspan and A. V. Johansson, "An Experimental Study of Flow Over an Impounding Dike," Study Application Math 64(3) 211-223, 1981.

(11) H. P. Greenspan and R. E. Young, "Flow Over a Containment Dike," J. Fluid Mechanics, 87:179-192, 1978.

(12) R. H. Haas and H. E. Walker, "Bank Stabilization by Revetments and Dikes," ASCE Proceedings 118, 849-879, 1953.

(13) R. S. Haupt and J. P. Olson, "Case History - Embankment Failure on Soft Varved Silt," ASCE Performance of Earth and Earth-Supported Structures, I-1, 1972.

BIBLIOGRAPHY (continued)

(14) E. J. Hayter and J. M. Ashish, "Verification of Changes in Flow Regime Due to Dike Breakthrough," J. Waterway, Port, Coastal and Ocean Division, ASCE, 79:729, 1979.

(15) Hydrotechnical Construction (Gidrotekhnicheskoie Stroitelstvo), "The Maximum Permissible Mean Velocity in Open Channels," Moscow, No. 5, PP. 5-7, May 1936.

(16) A. T. Ippen et al., "The Distribution of Boundary Shear Stress in Curved Trapezoidal Channels," Technical Report No. 43, MIT, Department of Civil Engineering, Hydrodynamics Lab, October 1960.

(17) K. Jetter, "Tests on Sand Dikes Protected Against Erosion by Overflowing Water," M.S. Thesis, University of Iowa, Iowa City, 1931.

(18) S. Karaki, K. Mahmood, E. V. Richardson, D. B. Simons, and M. A. Stevens, "River Environment, Hydraulic and Environmental Design Considerations," Federal Highway Administration, CER-73-74EVR-SK-KM-DBS-MAS49, 1974.

(19) V. C. Kartha and H. J. Lentheusser, "Distribution of Tractive Force in Open Channels," Journal of the Hydraulics Division, ASCE, HY7, 1970.

(20) J. W. King and J. B. Beard, "Measuring Rooting of Sodded Turfs," Agronomy Journal, Vol. 61, July-August, 1969, pp. 497-498.

(21) T. W. Lambe and R. V. Whitman, Soil Mechanics, Wiley and Sons, New York, 553 p., 1969.

(22) Y-D Lion, "Hydraulic Erodibility of Two Pure Clay Systems," Ph.D. Dissertation, Department of Civil Engineering, Colorado State University, 1970.

(23) H. K. Liu, J. N. Bradley, and E. J. Plate, "Backwater Effects of Piers and Abutments," Colorado State University, Civil Engineering, CER57HKL10, 364, 1957.

(24) H. S. Manamperi, "Tests of Graded Riprap for Protection of Erodible Material," M.S. Thesis, University of Iowa, Iowa City, 1952.

(25) T. E. Murphy and J. L. Grace, "Riprap for Overflow Embankments," Highway Research Board, HRR-30, 1963.

(26) H. Nasner, "Storm Surge Protection for the Elbe River," in 17th International Conference on Coastal Engineering, Sydney, Australia; Abstracts in Depth, 1980.

(27) E. M. O'Loughlin, S. C. Mehrotra, Y. C. Chang, and J. F. Kennedy, "Scale Effects in Hydraulic Model Tests of Rock Protected Structures," Iowa University, Iowa City Institute of Hydraulic Research, 37 p, 1970.

BIBLIOGRAPHY (continued)

(28) R. Q. Palmer and J. R. Walker, "Honolulu Reef Runway Dike," in Proceedings of 12th Coastal Engineering Conference, Wash., Vol. 3, Chapter 99, 1629-1646, 1970.

(29) E. Partheniades, "A Study of Erosion and Deposition of Cohesive Soils in Salt Water," Ph.D. Disseration, University of California, Berkeley, 1962.

(30) E. Partheniades, "Erosion and Deposition of Cohesive Soils," Journal of the Hydraulics Division, ASCE, Vol. 91, No. HY1, January 1965, pp. 105-139.

(31) V. C. Patel, "Calibration of the Preston Tube and Limitations on its Use in Pressure Gradients," Journal of Fluid Mechanics, Vol. 23, Part I, 1965.

(32) G. Pilot, "Study of Five Embankment Failures on Soft Soils," ASCE Performance of Earth and Earth-Supported Structures, I-1, 1972.

(33) T. J. Pokrefke and W. Franco, "Investigation of Proposed Dike Systems on the Mississippi River; Rpt. 2, New Madrid Bar Reach; Hydraulic Model Investigation," Vicksburg, MS, USAE Waterways Experiment Station, MPH-70-1, 30 p. 1981.

(34) C. J. Posey, "Flood Erosion Protection for Highway Fills," Trans. ASCE, Paper No. 2871, Vol. 122, pp. 531-555, 1957. Library Reference.

(35) J. H. Preston, "The Determination of Turbulent Skin Friction by Means of Pitot Tubes," Journal of the Royal Aeronautical Society, Vol. 58, 1954.

(36) P. L. Rowlison and G.L. Martin, "Rational Model Describing Slope Erosion," ASCE, Irrigation and Drainage 97, 39-50, 1971.

(37) P. G. Samuels, EMBER - A Numerical Model of an Embanked River," Wallingford Hydraulic Research Station, Report IT 183, 28 p, 1979.

(38) H. W. Schen, S. A. Schumm, and J. D. Nelson, "Methods for Assessment of Stream-Related Hazards to Highways and Bridges," FHWA/RD-80/160, 252 p, 1980.

(39) E. E. Seelye, Data Book for Civil Engineers, Vol. 1, NY, Wiley and Sons, 1966.

(40) P. Singh Shiwendra, "Highway Embankment Doubles As Dam," ASCE, Civil Engineering Journal, 79:80, 1979.

(41) D. B. Simons, Y. H. Chen and A. A. Fiuzat, "Stability Tests of Riprap in Flood Control Channels," for the U.S. Army Waterways Experiment Station, Vicksburg, Mississippi, 1981.

BIBLIOGRAPHY (continued)

(42) D. B. Simons, G. L. Lewis, and W. G. Field, "Embankment Protection at River Constrictions," Proceedings, Eleventh Annual Bridge Engineering Conference 1970, Department of Civil Engineering, Colorado State University, Fort Collins, Colorado, 1970.

(43) D. B. Simons, G. L. Lewis, "Flood Protection at Bridge Crossings," prepared for Wyoming State Highway Department, Planning and Research Division in Cooperation with the U.S. Department of Transportation, Federal Highway Administration, Bureau of Public Roads, 1970, CER70-71DBS-GLL31.

(44) D. B. Simons, R. M. Li, K. G. Eggert, D. M. Hartley, J.N.H. Ho, and R. Miskimins, "Computer Simulation for Evaluating the Effectiveness of Vegetation Buffer Strips," for Environmental Research Laboratory, Office of Research and Development, U.S. Environmental Protection Agency, 1981.

(45) M. A. Stevens and D. B. Simons, "Stability Analysis for Coarse Granular Material on Slopes," Chapter 17, River Mechanics, edited by H. W. Shen, Colorado State University, November 1971.

(46) E. Tautenhain and S. Kohlhase, "Investigation on Wave Run-Up and Overtopping at Sea Dikes," in Proceedings of International Conference of Water Resources Development, Taipei, Vol. 3, Taipei, Chinese Institute of Engineering, 873-882, 1980.

(47) M. T. Tseng, A. J. Knepp, and R. A. Schmalz, "Evaluation of Flood Risk Factors in the Design of Highway Stream Crossings," Fed. Highway Adm., FHWA-RD-75-54, 1975.

(48) U.S. Army Corps of Engineers, "Earth Embankments," US Government Printing Office, Washington, DC, EM-1110-2-2300, 1959.

(49) U.S. Army Corps of Engineers, "Seepage Control," US Government Printing Office, Washington, DC, EM-1110-2-1091, 1982.

(50) U.S. Bureau of Reclamation, "Method of Computing Erosion Rate for Failure of Earthfill Dams," Unpublished Report, USDI, B.R., Denver, CO, 1965.

(51) F. C. Walker and W. G. Holz, "Control of Embankment Material by Laboratory Testing," ASCE Proceedings 77, No. 108, Dec. 25 p, 1951.

(52) A. Weiss, "Construction Technique of Passing Floods Over Earth Dams," Trans. ASCE, V. 116, p. 1158, 1951.

(53) R. N. Yong and B. P. Warkentine, Introduction to Soil Behavior, MacMillan Co., New York, 1966.

(54) G. K. Young, R. S. Taylor, and L. S. Costello, "Evaluation of the Flood Risk Factor in the Design of Box Culverts," Report No. FHWA-RD-74-11, Vol. 1 of 2, FHWA HRS-42, Washington, DC 20590, September 1970.

204

FEDERALLY COORDINATED PROGRAM (FCP) OF HIGHWAY RESEARCH, DEVELOPMENT, AND TECHNOLOGY

The Offices of Research, Development, and Technology (RD&T) of the Federal Highway Administration (FHWA) are responsible for a broad research, development, and technology transfer program. This program is accomplished using numerous methods of funding and management. The efforts include work done in-house by RD&T staff, contracts using administrative funds, and a Federal-aid program conducted by or through State highway or transportation agencies, which include the Highway Planning and Research (HP&R) program, the National Cooperative Highway Research Program (NCHRP) managed by the Transportation Research Board, and the one-half of one percent training program conducted by the National Highway Institute.

The FCP is a carefully selected group of projects, separated into broad categories, formulated to use research, development, and technology transfer resources to obtain solutions to urgent national highway problems.

The diagonal double stripe on the cover of this report represents a highway. It is color-coded to identify the FCP category to which the report's subject pertains. A red stripe indicates category 1, dark blue for category 2, light blue for category 3, brown for category 4, gray for category 5, and green for category 9.

FCP Category Descriptions

1. **Highway Design and Operation for Safety**
   Safety RD&T addresses problems associated with the responsibilities of the FHWA under the Highway Safety Act. It includes investigation of appropriate design standards, roadside hardware, traffic control devices, and collection or analysis of physical and scientific data for the formulation of improved safety regulations to better protect all motorists, bicycles, and pedestrians.

2. **Traffic Control and Management**
   Traffic RD&T is concerned with increasing the operational efficiency of existing highways by advancing technology and balancing the demand-capacity relationship through traffic management techniques such as bus and carpool preferential treatment, coordinated signal timing, motorist information, and rerouting of traffic.

3. **Highway Operations**
   This category addresses preserving the Nation's highways, natural resources, and community attributes. It includes activities in physical maintenance, traffic services for maintenance zoning, management of human resources and equipment, and identification of highway elements that affect the quality of the human environment. The goals of projects within this category are to maximize operational efficiency and safety to the traveling public while conserving resources and reducing adverse highway and traffic impacts through protections and enhancement of environmental features.

4. **Pavement Design, Construction, and Management**
   Pavement RD&T is concerned with pavement design and rehabilititation methods and procedures, construction technology, recycled highway materials, improved pavement binders, and improved pavement management. The goals will emphasize improvements to highway performance over the network's life cycle, thus extending maintenance-free operation and maximizing benefits. Specific areas of effort will include material characterizations, pavement damage predictions, methods to minimize local pavement defects, quality control specifications, long-term pavement monitoring, and life cycle cost analyses.

5. **Structural Design and Hydraulics**
   Structural RD&T is concerned with furthering the latest technological advances in structural and hydraulic designs, fabrication processes, and construction techniques to provide safe, efficient highway structures at reasonable costs. This category deals with bridge superstructures, earth structures, foundations, culverts, river mechanics, and hydraulics. In addition, it includes material aspects of structures (metal and concrete) along with their protection from corrosive or degrading environments.

9. **RD&T Management and Coordination**
   Activities in this category include fundamental work for new concepts and system characterization before the investigation reaches a point where it is incorporated within other categories of the FCP. Concepts on the feasibility of new technology for highway safety are included in this category. RD&T reports not within other FCP projects will be published as Category 9 projects.